

Reactivity of Lewis Base Stabilized Pnictogenylboranes Towards Transition Metal Complexes



DISSERTATION
ZUR ERLANGUNG DES
DOKTORGRADES DER NATURWISSENSCHAFTEN
(DR. RER. NAT.)
DER FAKULTÄT FÜR CHEMIE UND PHARMAZIE
DER UNIVERSITÄT REGENSBURG

vorgelegt von
Jens Braese
aus Kulmbach
im Jahr 2018

Diese Arbeit wurde angeleitet von Prof. Dr. Manfred Scheer.

Promotionsgesuch eingereicht am: 30.11.2018

Tag der mündlichen Prüfung: 11.01.2019

Vorsitzender: Prof. Dr. Arnd Vogler

Prüfungsausschuss: Prof. Dr. Manfred Scheer

Prof. Dr. Henri Brunner

Prof. Dr. Frank-Michael Matysik



Universität Regensburg

Eidesstattliche Erklärung

Ich erkläre hiermit an Eides statt, dass ich die vorliegende Arbeit ohne unzulässige Hilfe Dritter und ohne Benutzung anderer als der angegebenen Hilfsmittel angefertigt habe; die aus anderen Quellen direkt oder indirekt übernommenen Daten und Konzepte sind unter Angabe des Literaturzitats gekennzeichnet.

Jens Braese

This thesis was elaborated within the period from April 2014 until March 2018 in the Institute of Inorganic Chemistry at the University of Regensburg, under the supervision of Prof. Dr. Manfred Scheer.

Parts of this work have already been published:

J. Braese, A. Schinabeck, M. Bodensteiner, H. Yersin, A. Y. Timoshkin, M. Scheer, *Chem. Eur. J.* **2018**, *24*, 10073–10077.

*"I'm just a simple man
trying to make my way in the universe."*

Jango Fett

***To my family, friends, supporters
and loved ones***

Preface

Some of the presented results have already been published during the preparation of this work (*vide supra*). The relevant content is reprinted with permission of the respective scientific publisher. The corresponding citation and the respective license numbers are given at the beginning of the particular chapters.

Each chapter includes a list of authors. At the beginning of each chapter the individual contribution of each author will be described. Additionally, if some of the presented results have already been partly discussed in other theses, it is stated at the beginning of the respective chapters.

To ensure a uniform design of this work, all chapters are subdivided into 'Introduction', 'Results and Discussion', 'Conclusion', 'References', and 'Supporting Information'. Furthermore, all chapters have the same text settings and the compound numeration begins anew. Due to different requirements of the journals and different article types, the presentation of figures for single crystal X-ray structures or the 'Supporting Information' may differ. In addition, a general introduction is given at the beginning and a comprehensive conclusion of all chapters is presented at the end of this thesis.

Table of Contents

1. Introduction	1
1.1 Bonding Situation and Structure Types of Group 13/15 Compounds	1
1.2 Academic Interest and Application	2
1.3 Inorganic Oligomeric and Polymeric Compounds from Dehydrocoupling reactions	3
1.4 Lewis Base Stabilized Pnictogenylboranes	6
1.5 References	8
2 Research Objectives	13
3 The Polymerization of Phosphinoborane by Titanium Complexes	17
3.1 Introduction	17
3.2 Results and Discussion	18
3.3 Conclusion	24
3.4 References	24
3.5 Supporting Information	27
3.5.1 Synthetic Procedures	27
3.5.2 Polymerization Experiments	28
3.5.3 NMR spectroscopy	33
3.5.4 ESI-MS	44
3.5.5 GPC and DLS	53
3.5.6 Computational Studies	56
3.5.7 References	57
4 Gold(I) Complexes Containing Phosphanyl- and Arsanylborane Ligands	61
4.1 Introduction	61
4.2 Results and Discussion	62

4.3	Conclusion	68
4.4	References	69
4.5	Supporting Information	72
4.5.1	General information.....	72
4.5.2	Syntheses of described compounds.....	72
4.5.3	Details of Crystal Structure Solution and Refinement	77
4.5.4	Crystal Structures.....	79
4.5.5	Crystallographic Information.....	87
4.5.6	NMR Spectroscopy	98
4.5.7	Computational Details	112
4.5.8	Photoluminescence.....	139
4.5.9	References.....	139
5	Coordination of Pnictogenylboranes Towards Monovalent Copper Compounds	143
5.1	Introduction	143
5.2	Results and Discussion	144
5.3	Conclusion	151
5.4	References	152
5.5	Supporting Information	154
5.5.1	General information.....	154
5.5.2	Syntheses of described compounds.....	154
5.5.3	References.....	167
6	Thesis Treasury	169
6.1	Reactivity of Phosphanylboranes towards Rh(I) complexes	169
6.1.1	Syntheses of described compounds.....	173
6.1.2	References.....	175
7	Conclusion	177
7.1	Polymerization of Pnictogenylboranes	177

7.2	Coordination towards Au(I) and Cu(I) compounds.....	182
7.3	References.....	185
8	Appendices.....	186
8.1	List of Abbreviations	186
8.2	Acknowledgments	189

1. Introduction

1.1 Bonding Situation and Structure Types of Group 13/15 Compounds

Compounds consisting of elements from both group 13 and group 15 with a direct bond between both elements are considered as inorganic analogues to hydrocarbon compounds: In a unit of two carbon atoms, substitution of one carbon atom by a group 13 element, e.g. B, and the other carbon atom by a group 15 element, e.g. N, leads to isoelectronic units.^[1] Boron, bearing one valence electron less than carbon, and nitrogen, bearing one more valence electron than carbon, can conjointly build isoelectronic molecules, saturated as well as unsaturated ones (Figure 1).

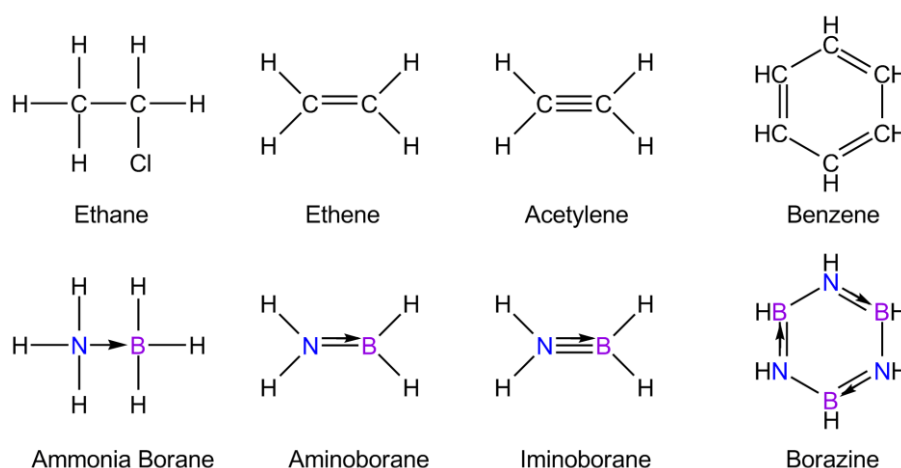


Figure 1. Isoelectronic analogy between hydrocarbons and group 13/15 compounds.

This analogy can also be observed in cyclic molecules like borazine (B₃N₃H₆), also called “inorganic benzene”, and even in solid state materials, for example boron nitride (BN)_n. While borazine shows some of the typical characteristics of its aromatic analogue benzene (C₆H₆), being a colourless liquid with aromatic odor,^[2] the aromaticity is significantly lower due to the polarity of the bonds between the group 13 and group 15 atoms. This is caused by the difference in the electronegativity between the boron and the nitrogen atom ($\Delta EN = 1.0$). Comparing ammonia borane (H₃N·BH₃) to ethane (C₂H₆), the bonding situation is pictorially better described as a dative bond from the nitrogen atom to the boron atom. In this work, the dative bond model is used if it’s adding clarity, otherwise plain bonds are depicted. A zwitterionic Lewis structure H₃N⁺-BH₃ could also

be used to describe the bonding situation, although computational studies show that just $0.2 e^-$ are transferred from nitrogen to boron, locating the bonding electron pair closer to nitrogen.^[3] In comparison to a C-C single bond, this leads to a weaker bond, which is subsequently influencing the reactivity. The bond length is elongated compared to hydrocarbons, the distance between the two atoms is approximately 0.04 \AA longer for all examples in Figure 1. The solid state material boron nitride $(\text{BN})_n$ occurs in the three different modifications, hexagonal (α), cubic (β) and wurtzite type (γ). A graphite like layer structure can be observed in the hexagonal phase, while the cubic β -BN shows a diamond like lattice. The γ -phase shows the same structure as lonsdaleite, the high pressure hexagonal diamond.

1.2 Academic Interest and Application

The first report of a group 13/15 compound dates back to the year 1809, a decade after the French revolution, when the ammonia-borane adduct $\text{H}_3\text{N}\cdot\text{BF}_3$ was described by the famous French scientist *Gay-Lussac*.^[4] The first description of the heavier congener $\text{H}_3\text{P}\cdot\text{BCl}_3$ took place much later in 1890, also containing a fully halogenated borane.^[5] The presence of trihydridoboron in $\text{Me}_3\text{N}\cdot\text{BH}_3$ was reported in 1937 by *Burg* and *Schlesinger*.^[6] Based on their work, the isolation of the fully hydrogen substituted ammonia borane $\text{H}_3\text{N}\cdot\text{BH}_3$ was achieved in 1955,^[7] followed by the characterization of $\text{H}_3\text{P}\cdot\text{BH}_3$ a decade later.^[8] These only hydrogen substituted compounds $\text{H}_3\text{E}\cdot\text{BH}_3$ (E = N, P, As, Sb) are of special academic interest because they represent the parent compounds of substituted pnictogen hydride boranes.^[9] For application, they are promising candidates for hydrogen storage materials, especially $\text{H}_3\text{N}\cdot\text{BH}_3$ due to its high hydrogen content up to 19.6 wt-%.^[10] Up to three equivalents of dihydrogen can be released by thermolysis. In this case, the thermodynamically very stable boron nitride $(\text{BN})_n$ is formed. Substitution on the main group elements can still be beneficial to improve the properties by electronical and sterical effects and influence the workability of resulting materials by altering e.g. the solubility or thermal stability.^[11] Catalysis by transition metal complexes can be applied to lower the activation barrier of the hydrogen release and control the degree of dehydrogenation. Recent studies showed also promising results in regenerating partially dehydrogenated compounds.^[12] Dehydrogenation can lead to formation of new bonds via dehydrocoupling, resulting in inorganic oligomeric and polymeric compounds, which will be discussed in the following chapter. Besides being promising candidates for hydrogen storage materials, poly(aminoborane)s are examined as potential preceramic materials. Processed into the desired shapes, subsequent pyrolyzation can then produce α -boron nitride forms. Boron

phosphide attracts significant interest due to its semiconducting properties,^[13] for which poly(phosphinoborane)s are discussed as precursors. Films of polymeric [(p-CF₃C₆H₄)HP-BH₂]_n were successfully tested for application in electron beam lithography.^[14] At present, group 13/15 compounds are already used as abrasives,^[15] flame retardants,^[16] high temperature ceramics^[1] or as semiconducting materials in opto- and microelectronic devices.^[17]

1.3 Inorganic Oligomeric and Polymeric Compounds from Dehydrocoupling reactions

Dehydrocoupling describes the process of the formation of a new chemical bond with simultaneous release of dihydrogen. This can lead to the aggregation of small molecules to bigger oligomeric and polymeric units. Subject for such reactions can be the release of dihydrogen or the generation of new materials or both. Especially dehydrocoupling reactions of amine- and phosphine-borane adducts have been intensively studied. The reaction can be induced either by thermolysis^[18] or with metal catalysts.^[19] The first metal catalyzed dehydrocoupling reaction of amine-boranes was mentioned in a patent in 1989.^[20] A decade later, *Manners et al.* described the first coupling of phosphine-borane Ph₂HP·BH₃ to dimeric species Ph₂HP-BH₂-Ph₂P-BH₃ (**I**, Figure 2), using the transition metal precatalysts [Rh(COD)₂][OTf] or [Rh(μ-Cl)(COD)]₂ (COD = cycloocta-1,5-diene).^[21] Using the mono-substituted phosphine-borane PhH₂P·BH₃ under similar conditions leads to the formation of polymeric product [PhHP-BH₂]_n (**II**). Later studies comprised the first in detail investigation on catalytic dehydrocoupling of amine-boranes, also using Rh(I) complexes or [RhCl₃·3H₂O].^[19c,22] Similar to dehydrocoupling reactions of phosphine-borane, the product is strongly influenced by the substitution on the pnictogen atom. Secondary amine-boranes RR'HN·BH₃ (R/R' = Me, Bn, 1,4-C₄H₈ = pyrrolidine) form cyclic dimers (**III**) by dehydrocoupling, while bulky substituents prevent dimerization and stabilize monomeric species like iPr₂N=BH₂ (**IV**). Mono-substituted compounds RH₂N·BH₃ (R = H, Me, Ph) afford cyclic trimers (**V**) upon dehydrocoupling. Subsequent heating leads to further hydrogen loss and formation of N-substituted borazines (**VI**). Since then, a variety of transition metal complexes and nanoparticles (Ti, Cr,^[23] Fe,^[24] Ni,^[25] CoCu,^[26] Zr, Ru,^[19f,27] Rh, Ir,^[28] Pt^[29]) and also main group compounds^[30] have been tested for catalytic activity in dehydrocoupling experiments of amine- and phosphine-borane adducts.

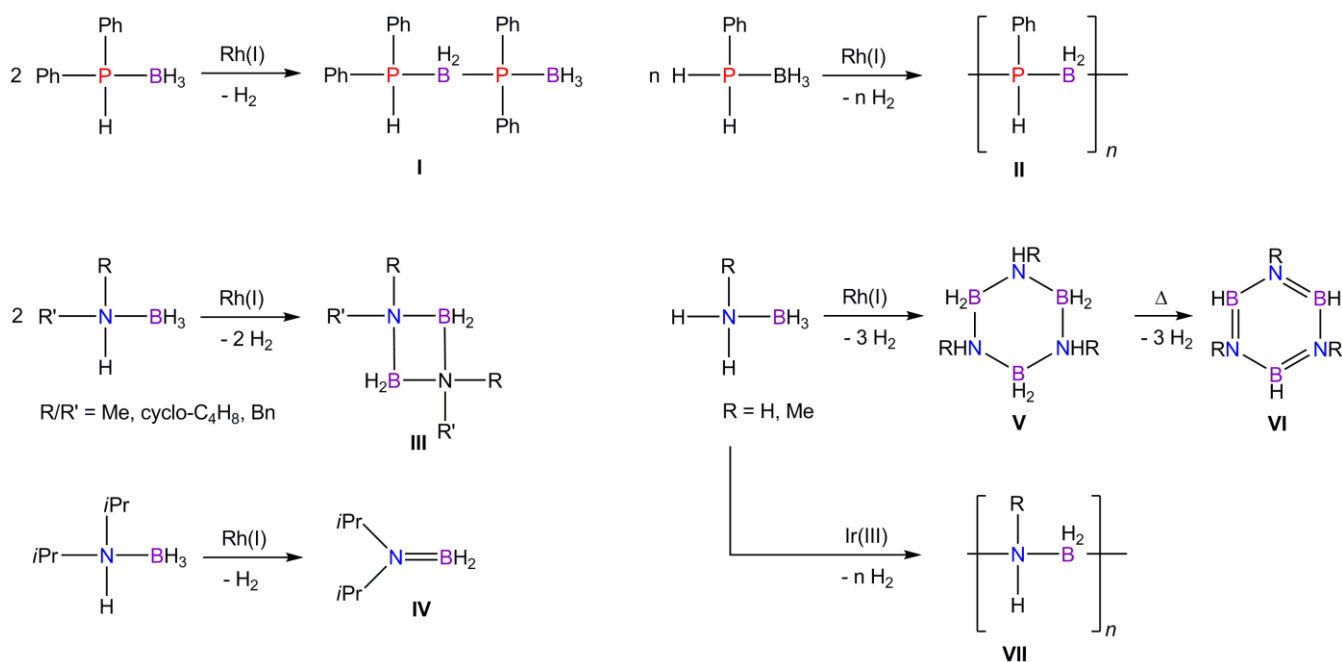


Figure 2. Dehydrocoupling of secondary and primary phosphine- and amine-boranes.

In addition to the Rh(I) species, exemplified results will be discussed in the following. An example for an active main group catalyst is the Lewis acid $B(C_6F_5)_3$, which was reacted with the in-situ generated parent compound $H_3P \cdot BH_3$.^[11b] Under evolution of hydrogen, the formation of poly(phosphinoborane) $[H_2P-BH_2]_n$ is assumed, although the product was not indubitable characterized due to its sensitivity. Substrate $Ph_2HP \cdot BH_3$ gives rise to the polymeric product $[PhHP-BH_2]_n$ (II), the same product as from Rh(I) catalysis. Recently, it was shown that also catalysts based on earth abundant Fe can be used for the synthesis of poly(phosphinoborane)s, while allowing the control of the molecular weight of the polymers.^[31] Worth mentioning is the use of *Brookhart's* $[IrH_2(POCOP)]$ catalyst ($POCOP = [\mu_3-1,3-(OPtBu_2)_2C_6H_3]$), which allows efficient dehydrocoupling of the parent compound $H_3N \cdot BH_3$, forming either cyclic pentamers $[H_2N-BH_2]_5$ ^[28a] or linear polymers $[H_2N-BH_2]_n$ from higher monomer concentrations.^[32] Similar to these findings, mono-substituted amine-boranes give rise to oligomeric compounds from reactions of lower monomer concentrations while higher concentrations lead to polymeric materials $[RHN-BH_2]_n$ ($R = H, Me, nBu$) (VII).^[32,33]

Another interesting class of catalysts are based on early transition metals titanium and its heavier homologue zirconium. $[Cp_2Ti]$, generated in situ from $[Cp_2TiCl_2]$ with 2 equivalents of $nBuLi$, functions as an efficient homogenous catalyst for the dehydrogenation of secondary amine-borane adducts. $R_2HN \cdot BH_3$ ($R = Me, iPr$) show total conversion at room temperature within minutes. The formed products are the same as with the use of Rh(I) catalysts.^[34] A series of active Ti^{II} and Zr^{II} precatalysts for

dehydrocoupling reactions has been investigated, of which the Ti-based precatalysts were found to be far more active than their Zr-based congeners.^[35,36,37] Mechanistic investigations propose a N-H bond activation and the formation of a M^{IV} intermediate (Figure 3), which was isolated for Zr^{IV} , but only proposed for Ti^{IV} . For subsequent steps, an off-metal process was suggested by *Luo* and *Ohn*,^[37] which involves hydride transfer from boron to the metal, resulting in monomeric $Me_2N=BH_2$ and $[Cp_2TiH_2]$. The former was supposed to dimerize towards a cyclic dimer (III), while the latter releases H_2 to reform $[Cp_2Ti]$. *Manners* and *Lloyd-Jones* on the other hand proposed a two-stage catalytic cycle, in which a linear diborazane intermediate $Me_2NH-BH_2-NMe_2-BH_3$ (similar to I) is formed (and also detected by NMR spectroscopy) after initial N-H activation. A subsequent on-metal ring closing dehydrogenation step gives rise to the cyclic dimer (III). Once again, an interplay of Ti^{II} and Ti^{IV} intermediates is postulated.^[38] However, this system was completely inactive towards the parent compound H_3N-BH_3 and it showed only negligible reaction rates towards primary amine-boranes. Interestingly, *Wolstenholme* and *McGrady* isolated a paramagnetic Ti^{III} species $[Cp_2Ti(NH_2BH_3)]$ (Figure 3) from reaction of $[Cp_2TiCl_2]$ with $Li[NH_2BH_3]$, which suggests that the presence of M^{III} ($M = Ti, Zr$) species on catalytic dehydrogenation reactions should not be dismissed.^[34b] From stoichiometric reactions of in-situ generated $[Cp_2Ti]$ with both secondary amine- and phosphine-boranes, further Ti^{III} complexes $[Cp_2Ti(NMe_2BH_3)]$ and $[Cp_2Ti(PPh_2BH_3)]$ (Figure 3) could be isolated.^[35] Both show activities as precatalysts for dehydrocoupling of Me_2HN-BH_3 , via a $Me_2NH-BH_2-NMe_2-BH_3$ intermediate, towards formation of a cyclic dimer (III). This strengthens the assumption of a key catalytic role of a paramagnetic Ti^{III} species in dehydrocoupling reactions of amine-boranes.

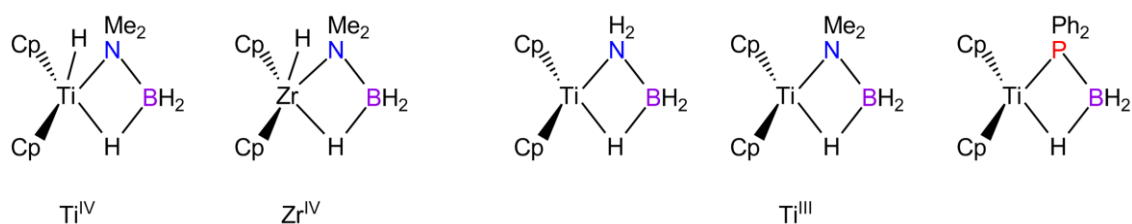


Figure 3. Proposed (Ti^{IV}) and isolated (Zr^{IV} and Ti^{III}) amido- and phosphidoborane species.

For phosphine-borane substrates, recent studies of the coordination chemistry at d-block metal centers gave insight into the formation of new P-B bonds via dehydrogenation in oligomeric and polymeric materials.^[39] The P-H moiety serves a double purpose: The activation of the P-H bond leads to the formation of metal-phosphidoborane intermediates and the P-B bond formation is promoted via dehydrogenative coupling of a protic P-H and a hydridic B-H moiety with simultaneous

release of dihydrogen.^[31a,39] Since the P-H bonds are essentially non-polar ($\Delta EN = 0.01$), this limits the reactions to substrates containing electron withdrawing effects from aryl groups on the phosphorus atom. Therefore, there are only very limited examples of poly(alkylphosphinoborane)s prepared via dehydrocoupling reactions, featuring electron donating alkyl substituents. $t\text{BuPH}_2\cdot\text{BH}_3$ ^[40] and $\text{FcCH}_2\text{PH}_2\cdot\text{BH}_3$ ^[41] in reaction with Rh(I) catalysts leads to the formation of polymeric materials, displaying rather unwanted properties like low molecular masses or high polydispersity indices when compared to other poly(phosphinoborane)s. Though it should be mentioned that there is a completely different pathway towards poly(alkylphosphinoborane)s which doesn't involve dehydrocoupling processes. Instead it makes use of Lewis base stabilized phosphanylboranes $\text{RR}'\text{PBH}_2\cdot\text{LB}$ ($\text{R/R}' = \text{H, alkyl, aryl}$; $\text{LB} = \text{NMe}_3, \text{SMe}_2$), which will be discussed in the following chapter.

1.4 Lewis Base Stabilized Pnictogenylboranes

Pnictogenylboranes $[\text{R}_2\text{EBR}'_2]$ ($\text{E} = \text{pnictogen atom}$; $\text{R/R}' = \text{H, alkyl, aryl}$) can be viewed as the inorganic equivalents of ethene, but as monomeric species they are commonly not stable under ambient conditions. This can be explained due to an empty p-orbital at the boron atom together with an available lone pair on the pnictogen atom (Figure 3). The free electron pair can interact with the vacant orbital of a second molecule, leading to a head-to-tail oligomerization/polymerization. This behavior, used in a controlled manner, can be utilized for the synthesis of new polymeric materials.

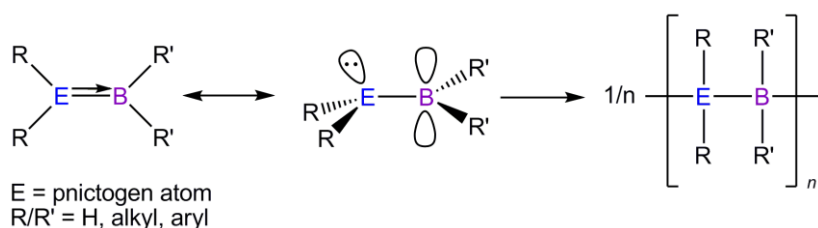


Figure 3. Head-to-tail oligomerization of pnictogenylboranes.

The monomeric species can be stabilized through steric hindrance, among other things, as observed e.g. in $t\text{Bu}_2\text{AsBMe}_2$.^[42] Less sterically hindered compounds, like the parent compound NH_2BH_2 , which could be isolated only at cryogenic conditions,^[43] can be stabilized in the coordination sphere of transition metal fragments like $[\text{RuH}_2(\text{PCy}_3)_2(\eta^2\text{-}\eta^2\text{-H}_2\text{NBH}_2)]$.^[44] Stabilization can also be realized through Lewis acids, which can accept the electron pair of the pnictogen atom, and Lewis bases, which can donate into the vacant orbital at the boron atom. Like this, stabilized parent compounds

$[\text{BH}_3\cdot\text{H}_2\text{NBH}_2\cdot\text{DMAP}]^{[45]}$ and $[\text{W}(\text{CO})_5\cdot\text{H}_2\text{EBH}_2\cdot\text{NMe}_3]^{[46]}$ (E = P, As) could be realized. Further investigations by our group gave rise to only Lewis base stabilized compounds $\text{H}_2\text{EBH}_2\cdot\text{NMe}_3$ (E = P, As) that can be achieved through abstraction of the $[\text{W}(\text{CO})_5]$ fragment by $\text{P}(\text{OMe})_3$.^[47] Such compounds can also be obtained by direct synthesis via salt metathesis reactions, giving access also to the heavier homologues $\text{H}_2\text{EBH}_2\cdot\text{LB}$ (E = P, As, Sb; LB = NMe_3 or NHC^{Me} for Sb).^[48] The azaborane $\text{H}_2\text{NBH}_2\cdot\text{LB}$ however is not accessible by these methods. Although it could be obtained by *Manners et al.* through the cleavage of polymers $[\text{H}_2\text{N}-\text{BH}_2]_n$ or $[\text{MeHN}-\text{BH}_2]_n$ by addition of the strong Lewis base NHC^{Dipp} .^[49] Moreover, mixed pnictogenylboranes could recently be stabilized by our group. Although also requiring both Lewis acid and Lewis base stabilization, $\text{W}(\text{CO})_5\cdot\text{PH}_2\text{BH}_2\text{ER}_2\text{BH}_2\cdot\text{LB}$ (E = P, As, Sb; R = H (except for Sb), SiMe_3 ; LB = NMe_3 or NHC^{Me} for Sb) could be obtained, which might be interesting building blocks for copolymers.^[50]

Thermal treatment of phosphanylboranes $\text{RR}'\text{PBH}_2\cdot\text{NMe}_3$ (R/R' = H, alkyl, aryl; LB = NMe_3) can lead to the elimination of the stabilizing Lewis base NMe_3 and a head-to-tail polymerization of the intermediate $[\text{RR}'\text{PBH}_2]$, giving rise to oligomeric and polymeric compounds. The resulting material is strongly influenced by the substituents on the phosphorus atom. Heating of parent compound $\text{H}_2\text{PBH}_2\cdot\text{NMe}_3$ results in a insoluble precipitate, presumably $[\text{H}_2\text{PBH}_2]_n$ and further small or branched oligomers.^[24] Electron withdrawing aryl-substituents increase the solubility, the thermally induced polymerization of $\text{Ph}_2\text{PBH}_2\cdot\text{NMe}_3$ resulted in oligomeric material $[\text{Ph}_2\text{PBH}_2]_n$, showing only a limited number of repeating units ($n < 6$). Gentle thermolysis of alkylated $\text{MeHPBH}_2\cdot\text{NMe}_3$ afford soluble poly(alkylphosphinoborane)s with at least 40 repeating units.^[51] The best results were obtained from mild thermolysis of $t\text{BuHPBH}_2\cdot\text{NMe}_3$ at 40 °C, resulting in well soluble, high molecular mass material $[t\text{BuHPBH}_2]_n$ with more than 2000 repeating units.^[24] Experiments in our group have shown that thermal treatment of the heavier homologues $\text{RR}'\text{EBH}_2\cdot\text{NMe}_3$ (E = As, Sb) does not result in the elimination of NMe_3 and the formation of new E-B bonds, but rather in the breaking of the already existing E-B bonds or a complete decomposition of the starting material.

To further promote poly- and oligomerization, the parent compound $\text{H}_2\text{PBH}_2\cdot\text{NMe}_3$ has been reacted with transition metal complex $[\text{Cp}_2\text{Ti}(\text{btmsa})]$ (btmsa = bis(trimethylsilyl)acetylene) as a source of $[\text{Cp}_2\text{Ti}]$, compare chapter 1.3. Initially, the adduct complex $[\text{Cp}_2\text{Ti}(\text{btmsa})(\text{H}_2\text{PBH}_2\cdot\text{NMe}_3)]$ is formed at -80 °C.^[52] Upon warming to room temperature, stepwise aggregation on titanium complex centers to form phosphinoborane oligomers ($n = 3, 4, 6$) can be observed (Figure 4). This process includes elimination of NMe_3 as well as dehydrocoupling steps to form new P-B (and also

P-P) bonds, while the catenae molecule is stabilized in the coordination sphere of $[\text{Cp}_2\text{Ti}]$ via Ti-P, Ti-B and Ti-H-B interactions.

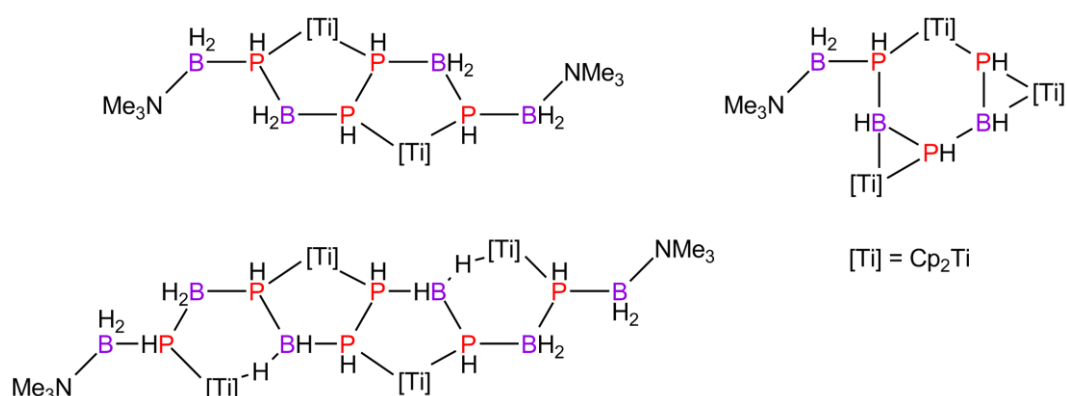


Figure 4. Phosphinoborane oligomers stabilized in the coordination sphere of $[\text{Cp}_2\text{Ti}]$.

Based on these findings, the reaction of Lewis base stabilized pnictogenylboranes towards transition metal complexes should be further investigated in this thesis.

1.5 References

- [1] A. F. Hollemann, E. Wiberg, *Lehrbuch der Anorganischen Chemie, Vol. 102*, Walter de Gruyter Verlag, Berlin-New York, **2007**, 1111-1126.
- [2] A. Stock, E. Pohland, *Ber. Dtsch. Chem. Ges.* **1926**, *59*, 2215–2223.
- [3] H. Umeyama, K. Morokuma, *J. Am. Chem. Soc.* **1976**, *98*, 7208–7220.
- [4] J. L. Gay-Lussac, J. L. Thénard, *Mem. de. Phys. et de. Chim. de la Soc. d’Arcueil* **1809**, *2*, 210 as cited in V. Jonas, G. Frenking, *J. Chem. Soc., Chem. Commun.* **1994**, 1489–1490.
- [5] A. Besson, *Comptes Rendus* **1890**, 516.
- [6] A. B. Burg, H. I. Schlesinger, *J. Am. Chem. Soc.* **1937**, *59*, 780–787.
- [7] S. G. Shore, R. W. Parry, *J. Am. Chem. Soc.* **1955**, *77*, 6084-6085.
- [8] R. W. Rudolph, R. W. Parry, C. F. Farran, *Inorg. Chem.* **1966**, *5*, 723-726.
- [9] R. T. Paine, H. Nöth, *Chem. Rev.* **1995**, *95*, 343–379.
- [10] C. W. Hamilton, R. T. Baker, A. Staubitz, I. Manners, *Chem. Soc. Rev.* **2009**, *38*, 279–293.
- [11] a) X. Feng, M. M. Olmstead, P. P. Power, *Inorg. Chem.* **1986**, *25*, 4615–4616; b) J.-M. Denis, H. Forintos, H. Szelke, L. Toupet, T.-N. Pham, P.-J. Madec, A.-C. Gaumont, *Chem. Commun.* **2003**, 54–55.
- [12] a) L. Winner, W. C. Ewing, K. Geetharani, T. Dellermann, B. Jouppi, T. Kupfer, M. Schäfer, H. Braunschweig, *Angew. Chem. Int. Ed.* **2018**, *57*, 12275–12279; *Angew. Chem.* **2018**, *130*, 12455-12459; b) C. Reller, F. O. R. L. Mertens, *Angew. Chem. Int. Ed.* **2012**, *51*, 11731–11735; *Angew. Chem.* **2012**, *124*, 11901–11905; c) B. L. Davis, D. A. Dixon, E. B. Garner, J. C. Gordon, M. H. Matus, B. Scott, F. H. Stephens, *Angew. Chem. Int. Ed.* **2009**, *48*, 6812–6816; *Angew. Chem.* **2009**, *121*, 6944–6948; d) A. D. Sutton, A. K. Burrell, D. A. Dixon, E. B. Garner III, J. C. Gordon, T. Nakagawa, K. C. Ott, J. P. Robinson, M. Vasiliu, *Science* **2011**, *331*, 1426–1429; e) A. P. M. Robertson, E. M. Leitao, I. Manners, *J. Am. Chem. Soc.* **2011**, *133*, 19322–19325; e) E. M. Leitao, N. E. Stubbs, A. P. M. Robertson, H.

- Helten, R. J. Cox, G. C. Lloyd-Jones, I. Manners, *J. Am. Chem. Soc.* **2012**, *134*, 16805–16816; f) P. Paetzold, *Adv. Inorg. Chem.* **1987**, *31*, 123–170.
- [13] Y. Kumashiro, *J. Mater. Res.* **1990**, *5*, 2933–2947.
- [14] T. J. Clark, J. M. Rodezno, S. B. Clendenning, S. Aouba, P. M. Brodersen, A. J. Lough, H. E. Ruda, I. Manners, *Chem. Eur. J.* **2005**, *11*, 4526–4534.
- [15] R. H. Todd, D. K. Allen, L. Alting, *Manufacturing Processes Reference Guide*, Industrial Press Inc, New York, **1994**, 43–48.
- [16] a) G. W. Parshall, *The Chemistry of Boron and its Compounds*; Muetterties, E. L., Ed.; Wiley: New York, **1967**, 617; b) Haiduc, I. *The Chemistry of Inorganic Ring Systems*; Wiley: New York, **1970**, 349.
- [17] a) R. L. Wells, W. L. Gladfelter, *J. Cluster Sci.* **1997**, *8*, 217–237; b) F. Maury, *Adv. Mater.* **1991**, *3*, 542–548;
- [18] a) S. Frueh, R. Kellett, C. Mallery, T. Molter, W. S. Willis, C. King'onde, S. L. Suib, *Inorg. Chem.* **2011**, *50*, 783–792; b) M. G. Hu, R. A. Geanangel, W. W. Wendlandt, *Thermochim. Acta* **1978**, *23*, 249–255; c) F. Baitalow, J. Baumann, G. Wolf, K. Jaenicke-Rössler, G. Leitner, *Thermochim. Acta* **2002**, *391*, 159–168; d) V. Sit, R. A. Geanangel, W. W. Wendlandt, *Thermochim. Acta* **1987**, *113*, 379–382; e) G. Wolf, J. Baumann, F. Baitalow, F. P. Hoffmann, *Thermochim. Acta* **2000**, *343*, 19–25; f) J. Baumann, F. Baitalow, G. Wolf, *Thermochim. Acta* **2005**, *430*, 9–14.
- [19] a) S. S. Mal, F. H. Stephens, R. T. Baker, *Chem. Commun.* **2011**, *47*, 2922–2924; b) T. Umegaki, J.-M. Yan, X.-B. Xiang, H. Shioyama, N. Kuriyama, Q. Xu, *Int. J. Hydrogen Energy* **2009**, *34*, 2303–2311; c) C. A. Jaska, K. Temple, A. J. Lough, I. Manners, *J. Am. Chem. Soc.* **2003**, *125*, 9424–9434; d) C. A. Jaska, I. Manners, *J. Am. Chem. Soc.* **2004**, *126*, 1334–1335; e) Y. Chen, J. L. Fulton, J. C. Linehan, T. Autrey, *J. Am. Chem. Soc.* **2005**, *127*, 3254–3255; f) N. Blaquiere, S. Diallo-Garcia, S. I. Gorelsky, D. A. Black, K. Fagnou, *J. Am. Chem. Soc.* **2008**, *130*, 14034–14035; g) W. R. H. Wright, E. Berkeley, L. G. Sneddon, R. T. Baker, *Chem. Commun.*, *Chem. Commun.* **2011**, *47*, 3177–3179.
- [20] Y. D. Blum, R. M. Laine, U.S. Pat. 4801439, **1989**.
- [21] H. Dorn, R. A. Singh, J. A. Massey, A. J. Lough, I. Manners, *Angew. Chem. Int. Ed.* **1999**, *38*, 3321–3323, *Angew. Chem.* **1999**, *111*, 3540–3543.
- [22] C. A. Jaska, K. Temple, A. J. Lough, I. Manners, *Chem. Commun.* **2001**, 962–963.
- [23] Y. Kawano, M. Uruichi, M. Shimoi, S. Taki, T. Kawaguchi, T. Kakizawa, H. Ogino, *J. Am. Chem. Soc.* **2009**, *131*, 14946–14957.
- [24] C. Marquardt, T. Jurca, K.-C. Schwan, A. Stauber, A. V. Virovets, G. R. Whittell, I. Manners, M. Scheer, *Angew. Chem. Int. Ed.* **2015**, *54*, 13782–13786; *Angew. Chem.* **2015**, *127*, 13986–13991.
- [25] a) R. J. Keaton, J. M. Blacquiere, R. T. Baker, *J. Am. Chem. Soc.* **2007**, *129*, 1844–1845; b) X. Yang, M. B. Hall, *J. Am. Chem. Soc.* **2008**, *130*, 1798–1799; c) P. M. Zimmerman, A. Paul, C. B. Musgrave, *Inorg. Chem.* **2009**, *48*, 5418–5433; d) L. Yang, W. Luo, G.-Z. Cheng, *Catal. Lett.* **2013**, *143*, 873–880.
- [26] C. Li, J. Zhou, W. Gao, J. Zhao, J. Liu, Y. Zhao, M. Wei, D. G. Evans, X. Duan, *J. Mater. Chem. A* **2013**, *1*, 5370–5376.
- [27] a) A. N. Marziale, A. Friedrich, I. Klopsch, M. Drees, V. R. Celinski, Schmedt auf der Günne, Jörn, S. Schneider, *J. Am. Chem. Soc.* **2013**, *135*, 13342–13355; b) D. F. Schreiber, C. O'Connor, C. Grave, Y. Ortin, H. Müller-Bunz, A. D. Phillips, *ACS Catal.* **2012**, *2*, 2505–2511; c) H. Ma, C. Na, *ACS Catal.* **2015**, *5*, 1726–1735; d) A. Friedrich, M. Drees, S. Schneider, *Chem. Eur. J.* **2009**, *15*, 10339–10342; e) M. Käß, A. Friedrich, M. Drees, S. Schneider, *Angew. Chem.* **2009**, *121*, 922–924; *Angew. Chem. Int. Ed.* **2009**, *48*, 905–907.
- [28] a) M. C. Denney, V. Pons, T. J. Hebden, D. M. Heinekey, K. I. Goldberg, *J. Am. Chem. Soc.* **2006**, *128*, 12048–12049; b) A. Paul, C. B. Musgrave, *Angew. Chem.* **2007**, *119*, 8301–8304; *Angew. Chem. Int. Ed.* **2007**, *46*, 8153–8156; c) T. J. Hebden, K. I. Goldberg, D. M. Heinekey, X. Zhang, T. J. Emge, A. S. Goldman, K.

- Krogh-Jespersen, *Inorg. Chem.* **2010**, *49*, 1733–1742; d) D. J. Nelson, B. J. Truscott, J. D. Egbert, S. P. Nolan, *Organometallics* **2013**, *32*, 3769–3772.
- [29] M. Roselló-Merino, J. López-Serrano, S. Conejero, *J. Am. Chem. Soc.* **2013**, *135*, 10910–10913.
- [30] a) J. Spielmann, G. Jansen, H. Bandmann, S. Harder, *Angew. Chem.* **2008**, *120*, 6386–6391; *Angew. Chem. Int. Ed.* **2008**, *47*, 6290–6295; b) D. J. Liptrot, M. S. Hill, M. F. Mahon, D. J. MacDougall, *Chem. Eur. J.* **2010**, *16*, 8508–8515; c) A. J. M. Miller, J. E. Bercaw, *Chem. Commun.* **2010**, *46*, 1709–1711; d) G. R. Whittell, E. I. Balmond, A. P. M. Robertson, S. K. Patra, M. F. Haddow, I. Manners, *Eur. J. Inorg. Chem.* **2010**, *25*, 3967–3975; e) M. M. Hansmann, R. L. Melen, D. S. Wright, *Chem. Sci.* **2011**, *2*, 1554–1559; f) H. Helten, A. P. M. Robertson, A. Staubitz, J. R. Vance, M. F. Haddow, I. Manners, *Chem. Eur. J.* **2012**, *18*, 4665–4680.
- [31] a) A. Schäfer, T. Jurca, J. Turner, J. R. Vance, K. Lee, V. A. Du, M. F. Haddow, G. R. Whittell, I. Manners, *Angew. Chem. Int. Ed.* **2015**, *54*, 4836–4841; *Angew. Chem.* **2015**, *127*, 4918–4923; b) J. R. Vance, A. Schäfer, A. P. M. Robertson, K. Lee, J. Turner, G. R. Whittell, I. Manners, *J. Am. Chem. Soc.* **2014**, *136*, 3048–3064.
- [32] A. Staubitz, A. P. Soto, I. Manners, *Angew. Chem. Int. Ed.* **2008**, *47*, 6212–6215, *Angew. Chem.* **2008**, *120*, 6308–6311.
- [33] B. L. Dietrich, K. I. Goldberg, D. M. Heinekey, T. Autrey, J.C. Linehan, *Inorg. Chem.* **2008**, *47*, 8583–8585.
- [34] a) T. J. Clark, C. A. Russell, I. Manners, *J. Am. Chem. Soc.* **2006**, *128*, 9582–9583; b) M. E. Sloan, A. Staubitz, T. J. Clark, C. A. Russell, G. C. Lloyd-Jones, I. Manners, *J. Am. Chem. Soc.* **2010**, *132*, 3831–3841.
- [35] H. Helten, B. Dutta, J. R. Vance, M. E. Sloan, M. F. Haddow, S. Sproules, D. Collison, G. R. Whittell, G. C. Lloyd-Jones, I. Manners, *Angew. Chem. Int. Ed.* **2013**, *52*, 437–440.
- [36] a) D. Pun, E. Lobkovsky, P. J. Chirik, *Chem. Commun.* **2007**, 3297–3299; b) T. Beweries, S. Hansen, M. Kessler, M. Klahn, U. Rosenthal, *Dalton Trans.* **2011**, *40*, 7689–7692.
- [37] Y. Luo, K. Ohno, *Organometallics* **2007**, *26*, 3597–3600.
- [38] M. E. Sloan, A. Staubitz, T. J. Clark, C. A. Russell, G. C. Lloyd-Jones, I. Manners, *J. Am. Chem. Soc.* **2010**, *132*, 3831–3841.
- [39] a) M. A. Huertos, A. S. Weller, *Chem. Commun.* **2012**, *48*, 7185–7187; b) M. A. Huertos, A. S. Weller, *Chem. Sci.* **2013**, *4*, 1881–1888; c) T. N. Hooper, M. A. Huertos, T. Jurca, S. D. Pike, A. S. Weller, I. Manners, *Inorg. Chem.* **2014**, *53*, 3716–3729; d) H. C. Johnson, T. N. Hooper, A. S. Weller, *Top. Organomet. Chem.* **2015**, *49*, 153–220.
- [40] H. Dorn, J. M. Rodezno, B. Brunnhöfer, E. Rivard, J. A. Massey, I. Manners, *Macromolecules* **2003**, *36*, 291–297.
- [41] S. Pandey, P. Lönnecke, E. Hey-Hawkins, *Eur. J. Inorg. Chem.* **2014**, 2456–2465.
- [42] a) M. A. Petrie, M. M. Olmstead, H. Hope, R. A. Bartlett, P. P. Power, *J. Am. Chem. Soc.* **1993**, *115*, 3221–3226; b) M. A. Mardones, A. H. Rowley, L. Contreras, R. A. Jones, *J. Organomet. Chem.* **1993**, *455*, C1–C2; c) P. P. Power, *Chem. Rev.* **1999**, *99*, 3463–3503.
- [43] C. Y. Tang, A. L. Thompson, S. Aldridge, *Angew. Chem. Int. Ed.* **2010**, *49*, 921–925; *Angew. Chem.* **2010**, *122*, 933–937.
- [44] G. Alcaraz, L. Vendier, E. Clot, S. Sabo-Etienne, *Angew. Chem. Int. Ed.* **2010**, *49*, 918–920; *Angew. Chem.* **2010**, *122*, 930–932.
- [45] A. C. Malcolm, K. J. Sabourin, R. McDonald, M. J. Ferguson, E. Rivard, *Inorg. Chem.* **2012**, *51*, 12905–12916.
- [46] U. Vogel, P. Hoemensch, K.-C. Schwan, A. Y. Timoshkin, M. Scheer, *Chem. Eur. J.* **2003**, *9*, 515–520.

-
- [47] K. Schwan, A. Timoshkin, M. Zabel, M. Scheer, *Chem. Eur. J.* **2006**, *12*, 4900–4908.
- [48] C. Marquardt, O. Hegen, M. Hautmann, G. Balázs, M. Bodensteiner, A. V. Virovets, A. Y. Timoshkin, M. Scheer, *Angew. Chem. Int. Ed.* **2015**, *54*, 13122–13125; *Angew. Chem.* **2015**, *127*, 13315–13318.
- [49] N. E. Stubbs, T. Jurca, E. M. Leitao, C. H. Woodall, I. Manners, *Chem. Commun.* **2013**, *49*, 9098–9100.
- [50] O. Hegen, C. Marquardt, A. Y. Timoshkin, M. Scheer, *Angew. Chem. Int. Ed.* **2017**, *56*, 12783–12787; *Angew. Chem.* **2017**, *129*, 12959–12963.
- [51] A. Stauber, T. Jurca, C. Marquardt, M. Fleischmann, M. Seidl, G. R. Whittell, I. Manners, M. Scheer, *Eur. J. Inorg. Chem.* **2016**, *17*, 2684–2687.
- [52] C. Thoms, C. Marquardt, M. Bodensteiner, M. Scheer, *Angew. Chem. Int. Ed.* **2013**, *52*, 5150–5154; *Angew. Chem.* **2013**, *125*, 5254–5259.

2 Research Objectives

Since the parent compound $\text{H}_2\text{PBH}_2\cdot\text{NMe}_3$ has been successfully reacted with the transition metal complex $[\text{Cp}_2\text{Ti}(\text{btmsa})]$ to promote oligomerization, the reaction of Lewis base stabilized pnictogenylboranes towards transition metal complexes should be further investigated. Known precatalysts for dehydrocoupling reactions of group 13/15 compounds as well as new complexes should be tested for possible catalytic activities with Lewis base stabilized pnictogenylboranes. This includes testing of complexes known for activation of E-H bonds in small molecules as well as a series of monovalent salts MX (M = transition metal, X = Cl, Br, I), which showed in the past great potential of building multinuclear complexes in our group. As we know, the substituents on the pnictogen atom play a key role in the formation of new oligomeric and polymeric species. Therefore, a series of substituted pnictogenylboranes $\text{RR}'\text{EBH}_2\cdot\text{NMe}_3$ (E = P, As, Sb; R = H, alkyl, aryl) should be tested in these reactions. Especially alkyl-substituted phosphinoboranes are of interest for the synthesis of poly(alkylphosphinoborane)s, because these kinds of inorganic polymers are hard to access via dehydrocoupling reactions. Because reactions of the heavier homologues $\text{RR}'\text{EBH}_2\cdot\text{NMe}_3$ (E = As, Sb) are not suitable for thermolysis, lowering the activation barrier via the addition of a transition metal precatalyst might bring new perspectives to this field. The reactions are to be carried out in stoichiometric ratios with the goal of isolating transient species that also come into play in catalytic reactions or coordination complexes of non-catalytic reactions. Sub stoichiometric amounts of metal complexes in different amounts and varying ambient conditions should be used in case of catalytic activities to get further insight into the ongoing reaction pathway. Proper characterization of the obtained oligomeric or polymeric products is essential for these investigations. The release of a free oligomer or polymer would represent a new class of catalytic polymerization reaction of Lewis base stabilized pnictogenylboranes. Reaction with active precatalysts for oligomerization/polymerization reactions includes:

- Stoichiometric reactions with the goal of isolating coordination products (including transient species) and characterization of the obtained products.
- Substoichiometric reactions applying different reaction conditions to get further insight into the ongoing reaction pathway.
- Characterization of possible oligomeric and polymeric products.
- Evaluation of the substrate scope and synthesis of new starting materials.

Not all reactions of transition metal complexes with pnictogenylboranes lead to an oligomerization or polymerization of the group 13/15 compounds. Coordination towards transition metal centers is a first step in the coordination chemistry of pnictogenylboranes and can result in complexes with intriguing properties. Lewis base stabilized pnictogenylboranes $R_2EBH_2 \cdot NMe_3$ ($E = P, As$; $R = H, alkyl, aryl$) are special phosphines and arsines: they are good σ -donors, they feature an electropositive $BH_2 \cdot NMe_3$ substituent and the sterical and electronical environment can be easily controlled through the variation of the organic substituents. Moreover, the parent compounds $H_2EBH_2 \cdot NMe_3$ ($E = P, As$) can be used as special primary phosphine or arsine ligands respectively, which are much less common than their fully organic substituted derivatives. Coordination to a metal center can result in complexes that are unprecedented with such small, primary ligands, especially for $H_2AsBH_2 \cdot NMe_3$. The newly obtained complexes might feature interesting properties and will be thoroughly characterized. The influence of the heavier pnictogen atoms P, As and Sb will be determined by the comparison to the widely used N- and P-based ligands. Additionally, the influence of the unusual boranyl group $BH_2 \cdot NMe_3$ will be estimated by comparing the results to more common organic substituents. Since coordination towards Lewis acids is an important step in many reactions of pnictogenylboranes, this can help in better understanding and predicting the outcome of future experiments.

Preface

The following chapter has been compiled for future publication.

Authors

Jens Braese, Vincent Annibale, Rüdiger Beckhaus, Ian Manners and Manfred Scheer

Author contributions

The syntheses and characterization of compounds **2a-e**, **2g**, **2h** were performed by Jens Braese. Compounds **2f** and **2i** were synthesized by Dr. Oliver Hegen (Universität Regensburg). Subsequent polymerization reactions were performed by Jens Braese. Compound **1** was a donation by Prof. Dr. Rüdiger Beckhaus (Universität Oldenburg). The characterization of the polymeric materials was performed by Jens Braese (NMR spectroscopy, DLS) and Dr. Vincent Annibale (ESI-MS, GPC; University of Bristol).

The manuscript (including supporting information, figures, schemes and graphical abstract) was written by Jens Braese.

3 The Polymerization of Phosphinoborane by Titanium Complexes

Abstract: Reaction of Lewis base stabilized phosphinoborane monomer $t\text{BuHPBH}_2\text{NMe}_3$ (**2a**) with catalytic amounts of bis(η^5 : η^1 -adamantylidenepentafulvene)titanium (**1**) provide a convenient new route to polyphosphinoboranes $[\text{tBuPH-BH}_2]_n$ (**3a**). This method offers access to high molecular mass materials under mild conditions and short reaction times. It represents an unprecedented example of a transition-metal mediated polymerization of Lewis base stabilized Group 13/15 compounds. For this reaction a variety of different monomers of the type $\text{RR}'\text{EBH}_2\text{NMe}_3$ ($\text{E} = \text{P}, \text{As}$; $\text{R/R}' = \text{H}, \text{alkyl}, \text{aryl}$) has been tested.

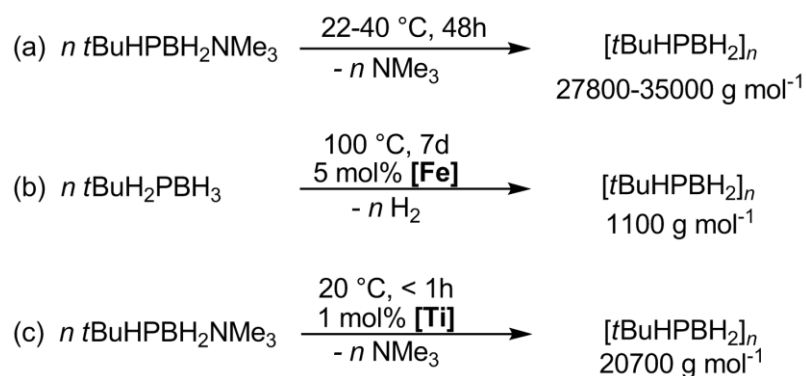
3.1 Introduction

Inorganic polymers, based on main-group elements other than carbon, provide attractive materials with specific uses as elastomers, lithographic resistant layers, biomaterials, polyelectrolytes, ceramic precursors and in optoelectronics.^[1] The inorganic monomers for polymerization reactions are comparable to their organic analogues. Ammonia borane H_3NBH_3 can be regarded as an ethane analogue. It is in the focus of current studies due to its high hydrogen content.^[2] Recently, a progress in the regeneration of the dehydrogenated polymeric residue was achieved.^[3] The metal induced polymerization is comprehensively studied.^[4] The heavier homologue H_3PBH_3 is very labile even at low temperatures, but nonetheless has been reported to give a polymer in dehydrocondensation reactions catalysed by $\text{B}(\text{C}_6\text{F}_5)_3$.^[5] Poly(phosphinoboranes) $[\text{RHP-BH}_2]_n$ have been prepared over the past decade as high-molar-mass materials by rhodium- and iron-catalyzed dehydrocoupling reactions of primary phosphine-boranes.^[6] Catalytic dehydrocoupling-routes have relied on the electron-withdrawing effect of the aryl groups on the phosphorus to promote the reaction since the P-H bonds are essentially nonpolar. This limits the substrate scope, with only very special examples of generated poly(alkylphosphinoborane)s^[6c,e] with modest molecular masses compared to other poly(phosphinoborane)s. Following the carbon analogue comparison, the inorganic BN congener of ethylene would be aminoborane H_2NBH_2 , which has been isolated under cryogenic conditions.^[7] The heavier homologue H_2PBH_2 does not exist and was not obtained even by matrix-isolation techniques.^[8] But it can be stabilized by Lewis bases to give monomeric phosphinoboranes such as

$\text{H}_2\text{PBH}_2\text{NMe}_3$.^[9] Moreover, a variety of organic substituted derivatives^[10] and heavier Group 15 elements derivatives have been synthesized over the years.^[11]

3.2 Results and Discussion

Reactions with $[\text{Cp}_2\text{Ti}(\text{btmsa})]$ (btmsa = bis(trimethylsilyl)acetylene) have shown that $\text{H}_2\text{PBH}_2\text{NMe}_3$ is an excellent ethylene-like monomer for the stepwise aggregation to form oligomers that are stabilized in the coordination sphere of titanium complexes.^[12] These phosphinoborane chains are a result of the loss of the stabilizing NMe_3 entity, leading to a head-to-tail aggregation, as well as to an additional P-P coupling via dehydrocoupling due to the achieved P-H activation. Furthermore, the mild metal-free thermolysis of the derivative $t\text{BuHPBH}_2\text{NMe}_3$ leads to a transient free phosphinoborane $t\text{BuHPBH}_2$ via elimination of the initially stabilizing Lewis base. Subsequent head-to-tail polymerization results in high molecular mass poly(alkylphosphinoborane)s,^[10b] which are hard to access via catalytic dehydrocoupling reactions due to the unpolar P-H bonds (Scheme 1). Several attempts to use late transition metal complexes to initiate a polymerization reaction have not been successful,^[9,13] thus a transition metal mediated polymerization of Lewis base stabilized phosphanylboranes is unknown so far. Consequently, the quest for a metal mediated polymerization of Lewis base stabilized pnictogenylboranes at low temperature to yield high molecular mass polymers without cross links was still open. Moreover, some of the heavier homologues $\text{H}_2\text{EBH}_2\text{-NMe}_3$ (E = As, Sb) are not suitable for thermolysis, therefore lowering the activation barrier via addition of a transition metal catalysis might bring new perspectives to this field. We chose an $\eta^5:\eta^1$ -pentafulvene titanium complex due to its similarities to titanocene but showing flexible reactivity. They are known for E-H bond activations under mild conditions and also for insertion reactions of polar multiple bond substrates,^[14] which might influence the molecular mass or size distribution of resulting polymers.



Scheme 1. Comparison of different routes to poly(*tert*-butylphosphino)boranes]. a) metal free thermolysis, b) dehydrocoupling using $[\text{Fe}] = [\text{Cp}(\text{CO})_2\text{Fe}(\text{OSO}_2\text{CF}_3)]$, c) new route using $[\text{Ti}] = [(\eta^5:\eta^1\text{-C}_5\text{H}_4\text{C}_{10}\text{H}_{14})_2\text{Ti}]$ (**1**).

Preliminary experiments showed a polymerization reaction of *t*BuHPBH₂NMe₃ (**2a**) takes place in the presence of 5 mol% of the sterically encumbered bis(η^5 : η^1 -adamantylidenepentafulvene)titanium (**1**) in toluene at room temperature (Scheme 1c). Full conversion to the polymer [*t*BuPH-BH₂]_{*n*} (**3a**) was observed within 30 minutes, detected by ¹H, ¹¹B, and ³¹P NMR spectroscopy, featuring a release of the stabilizing Lewis base by observing free NMe₃. The ³¹P{¹H} NMR spectrum of the polymer **3a**, which was isolated by precipitation into acetonitrile, showed a set of three broad signals at $\delta = -19, -22$ and -24 ppm, similar to the polymer reported previously.^[10b] In the ³¹P NMR spectrum, further broadening and splitting into poorly defined doublets was observed. A very broad signal at $\delta = -38$ ppm was found in ¹¹B{¹H} NMR spectrum. While the total conversion of the monomer **2a** happens much faster and at lower temperatures than the metal free polymerization reaction (48h at 40 °C), however the molecular weight of polymer **3a** was lower ($M_n = 5511$ g mol⁻¹, PDI = 2.0, PDI = polydispersity index).

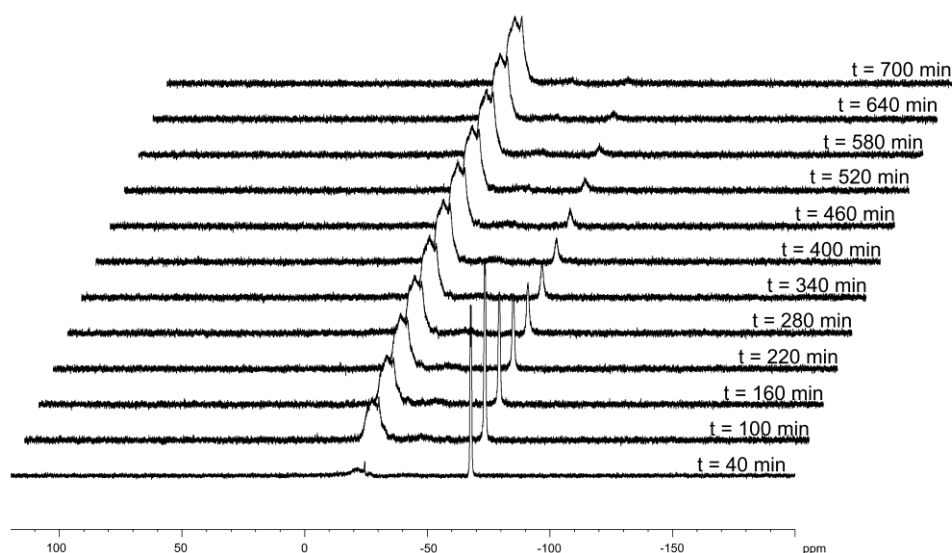


Figure 1. ³¹P{¹H} NMR Spectra of the reaction of **2a** with 5 mol% [(η^5 : η^1 -C₅H₄C₁₀H₁₄)₂Ti] (**1**) at 0 °C. $\delta = -67.6$ ppm: *t*BuHP-BH₂NMe₃, $\delta = -16.0 - 32.0$ ppm: [*t*BuHP-BH₂]_{*n*}.

By lowering the load of the catalyst to only 1 mol% of **1**, the conversion of *t*BuHPBH₂NMe₃ (**2a**) proceeds quantitatively at room temperature to higher molecular mass polymer ($M_n = 20732$ g mol⁻¹, $M_w = 44937$ g mol⁻¹, PDI = 2.2). Samples from this method were analyzed by DLS at optimized concentrations in CH₂Cl₂. The value of R_h of 4.95 nm corresponds to a molar mass of 35400 g mol⁻¹ for monodisperse polystyrene samples in THF,^[15] confirming the presence of higher molecular weight polymer obtained by lower catalyst concentrations. Even lower catalyst loadings presumably lead to a competitive reaction between the catalyzed polymerization and the metal free polymerization reaction, as reaction times progressively approach the values of the

uncatalyzed reaction. Experiments with significant higher amounts than 5 mol% of **1** show the presence of unreacted starting material **1** in the ^1H NMR spectra. To evaluate the influence of the titanium complex on the polymerization reaction, we conducted the experiments at different temperatures. With 5 mol% of **1** at 40 °C, the same temperature as metal free polymerization reaction, the observed molecular mass of the polymer was still significant lower ($M_n = 3902 \text{ g mol}^{-1}$, PDI = 2.3). At 0 °C, no conversion of the monomer **2a** is observed without the help of the metal complex. The addition of 5 mol% of **1** at 0 °C gives a slowed down polymerization reaction with full conversion to the polymer **3a** within 20h, giving the definite proof of the enhancing influence of the metal complex on the polymerization reaction as well as a reasonable time scale for multinuclear NMR spectroscopy experiments.

Monitoring the reaction between $t\text{BuHPBH}_2\text{NMe}_3$ (**2a**) and 5 mol% of bisfulvene titanium complex (**1**) at 0 °C by ^1H and $^{31}\text{P}\{^1\text{H}\}$ NMR spectroscopy shows the consumption of the monomer (**2a**) and the release of an equivalent amount of free NMe_3 as well as the formation of the polymer $[\text{tBuPH-BH}_2]_n$ (**3a**) over the course of 20h (Figure 1 and 2). Figure 1 shows the decline of the relative sharp signal of the monomer at $\delta = -67.6 \text{ ppm}$ in the $^{31}\text{P}\{^1\text{H}\}$ NMR spectra and the growth of the broad, structured signal for the polymer at about $\delta = -20 \text{ ppm}$. The decline of the stabilizing Lewis base NMe_3 in $t\text{BuHPBH}_2\text{NMe}_3$ and the appearance of free NMe_3 in the ^1H NMR spectra over the time gives a first idea of the involved kinetics. The natural logarithm of the monomer concentration versus time can be fitted linearly, suggesting first order kinetics of the reaction in respect to the monomer concentration with a reaction rate constant $k = 0.00318 \text{ s}^{-1}$ at 0 °C (Figure 2).

The resulting polymers were also studied by ESI-MS in the positive ion mode with CH_2Cl_2 as solvent (Figure 3 and 4). The observed m/z is around 4000 for all samples, showing the limitation for molecular weight determination in such polyphosphinoboranes. ESI-MS from the metal free polymer showed m/z up to 2000, while GPC analysis shows a molecular mass up to 35000 g mol^{-1} .^[10b] These limitations are also known for polyaminoboranes.^[4d,16] The mass spectroscopy analysis for **2** shows a degree of polymerization up to 47 ($\sim 4800 \text{ g mol}^{-1}$). Three product distributions were identified, two major distributions corresponding to linear material $[\text{H}(\text{tBuHPBH}_2)_n\text{NMe}_3]^+$ and $[\text{Me}_3\text{NBH}_2(\text{tBuHPBH}_2)_n\text{NMe}_3]^+$ and a minor distribution for which best matches $[\text{H}(\text{tBuHPBH}_2)_n\text{PH}_2\text{tBu}]^+$ (Figure 3). All detected repeating units of are of $m/z = 102$ and show the release of $t\text{BuHPBH}_2$ (Figure 4).

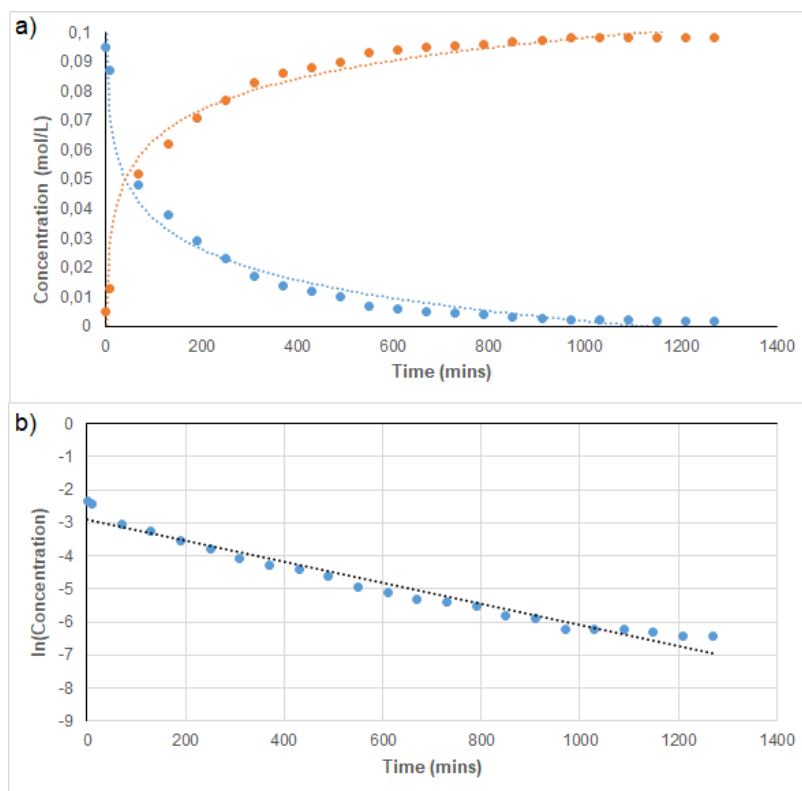


Figure 2. a) Plot of the consumption of monomer **2a** (blue)/ release of free NMe₃ (orange) in time using 5 mol% [(η^5 : η^1 -C₅H₄C₁₀H₁₄)₂Ti] (**1**) at 0 °C. b) natural logarithm of the monomer concentration; linear fit for a first order reaction with reaction rate constant of $k = 0.00318 \text{ s}^{-1}$ at 0 °C.

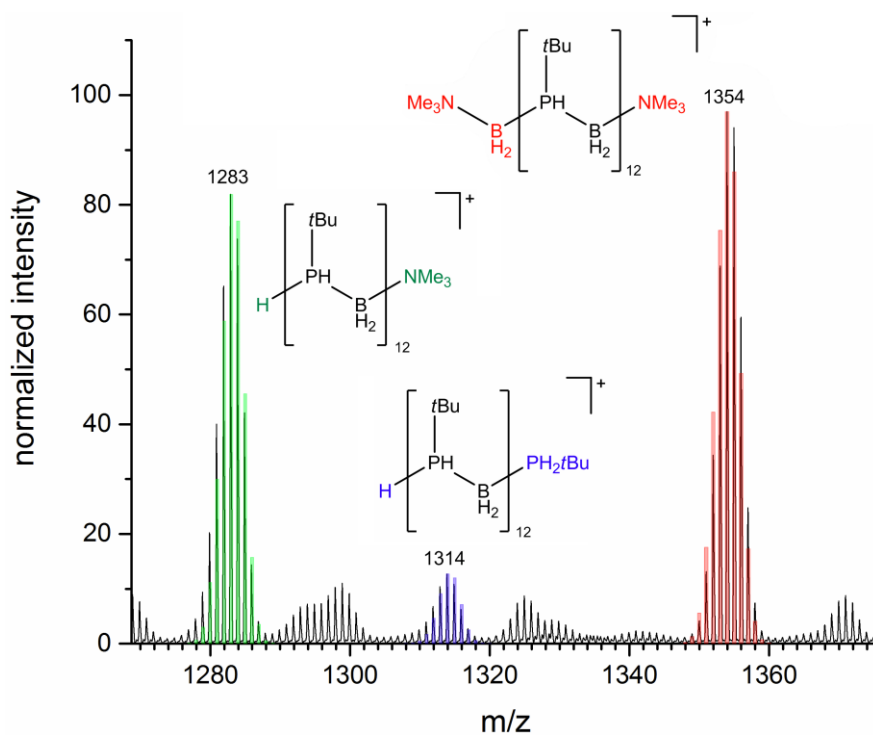


Figure 3. ESI-MS of polyphosphinoborane (**3a**) from reaction with 5 mol% [(η^5 : η^1 -C₅H₄C₁₀H₁₄)₂Ti] (**1**) at 0 °C, showing three different possible end groups.

In order to get more insight into the polymerization pathway and the scope of substrates, we tested the reactivity of different substituted phosphanylboranes towards bis(η^5 : η^1 -adamantylidenepentafulvene)titanium (**1**). Following adjusted procedures of our group,^[10,11] RR'EBH₂NMe₃ (**2a**: E = P, R = H, R' = *t*Bu; **2b**: E = P, R = R' = H; **2c**: E = P, R = H, R' = Me; **2d**: E = P, R = H, R' = *n*Pr; **2e**: E = P, R = H, R' = *n*Hex; **2f**: E = P, R = Me, R' = *t*Bu; **2g**: E = P, R = R' = Ph, **2h**: E = As, R = R' = H; **2i**: E = As, R = H, R' = *t*Bu) have been synthesized and were reacted with 5 mol % of **1** at room temperature. The sterical hinderance of the monomer, the electron density on the phosphorus atom

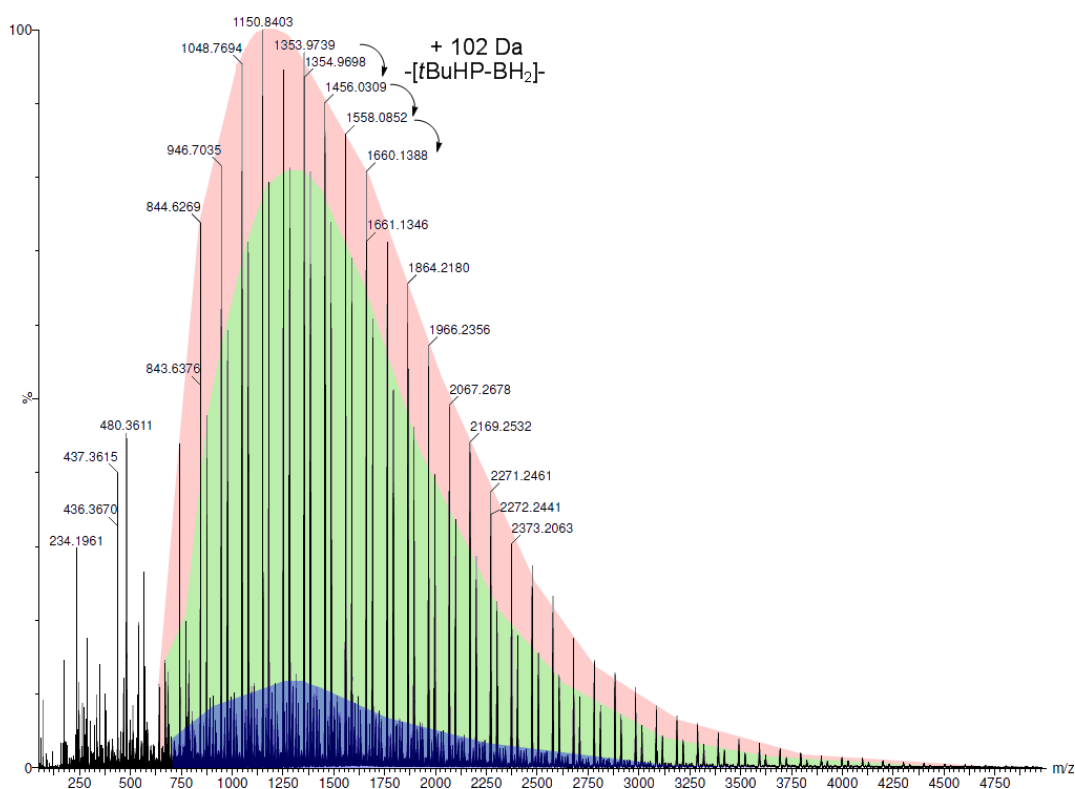
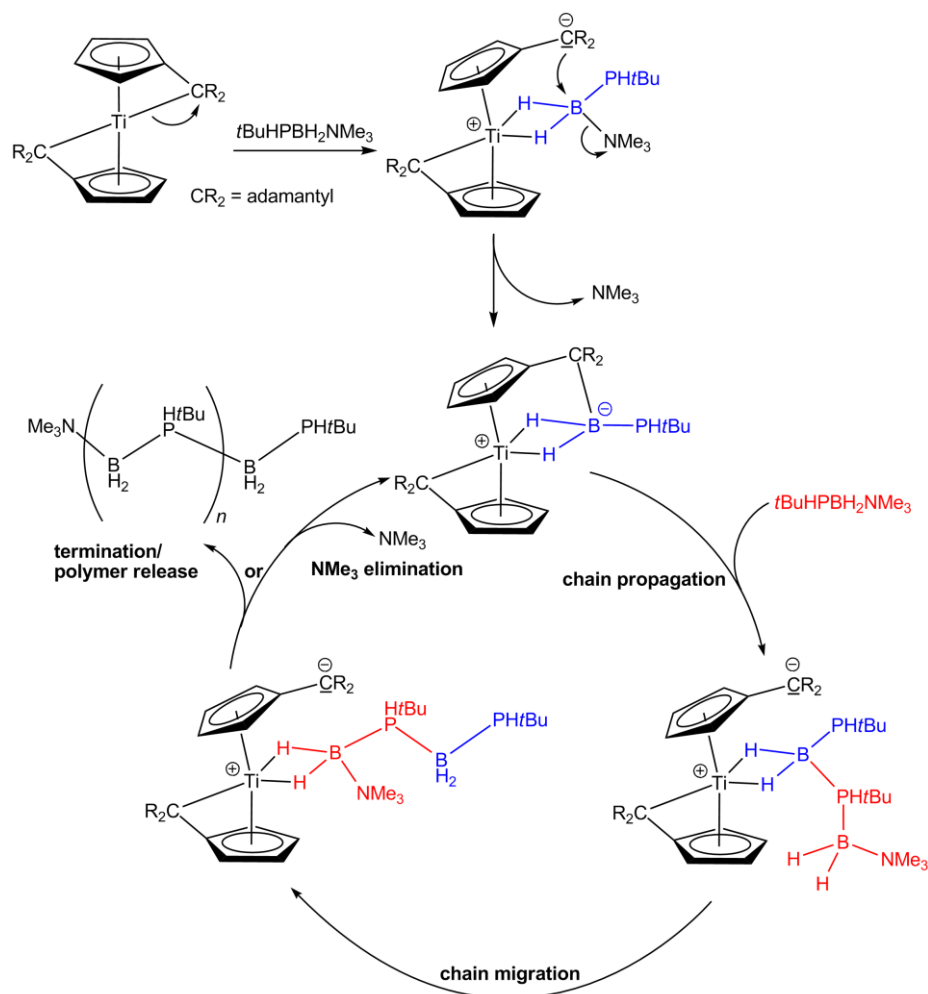


Figure 4. ESI-MS of polyphosphinoborane (**3a**) from reaction with 5 mol% [(η^5 : η^1 -C₅H₄C₁₀H₁₄)₂Ti] (**1**) at 0 °C, showing distributions of the three possible end groups. Mass increase by 102 Da corresponds to one *t*BuHP-BH₂ unit.

as well as the solubility of the resulting polymer are key factors for the formation for polyphosphinoboranes^[10] and can be recognized in these reactions as well. The sterically encumbered catalyst **1** is already very well soluble in unpolar solvents. The polymerization from the monosubstituted *t*BuHPBH₂NMe₃ (**2a**) to polymer [*t*BuPH-BH₂]_{*n*} (**3a**) works best, while reactions with *n*PrHPBH₂NMe₃ (**2d**) and *n*HexHPBH₂NMe₃ (**2e**) show signals for oligomeric and polymeric product species in the ¹H, ¹¹B, and ³¹P NMR spectra.^[17] MeHPBH₂NMe₃ (**2c**), *t*BuMePBH₂NMe₃ (**2f**) and Ph₂PBH₂NMe₃ (**2g**) don't show any reactivity towards **1** at room temperature, neither do the arsenic derivatives H₂AsBH₂NMe₃ (**2h**) and *t*BuHAsBH₂NMe₃ (**2i**). H₂PBH₂NMe₃ (**2b**) shows a completely

different reaction pathway including formation of paramagnetic coordination complexes that have not yet been doubtlessly identified, but no polymerization reactions takes place.^[17] Therefore, we assume that the substrate has to be sterically hindered at the phosphorus atom, as it is the case for monoalkylated substrates, so that a P-Ti bond formation as in the reaction with $\text{H}_2\text{PBH}_2\text{NMe}_3$ (**2b**) is prevented, but also has to be not that bulky as in **2f-g**. The electron density on the group 15 atom is of importance as well, as we see no reaction on substrates **2c** and **2g-2i** with comparably low electron density on the P or As atom. Good solubility increases the molar mass due to prevention of premature precipitation of the polymer. These findings were used for the consideration of the reaction pathway. We discovered that the oligomerization of $\text{H}_2\text{PBH}_2\text{NMe}_3$ (**2b**) on $[\text{Cp}_2\text{Ti}]$ fragments include the formation of B-Ti and B-H \cdots Ti bonds,^[12] so does the oligomerization of aminoboranes.^[18] Since we observed that sterical hinderance is beneficial and prevents P-Ti bond formation, we propose that the first step involves a B-H \cdots Ti interaction and thereby the fixation of the first monomer on the metal center. The exo carbon can subsequently assist in the elimination of the stabilizing Lewis base NMe_3 ,



Scheme 2. Proposed catalytic cycle for the chain-growth coordination polymerization of **2a** (scheme showing one insertion event).

lowering the reaction barrier for the chain propagation (Scheme 2). Computational studies show that the hydrogen atoms on the terminal BH₂ group next to the NMe₃ are more electronegative than hydrogens on the BH₂ moiety between two *t*BuHP groups,^[19] so a chain migration is likely to happen. This step can be followed up once again by NMe₃ elimination for further chain growth or by a termination step and release of the free polymer later in the cycle. While additional experiments as well as more detailed computational studies are necessary to verify this mechanism, the current model fits the present data, presenting a first order chain growth mechanism.

3.3 Conclusion

In summary, we report the first example of a transition-metal mediated polymerization of a Lewis base stabilized Group 13/15 compound. The reaction appears to be homogenous in nature, presumably via a chain-growth coordination-polymerization mechanism. While the metal free polymerization of *t*BuHPBH₂NMe₃ provides a higher molecular mass of the resulting polymer, the addition of bis(η⁵:η¹-adamantylidenepentafulvene)titanium offers a much faster generation of the polymer and allows working at milder reaction conditions for a wider substrate scope. These discoveries will stimulate future developments of the field of inorganic main group polymers.

3.4 References

- [1] a) M. Liang, I. Manners, *J. Am. Chem. Soc.* **1991**, *113*, 4044-4045; b) H. R. Allcock, *Chem. Mater.* **1994**, *6*, 1476-1491; c) C. H. Honeyman, I. Manners, C. T. Morrissey, H. R. Allcock, *J. Am. Chem. Soc.* **1995**, *117*, 7035-7036; d) R. D. Archer, *Inorganic and Organometallic Polymers*, Wiley-VCH, New York, **2001**; e) I. Manners, *Angew. Chem. Int. Ed.* **1996**, *35*, 1602-1621; f) S. J. Clarson, J. A. Semlyen, *Siloxane Polymers*, Prentice Hall, Englewood Cliffs, **1993**; g) R. H. Neilson, P. Wisian-Neilson, *Chem. Rev.* **1988**, *88*, 541-562; h) R. D. Miller, J. Michl, *Chem. Rev.* **1989**, *89*, 1359-1410; i) R. De Jaeger, M. Gleria, *Prog. Polym. Sci.* **1998**, *23*, 179-276; j) R. West, *J. Organomet. Chem.* **1986**, *300*, 327-346; k) T. Imori, V. Lu, H. Cai, T. D. Tilley, *J. Am. Chem. Soc.* **1995**, *117*, 9931-9940; l) X. He, T. Baumgartner, *RSC Adv.* **2013**, *3*, 11334-11350; m) S. Wilfert, H. Henke, W. Schoefberger, O. Brüggemann, I. Teasdale, *Macromol. Rapid Commun.* **2014**, *35*, 1135-1141; n) W. Cao, Y. Gu, M. Meineck, T. Li, H. Xu, *J. Am. Chem. Soc.* **2014**, *136*, 5132-5137; o) F. Choffat, S. Käser, P. Wolfer, D. Schmid, R. Mezzenga, P. Smith, W. Caseri, *Macromolecules* **2007**, *40*, 7878-7889; p) J. Linshoef, E. J. Baum, A. Hussain, P. J. Gates, C. Näther, A. Staubitz, *Angew. Chem. Int. Ed.* **2014**, *53*, 12916-12920; q) B. W. Rawe, C. P. Chun, D. P. Gates, *Chem. Sci.* **2014**, *5*, 4928-4938; r) P. J. Fazen, J. S. Beck, A. T. Lynch, E. E. Remsen, L. G. Sneddon, *Chem. Mater.* **1990**, *2*, 96-97; s) F. Jäkle, *Chem. Rev.* **2010**, *110*, 3985-4022; t) H. Kutz, F. Cheng, S. Schwedler, L. Böhling, A. Brockhinke, L. Weber, K.

- Parab, F. Jäkle, *ACS Macro Lett.* **2012**, *1*, 555-559; u) Z. M. Hudson, D. J. Lunn, M. A. Winnik, I. Manners, *Nat. Commun.* **2014**, *5*, 3372; v) A. Lorbach, M. Bolte, H. Li, H.-W. Lerner, M. C. Holthausen, F. Jäkle, M. Wagner, *Angew. Chem. Int. Ed.* **2009**, *48*, 4584-4588; w) A. Hübner, Z.-W. Qu, U. Englert, M. Bolte, H.-W. Lerner, M. C. Holthausen, M. Wagner, *J. Am. Chem. Soc.* **2011**, *133*, 4596-4609; x) G. Zhang, G. M. Palmer, M. W. Dewhirst, C. L. Fraser, *Nat. Mater.* **2009**, *8*, 747-751.
- [2] a) Z. Liu, T. B. Marder, *Angew. Chem.* **2008**, *120*, 248-250; b) V. Pons, R. T. Baker, *Angew. Chem. Int. Ed.* **2008**, *47*, 9600-9602; c) F. H. Stephens, V. Pons, R. T. Baker, *Dalton Trans.* **2007**, 2613-2626; d) G. Alcaraz, S. Sabo-Etienne; *Angew. Chem. Int. Ed.* **2010**, *49*, 7170-7179; e) M. E. Sloan, A. Staubitz, T. J. Clark, C. A. Russell, G. C. Lloyd-Jones, I. Manners, *J. Am. Chem. Soc.* **2010**, *132*, 3831-3841; f) A. Staubitz, A. P. M. Robertson, I. Manners, *Chem. Rev.* **2010**, *110*, 4023-4078.
- [3] a) L. Winner, W. C. Ewing, K. Geetharani, T. Dellermann, B. Jouppi, T. Kupfer, M. Schäfer, H. Braunschweig, *Angew. Chem. Int. Ed.* **2018**, *57*, 12275-12279; b) C. Reller, F. O. R. L. Mertens, *Angew. Chem. Int. Ed.* **2012**, *51*, 11731-11735; c) B. L. Davis, D. A. Dixon, E. B. Garner, J. C. Gordon, M. H. Matus, B. Scott, F. H. Stephens, *Angew. Chem. Int. Ed.* **2009**, *48*, 6812-6816; d) A. D. Sutton, A. K. Burrell, D. A. Dixon, E. B. Garner III, J. C. Gordon, T. Nakagawa, K. C. Ott, J. P. Robinson, M. Vasiliu, *Science* **2011**, *331*, 1426-1429; e) A. P. M. Robertson, E. M. Leitao, I. Manners, *J. Am. Chem. Soc.* **2011**, *133*, 19322-19325; e) E. M. Leitao, N. E. Stubbs, A. P. M. Robertson, H. Helten, R. J. Cox, G. C. Lloyd-Jones, I. Manners, *J. Am. Chem. Soc.* **2012**, *134*, 16805-16816; f) P. Paetzold, *Adv. Inorg. Chem.* **1987**, *31*, 123-170.
- [4] a) A. Staubitz, A. Presa Soto, I. Manners, *Angew. Chem. Int. Ed.* **2008**, *47*, 6212-6215; b) J. R. Vance, A. P. M. Robertson, K. Lee, I. Manners, *Chem. Eur. J.* **2011**, *17*, 4099-4103; c) R. Dallanegra, A. P. M. Robertson, A. B. Chaplin, I. Manners, A. S. Weller, *Chem. Commun.* **2011**, *47*, 3763-3765; d) A. Staubitz, M. E. Sloan, A. P. M. Robertson, A. Friedrich, S. Schneider, P. J. Gates, J. Schmedt auf der Günne, I. Manners, *J. Am. Chem. Soc.* **2010**, *132*, 13332-13345; e) B. L. Dietrich, K. I. Goldberg, D. M. Heinekey, T. Autrey, J. C. Linehan, *Inorg. Chem.* **2008**, *47*, 8583-8585; f) H. C. Johnson, A. P. M. Robertson, A. B. Chaplin, L. J. Sewell, A. L. Thompson, M. F. Haddow, I. Manners, A. S. J. Weller, *J. Am. Chem. Soc.* **2011**, *133*, 11076-11079.
- [5] J.-M. Denis, H. Forintos, H. Szelke, L. Toupet, T.-N. Pham, P.-J. Madec, A.-C. Gaumontz, *Chem. Commun.* **2003**, 54-55.
- [6] a) H. Dorn, R. A. Singh, J. A. Massey, A. J. Lough, I. Manners, *Angew. Chem. Int. Ed.* **1999**, *38*, 3321-3323; b) H. Dorn, R. A. Singh, J. A. Massey, J. M. Nelson, C. A. Jaska, A. J. Lough, I. Manners, *J. Am. Chem. Soc.* **2000**, *122*, 6669-6678; c) H. Dorn, J. M. Rodezno, B. Brunnhöfer, E. Rivard, J. A. Massey, I. Manners, *Macromolecules* **2003**, *36*, 291-297; d) T. J. Clark, J. M. Rodezno, S. B. Clendenning, S. Aouba, P. M. Brodersen, A. J. Lough, H. E. Ruda, I. Manners, *Chem. Eur. J.* **2005**, *11*, 4526-4534; e) S. Pandey, P. Lönnecke, E. Hey-Hawkins, *Eur. J. Inorg. Chem.* **2014**, 2456-2465; f) D. Jacquemin, C. Lambert, E. A. Perpète, *Macromolecules* **2004**, *37*, 1009-1015; g) A. Schäfer, T. Jurca, J. Turner, J. R. Vance, K. Lee, V. A. Du, M. F. Haddow, G. R. Whittell, I. Manners, *Angew. Chem. Int. Ed.* **2015**, *54*, 4836-4841.
- [7] C. T. Kwon, H. A. Jr. McGee, *Inorg. Chem.* **1970**, *9*, 2458-2461.
- [8] Only theoretical calculations give insight into the bonding situation of such monomers: a) T. L. Allen, W. H. Fink, *Inorg. Chem.* **1992**, *31*, 1703-1705; b) T. L. Allen, A. C. Scheiner, H. F. Schaefer III, *Inorg. Chem.* **1990**, *29*, 1930-1936; c) M. B. Coolidge, W. T. Borden, *J. Am. Chem. Soc.* **1990**, *112*, 1704-1706; d) H.-J. Himmel, *Dalton Trans.* **2003**, 3639-3649; e) H.-J. Himmel, *Eur. J. Inorg. Chem.* **2003**, 2153-2163.

- [9] K.-C. Schwan, A. Timoshkin, M. Zabel, M. Scheer, *Chem. Eur. J.* **2006**, *12*, 4900-4908; for the precursor compounds cf.: U. Vogel, P. Hoemensch, K.-C. Schwan, A. Y. Timoshkin, M. Scheer, *Chem. Eur. J.* **2003**, *9*, 515-519.
- [10] a) A. Stauber, T. Jurca, C. Marquardt, M. Fleischmann, M. Seidl, G. R. Whittell, I. Manners, M. Scheer, *Eur. J. Inorg. Chem.* **2016**, 2684-2687; b) C. Marquardt, T. Jurca, K.-C. Schwan, A. Stauber, A. V. Virovets, G. R. Whittell, I. Manners, M. Scheer, *Angew. Chem. Int. Ed.* **2015**, *54*, 13782-13786.
- [11] C. Marquardt, A. Adolf, A. Stauber, M. Bodensteiner, A. V. Virovets, A. Y. Timoshkin, M. Scheer, *Chem. Eur. J.* **2013**, *19*, 11887-11891; C. Marquardt, O. Hegen, M. Hautmann, G. Balázs, M. Bodensteiner, A. V. Virovets, A. Y. Timoshkin, M. Scheer, *Angew. Chem. Int. Ed.* **2015**, *54*, 13122-13125.
- [12] C. Thoms, C. Marquardt, M. Bodensteiner, M. Scheer, *Angew. Chem. Int. Ed.* **2013**, *52*, 5150-5154.
- [13] a) U. Vogel, K.-C. Schwan, P. Hoemensch, M. Scheer, *Eur. J. Inorg. Chem.* **2005**, *8*, 1453-1458; b) K. Schwan, A. Adolf, M. Bodensteiner, M. Zabel, M. Scheer, *Z. Anorg. Allg. Chem.* **2008**, *634*, 1383-1387; c) J. Braese, A. Schinabeck, M. Bodensteiner, H. Yersin, A. Y. Timoshkin, M. Scheer, *Chem. Eur. J.* **2018**, *24*, 10073-10077.
- [14] a) T. Oswald, T. Gelert, C. Lasar, M. Schmidtman, T. Klüner, R. Beckhaus, *Angew. Chem. Int. Ed.* **2017**, *56*, 12297-12301; b) T. Oswald, M. Diekmann, A. Frey, M. Schmidtman, R. Beckhaus, *Acta Crystallogr. Sect. E* **2017**, *73*, 691-693; c) M. Manßen, I. Töben, C. Kahrs, J.-H. Bölte, M. Schmidtman, R. Beckhaus, *Organometallics* **2017**, *36*, 2973-2981; d) M. Manßen, N. Lauterbach, T. Woriescheck, M. Schmidtman, R. Beckhaus, *Organometallics* **2017**, *36*, 867-876; e) M. Manßen, C. Kahrs, I. Töben, J.-H. Bölte, M. Schmidtman, R. Beckhaus, *Chem. Eur. J.* **2017**, *23*, 15827-15833; f) C. Adler, M. Diekmann, M. Schmidtman, R. Beckhaus, *Z. Anorg. Allg. Chem.* **2017**, *643*, 732-735; g) M. Manßen, N. Lauterbach, J. Dörfler, M. Schmidtman, W. Saak, S. Doye, R. Beckhaus, *Angew. Chem. Int. Ed.* **2015**, *54*, 4383-4387.
- [15] L. J. Fetters, N. Hadjichristidis, J. S. Lindner, J. W. Mays, *J. Phys. Chem. Ref. Data* **1994**, *23*, 619-640.
- [16] A. L. Colebatch, B. W. Hawkey Gilder, G. R. Whittell, N. L. Oldroyd, I. Manners, A. S. Weller, *Chem. Eur. J.* **2018**, *24*, 5450-5455.
- [17] See Supporting Information, section 3.5.2.
- [18] a) H. Helten, B. Dutta, J. R. Vance, M. E. Sloan, M. F. Haddow, S. Sproules, D. Collison, G. R. Whittell, G. C. Lloyd-Jones, I. Manners, *Angew. Chem. Int. Ed.* **2013**, *52*, 437-440; b) O. J. Metters, S. R. Flynn, C. K. Dowds, H. A. Sparkes, I. Manners, D. F. Wass, *ACS Catal.* **2016**, *6*, 6601-6611.
- [19] see Supporting Information, section 3.5.6.

3.5 Supporting Information

3.5.1 Synthetic Procedures

All manipulations, except stated otherwise, were performed under an atmosphere of dry argon using standard glovebox and Schlenk techniques. All solvents are degassed and purified by standard procedures.

The compounds $[(\eta^5:\eta^1\text{-C}_5\text{H}_4\text{C}_{10}\text{H}_{14})_2\text{Ti}]$ (**1**),^[1] $t\text{BuHPBH}_2\cdot\text{NMe}_3$ (**2a**),^[2] $\text{H}_2\text{PBH}_2\text{NMe}_3$ (**2b**),^[3] $\text{MeHPBH}_2\cdot\text{NMe}_3$ (**2c**),^[4] $\text{Ph}_2\text{PBH}_2\text{NMe}_3$ (**2g**),^[2] $\text{H}_2\text{AsBH}_2\text{NMe}_3$ (**2h**),^[3] were prepared according to literature procedures.

Following the literature procedure for $\text{MeHPBH}_2\cdot\text{NMe}_3$ (**2c**),^[4] $n\text{PrHPBH}_2\cdot\text{NMe}_3$ (**2d**) and $n\text{HexHPBH}_2\cdot\text{NMe}_3$ (**2e**) were prepared. $n\text{PrI}$ and $n\text{HexI}$ respectively were used as a substitute for MeI .

Following the literature procedure for $\text{MeHPBH}_2\cdot\text{NMe}_3$ (**2c**),^[4] $t\text{BuMePBH}_2\cdot\text{NMe}_3$ (**2f**) was prepared. $t\text{BuHPBH}_2\cdot\text{NMe}_3$ was used as a substitute for $\text{H}_2\text{PBH}_2\text{NMe}_3$.

Following the literature procedure for $t\text{BuHPBH}_2\cdot\text{NMe}_3$ (**2a**),^[2] $t\text{BuHAsBH}_2\cdot\text{NMe}_3$ (**2i**) was prepared. $t\text{BuH}_2\text{As}$ ^[5] was used as a substitute for $t\text{BuH}_2\text{P}$.

The NMR spectra were recorded on an Avance 400 spectrometer (^1H : 400.13 MHz, ^{31}P : 161.976 MHz, ^{11}B : 128.378 MHz, $^{13}\text{C}\{^1\text{H}\}$: 100.623 MHz with δ [ppm] referenced to external SiMe_4 (^1H , ^{13}C), H_3PO_4 (^{31}P) or $\text{BF}_3\cdot\text{Et}_2\text{O}$ (^{11}B).

The ESI-MS spectra were obtained using a Waters Synapt G2S instrument equipped with a nanospray ionization module (Advion TriVersa Nanomate). Solutions (40 μL) of approximately 1 mg/mL were loaded under ambient conditions in air into the sample tray, and aliquots of 3 μL were introduced into the spectrometer using a spray voltage of 1.5 kV. Positive and negative ion spectra were recorded at a rate of 1 scan/second and summed to obtain the final spectra.

GPC was performed on a Malvern RI max Gel Permeation Chromatograph, equipped with an automatic sampler, a pump, an injector, and inline degasser. The columns (T5000) were contained within an oven (35 $^\circ\text{C}$) and consisted of styrene/divinyl benzene gels. Sample elution was detected by means of a differential refractometer. THF (Fisher), containing 0.1 wt% $[n\text{Bu}_4\text{N}][\text{Br}]$, was used as the eluent at a flow rate of 1 mL/min. Samples were dissolved in the eluent (2 mg/mL) and filtered with a Ministart SRP15 filter poly(tetrafluoroethylene) membrane of 0.45 μm pore size) before analysis. The

calibration was conducted using monodisperse polystyrene standards obtained from Aldrich. The lowest molecular weight standard used was 2300 Da.

3.5.2 Polymerization Experiments

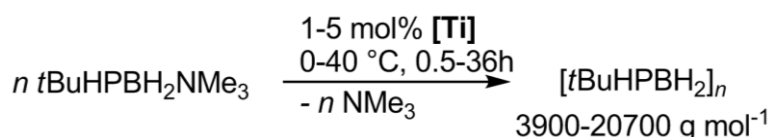
Polymerization of $t\text{BuHPBH}_2\cdot\text{NMe}_3$ (**2a**) to form $[\text{tBuPH-BH}_2]_n$ (**3a**)

Five methods were employed to monitor the influence of temperature, catalyst loading and precipitation on the resulting polymers **P1-P5** of $[\text{tBuPH-BH}_2]_n$ (**3a**):

Table S1: Reaction conditions for the formation of polymer $[\text{tBuPH-BH}_2]_n$ (**3a**): **P1-P5**

	P1	P2	P3	P4	P5
T / °C	0	20	40	20	20
Loading / mol%	5	5	5	5	1
Precipitation	No	No	No	Yes	Yes
Reaction Time / h	36	16	16	16	16

Complete conversion to the polymer happens in less than 30min, except at 0°C, but was stirred regardlessly for 16h.



Scheme 1: Route to $[\text{tBuPH-BH}_2]_n$ (**3a**) using catalytic amounts of $[\text{Ti}] = [(\eta^5\text{-}\eta^1\text{-C}_5\text{H}_4\text{C}_{10}\text{H}_{14})_2\text{Ti}]$ (**1**).

Synthesis of P1-3: A solution of 11 mg (0.025 mmol) $[(\eta^5\text{-}\eta^1\text{-C}_5\text{H}_4\text{C}_{10}\text{H}_{14})_2\text{Ti}]$ (**1**) in 1 mL toluene was added to a stirred solution of 81 mg (0.5 mmol) $t\text{BuHPBH}_2\cdot\text{NMe}_3$ (**2a**) in 5 mL toluene at given temperature. The solution was stirred for 16h (36h for **P1**). After removing all the volatiles under vacuum, NMR spectra in C_6D_6 were carried out.

Synthesis of P4: A solution of 11 mg (0.025 mmol) $[(\eta^5\text{-}\eta^1\text{-C}_5\text{H}_4\text{C}_{10}\text{H}_{14})_2\text{Ti}]$ (**1**) in 1 mL toluene was added to a stirred solution of 81 mg (0.5 mmol) $t\text{BuHPBH}_2\cdot\text{NMe}_3$ (**2a**) in 5 mL toluene. The solution was stirred for 16h. After removing all the volatiles under vacuum, **P4** was dissolved in 1mL of hexane. The viscous solution was added drop wise to vigorously stirred acetonitrile (ca. 50 mL) and a off-white rubber-like solid precipitated.

Synthesis of P5: A solution of 9 mg (0.02 mmol) $[(\eta^5\text{-}\eta^1\text{-C}_5\text{H}_4\text{C}_{10}\text{H}_{14})_2\text{Ti}]$ (**1**) in 1 mL toluene was added to a stirred solution of 322 mg (2 mmol) $t\text{BuHPBH}_2\cdot\text{NMe}_3$ (**2a**) in 5 mL toluene. The solution was stirred for 16h. After removing all the volatiles under vacuum, **P4** was dissolved in 4mL of hexane. The viscous solution was added drop wise to vigorously stirred acetonitrile (ca. 200 mL) and an off-white rubber-like solid precipitated.

Yield:

P1: 41 mg (80%), **P2:** 36 mg (71%), **P3:** 48 mg (94%), **P4:** 20 mg (39%), **P5:** 96 mg (47 %)

NMR shifts for $[t\text{BuPH-BH}_2]_n$ (**3a**, **P1**):

^1H NMR (C_6D_6 , 20°C): δ [ppm] = 0.9 - 1.9 (s, v br, BH_2), 1.35 (s, br, $t\text{Bu}$), 4.06 (d, br, $^1J_{\text{H,P}} = 330$ Hz PH). ^{31}P NMR (C_6D_6 , 20°C): δ [ppm] = -17 to -28 (br, PH). $^{31}\text{P}\{^1\text{H}\}$ NMR (C_6D_6 , 20°C): δ [ppm] = -17 to -28 (br, PH). ^{11}B NMR (C_6D_6 , 20°C): δ [ppm] = -38 (br, BH_2). $^{11}\text{B}\{^1\text{H}\}$ NMR (C_6D_6 , 20°C): δ [ppm] = -38 (br, BH_2). ^{13}C NMR (C_6D_6 , 20°C) δ [ppm] = 29.1 - 27.2 (m, v br, $t\text{Bu}$).

The spectra from all polymerization reactions are shown in section 3.5.3 of the supporting information. The NMR spectra of **P1-P5** are similar to each other and similar to polymer $[t\text{BuPH-BH}_2]_n$ from the metal free polymerization,^[2] although the ratio of the overlapped resonances in the $^{31}\text{P}\{^1\text{H}\}$ NMR spectra differ slightly (Figure S23). The overlapping resonances have previously been assigned to tacticity,^[2] therefore we assume a possible change in tacticity for the transition-metal mediated polymers. Other factors like chain length, branching and different end groups have to be considered as well. Further investigations are underway.

For time dependent NMR spectroscopy, a solution of 2.2 mg (0.005 mmol) $[(\eta^5\text{-}\eta^1\text{-C}_5\text{H}_4\text{C}_{10}\text{H}_{14})_2\text{Ti}]$ (**1**) in 0.4 mL toluene- d_8 at -80 °C was layered inside an NMR tube with a solution of 16 mg (0.1 mmol) $t\text{BuHPBH}_2\cdot\text{NMe}_3$ (**2a**) in 0.4 mL toluene- d_8 at -80 °C. Right before the start of the measurement, the solutions were mixed by vigorous shaking and warmed up to 0 °C inside of the machine, followed by an immediate start of the measurement.

Attempted polymerization of RR'EBH₂NMe₃ (E = P, As; R/R' = H, alkyl, aryl) (2b-i) to form the corresponding polymer [RR'EH-BH₂]_n

*t*BuHPBH₂·NMe₃ (**2a**) in reaction with 1–100 mol% of [(η⁵:η¹-C₅H₄C₁₀H₁₄)₂Ti] (**1**) in organic solvents forms polymer [*t*BuPH-BH₂]_n (**3a**), although the reactions show the presence of unreacted starting material **1** in the ¹H NMR spectra if more than 5 mol% of **1** is used. Therefore, we started the reactions of RR'EBH₂NMe₃ (**2b**: E = P, R = R' = H; **2c**: E = P, R = H, R' = Me; **2d**: E = P, R = H, R' = *n*Pr; **2e**: E = P, R = H, R' = *n*Hex; **2f**: E = P, R = Me, R' = *t*Bu; **2g**: E = P, R = R' = Ph, **2h**: E = As, R = R' = H; **2i**: E = As, R = H, R' = *t*Bu) with substoichiometric amounts of [(η⁵:η¹-C₅H₄C₁₀H₁₄)₂Ti] (**1**), but increased the load of **1** to stoichiometric amounts if no reaction was observed before.

A solution of 2 mmol *n*PrHPBH₂NMe₃ (**2d**) in 1.5 mL C₆D₆ was splitted into two batches. 0.7 mL of the solution was reacted with 15 mg (0.034 mmol) [(η⁵:η¹-C₅H₄C₁₀H₁₄)₂Ti] (**1**) at room temperature. 0.7 mL of the solution without addition of **1** was heated to 40 °C for 48h to compare the transition-metal mediated reaction with the metal free thermolysis. Figure S1 shows the results of these preliminary experiments, showing a fast reaction of the monomeric species in the ³¹P{¹H} NMR spectra at δ = -131 ppm to assumed oligomeric and polymeric species showing broad signals from δ = -70 to -56 ppm and δ = -41 to -36 ppm respectively. These chemical shifts were in the expected region on the basis of previous reports on poly(phosphinoborane) [R¹R²P-BH₂]_n oligomers.^[2,4,6] Metal free thermolysis (40 °C, 48h) leads to identical products, although remarkably slower and in different ratio. The products have to be further characterized.

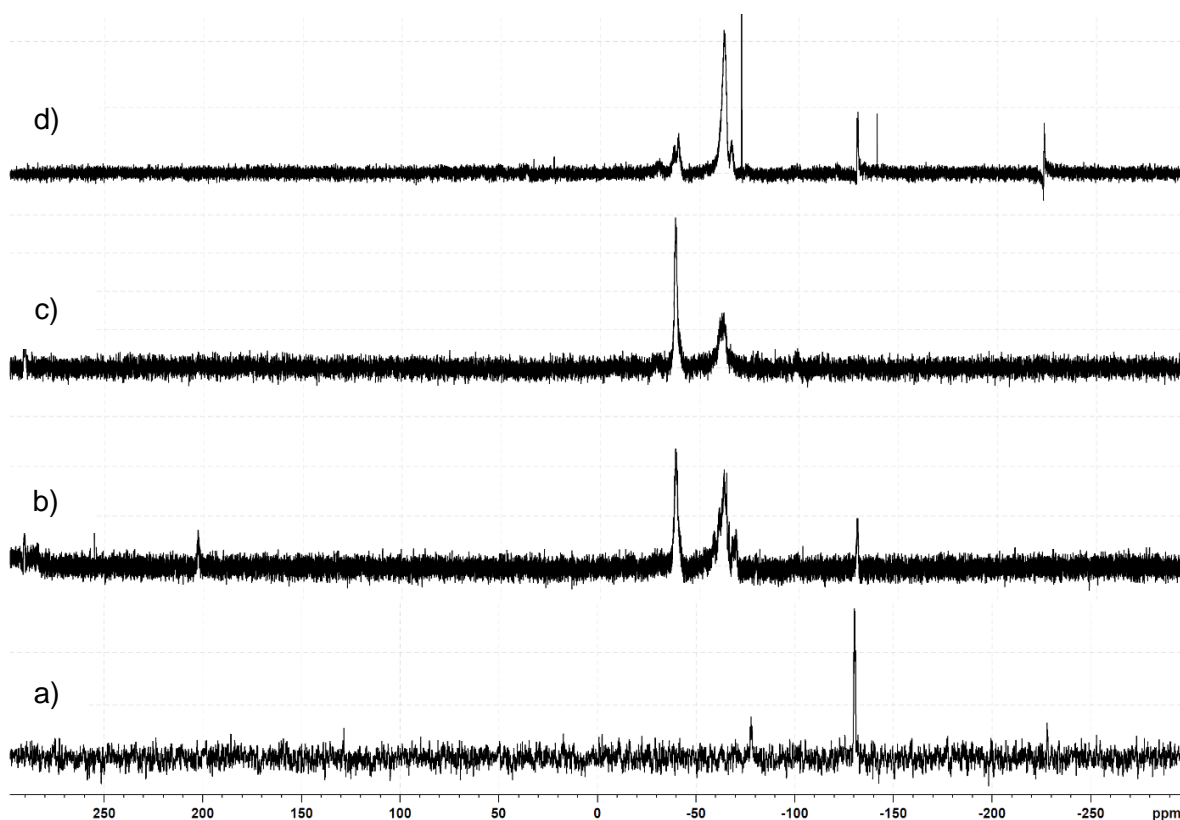


Figure S1: $^{31}\text{P}\{^1\text{H}\}$ NMR spectra of attempted polymerization of $n\text{PrHPBH}_2\text{NMe}_3$ (**2d**) in C_6D_6 . From bottom to top: a) monomeric $n\text{PrHPBH}_2\text{NMe}_3$ (**2d**) b) 30 min after addition of $[(\eta^5\text{-}\eta^1\text{-C}_5\text{H}_4\text{C}_{10}\text{H}_{14})_2\text{Ti}]$ (**1**) c) 48h after addition of **1** d) 48h at 40 °C without addition of **1**.

A solution of 2 mmol of $n\text{HexHPBH}_2\text{NMe}_3$ (**2e**) in 1.5 mL C_6D_6 was splitted into two batches. 0.7 mL of the solution was reacted with 15 mg (0.034 mmol) $[(\eta^5\text{-}\eta^1\text{-C}_5\text{H}_4\text{C}_{10}\text{H}_{14})_2\text{Ti}]$ (**1**) at room temperature. 0.7 mL of the solution without addition of **1** was heated to 40 °C for 48h to compare the transition-metal mediated reaction with the metal free thermolysis. Figure S2 shows the results of these preliminary experiments, showing a fast reaction of the monomeric species in the $^{31}\text{P}\{^1\text{H}\}$ NMR spectra at $\delta = -128$ ppm to assumed oligomeric and polymeric species showing broad signals from $\delta = -67$ to -54 ppm and $\delta = -42$ to -34 ppm respectively. These chemical shifts were in the expected region on the basis of previous reports on poly(phosphinoborane) $[\text{R}^1\text{R}^2\text{P-BH}_2]_n$ oligomers.^[2,4,6] Metal free thermolysis (40 °C, 48h) leads to the same products, although the reaction seems to be less selective and less influenced by the addition of **1** compared to the reaction of $n\text{PrHPBH}_2\text{NMe}_3$ (**2d**) or $t\text{BuHPBH}_2\text{NMe}_3$ (**2a**). The products have to be further characterized.

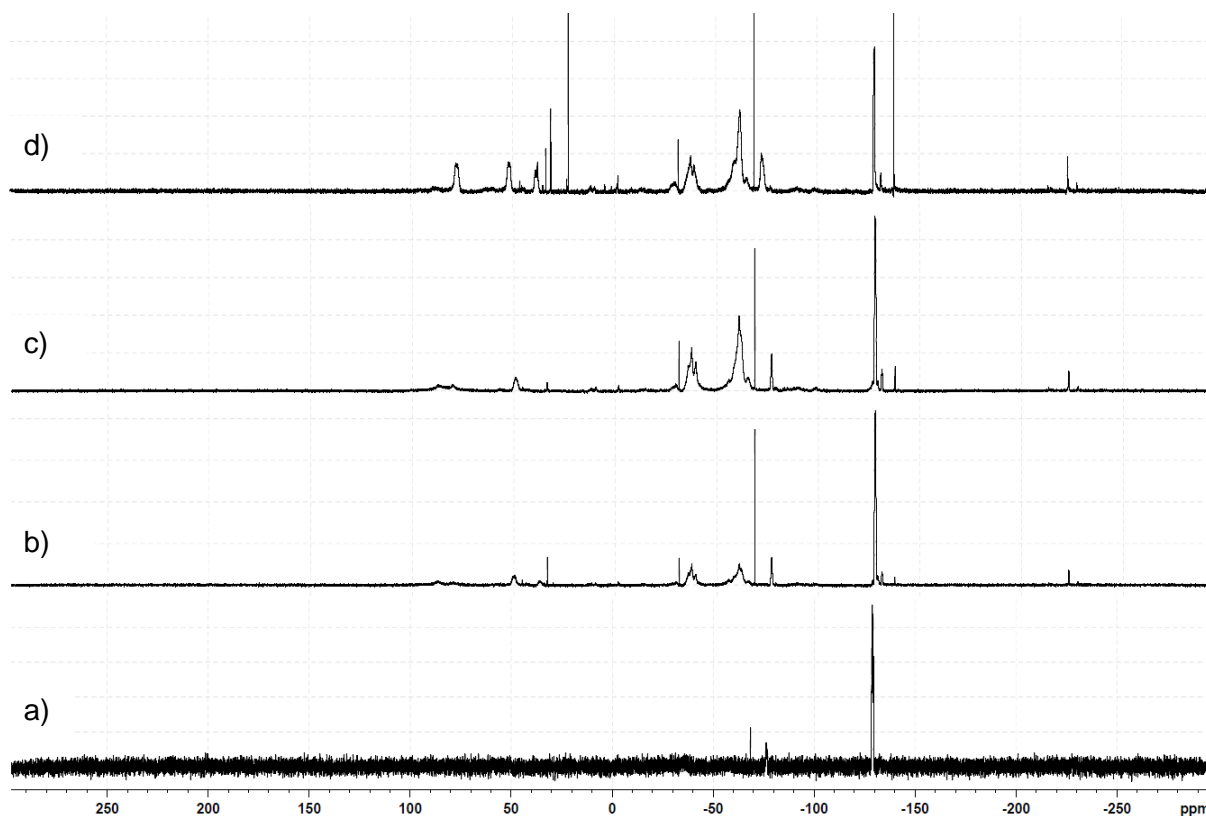


Figure S2: $^{31}\text{P}\{^1\text{H}\}$ NMR spectra of attempted polymerization of $n\text{HexHPBH}_2\text{NMe}_3$ (**2e**) in C_6D_6 . From bottom to top: a) monomeric $n\text{HexHPBH}_2\text{NMe}_3$ (**2e**) b) 30 min after addition of $[(\eta^5:\eta^1\text{-C}_5\text{H}_4\text{C}_{10}\text{H}_{14})_2\text{Ti}]$ (**1**) c) 48h after addition of **1** d) 48h at 40 °C without addition of **1**.

Reaction of $\text{MeHPBH}_2\text{NMe}_3$ (**2c**), $t\text{BuMePBH}_2\text{NMe}_3$ (**2f**), $\text{Ph}_2\text{PBH}_2\text{NMe}_3$ (**2g**), $\text{H}_2\text{AsBH}_2\text{NMe}_3$ (**2h**) and $t\text{BuHAsBH}_2\text{NMe}_3$ (**2i**) with $[(\eta^5:\eta^1\text{-C}_5\text{H}_4\text{C}_{10}\text{H}_{14})_2\text{Ti}]$ (**1**) in organic solvents at room temperature didn't show any reactivity within 48h besides formation of minor amounts of decomposition products.

Reactions of $\text{H}_2\text{PBH}_2\text{NMe}_3$ (**2b**) with substoichiometric amounts of $[(\eta^5:\eta^1\text{-C}_5\text{H}_4\text{C}_{10}\text{H}_{14})_2\text{Ti}]$ (**1**) in toluene at room temperature showed a colour change from blue to orange, while no new signals show in the NMR spectra can be observed. Reactions of one or two equivalents of $\text{H}_2\text{PBH}_2\text{NMe}_3$ (**2b**) with $[(\eta^5:\eta^1\text{-C}_5\text{H}_4\text{C}_{10}\text{H}_{14})_2\text{Ti}]$ (**1**) in toluene show a colour change from blue to red, while no signals can be observed in the ^{11}B and ^{31}P NMR spectra. While isolation and identification of the products failed so far and is an important task for the future, we attribute the behavior of the NMR spectroscopy and the colour change to formation of paramagnetic coordination complexes that yet have to be indubitably characterized. Reaction mixtures are also sensitive to ESR spectroscopy.

3.5.3 NMR spectroscopy

P1

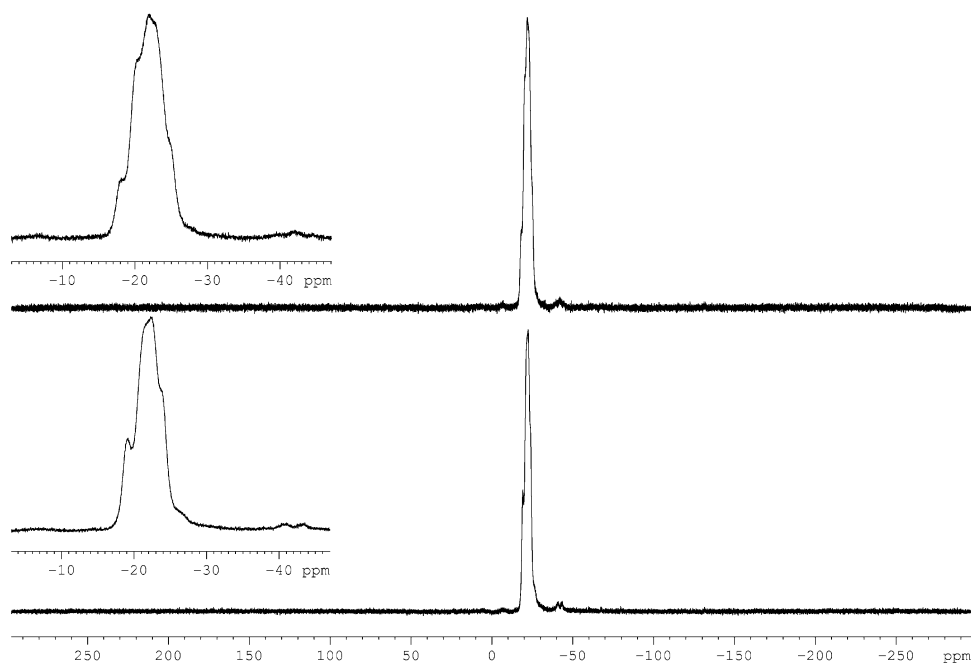


Figure S3: ³¹P (top) and ³¹P{¹H} NMR spectrum (bottom) of P1 in C₆D₆.

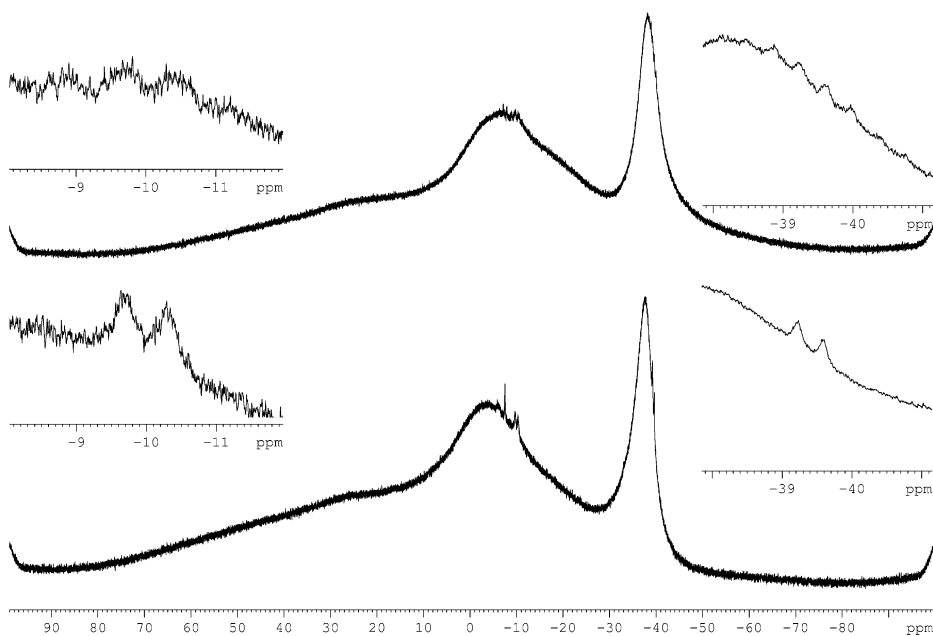


Figure S4: ¹¹B (top) and ¹¹B{¹H} NMR spectrum (bottom) of P1 in C₆D₆.

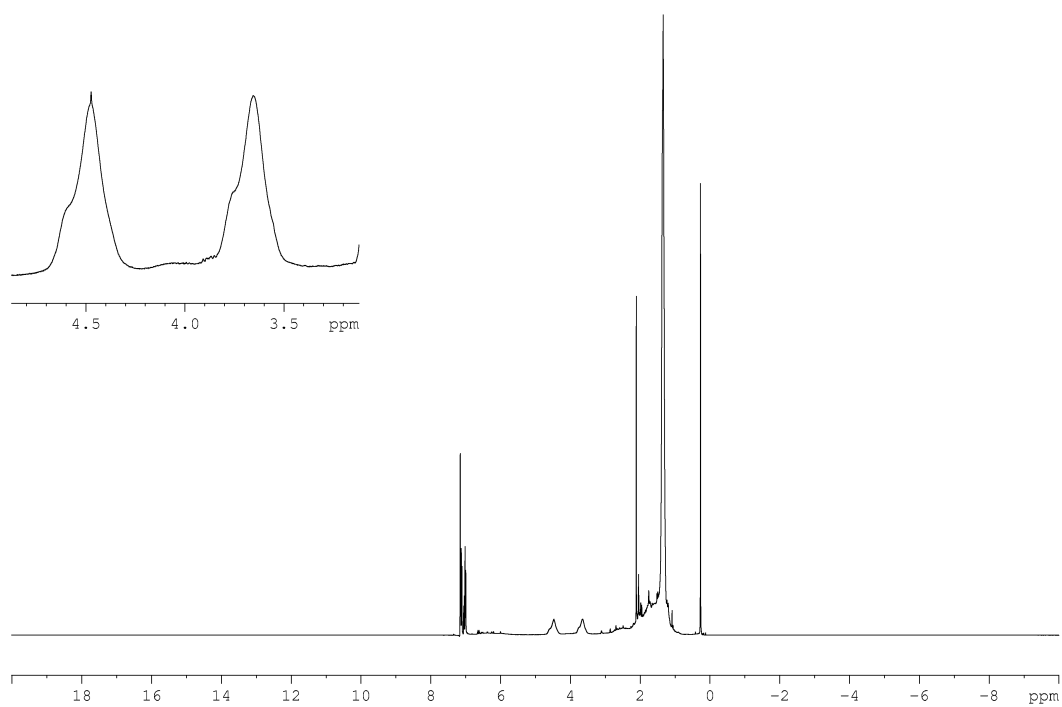


Figure S5: ^1H NMR spectrum of P1 in C_6D_6 .

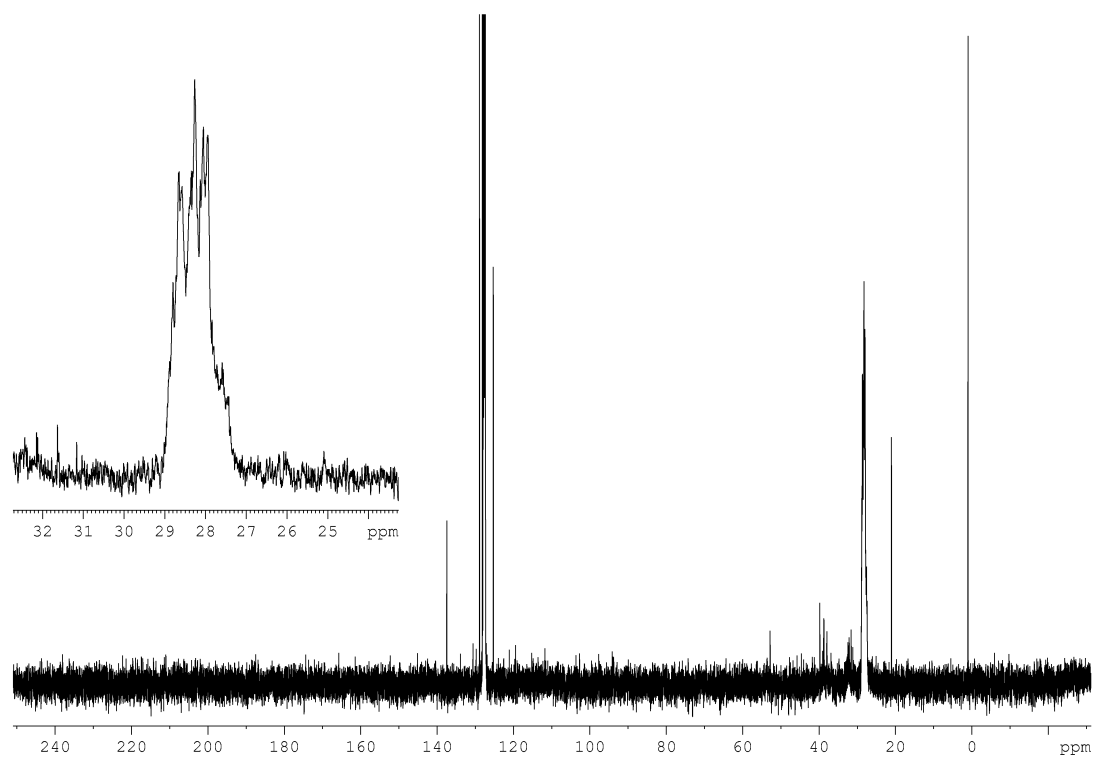


Figure S6: $^{13}\text{C}\{^1\text{H}\}$ NMR spectrum of P1 in C_6D_6 .

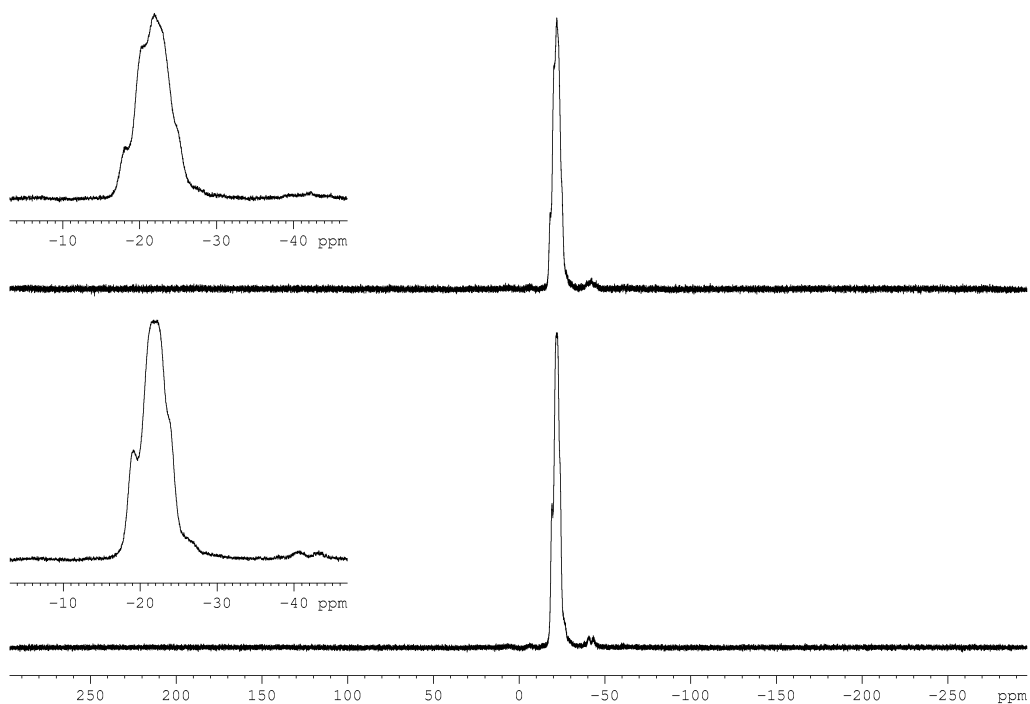
P2

Figure S7: ³¹P (top) and ³¹P{¹H} NMR spectrum (bottom) of **P2** in C₆D₆.

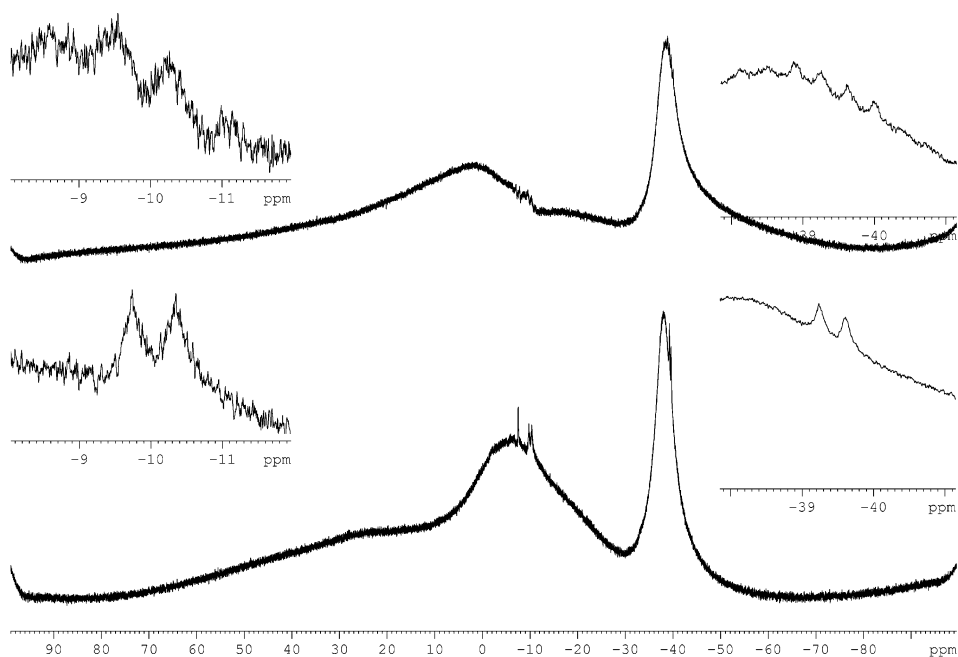


Figure S8: ¹¹B (top) and ¹¹B{¹H} NMR spectrum (bottom) of **P2** in C₆D₆.

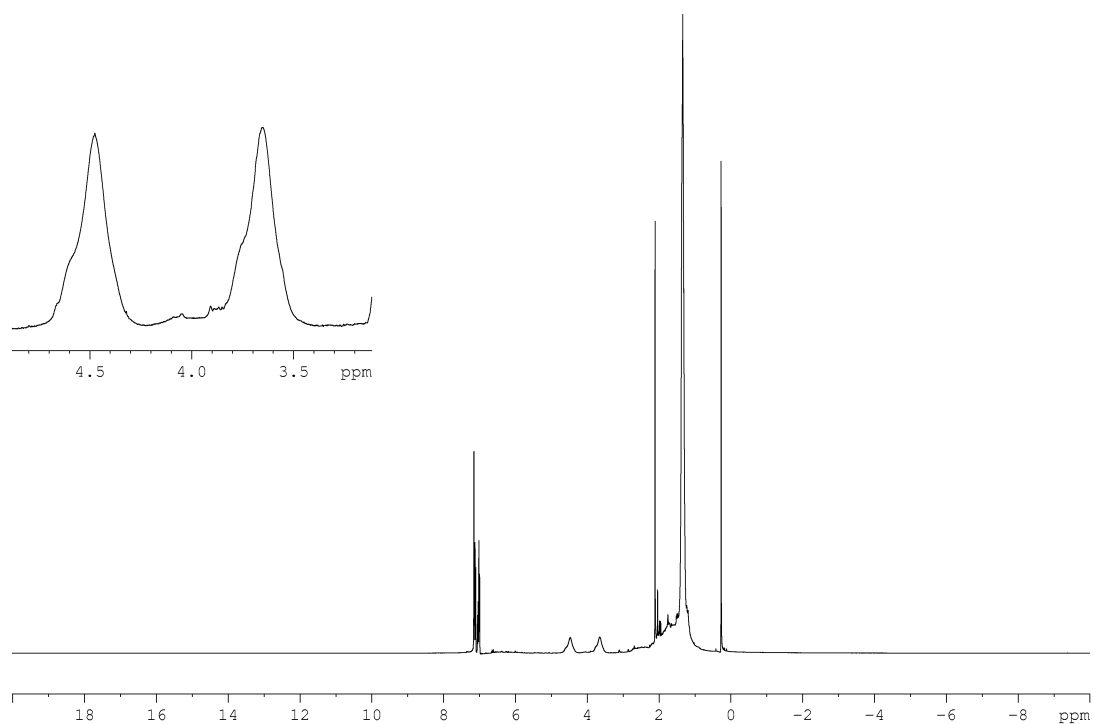


Figure S9: ^1H NMR spectrum of P2 in C_6D_6 .

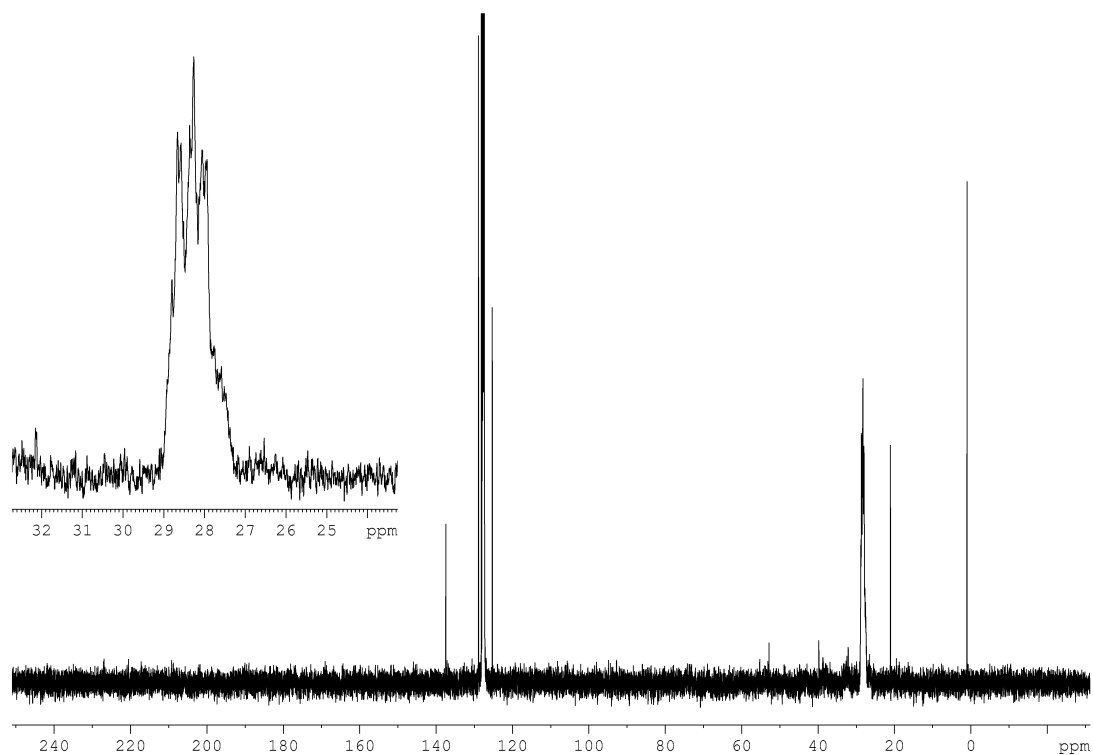


Figure S10: $^{13}\text{C}\{^1\text{H}\}$ NMR spectrum of P2 in C_6D_6 .

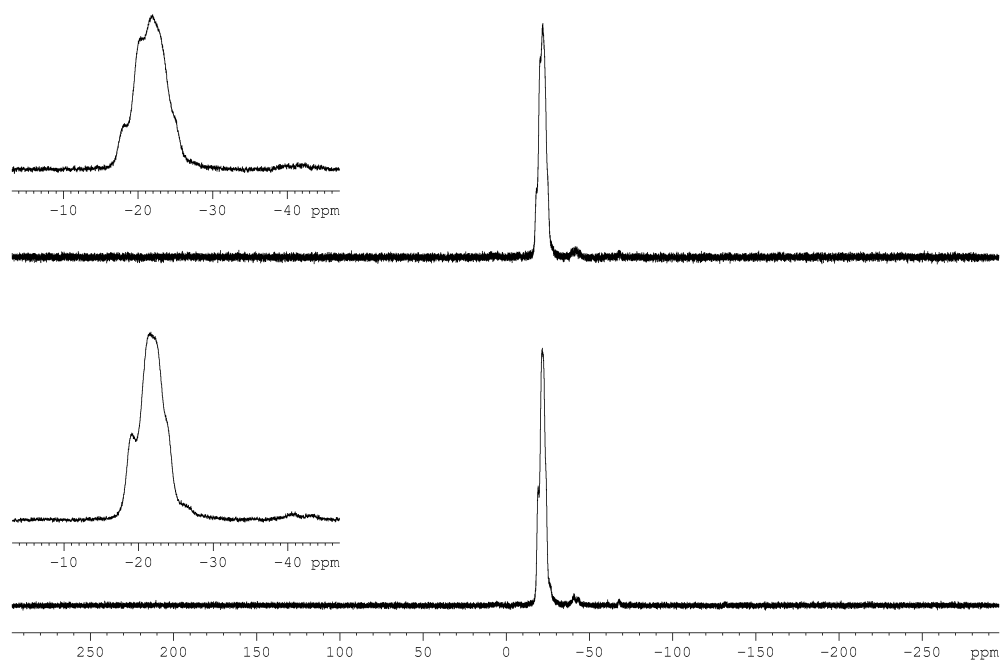
P3

Figure S11: ³¹P (top) and ³¹P{¹H} NMR spectrum (bottom) of P3 in C₆D₆.

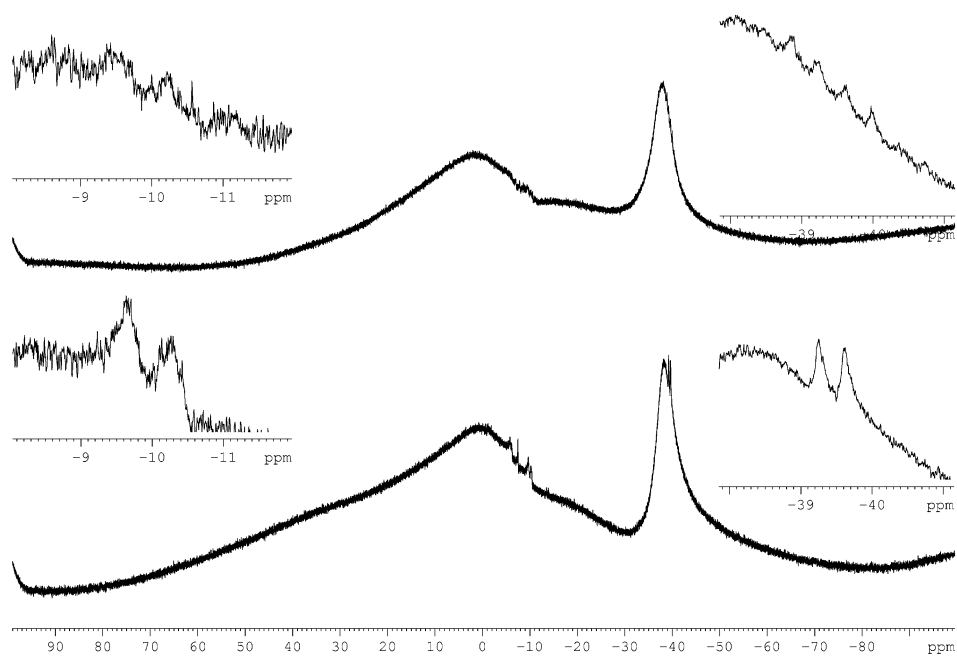


Figure S12: ¹¹B (top) and ¹¹B{¹H} NMR spectrum (bottom) of P3 in C₆D₆.

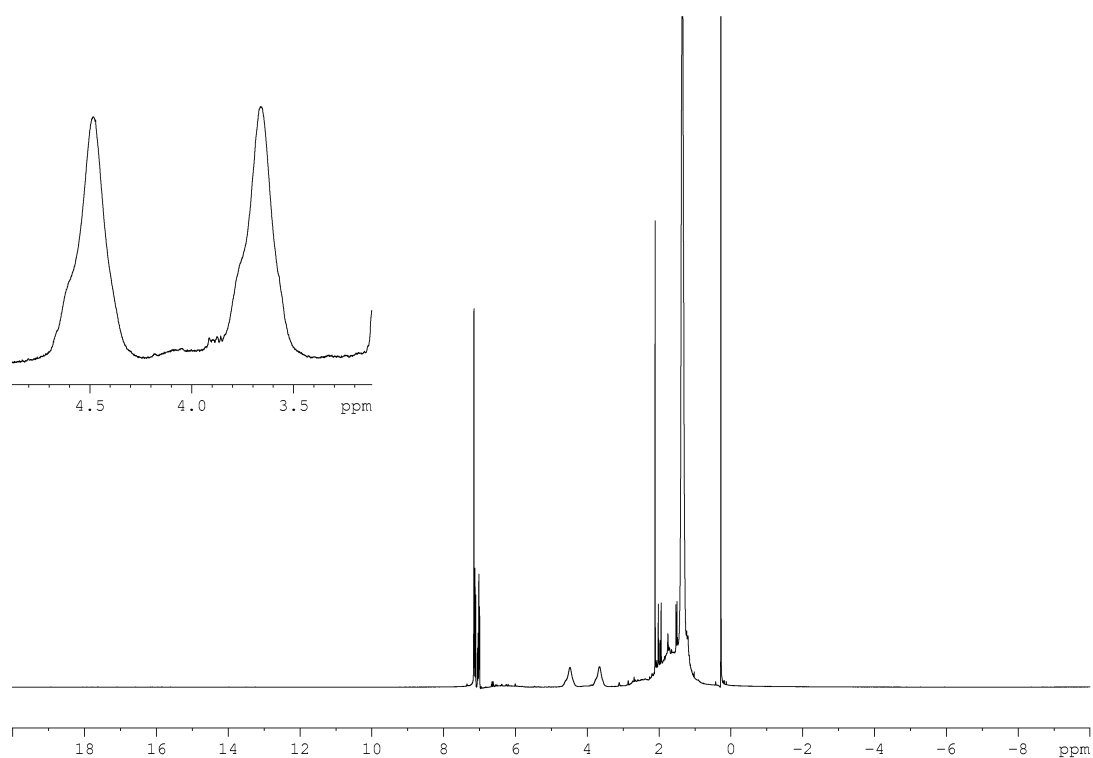


Figure S13: ^1H NMR spectrum of **P3** in C_6D_6 .

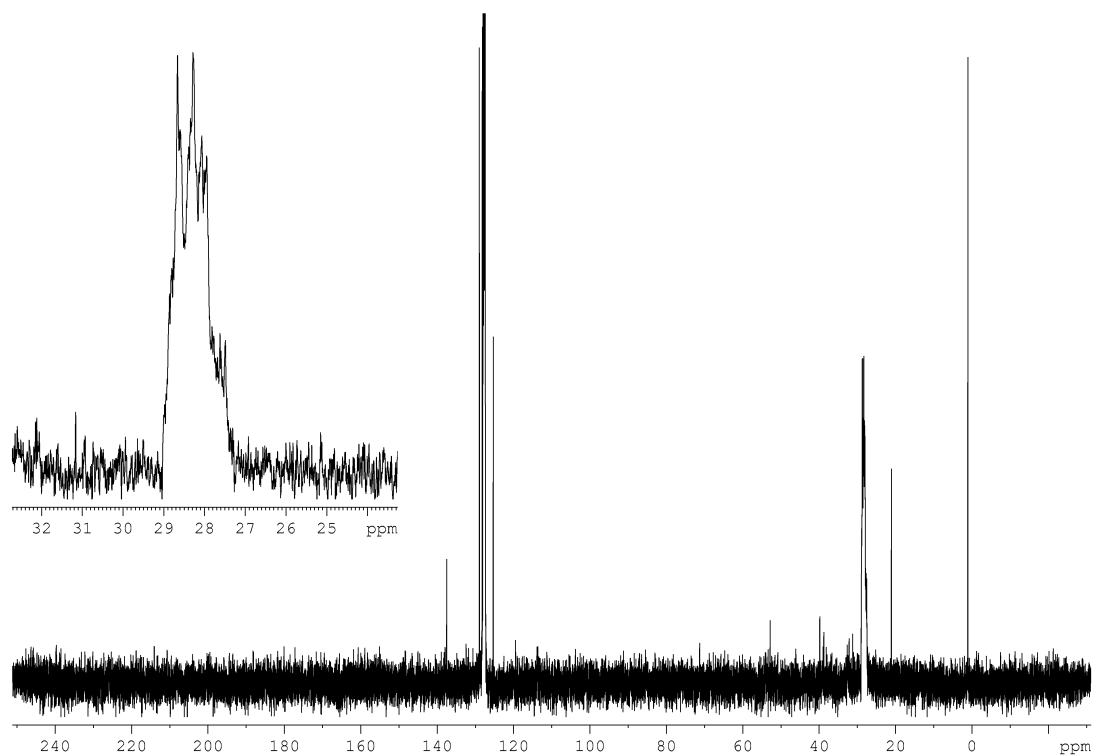


Figure S14: $^{13}\text{C}\{^1\text{H}\}$ NMR spectrum of **P3** in C_6D_6 .

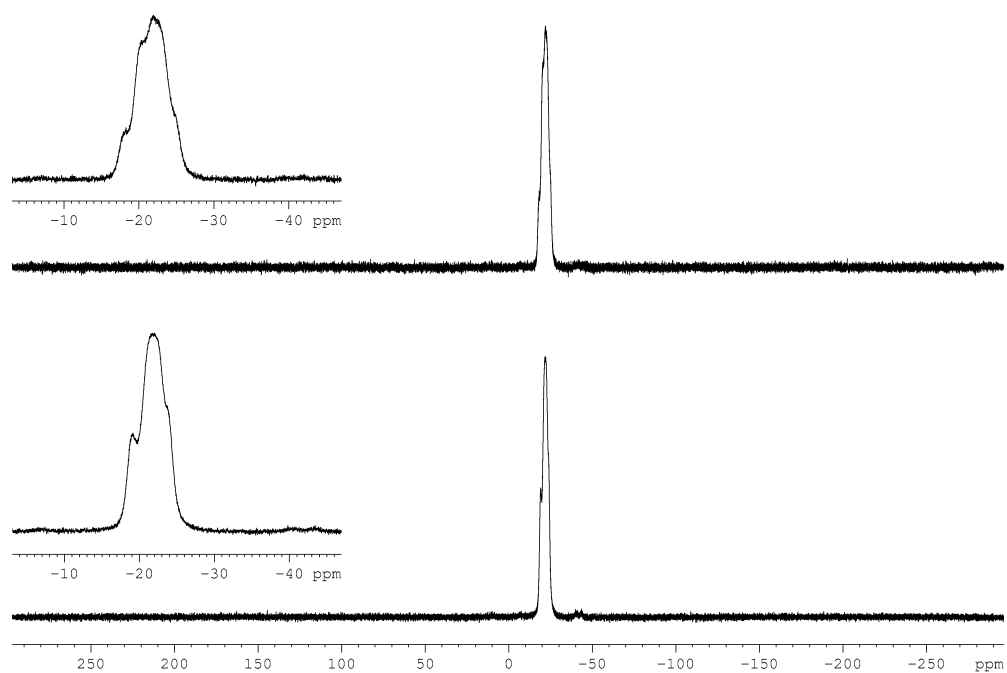
P4

Figure S15: ³¹P (top) and ³¹P{¹H} NMR spectrum (bottom) of **P4** in C₆D₆.

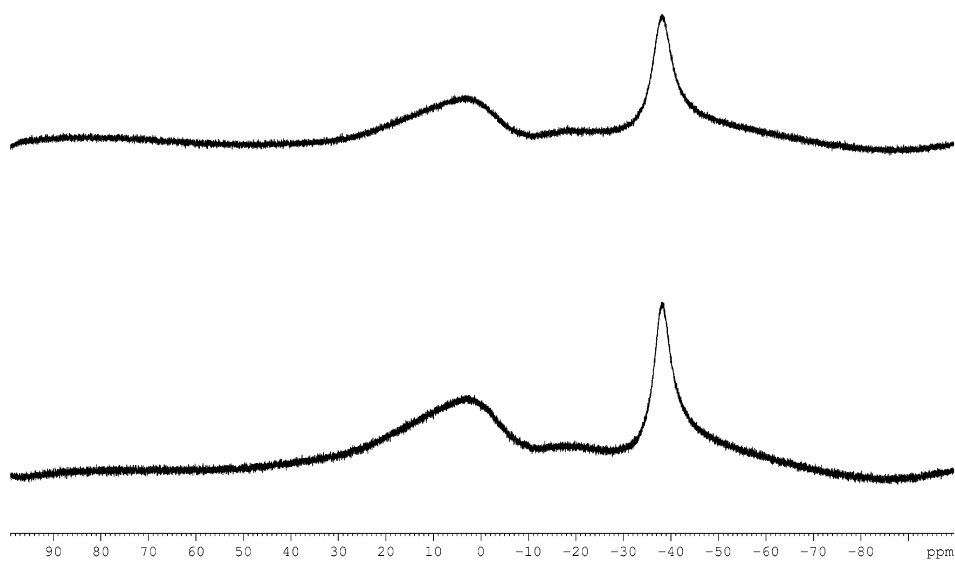


Figure S16: ¹¹B (top) and ¹¹B{¹H} NMR spectrum (bottom) of **P4** in C₆D₆.

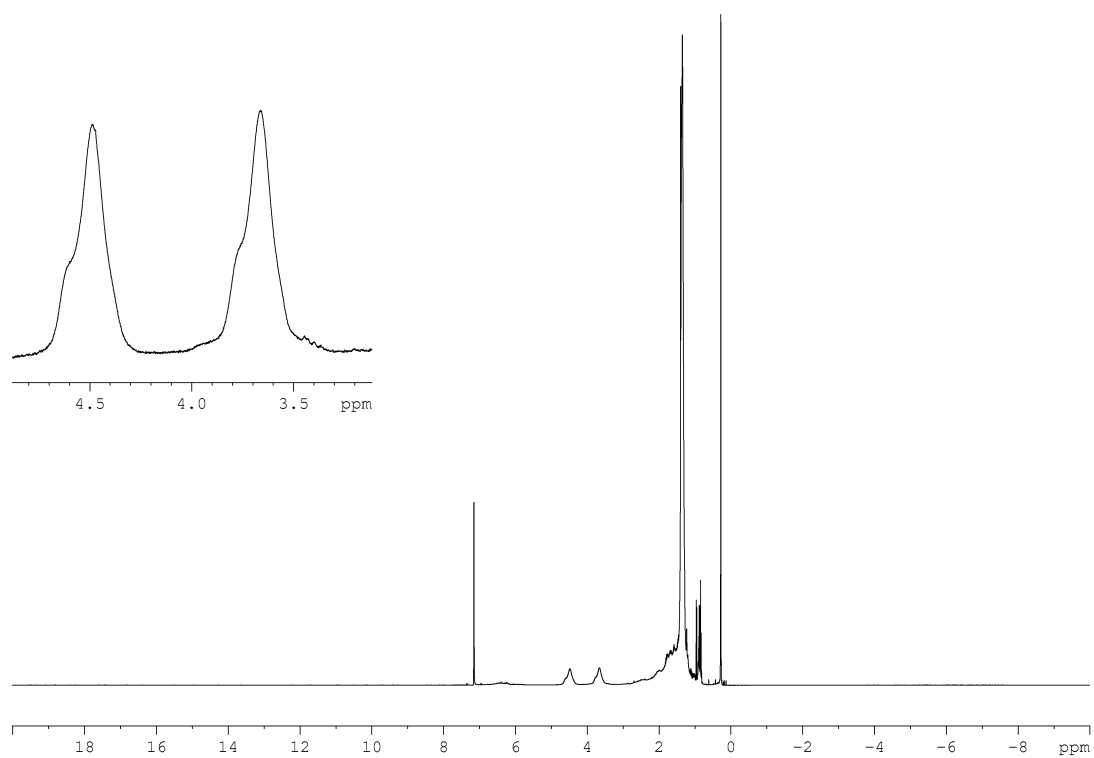


Figure S17: ^1H NMR spectrum of **P4** in C_6D_6 .

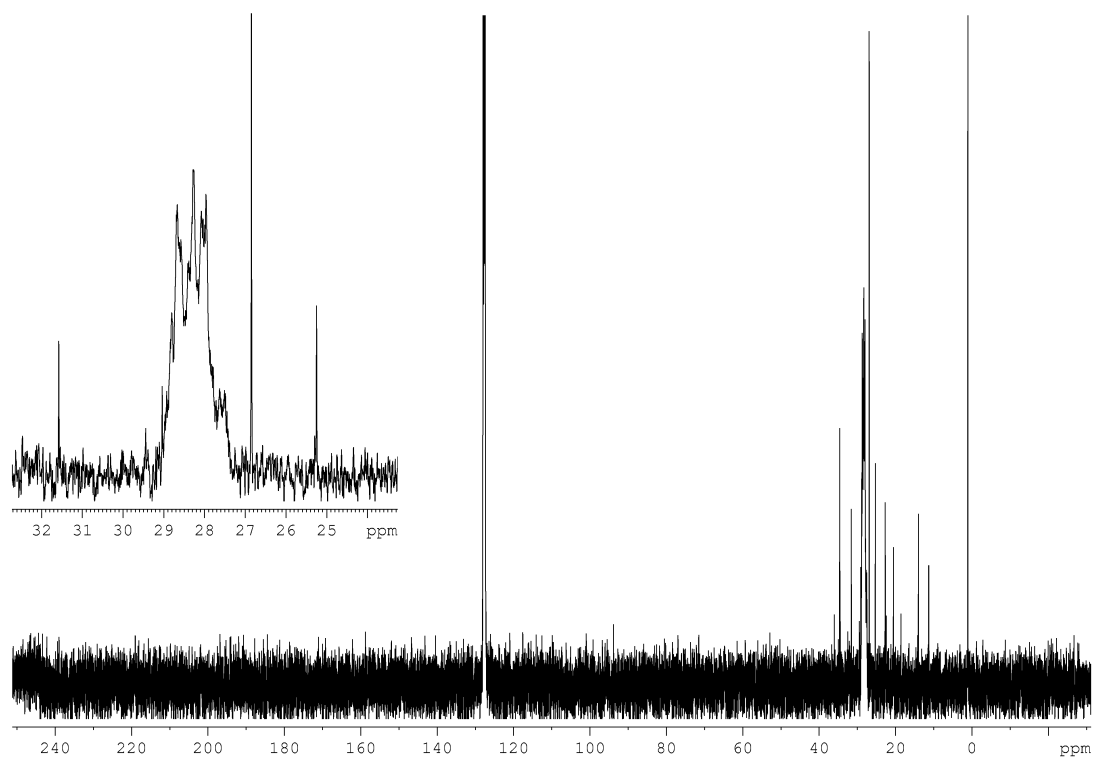


Figure S18: $^{13}\text{C}\{^1\text{H}\}$ NMR spectrum of **P4** in C_6D_6 .

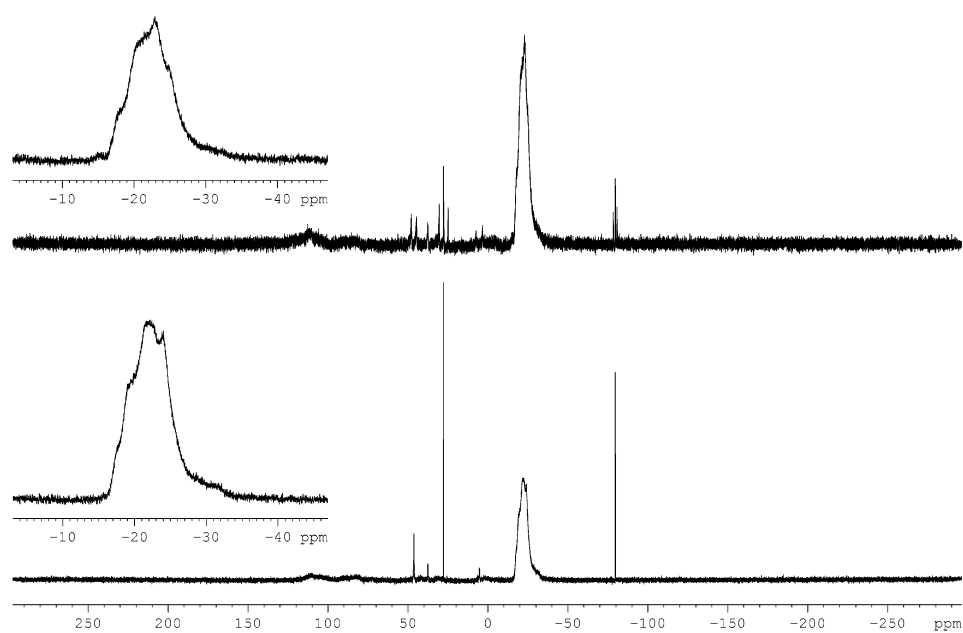
P5

Figure S19: ³¹P (top) and ³¹P{¹H} NMR spectrum (bottom) of **P5** in C₆D₆.

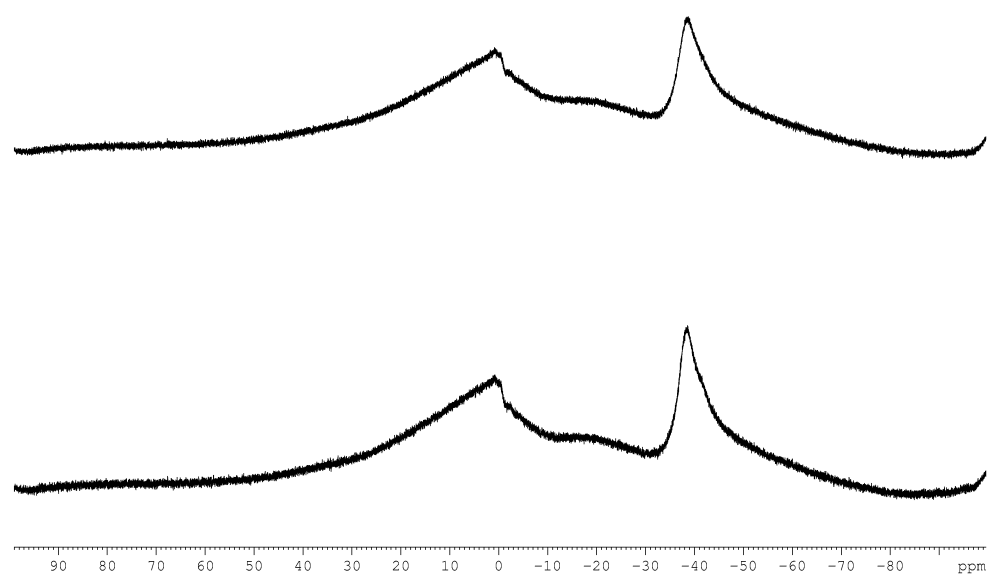


Figure S20: ¹¹B (top) and ¹¹B{¹H} NMR spectrum (bottom) of **P5** in C₆D₆.

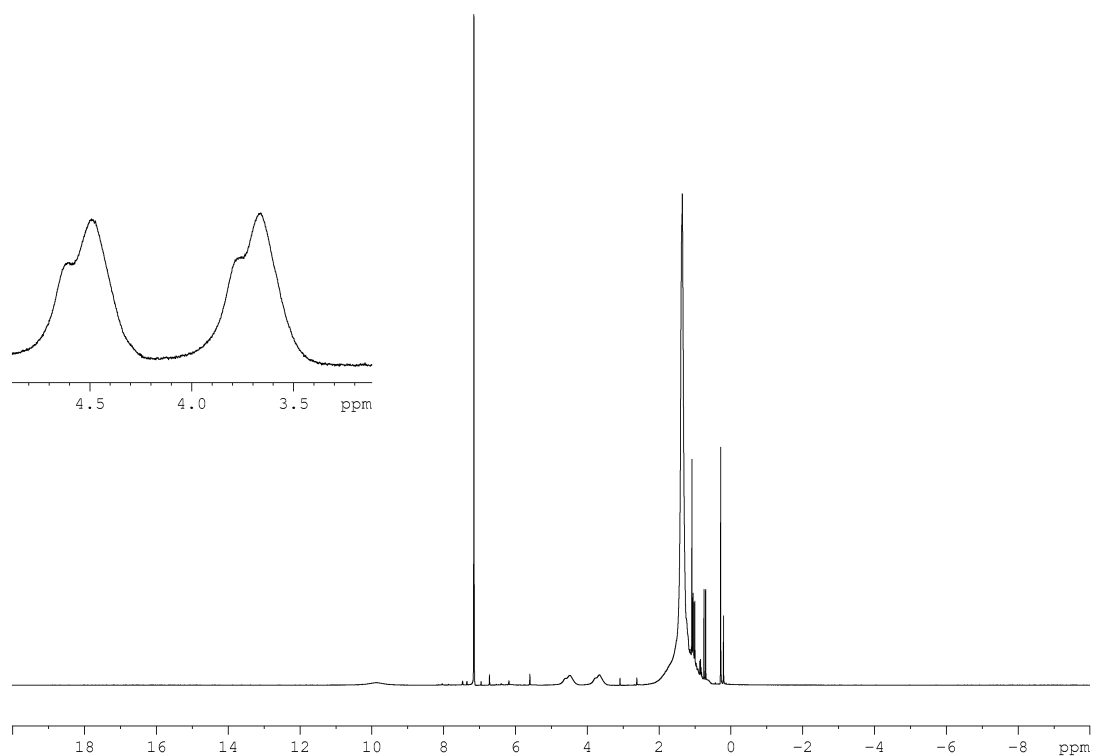


Figure S21: ^1H NMR spectrum of **P5** in C_6D_6 .

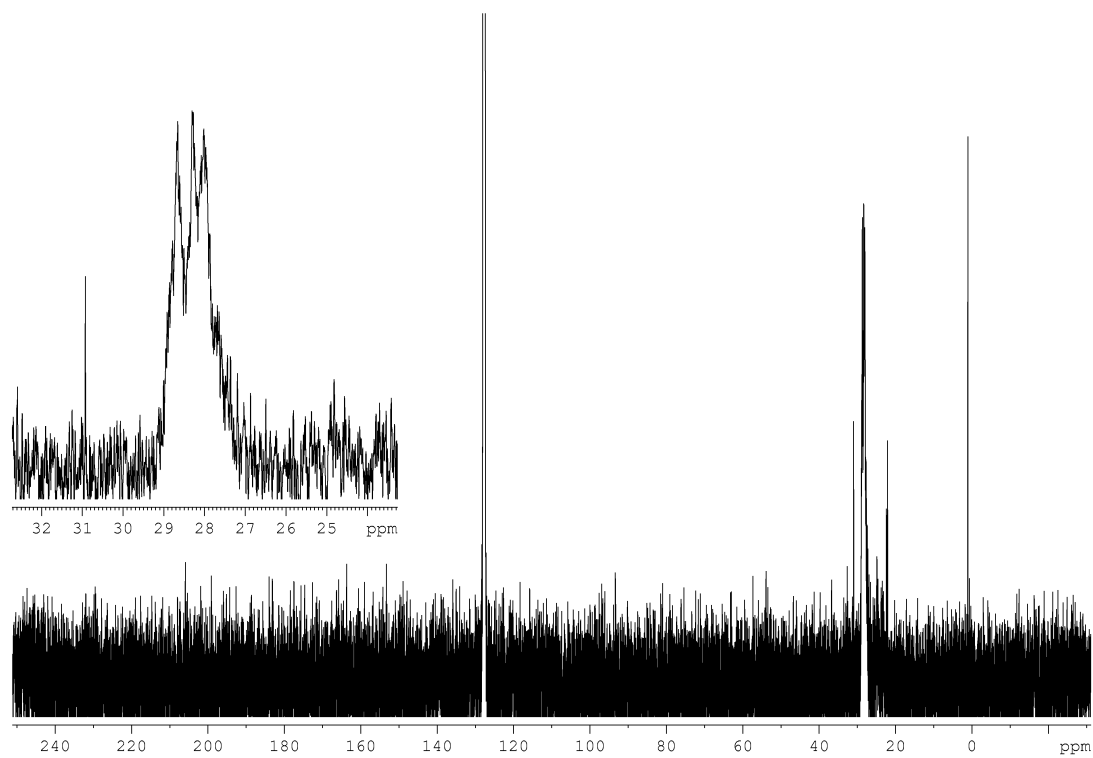


Figure S22: $^{13}\text{C}\{^1\text{H}\}$ NMR spectrum of **P5** in C_6D_6 .

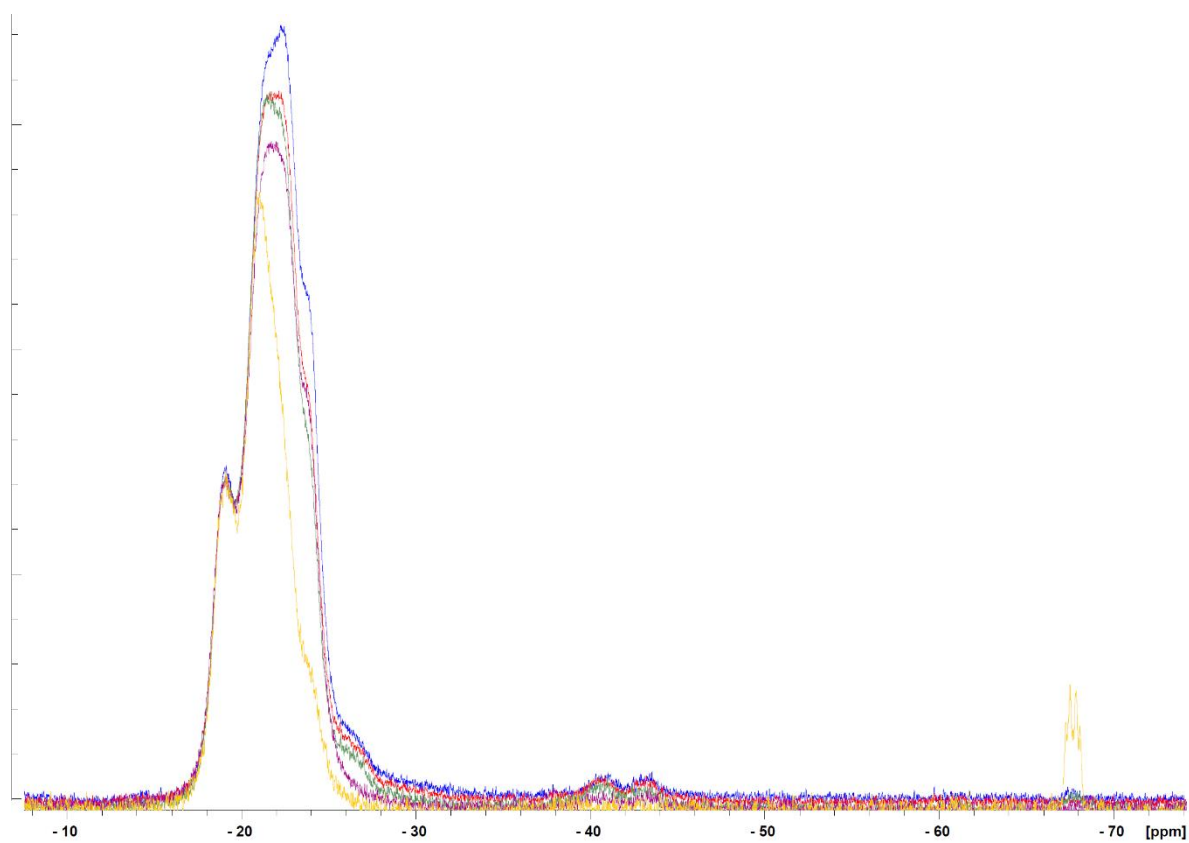


Figure S23: $^{31}\text{P}\{^1\text{H}\}$ NMR spectra overlay: **P1:** blue, **P2:** red, **P3:** green, **P4:** purple, thermal 20°C 72h: yellow; * = monomeric $t\text{BuHPBH}_2\cdot\text{NMe}_3$ (**2a**).

3.5.4 ESI-MS

P1

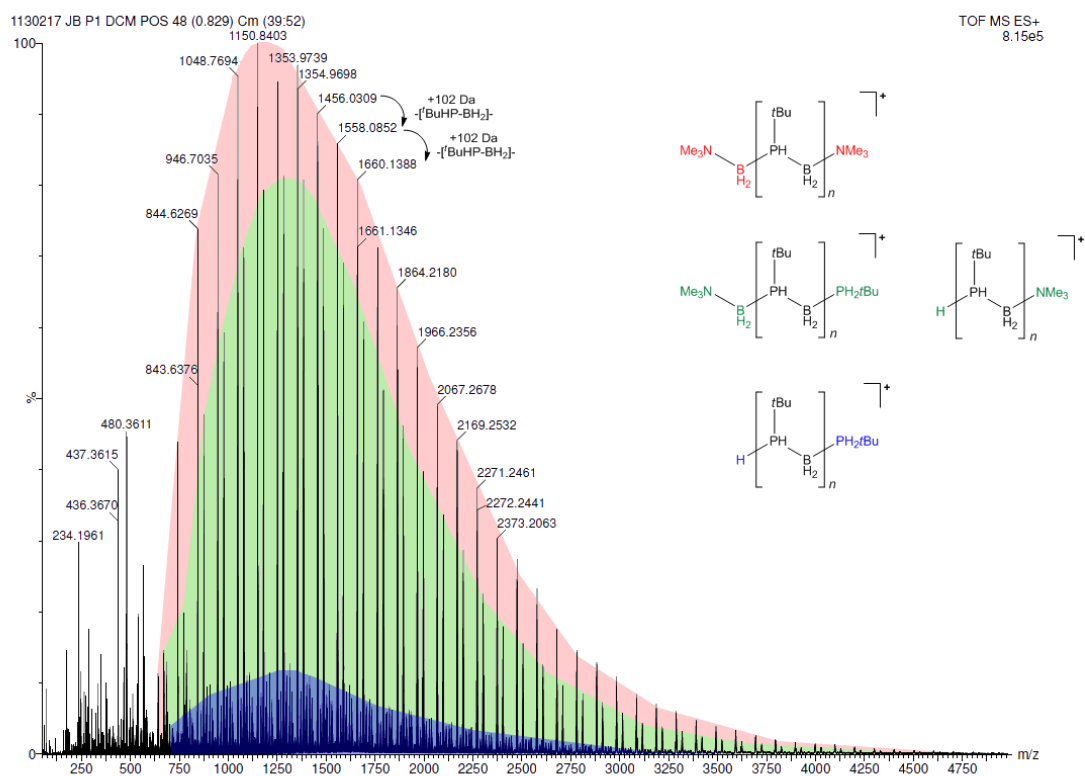


Figure S24: ES⁺ mass spectrum of **P1** with possible end groups.

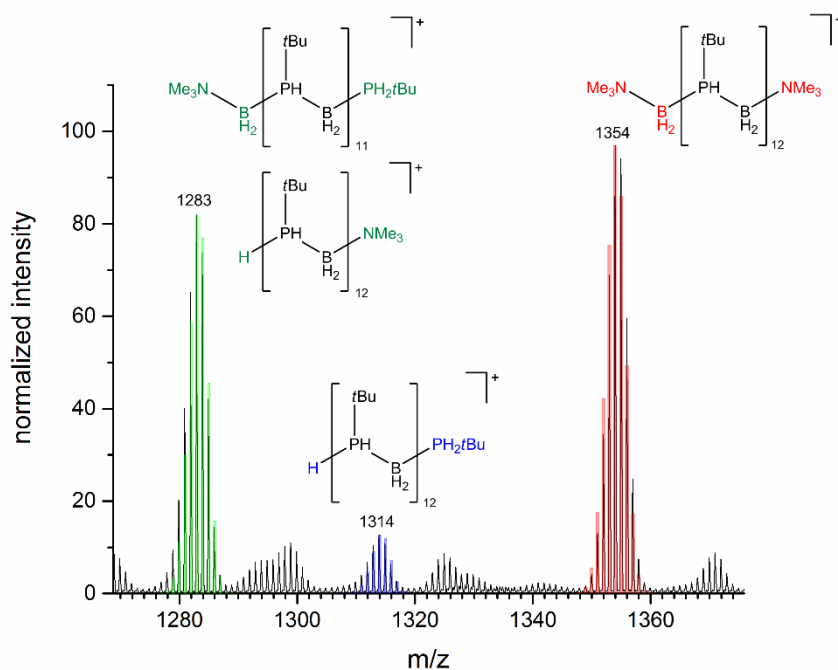


Figure S25: ES⁺ mass spectrum of **P1**, simulated MS represented in coloured bars.

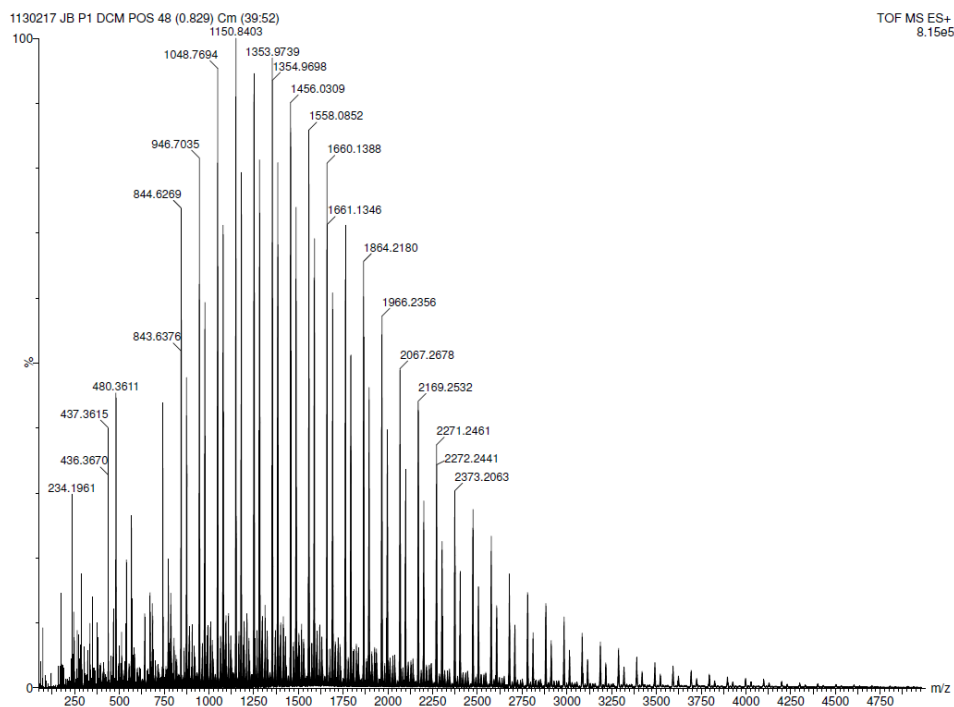


Figure S26: ES+ mass spectrum of P1.

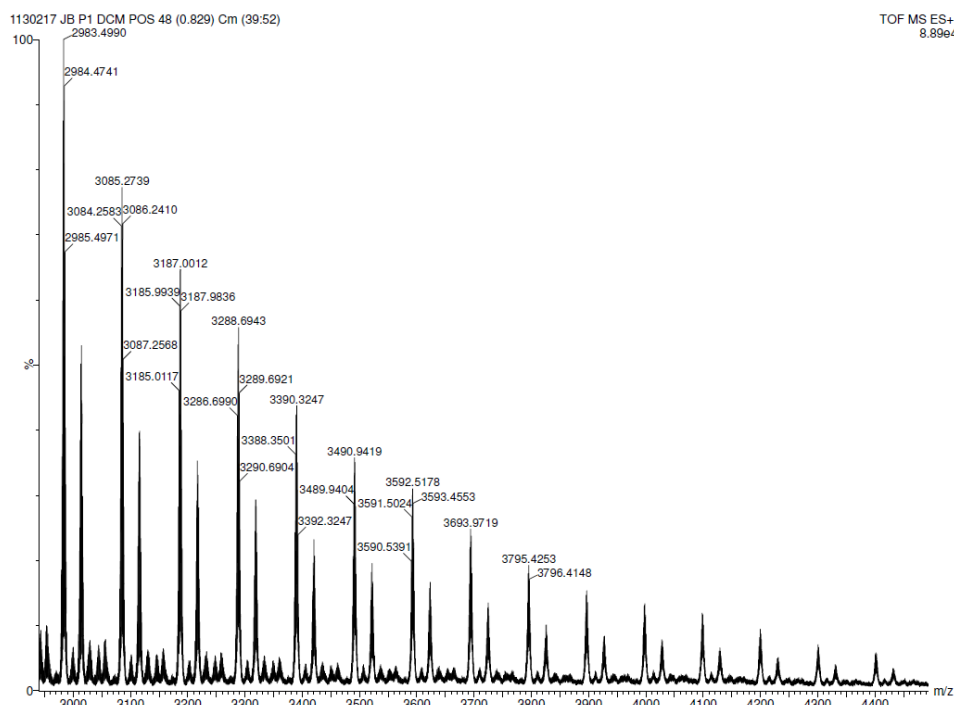


Figure S27: ES+ mass spectrum of P1.

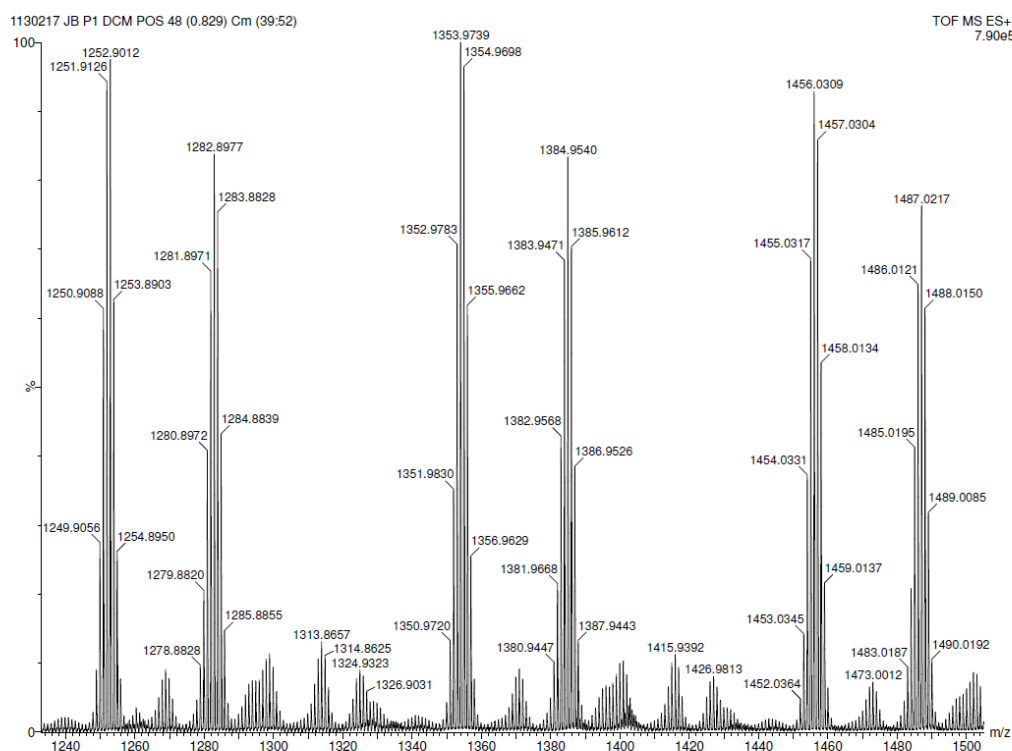


Figure S28: ES+ mass spectrum of P1.

P2

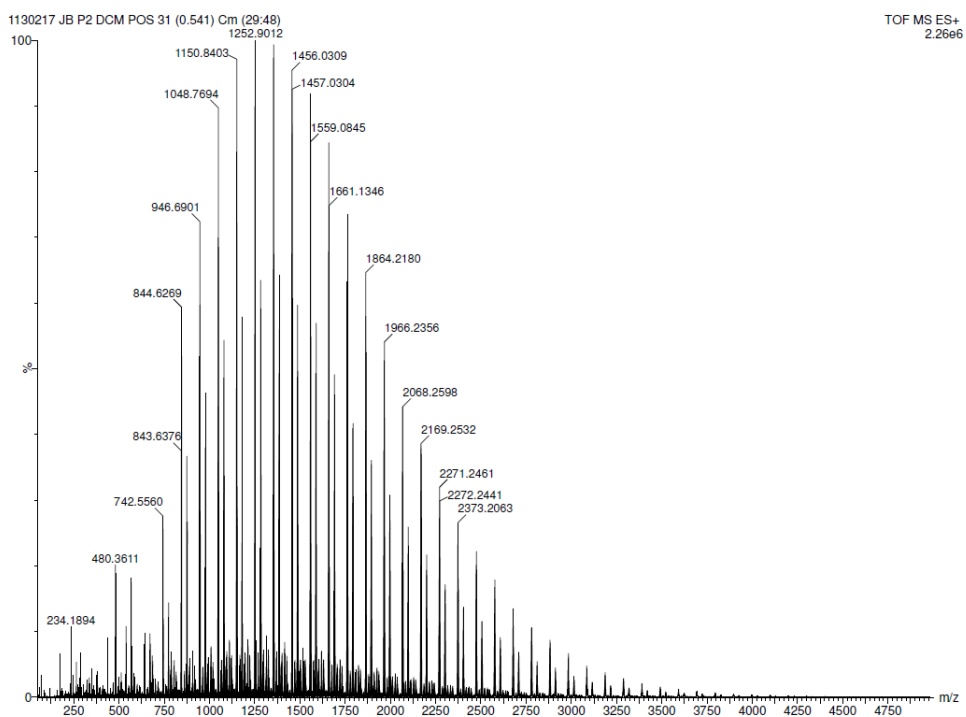


Figure S29: ES+ mass spectrum of P2.

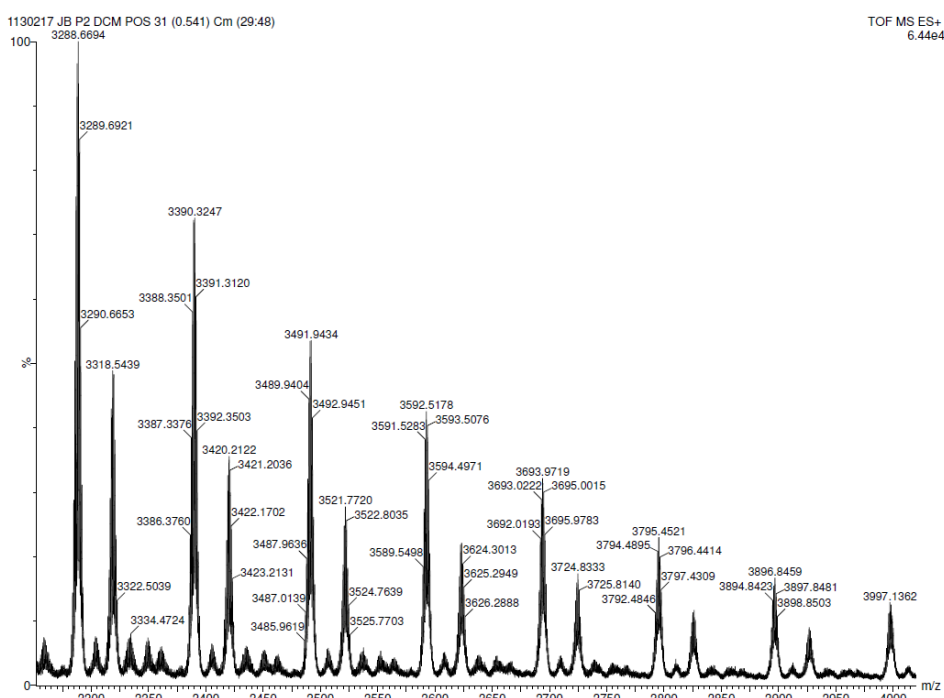


Figure S30: ES+ mass spectrum of P2.

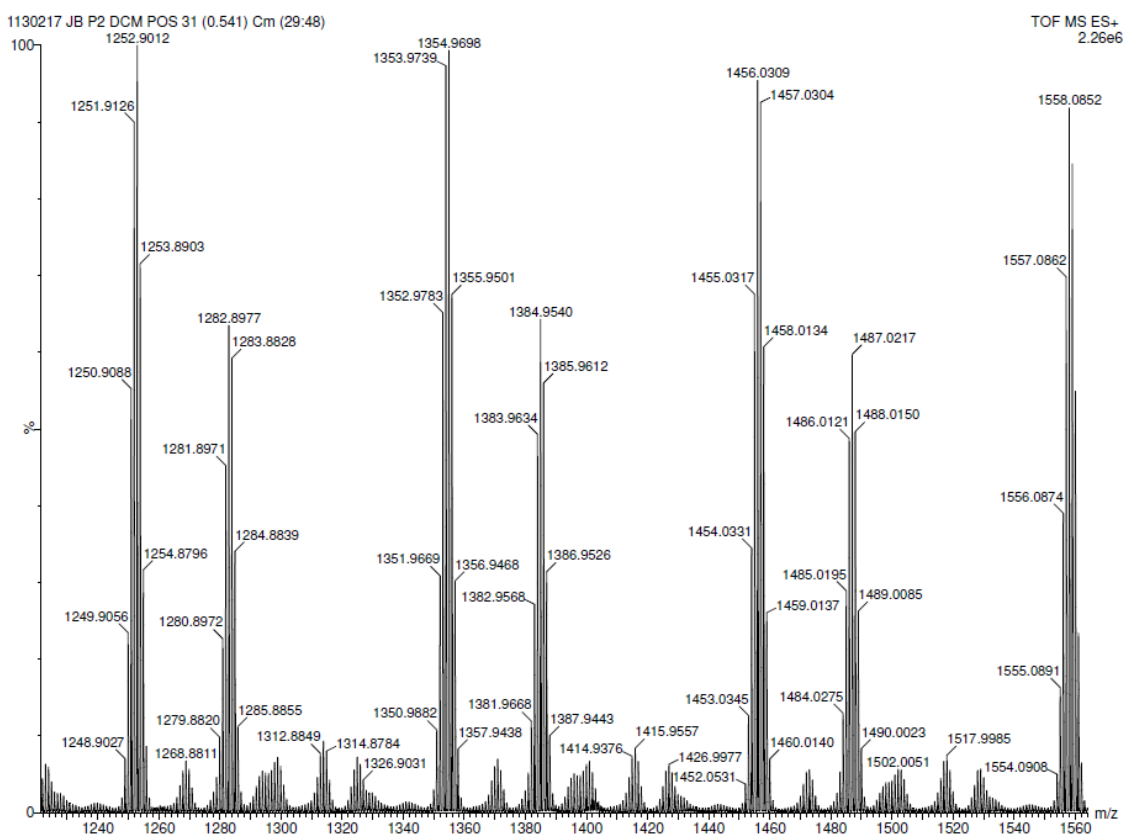


Figure S31: ES+ mass spectrum of P2.

P3

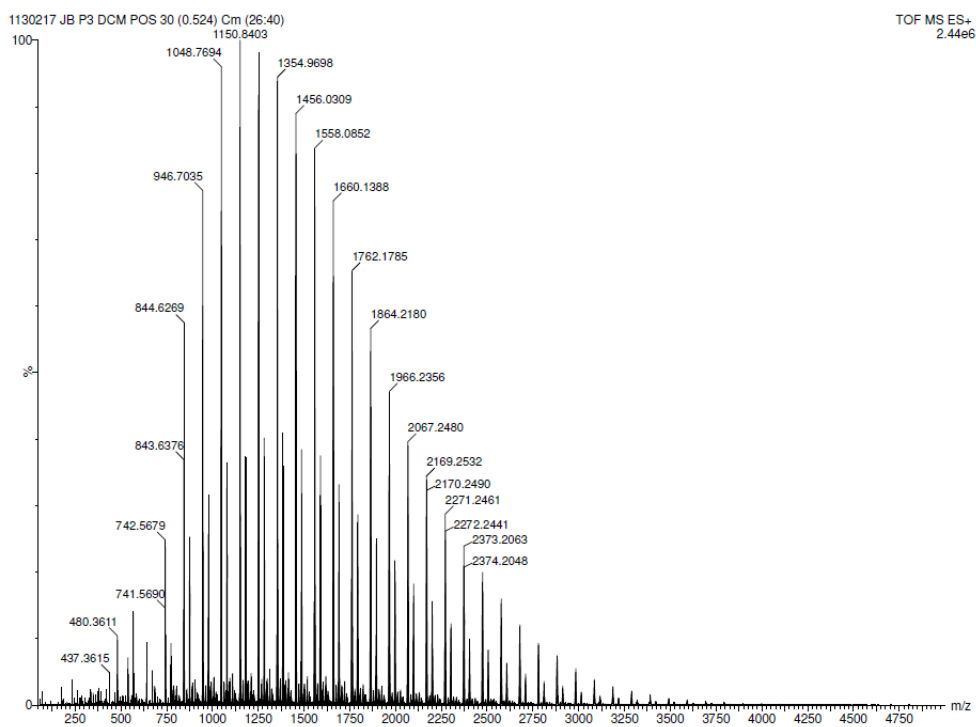


Figure S32: ES+ mass spectrum of P3.

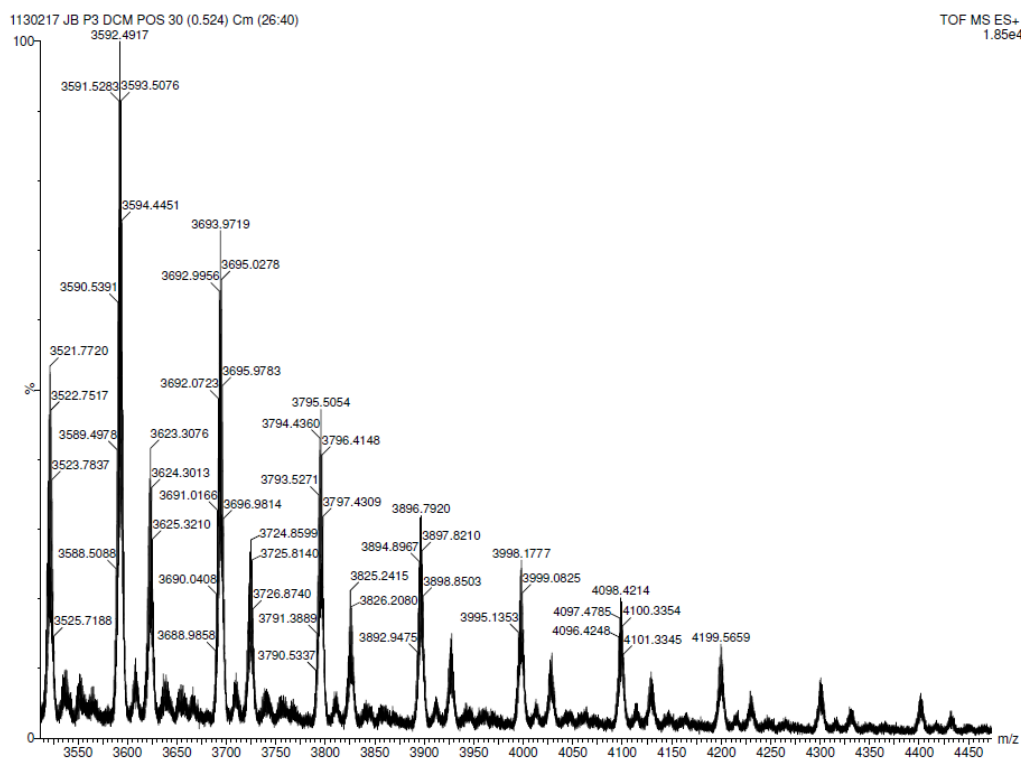


Figure S33: ES+ mass spectrum of P3.

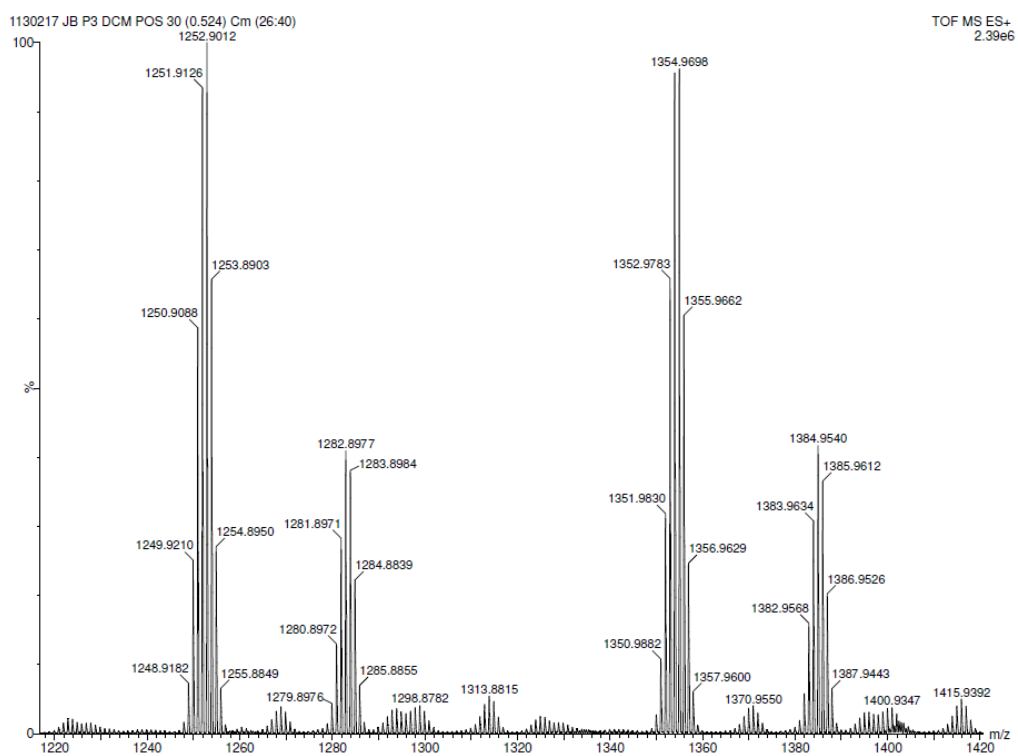


Figure S34: ES+ mass spectrum of P3.

P4

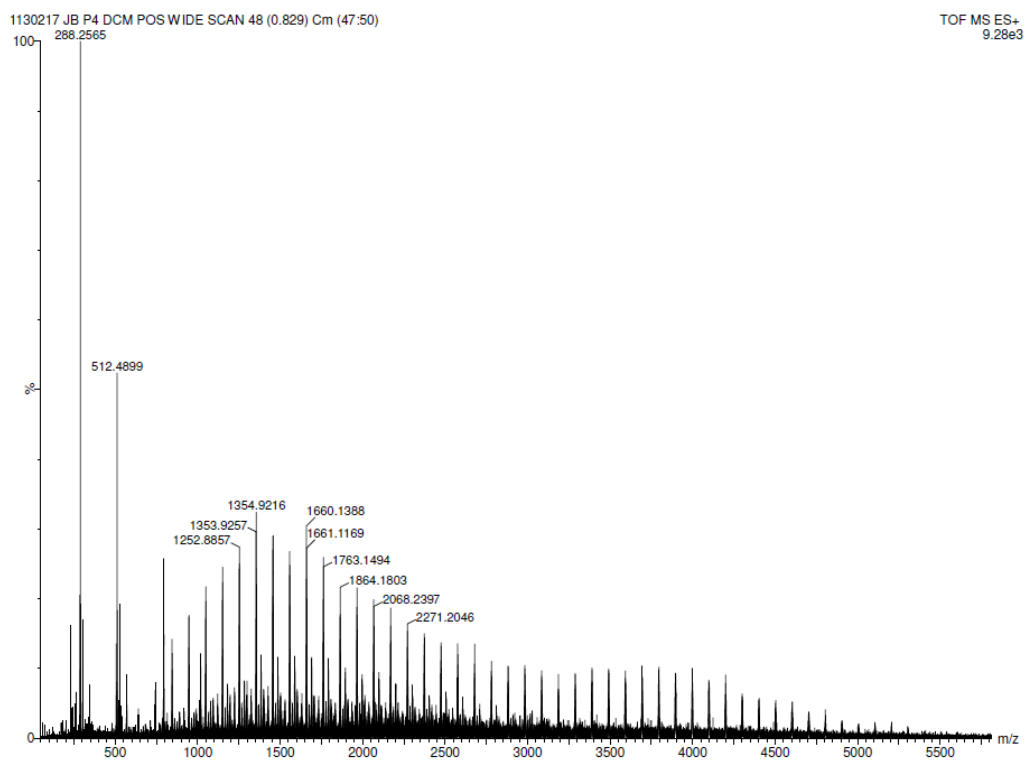


Figure S35: ES+ mass spectrum of P4.

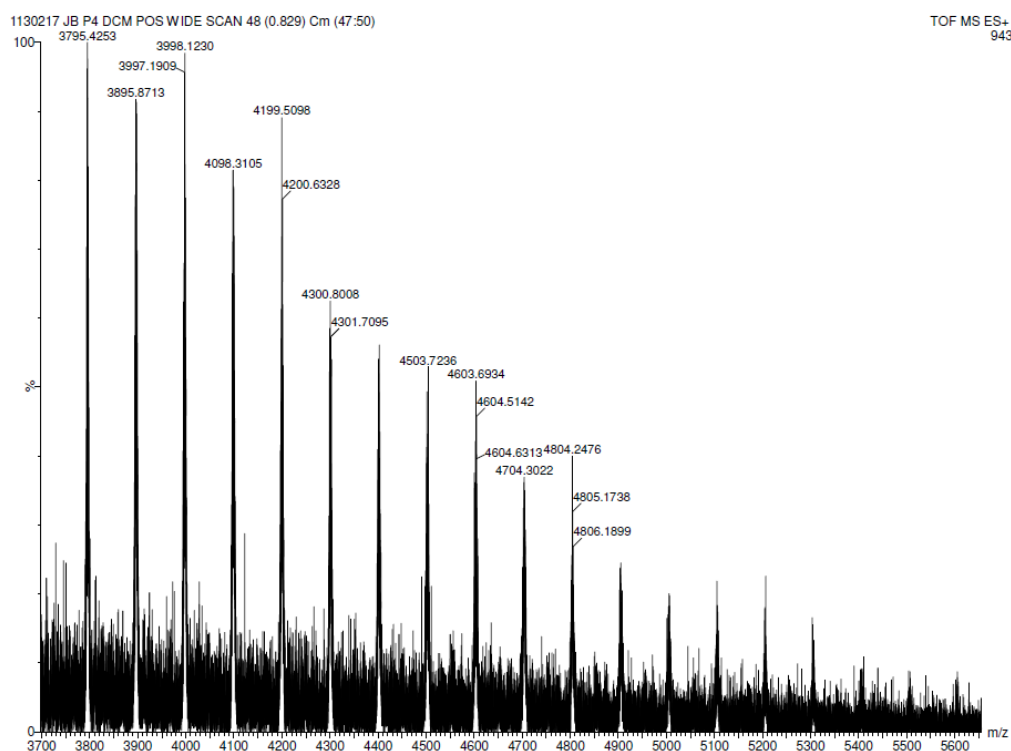


Figure S36: ES+ mass spectrum of P4.

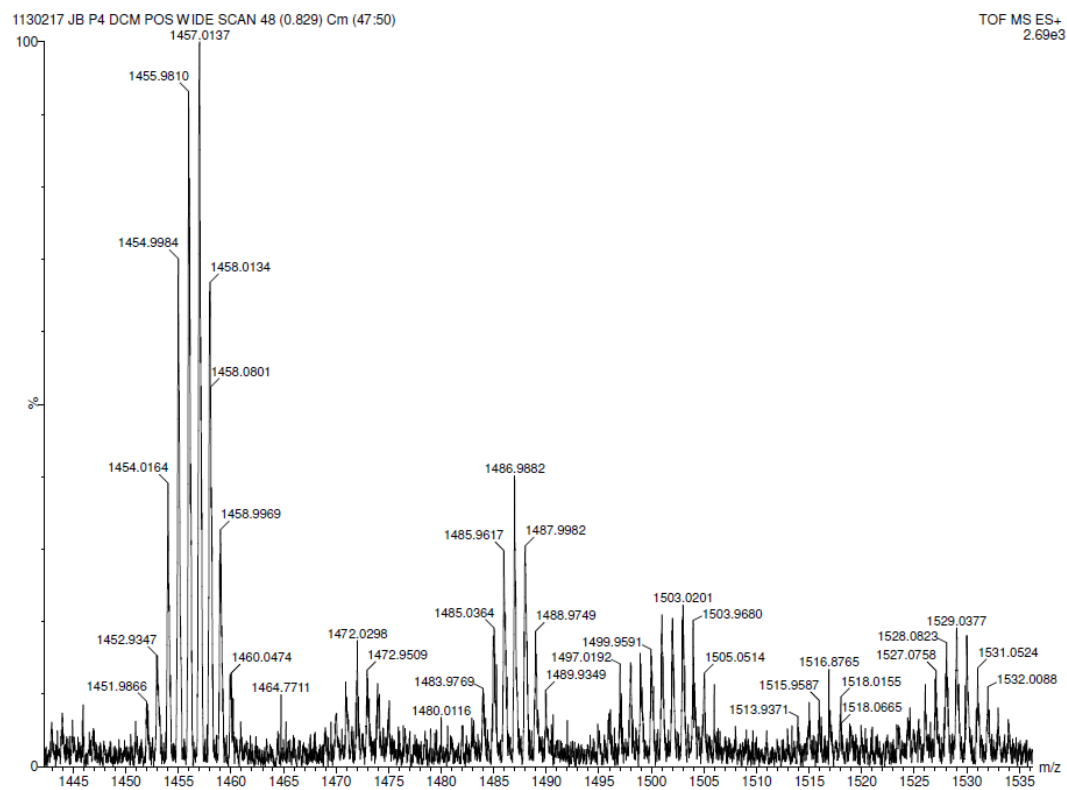


Figure S37: ES+ mass spectrum of P4.

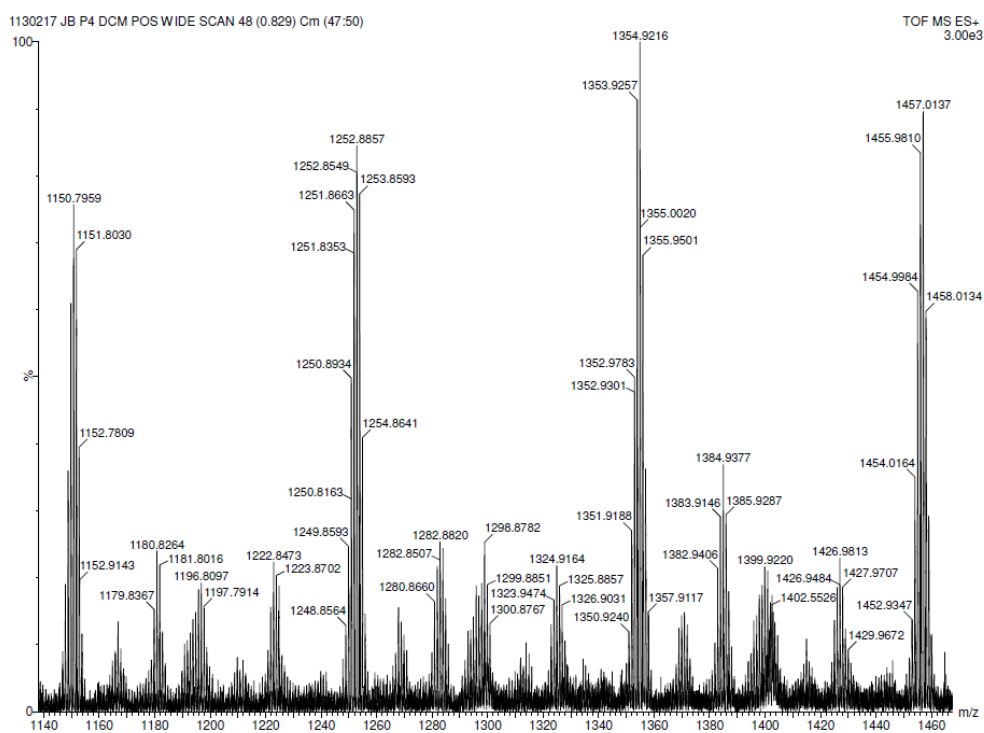


Figure S38: ES+ mass spectrum of P4.

P5

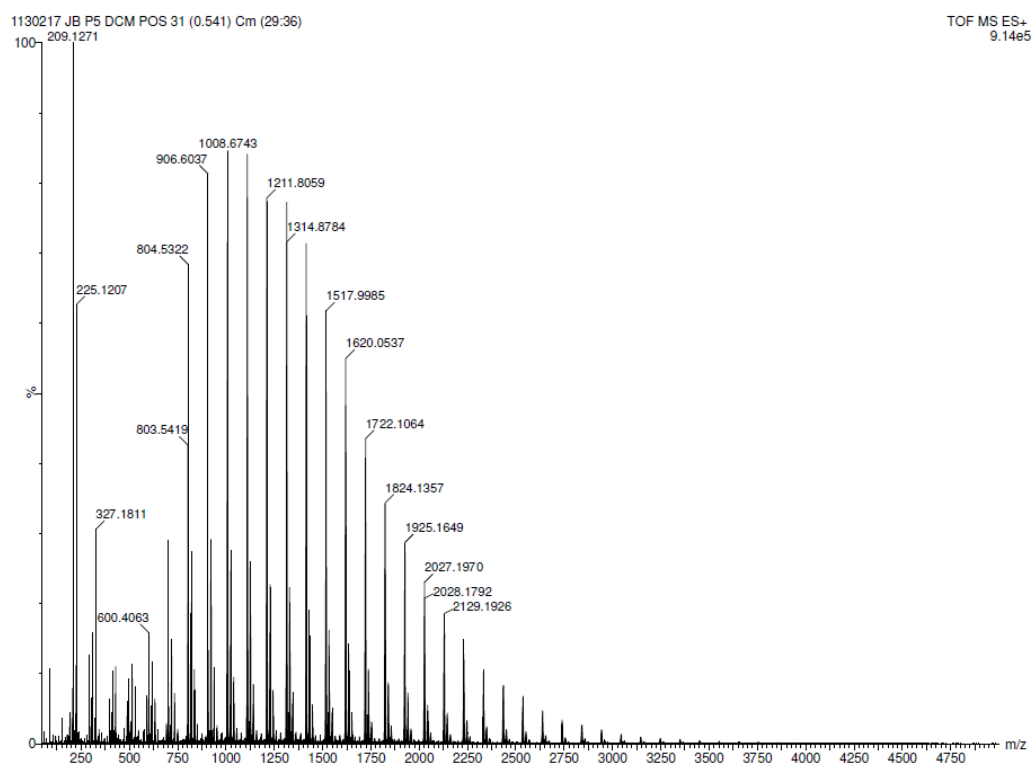


Figure S39: ES+ mass spectrum of P5.

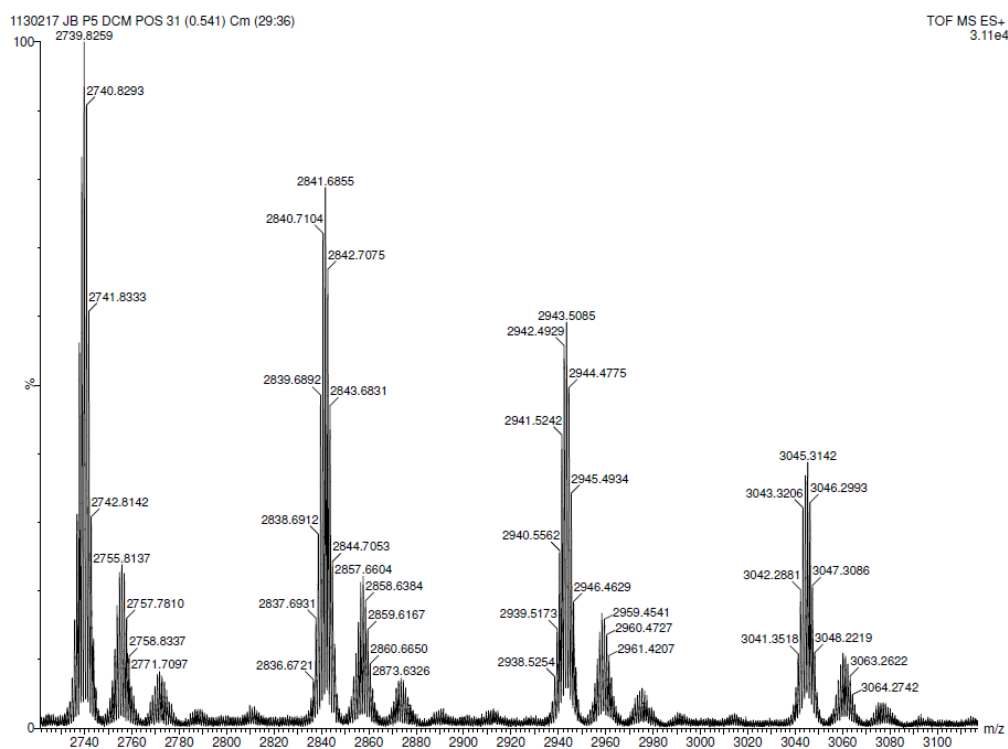


Figure S40: ES+ mass spectrum of P5.

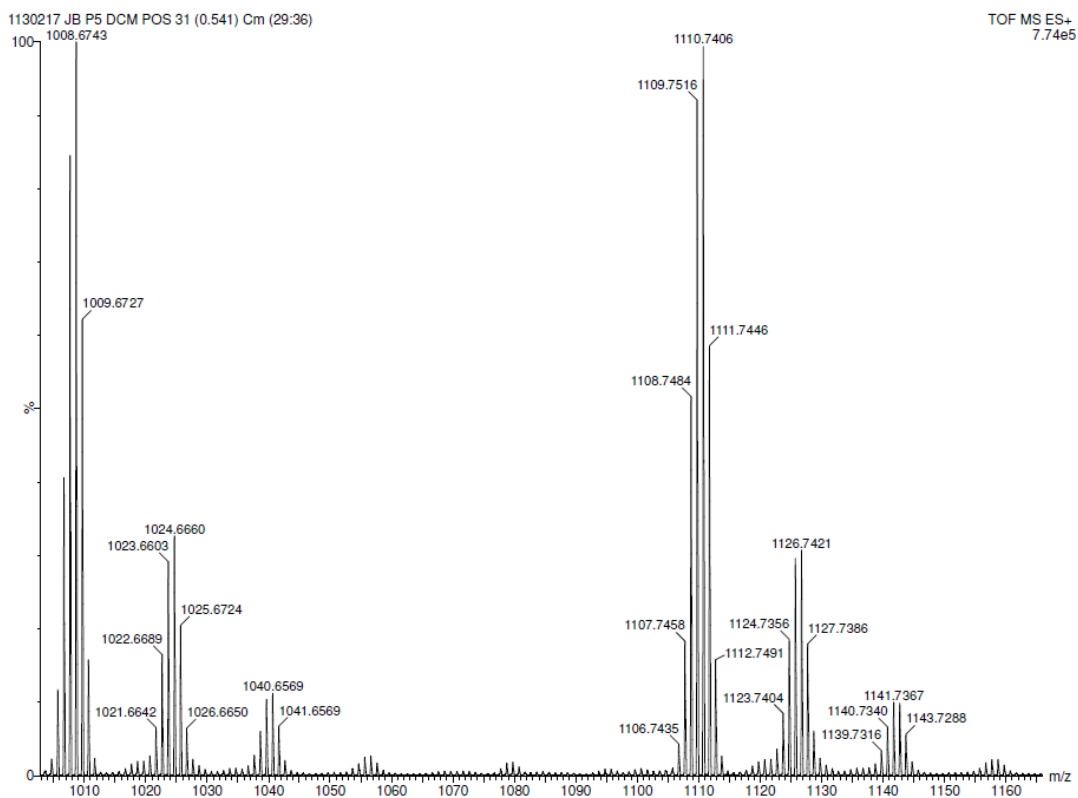


Figure S41: ES+ mass spectrum of P5.

3.5.5 GPC and DLS

Table S2: GPC data of polymers **P1-P5** in THF.

	P1	P2	P3	P4	P5
T / °C	0	20	40	20	20
Loading / mol%	5	5	5	5	1
Precipitation	No	No	No	Yes	Yes
Reaction Time / h	36	16	16	16	16
GPC Peak2 RV / mL	19.440	18.857	20.230	19.377	18.043
PDI (Mw/Mn)	2.032	2.012	2.255	2.014	2.168
GPC Mn / Da	4405	4189	3902	5511	20732
GPC Mw / Da	8950	8430	8798	11098	44937
GPC Mz / Da	15380	14765	16419	20221	67042
GPC Mp / Da	6337	15546	1368	7049	41040

Table S3: DLS data of polymer **P5** in CH₂Cl₂

Sample	T / °C	c / mg/mL	R_h / nm	Mw / g mol⁻¹
P5	20	2	4.95	35400

Similar to the polymer from metal free thermolysis,^[2] GPC analysis of polymer **P1-P5** conducted with THF as eluent resulted in two peaks. A lower molecular weight component ranging from Mn = 3900 to 20700 g mol⁻¹, and an apparent higher molecular weight component ranging from Mn = 79300 to 83900 g mol⁻¹. The lower molecular weight component is consistent with DLS data. The absence of such a size population by DLS that corresponds to the high molecular weight component is suggestive that the presence of this species is dependent on the conditions applied, and most probably larger aggregates form in diluted THF solutions but not in solutions of CH₂Cl₂. Similar phenomena have also been observed for poly(phenylphosphinoborane).^[2,6a]

P5 was analyzed by DLS at optimized concentrations (2 mg/mL) in CH₂Cl₂. The value of R_h of 4.95 nm corresponds to a molar mass of 35400 g mol⁻¹ for monodisperse polystyrene samples in THF.^[7]

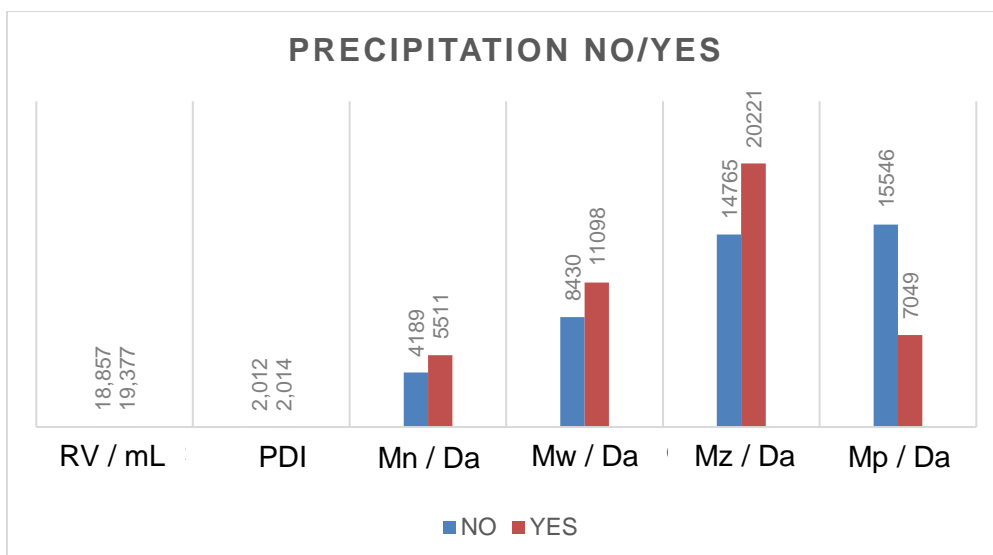


Figure S42: GPC data of non-precipitated (**P2**) and precipitated (**P4**) polymers.

Precipitated polymer showed a higher molecular mass in the GPC analysis, while the polydispersity index (PDI) is roughly the same. This might be due to washing out of lower molecular compounds during precipitation in MeCN. At the same time the PDI doesn't change significantly, which suggest a shift to higher masses without changing the distribution of high to low molecular mass polymers.

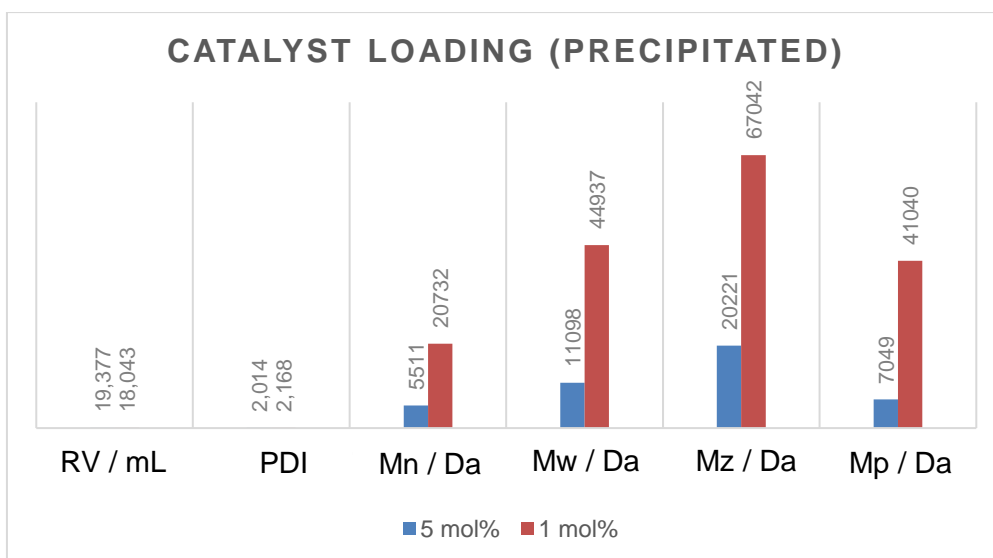


Figure S43: GPC data of precipitated polymers with different catalyst loadings: 5mol% (**P4**) and 1mol% (**P5**) of $[(\eta^5\text{-}\eta^1\text{-C}_5\text{H}_4\text{C}_{10}\text{H}_{14})_2\text{Ti}]$ (**1**).

Higher loadings of catalyst $[(\eta^5\text{-}\eta^1\text{-C}_5\text{H}_4\text{C}_{10}\text{H}_{14})_2\text{Ti}]$ (**1**) showed a lower molecular mass in the resulting polymer in GPC analysis, while the PDI is roughly the same, slightly lower for higher catalyst loadings. This might indicate a chain growth mechanism, which

leads to shorter chains, the higher concentration of active sites is during the growth reaction. The slightly higher PDI might be due to a competitor reaction between the catalytic and thermal polymerization at low catalyst concentrations.

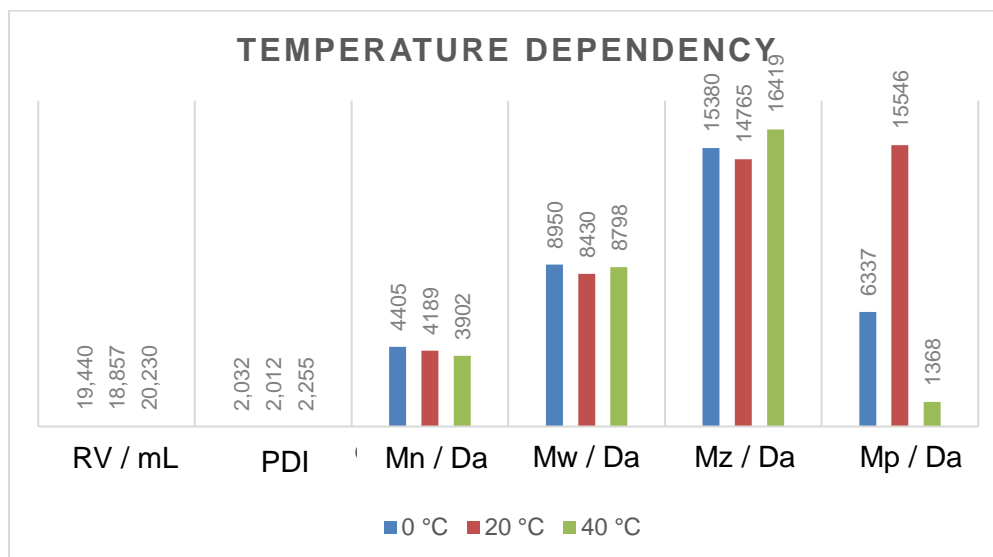


Figure S44: GPC data of polymers, synthesized at different temperatures: 0 °C (P1), 20 °C (P2), 40 °C (P3).

Variation of reaction temperature didn't show a clear trend in the GPC analysis of the resulting polymers. Complete conversion of the monomer to the polymer is faster at higher temperatures. The PDI of the polymer synthesized at 40 °C is slightly higher than the other, indicating a faster and less organized reaction.

3.5.6 Computational Studies

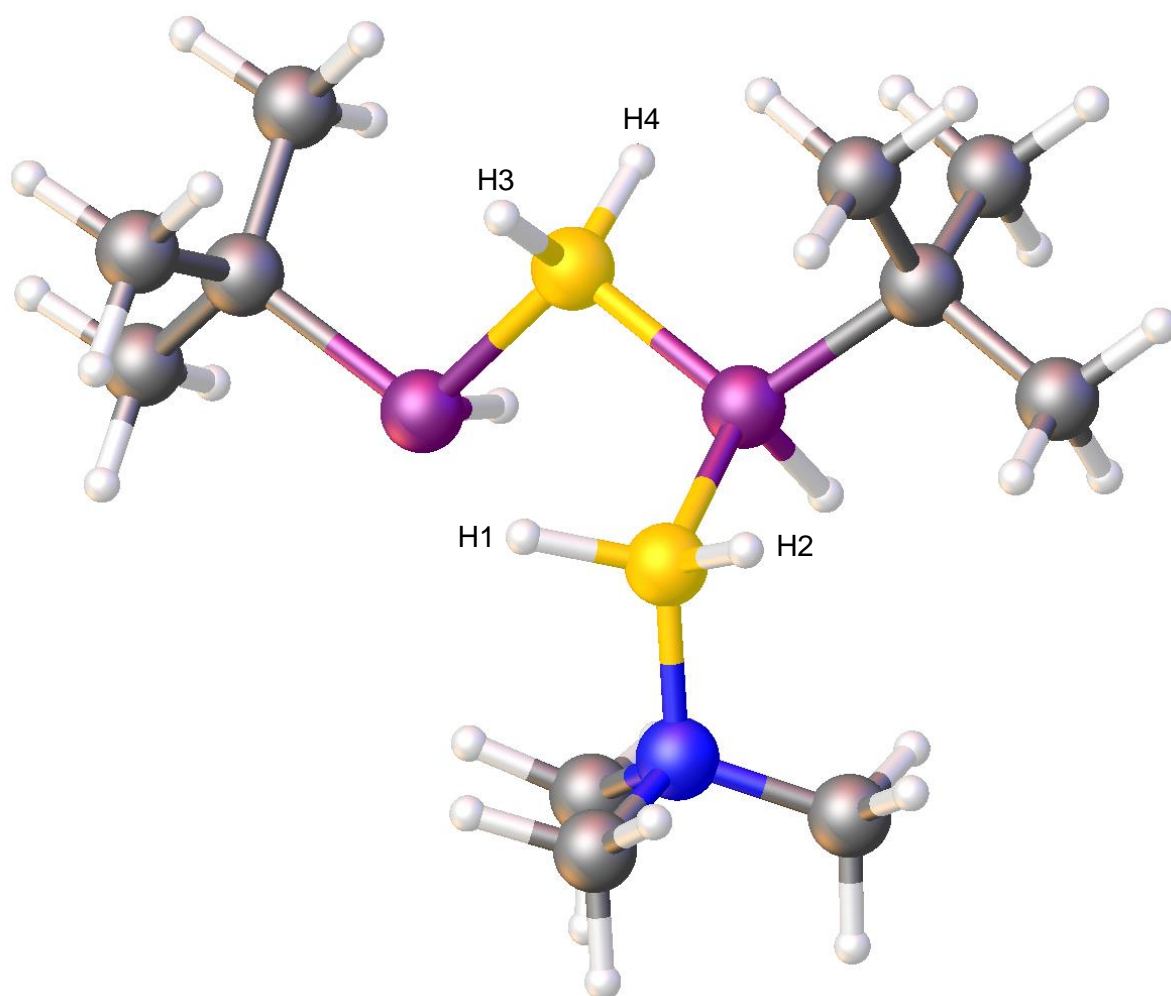


Figure S45: Optimized Geometrie of dimer $[\text{Me}_3\text{N}\cdot\text{BH}_2\text{-PtBuH-BH}_2\text{-PtBuH}]$.

All calculations have been performed with the TURBOMOLE program package^[8] at the RI^[9]-B3LYP^[10]/def2-TZVP^[11] level of theory. The solvent effects were incorporated via the Conductor-like Screening Model (COSMO)^[12] using the dielectric constant of THF ($\epsilon = 7.250$). The natural population analysis^[13] was performed as implemented in TURBOMOLE. The studies show that the hydrogen atoms H1 and H2 on the terminal BH₂ group next to the NMe₃ are more electronegative than hydrogens H3 and H4 on the BH₂ between two *t*BuHP groups, so a chain migration is likely to happen.

Summary of Natural Population Analysis:

Atom	Natural	----- Natural Population -----			
	Charge	Core	Valence	Rydberg	Total
H1	-0.02468	0.00000	1.01818	0.00650	1.02468
H2	-0.02500	0.00000	1.02268	0.00232	1.02500
H3	0.01603	0.00000	0.98165	0.00232	0.98397
H4	-0.00028	0.00000	0.99763	0.00265	1.00028

Atomic populations from total density:

Atom	Charge	n(s)	n(p)	n(d)	n(f)	n(g)
H1	-0.02468	1.02074	0.00394	0.00000	0.00000	0.00000
H2	-0.02500	1.02331	0.00169	0.00000	0.00000	0.00000
H3	0.01603	0.98248	0.00149	0.00000	0.00000	0.00000
H4	-0.00028	0.99874	0.00154	0.00000	0.00000	0.00000

3.5.7 References

- [1] M. Diekmann, G. Bockstiegel, A. Lützen, M. Friedemann, W. Saak, D. Haase, R. Beckhaus, *Organometallics* **2006**, *25*, 339-348.
- [2] C. Marquardt, T. Jurca, K.-C. Schwan, A. Stauber, A. V. Virovets, G. R. Whittell, I. Manners, M. Scheer, *Angew. Chem. Int. Ed.* **2015**, *54*, 13782-13786.
- [3] C. Marquardt, A. Adolf, A. Stauber, M. Bodensteiner, A. V. Virovets, A. Y. Timoshkin, M. Scheer, *Chem. Eur. J.* **2013**, *19*, 11887-11891.
- [4] A. Stauber, T. Jurca, C. Marquardt, M. Fleischmann, M. Seidl, G. R. Whittell, I. Manners, M. Scheer, *Eur. J. Inorg. Chem.* **2016**, 2684-2687.
- [5] A. Tzschach, W. Deylig, *Z. Anorg. Allg. Chem.* **1965**, *336*, 36-41.
- [6] a) H. Dorn, R. A. Singh, J. A. Massey, J. M. Nelson, C. A. Jaska, A. J. Lough, I. Manners, *J. Am. Chem. Soc.* **2000**, *122*, 6669-6678; b) H. Dorn, J. M. Rodezno, B. Brunnhofer, E. Rivard, J. A. Massey, I. Manners, *Macromolecules* **2003**, *36*, 291-297; c) T. J. Clark, J. M. Rodezno, S. B. Clendenning, S. Aouba, P. M. Brodersen, A. J. Lough, H. E. Ruda, I. Manners, *Chem. Eur. J.* **2005**, *11*, 4526-4534; d) S. Pandey, P. Lonneck, E. Hey-Hawkins, *Eur. J. Inorg. Chem.* **2014**, 2456-2465; e) D. Jacquemin, C. Lambert, E. A. Perpete, *Macromolecules* **2004**, *37*, 1009-1015; f) A. Schafer, T. Jurca, J. R. Vance, K. Lee, V. A. Du, M. F. Haddow, G. R. Whittell, I. Manners, *Angew. Chem. Int. Ed.* **2015**, *54*, 4836-4841; *Angew. Chem.* **2015**, *127*, 4918-4923; g) J.-M. Denis, H. Forintos, H. Szelke, L. Toupet, T.-N. Pham, P.-J. Madec, A.-C. Gaumont, *Chem. Commun.* **2003**, 54-55.
- [7] L. J. Fetters, N. Hadjichristidis, J. S. Lindner, J. W. Mays, *J. Phys. Chem. Ref. Data* **1994**, *23*, 619-640.
- [8] a) F. Furche, R. Ahlrichs, C. Hättig, W. Klopper, M. Sierka, F. Weigend, *WIREs Comput. Mol. Sci.* **2014**, *4*, 91-100; b) R. Ahlrichs, M. Bär, M. Häser, H. Horn, C. Kölmel, *Chem. Phys. Lett.* **1989**, *162*, 165-169; c) O. Treutler, R. Ahlrichs, *J. Chem. Phys.* **1995**, *102*, 346-354.

- [9] a) M. Sierka, A. Hogekamp, R. Ahlrichs, *J. Chem. Phys.* **2003**, *118*, 9136; c) K. Eichkorn, O. Treutler, H. Oehm, M. Häser, R. Ahlrichs, *Chem. Phys. Lett.* **1995**, *242*, 652–660; b) K. Eichkorn, F. Weigend, O. Treutler, R. Ahlrichs, *Theor. Chem. Acc.* **1997**, *97*, 119.
- [10] a) P. A. M. Dirac, *Proc. Royal Soc.A*, **1929**, *123*, 714. b) J. C. Slater, *Phys. Rev.***1951**, *81*, 385. c) S. H. Vosko, L. Wilk, M. Nusair, *Can. J. Phys.***1980**, *58*, 1200. d) A. D. Becke, *Phys. Rev. A*, **1988**, *38*, 3098. e) C. Lee, W. Yang, R. G. Parr, *Phys. Rev. B*,**1988**, *37*, 785. f) A. D. Becke, *J. Chem. Phys.* **1993**, *98*, 5648.
- [11] a) A. Schäfer, C. Huber, R. Ahlrichs, *J. Chem. Phys.***1994**, *100*, 5829; b) K. Eichkorn, F. Weigend, O. Treutler, R. Ahlrichs, *Theor. Chem. Acc.***1997**, *97*, 119.
- [12] a) A. Klamt, G. Schüürmann *J. Chem. Soc. Perkin Trans. 2* **1993**, 799–805; b) A. Schäfer, A. Klamt, D. Sattel, J. C. W. Lohrenz, F. Eckert *Phys. Chem. Chem. Phys.* **2000**, *2*, 2187–2193.
- [13] A. E. Reed, R. B. Weinstock, F. Weinhold, *J. Chem. Phys.* **1985**, *83*, 735–746.

Preface

The following chapter has already been published:

Chem. Eur. J. **2018**, *24*, 10073–10077.

The article is reprinted with slight modifications with permission of “John Wiley and Sons”. License Number: 4470780574113.

Authors

Jens Braese, Alexander Schinabeck, Michael Bodensteiner, Hartmut Yersin, Alexej Y. Timoshkin and Manfred Scheer

Author contributions

The syntheses and characterization of compounds **1a-d**, **2a-d**, **3a-d** were performed by Jens Braese. The characterization of the luminescent materials was performed by Alexander Schinabeck (Universität Regensburg) and Jens Braese. DFT-calculations were performed by Prof. Dr. Alexej Y. Timoshkin (St. Petersburg State University). X-ray structural analyses of all compounds were performed by Jens Braese and Dr. Michael Bodensteiner (Universität Regensburg).

The manuscript (including supporting information, figures, schemes and graphical abstract) was written by Jens Braese. The photophysical part of the manuscript was written by Prof. Dr. Hartmut Yersin (Universität Regensburg).

Commentary

The influence of the heavier pnictogen atoms P, As and Sb in comparison to the widely used N- and P-based ligands is part of this thesis and will become apparent in the following chapter. The parent compound $\text{H}_2\text{SbBH}_2\text{NMe}_3$ has been used in the same reactions as $\text{H}_2\text{PBH}_2\text{NMe}_3$ and $\text{H}_2\text{AsBH}_2\text{NMe}_3$, although no products could be identified. This is due to redox processes taking place between $\text{H}_2\text{SbBH}_2\text{NMe}_3$ and the Au(I) compounds, resulting in the quick formation of a black precipitate, even at low temperatures.

4 Gold(I) Complexes Containing Phosphanyl- and Arsanylborane Ligands

Abstract: The structural and photophysical properties of a series of new Au(I) compounds have been studied. The reactions of AuCl(tht) with the phosphanyl- and arsanylboranes RR'EBH₂NMe₃ (E = P, As; R = H, Ph; R' = H, Ph, *t*Bu) afford the complexes [AuCl(RR'EBH₂NMe₃)]. In the solid state, [AuCl(H₂PBH₂NMe₃)₂] (**2a**) is a dimer showing unsupported intermolecular aurophilic interactions with short Au⋯Au distances. In contrast, [AuCl(H₂AsBH₂NMe₃)_n] (**2b**) aggregates to form 1D chains. Organic substituents on the pnictogen atoms lead to discrete molecules in [AuCl(RR'PBH₂NMe₃)] (**2c**: R = H, R' = *t*Bu; **2d**: R = R' = Ph). To increase the aurophilicity, the ionic homoleptic complexes [Au(RR'EBH₂NMe₃)₂][AlCl₄] (**3a-d**) have been synthesized for which **3a,b** form chains in the solid state and exhibit luminescence. The emissions show a drastic redshift with temperature decrease correlating with decreasing Au⋯Au distances. DFT calculations provide insight into the bonding situation of the products.

4.1 Introduction

For several decades, gold complexes have been of interest because of their various applications as drugs,^[1] sensors,^[2] dopant emitters^[3] and catalysts.^[4] Under suitable conditions, gold centers in the oxidation state +1 can aggregate with close intermetallic distances in the range of 2.50 to 3.50 Å,^[5] which is well below the sum of the van der Waals radii of 3.80 Å. The strength of such aurophilic interactions is found to be in the range of hydrogen bonding thus being remarkably stronger than simple van der Waals forces.^[6] Two or more gold atoms can be forced to Au⋯Au interactions by a bridging ligand (supported contacts).^[7] Unsupported complexes are also known in which a short Au⋯Au distance is essentially the result of the aurophilicity.^[5,8] Gold(I) complexes with aurophilic interactions generally display interesting luminescence properties with high emission intensities, long-lived photoluminescence as well as a wide range of emission energies.^[9] The luminescence can be fine-tuned through variations of the organic substituents and of the auxiliary ligands.^[10] In order to allow short Au⋯Au distances, the ligands should not be too sterically demanding.^[11] In linear Au(I) complexes, the combination of neutral ligands L and anionic ligands X enables the access to neutral complexes [L-Au-X] or cationic complexes [L-Au-L]⁺.^[12] Even though Coulomb repulsion between equally charged complexes must be overcome,^[5] aurophilic interactions can be present. Non-bulky primary phosphines are well-suited ligands to promote aurophilic

interactions,^[11b,13] while complexes with the heavier homologue arsine are comparatively rare, constrained mainly to AsPh_3 .^[14] This sterically demanding ligand prevents proximity of the gold centers, while gold(I) complexes bearing smaller primary arsines are unknown. Furthermore, chain-like arrangements of cationic gold complexes are limited without the help of bridging ligands,^[15] and there are no such examples known with phosphine or arsine ligands. Therefore, the quest for first unsupported (not bridged) neutral and cationic chain-like phosphine complexes of Au that might reveal luminescence properties was still open. Moreover, because of the lack of Au complexes with primary arsine ligands, the question of the synthesis of such unprecedented derivatives was to be answered, and, if accessible, a comparison of their properties to related primary phosphines was needed.

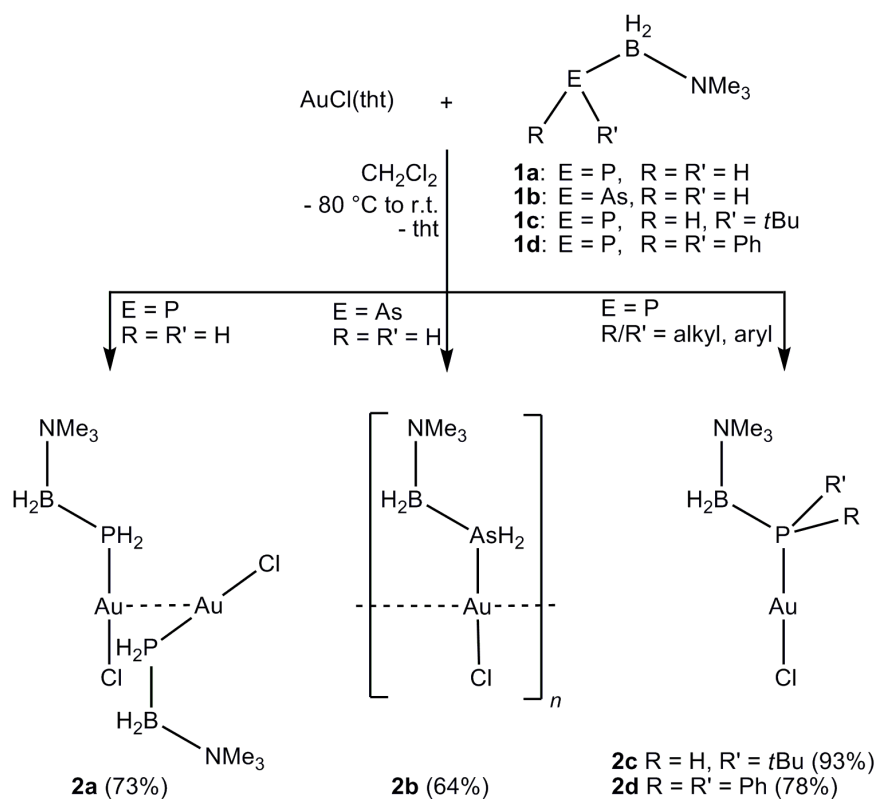
We reported recently the high yield syntheses of the parent pnictogenylboranes $[\text{EH}_2\text{BH}_2\text{NMe}_3]$ ($\text{E} = \text{P}$ (**1a**), As (**1b**)),^[16] which are excellent building blocks for the formation of main group oligomeric^[17] and polymeric^[18] compounds. In the reaction of the phosphanylborane with early transition metal compounds, dehydrocoupling was observed leading to oligomeric chains stabilized in the coordination sphere of transition metals.^[19] Cluster formation was observed with Cu(I) complexes.^[20] Therefore, these distinct primary phosphine and arsine ligands (**1a,b**) are of interest to study if Au complexes are achievable and, if so, whether aurophilic interactions do occur.

4.2 Results and Discussion

Herein we describe the structural and photophysical properties of mononuclear, dinuclear as well as polymeric neutral and cationic Au(I) complexes containing phosphanyl- and arsanylboranes of the formulae $\text{RR}'\text{EBH}_2\text{NMe}_3$ (**1a**: $\text{E} = \text{P}$, $\text{R} = \text{R}' = \text{H}$; **1b**: $\text{E} = \text{As}$, $\text{R} = \text{R}' = \text{H}$; **1c**: $\text{E} = \text{P}$; $\text{R} = \text{H}$, $\text{R}' = \text{tBu}$; **1d**: $\text{E} = \text{P}$; $\text{R} = \text{R}' = \text{Ph}$) as ligands. These ligands are well suited for gold chemistry, as their sterical demand can be easily controlled by the substitution with organic groups at the pnictogen atom.^[18] Moreover, first gold complexes with a primary arsine could be realized.

To avoid oxidation, the reaction of $\text{AuCl}(\text{tht})$ with the phosphanyl- and arsanylboranes $\text{RR}'\text{EBH}_2\text{NMe}_3$ (**1a-d**) was started at $-80\text{ }^\circ\text{C}$. According to the NMR spectra of the reaction mixture, the latter proceed selectively to the products $[\text{AuCl}(\text{RR}'\text{EBH}_2\text{NMe}_3)]$ (**2a-d**), which were isolated in high yields (Scheme 1). All products are well soluble in dichloromethane and were comprehensively characterized.

The solid state structures of the compounds with organic substituents on the phosphorus atoms (**2c,d**) reveal monomeric species,^[21] whereas the unsubstituted primary phosphine and arsine compounds $[\text{AuCl}(\text{H}_2\text{EBH}_2\text{NMe}_3)]_n$ (**2a,b**) form extended



Scheme 1. Synthesis of Au(I) phosphine and arsine complexes with mononuclear, dinuclear as well as polymeric arrangements in the solid state.

structures due to the aurophilic interactions (Figure 1). Interestingly, whereas the phosphorus-containing compound $[\text{AuCl}(\text{H}_2\text{PBH}_2\text{NMe}_3)]_2$ (**2a**) forms a dimer,^[22] the arsenic derivative $[\text{AuCl}(\text{H}_2\text{AsBH}_2\text{NMe}_3)]_n$ (**2b**) shows a 1D chain structure. In both compounds, the distances between the gold atoms are shorter than the sum of the van der Waals radii. The distances are shorter in the phosphorus compound **2a** (3.103(1) Å) than in the arsenic derivative **2b** (3.251(1) Å). This observation goes along with reports

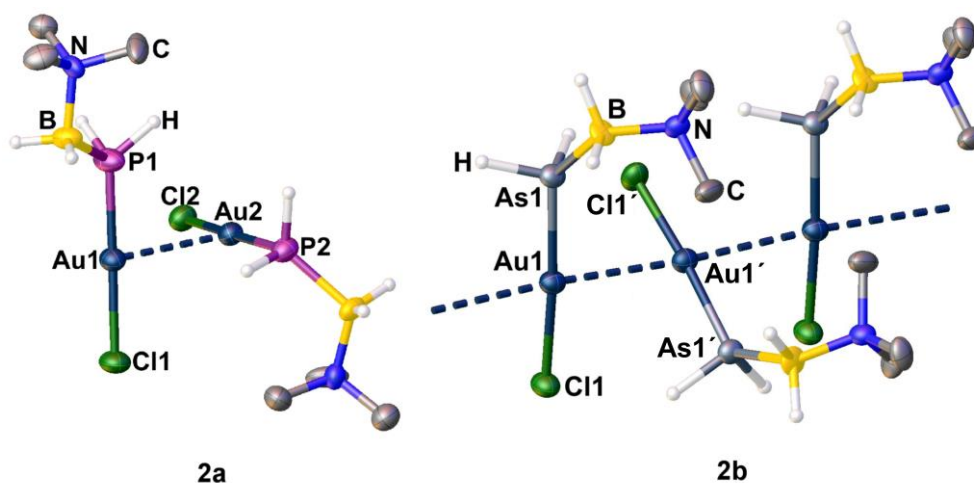
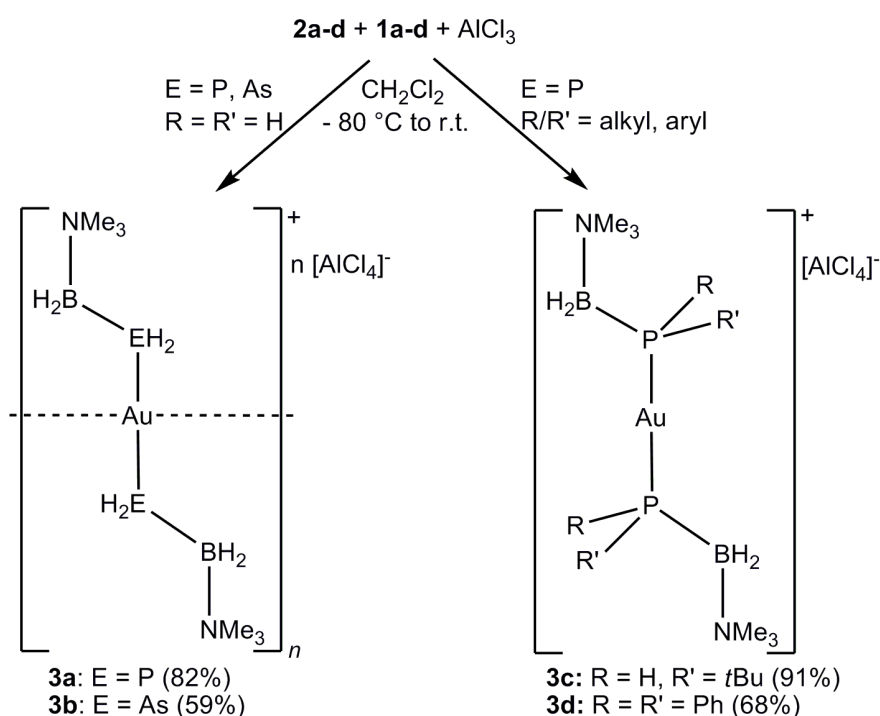


Figure 1. Molecular structures and arrangements of the complexes **2a** and **2b** in the solid state. Thermal ellipsoids are at 50% probability. The hydrogen atoms bonded to carbon atoms are omitted for clarity.

on the increasing influence of softer Lewis bases coordinated to Au(I) centers to form multiple Au...Au interactions compared to harder Lewis bases.^[12,13b] Therefore, not only smaller ligands but also softer coligands form extended polymeric structures in the solid state.^[11b,13] In the dimer **2a**, the two fragments align perfectly orthogonally with a P-Au-Au'-P' torsion angle of 90°. In the arsenic polymer (**2b**), this angle is widened to 127° and the linear chain is slightly bent with an Au-Au-Au angle of 177°. This 1D polymer shows no photoluminescence. For the sterically more hindered derivatives [AuCl(*t*BuHPBH₂NMe₃)] (**2c**) and [AuCl(Ph₂PBH₂NMe₃)] (**2d**), also a linear coordination of the gold center was found, without close Au...Au distances in the solid state.^[21]

To trigger more aurophilic interactions and to gain access to luminescent materials, we targeted on the synthesis of the corresponding homoleptic cationic derivatives of **2a-d**. The reactions of **2a-d** with a second equivalent of the respective ligand **1a-d** in the presence of AlCl₃ as a chloride abstractor leads to the selective formation of the products [Au(RR'EBH₂NMe₃)₂][AlCl₄] (**3a-d**) with almost no side reactions according to the multinuclear NMR spectra of the reaction mixtures (Scheme 2). The reactions were carried out starting at a low temperature (-80°C), otherwise a black precipitate is formed. This is especially important for the reactions with the arsanylborane (**1b**). The good isolated yields confirm these clean reactions.



Scheme 2. Synthesis of charged homoleptic Au(I) phosphine and arsine complexes.

The ionic products **3a-d** are soluble in polar solvents and were comprehensively characterized inclusive of single crystal X-ray diffraction. Only for [Au(Ph₂PBH₂NMe₃)₂][AlCl₄] (**3d**), no single crystals could be obtained. Several attempts

of crystallization gave repeatedly crystals of the starting material $[\text{AuCl}(\text{Ph}_2\text{PBH}_2\text{NMe}_3)]$ (**2d**). The ^{31}P -NMR spectra of **3d** show a minor presence of **2d**, indicating an equilibrium reaction. Because of the modulated nature of the crystals of **3b**, only an average model could be refined.^[23] For the compounds $[\text{Au}(\text{tBuHPBH}_2\text{NMe}_3)_2][\text{AlCl}_4]$ (**3c**) and $[\text{Au}(\text{Ph}_2\text{PBH}_2\text{NMe}_3)_2][\text{AlCl}_4]$ (**3d**) with bulkier organic substituents on the phosphorus atom, only monomeric complexes could be obtained.^[21] However, the solid state structures of the compounds $[\text{Au}(\text{H}_2\text{PBH}_2\text{NMe}_3)_2][\text{AlCl}_4]$ (**3a**) and $[\text{Au}(\text{H}_2\text{AsBH}_2\text{NMe}_3)_2][\text{AlCl}_4]$ (**3b**) show isostructural extended cationic chains of gold atoms (Figure 2). The softer phosphorus ligand in **3a** instead of the harder chloride ligand in the educt **2a** might cause the difference between a dimer and a chain-like structure.^[12,13b] In **3a** and **3b**, the Au(I) center is coordinated linearly. The Au-Au-Au angle forms a nearly perfect linear chain. Two neighboring linear fragments align nearly orthogonal to each other with a E-Au-Au'-E' torsion angle of 99° (E = P) and 93° (E = As), respectively. Usually, if gold(I) centers are positively charged one would expect significant coulomb repulsion. However, for **3a** and **3b** short Au...Au distances were found, which are slightly longer for the phosphorus derivative **3a** (3.208(2) Å) than for the starting complex **2a** (3.103(1) Å). Interestingly in the arsenic compound **3b** the gold distances (3.1132(1) Å) are significantly shorter than in starting material **2b** (3.251(1) Å), despite the positive charge of the gold atoms. This as well might be caused by the softer arsenic ligand compared the e.g. Cl⁻ ligand. While comparable in size, the arsenic ligand causes shorter intermetallic distances in the resulting complex **3b** than the phosphorus ligand in **3a**. Extended chains of Au(I) complexes through aurophilic interactions are

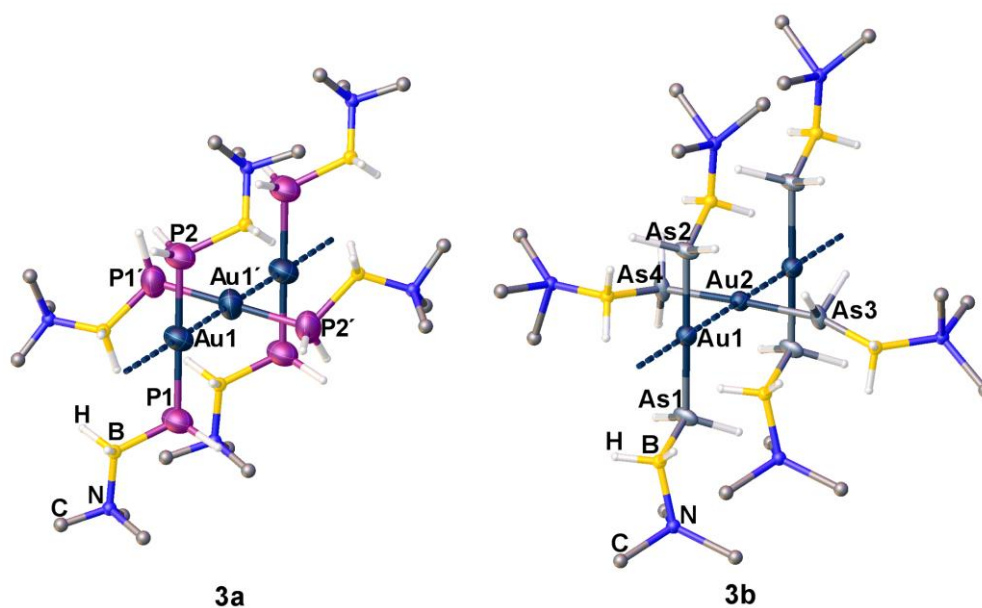


Figure 2. Section of the solid state structures of the luminescent compounds **3a** and **3b**. $[\text{AlCl}_4]$ counter ions not shown. Thermal ellipsoids are at 50% probability. The hydrogen atoms bonded to carbon atoms are omitted for clarity.

relatively uncommon,^[14] especially for positively charged gold(I) centers. Non-bridging phosphine and arsine ligands were used for the first time to synthesize such complexes. The distances between the gold atoms are slightly shorter than in other known cationic gold polymers, usually carrying carbene ligands.^[24]

In addition, we investigated the Au...Au distances for the chain-like compounds **3a** and **3b** at different temperatures (300, 230, 160, 90 K) by single crystal X-ray diffraction. With decreasing temperature, the Au...Au distance decreases (Figure 3).^[25]

To gain insight into how the energetics of interactions changes with changing temperatures, single point energy computations using the experimentally determined geometries of **3a** at 90 K and 300 K, respectively, were performed, applying gradient-corrected density functional theory (DFT). For this calculation, a cationic tetrameric unit was extracted from the experimental data, the tetramer was subsequently divided into the two dimers and four monomers. The counterions were not included in the computation.^[26] The interaction energies between the positively charged monomers are highly endothermic. Nevertheless, one can compare the energetic data for **3a** at the geometries determined at 90 K and 300 K. The energy difference $\Delta(\Delta E_{300} - \Delta E_{90})$ indicates that the Au...Au bond is by 2-4 kJ mol⁻¹ stronger for the structure at 90 K than for the one at 300 K. This result is in accordance with the Wiberg bond index (WBI) trends. The WBI of the Au...Au bonds in **3a** increases by 7% when going from 300 K to 90 K, which confirms the experimentally observed shorter Au...Au distances at 90 K compared to 300 K (3.160(1) Å and 3.214(1) Å). The temperature dependency of the

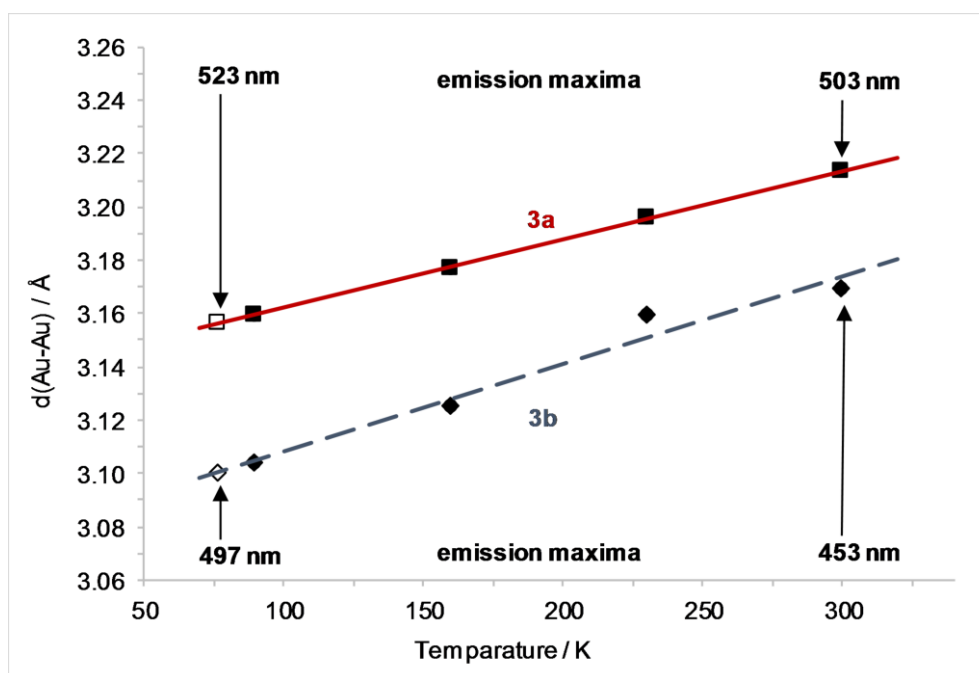


Figure 3. Temperature dependence of the Au...Au distance. Additionally, emission maxima are given for 77 K and 300 K.

Au...Au distance is of additional interest because **3a** and **3b** exhibit luminescence in the solid state. The emission shows a significant red shift with decreasing temperature (Figure 3). The luminescence properties are no longer present in the dissolved material, therefore it is assumed that the chainlike structures exist only in the solid state.^[27]

Frequently, interacting Au(I) complexes with short metal-metal separations show significant photoluminescence,^[9,28,29,30,31] while mononuclear or dissolved complexes mostly do not emit (for an exception see [32]). The solid state compounds show emissions, which are bright for **3a** ($\Phi_{\text{PL}} = 24\%$), but relatively weak for **3b** ($\Phi_{\text{PL}} \approx 1\%$). The ambient temperature emission bands with peak maxima at $\lambda_{\text{max}} = 503\text{ nm}$ (**3a**, $19\,880\text{ cm}^{-1}$) and at 453 nm (**3b**, $22\,080\text{ cm}^{-1}$), respectively, are very broad with halfwidths of about $3\,600\text{ cm}^{-1}$. For both compounds, weak shoulders occur at the high energy side of the broad bands (Table 1).^[33]

The related low-energy electronic transitions of the solid state materials are associated with the linear chain structures showing relatively short Au...Au separations. In this situation, a significant overlap of orbitals of adjacent metal centers occurs, leading to energy bands. The analysis of the molecular orbitals by DFT calculations of a tetrameric unit of **3a** reveals that the largest contributions to HOMO and LUMO are from the Au atoms (72% for HOMO and 77% for LUMO). The HOMO is essentially formed by mixing $5d_{z^2}$ and $6s$ orbitals of the adjacent Au atoms, while the LUMO is mainly formed by overlapping $6p_z$ orbitals. Thus, in the chain, the occupied valence band results predominantly from overlapping Au $5d_{z^2}$ orbitals mixed with Au $6s$ orbitals.^[28,29,30] The lowest unoccupied electron band, the conduction band, stems from overlapping Au $6p_z$ orbitals. These are mixed with small contributions of ligand orbitals.^[26,28,29,34]

Accordingly, the low-lying optical transitions can be tracked back to inter-band excitations by creating a hole in the valence band and an electron in the conduction band. However, this classification represents only a very coarse assignment, since

Table 1. Photophysical data of the linear chain Au...Au compounds. ^a Peak maximum, ^b shoulder, ^c photoluminescence quantum yield, ^d emission decay time measured at λ_{max} .

complex	300 K	77 K
[Au(H ₂ PBH ₂ NMe ₃) ₂][AlCl ₄] 3a	$\lambda_{\text{max}} = 503\text{ nm}^{\text{a}}$ sh. $\approx 450\text{ nm}^{\text{b}}$ $\Phi_{\text{PL}} = 24\%^{\text{c}}$ $\tau \approx 2\ \mu\text{s}^{\text{d}}$	$\lambda_{\text{max}} = 523\text{ nm}^{\text{a}}$ $\tau \approx 5\ \mu\text{s}^{\text{d}}$
[Au(H ₂ AsBH ₂ NMe ₃) ₂][AlCl ₄] 3b	$\lambda_{\text{max}} = 453\text{ nm}^{\text{a}}$ sh. $\approx 400\text{ nm}^{\text{b}}$ $\Phi_{\text{PL}} = 1\%^{\text{c}}$	$\lambda_{\text{max}} = 497\text{ nm}^{\text{a}}$

several important effects^[28,35,36] are not taken into account: (i) hole-electron interaction leading to an energy stabilization (formation of excitons), (ii) increase of aurophilic bonding and decrease of the Au...Au separation in the excited electronic state as compared to the electronic ground state S_0 ,^[37] (iii) exchange interaction leading to electronic singlet (S_1) and triplet (T_1) states. Thus, the emission observed stems from singlet and/or triplet states of a chain segment with a distorted (relaxed) geometry (self-trapped states). Usually, the related emission bands are very broad and unstructured, just as observed in the present case. A similar behavior has already been discussed for $[\text{Au}(\text{CN})_2]^-$ two-dimensional structures^[28] and for $[\text{Pt}(\text{CN})_4]^{2-}$ one-dimensional chain structures.^[35] The emission found for **3a** exhibits a relatively long decay time of about 2 μs (300 K) and 5 μs (77 K), respectively. Accordingly, this emission is assigned as a phosphorescence ($T_1 \rightarrow S_0$) that can be traced back to a geometry-relaxed (self-trapped) excited state predominantly being of $^3[(\text{Au}5d_z^2-6s)(\text{Au}6p_z)]$ character, whereby π^* ligand admixtures can also be of importance. For completeness, the mentioned weak shoulder at the blue energy side of the emission spectra of **3a,b** may tentatively be assigned, in analogy to Ref. [36], to a short-lived fluorescence stemming from a state of $^1[(\text{Au}5d_z^2-6s)(\text{Au}6p_z)]$ character.

With temperature decrease from $T = 300$ K to 77 K, the compounds **3a** and **3b** exhibit significant shortenings of the Au...Au separation by 0.057 Å and 0.069 Å, respectively (Figure 3). Such a decrease leads to a stronger overlap, in particular, of the orbitals of adjacent Au(I) centers. Accordingly, the electronic band gaps between valence and conduction bands become smaller, which is confirmed by calculations showing a decreasing HOMO-LUMO gap in the tetrameric unit. Thus, the related transition energies are red-shifted with temperature decrease. Indeed, this behavior is clearly observed for **3a,b** as marked in Figure 3 and Table 1. Also in this respect, the properties of the Au chains show a close similarity to those of the linear-chain $[\text{Pt}(\text{CN})_4]^{2-}$ compounds.^[38]

4.3 Conclusion

In summary, we were able to synthesize novel neutral Au(I) chloride compounds (**2a-d**) with phosphanyl- and arsanylborane ligands. Depending on the nature of the ligands, aurophilic interactions could be observed (**2a, 2b**). This was not found for the organic substituted phosphanylboranes, which reveal monomeric AuCl complexes. By abstraction of the chloride substituent by AlCl_3 and addition of a corresponding pnictogenylborane ligand, cationic Au(I) complexes are formed, which give, in the case of the parent ligands **1a,b**, infinite 1D chain products (**3a,b**). In the solid state, the Au...Au distances in the cationic chains of **3a,b** decrease with lower temperature and reveal

luminescence. The emission shows a red shift with temperature decrease, being correlated with decreasing intermetallic distances. These findings were confirmed by DFT calculations. Therefore, light-emitting cationic chain complexes of Au(I) with non-bridging phosphine and arsine ligands were obtained for the first time, resulting in remarkably short Au \cdots Au distances. Moreover, unprecedented primary arsine gold complexes could be synthesized (**2b**, **3b**), which show a high tendency to form multiple Au \cdots Au bonds, resulting in both cases in 1D chain arrangements in the solid state. Further investigations of the influences between ligand design, solid-state structure and luminescence properties are underway.

4.4 References

- [1] a) R.V. Parish, S. M. Cottrill, *Gold Bull.* **1987**, *20*, 3-12; b) D. Michael P. Mingos, *Dalton Trans.* **1996**, *5*, 561-566.
- [2] a) C. E. Strasser, V. J. Catalano, *J. Am. Chem. Soc.* **2010**, *132*, 10009-10011; b) A. Laguna, T. Lasanta, J. M. Lopez-de-Luzuriaga, M. Monge, P. Naumov, M. E. Olmos, *J. Am. Chem. Soc.* **2010**, *132*, 456-457; c) E. J. Fernández, J. M. Lopez-de-Luzuriaga, M. Monge, M. E. Olmos, R. C. Puelles, A. Laguna, A. A. Mohamed, J. P. Fackler Jr, *Inorg. Chem.* **2008**, *47*, 8069-8076; d) Y. Sagara, T. Kato, *Nat. Chem.* **2009**, *1*, 605-610.
- [3] a) V. K.-M. Au, K. M.-C. Wong, D. P.-K. Tsang, M.-Y. Chan, N. Zhu and V. W.-W. Yam, *J. Am. Chem. Soc.* **2010**, *132*, 14273-14278; b) R. C. Evans, P. Douglas, C. J. Winscom, *Coord. Chem. Rev.* **2006**, *250*, 2093-2126.
- [4] a) H. Schmidbaur, A. Schier, *Organometallics* **2010**, *29*, 2-23; b) J. Petuskova, H. Bruns, M. Alcarazo, *Angew. Chem. Int. Ed.* **2011**, *50*, 3799-3802; c) G. Zhang, Y. Peng, L. Cui, L. Zhang, *Angew. Chem. Int. Ed.* **2009**, *48*, 3112-3115; d) L. Cui, Y. Peng, L. Zhang, *J. Am. Chem. Soc.* **2009**, *131*, 8394-8395; e) A. S. K. Hashmi, S. Pankajakshan, M. Rudolph, E. Enns, T. Bander, F. Rominger, W. Frey, *Adv. Synth. Catal.* **2009**, *351*, 2855-2975; f) S. Han, Y. Y. Yoon, O. Jung, Y. Lee, *Chem. Commun.* **2011**, *47*, 10689-10691.
- [5] H. Schmidbaur, A. Schier, *Chem. Soc. Rev.* **2012**, *41*, 370-412.
- [6] H. Schmidbaur, *Gold Bull.* **2000**, *33*, 3-10.
- [7] a) M. Streitberger, A. Schmied, E. Hey-Hawkins, *Inorg. Chem.* **2014**, *53*, 6794-6804; b) H. Schmidbaur, A. Wohlleben, F. Wagner, O. Orama, G. Huttner, *Chem. Ber.* **1977**, *110*, 1748-1754; c) J.-C. Shi, B.-S. Kang, T. C. W. Mak, *J. Chem. Soc., Dalton Trans.* **1997**, 2171-2176; d) A. Himmelspach, M. Finze, S. Raub, *Angew. Chem. Int. Ed.* **2011**, *50*, 2628-2631; e) V. Pawlowski, H. Kunkely, A. Vogler, *Inorg. Chim. Acta* **2004**, *257*, 1309-1312; f) D. V. Partyka, T. S. Teets, M. Zeller, J. B. Updegraff, A. D. Hunter, T. G. Gray, *Chem. Eur. J.* **2012**, *18*, 2100-2112; g) A. R. Browne, N. Deligonul, B. L. Anderson, A. L. Rheingold, T. G. Gray, *Chem. Eur. J.* **2014**, *20*, 17552-17564; h) D. Y. Melgarejo, G. M. Chiarella, J. P. Fackler Jr., *Inorg. Chem.* **2016**, *55*, 11883-11889;
- [8] A. Battisti, O. Bellina, P. Diversi, S. Losi, F. Marchetti, P. Zanella, *Eur. J. Inorg. Chem.* **2007**, *6*, 865-875.
- [9] a) V. W.-W. Yam, K. K.-W. Lo, *Chem. Soc. Rev.*, **1999**, *28*, 323-334; b) A. Vogler, H. Kunkely, *Coord. Chem. Rev.* **2001**, *219-221*, 489-507; c) V. W.-W. Yam, V. K.-M. Au, S. Y.-L. Leung, *Chem. Rev.* **2015**, *115*, 7589-7728; d) J. T. Markert, N.

- Blom, G. Roper, A. D. Perregaux, N. Nagasundaram, M. R. Corson, A. Ludi, J. K. Nagle, H. H. Patterson, *Chem. Phys. Letters* **1985**, *118*, 258-262.
- [10] a) J. R. Shakirova, E. V. Grachova, V. V. Sizov, G. L. Starova, I. O. Koshevoy, A. S. Melnikov, M. C. Gimeno, A. Laguna, S. P. Tunik, *Dalton Trans.* **2017**, *46*, 2516–2523, b) M. C. Gimeno, A. Laguna in *Comprehensive Coordination Chemistry II*, Vol. 6, Elsevier Pergamon, Amsterdam, **2004**, pp. 911-1145; c) L. D. Earl, J. K. Nagle, M. O. Wolf, *Inorg. Chem.* **2014**, *53*, 7106-7117.
- [11] a) C. A. Tolman, *Chem. Rev.* **1977**, *77*, 313-348; b) K. Angermaier, E. Zeller, H. Schmidbaur, *J. Organomet. Chem.* **1994**, *472*, 371-376.
- [12] R. J. Puddephatt, *The Chemistry of Gold*, Elsevier, Amsterdam, **1978**.
- [13] a) H. Schmidbaur, G. Weidenhiller, O. Steigelmann, G. Müller, *Z. Naturforsch.* **1990**, *45b*, 747-752; b) S. Ahrland, B. Aurivillius, K. Dreisch, B. Norén, Å. Oskarsson, *Acta Chem. Scand.* **1992**, *A46*, 262-265.
- [14] a) M. Bardají, P. G. Jones, A. Laguna, A. Moracho, A. K. Fischer, *J. Organomet. Chem.* **2002**, *648*, 1-7; b) U. M. Tripathi, A. Bauer, H. Schmidbaur, *J. Chem. Soc., Dalton Trans.* **1997**, 2865-2868; c) J. Vicente, A. Arcas, M. Mora, X. Solans, M. Font-Altaba, *J. Organomet. Chem.* **1986**, *309*, 369-378; d) R. Usón, A. Laguna, J. Vicente, *Synth. React. Inorg. Met.-Org. Chem.* **1997**, *7*, 463-496; e) P. G. Jones, A. F. Williams, *J. Chem. Soc., Dalton Trans.* **1977**, 1430-1434; f) R. Usón, A. Laguna, J. Pardo, *Synth. React. Inorg. Met.-Org. Chem.* **1974**, *4*, 499-513; g) G. E. Coates, C. Parkin, *J. Chem. Soc.* **1962**, 3220-3226; h) N. A. Barnes, K. R. Flower, S. A. Fyyaz, S. M. Godfrey, A. T. McGown, P. J. Miles, R. G. Pritchard, J. E. Warren, *CrystEngComm*, **2010**, *12*, 784-794.
- [15] a) D. Rios, D. M. Pham, J. C. Fettinger, M. M. Olmstead, A. L. Balch, *Inorganic Chemistry* **2008**, *47*, 3442-3451; b) R. L. White-Morris, M. M. Olmstead, F. Jiang, A. L. Balch, *Inorg. Chem.* **2002**, *41*, 2313-2315; c) M. Saitoh, A. L. Balch, J. Yuasa, T. Kawai, *Inorg. Chem.* **2010**, *49*, 7129-7134; d) J. Y. Z. Chiou, S. C. Luo, W. C. You, A. Bhattacharyya, C. S. Vasam, C. H. Huang, I. J. B. Lin, *Eur. J. Inorg. Chem.* **2009**, *13*, 1950–1959; e) P. C. Kunz, C. Wetzel, S. Kögel, M. U. Kassack, B. Spingler, *Dalton Trans.* **2011**, *40*, 35–37.
- [16] a) K.-C. Schwan, A. Y. Timoskin, M. Zabel, M. Scheer, *Chem. Eur. J.* **2006**, *12*, 4900-4908; b) C. Marquardt, A. Adolf, A. Stauber, M. Bodensteiner, A. V. Virovets, A. Y. Timoshkin, M. Scheer, *Chem. Eur. J.* **2013**, *19*, 11887-11891; c) C. Marquardt, O. Hegen, M. Hautmann, G. Balázs, M. Bodensteiner, A. V. Virovets, A. Y. Timoshkin, M. Scheer, *Angew. Chem. Int. Ed.* **2015**, *54*, 13122-13125.
- [17] a) C. Marquardt, T. Kahoun, A. Stauber, G. Balázs, M. Bodensteiner, A. Y. Timoshkin, M. Scheer, *Angew. Chem. Int. Ed.* **2016**, *55*, 14828-14832; b) C. Marquardt, C. Thoms, A. Stauber, G. Balázs, M. Bodensteiner, M. Scheer, *Angew. Chem. Int. Ed.* **2014**, *53*, 3727-3730.
- [18] a) C. Marquardt, T. Jurca, K.-C. Schwan, A. Stauber, A. V. Virovets, G. R. Whittell, I. Manners, M. Scheer, *Angew. Chem. Int. Ed.* **2015**, *54*, 13782-13786; b) A. Stauber, T. Jurca, C. Marquardt, M. Fleischmann, M. Seidl, G. R. Whittell, I. Manners, M. Scheer, *Eur. J. Inorg. Chem.* **2016**, 2684-2687.
- [19] C. Thoms, C. Marquardt, M. Bodensteiner, M. Scheer, *Angew. Chem. Int. Ed.* **2013**, *52*, 5150-5154.
- [20] K.-C. Schwan, A. Adolf, M. Bodensteiner, M. Zabel, M. Scheer, *Z. Anorg. Allg. Chem.* **2008**, *634*, 1383-1387.
- [21] See supporting information section 4.5.4.
- [22] N. Runeberg, M. Schütz, H.-J. Werner, *J. Chem. Phys.* **1999**, *110*, 7210-7215; also see supporting information section 4.5.7.
- [23] See supporting information section 4.5.4. (double due to transfer from publication)
- [24] R. L. White-Morris, M. M. Olmstead, F. Jiang, D. S. Tinti, A. L. Balch, *J. Am. Chem. Soc.* **2002**, *124*, 2327-2336; Compare values for d(Au···Au) at the same

- temperature (90 K): 3.1595(4) Å for **3a**, 3.1037(4) Å for **3b** vs. 3.1882(1) Å for [Au{C(NHMe)₂}₂](PF₆).
- [25] cf. a) M. M. Ghimire, V. N. Nesterov, M. A. Omary, *Inorg. Chem.* **2017**, *56*, 12086–12089; b) J. L. Korčok, M. J. Katz, D. B. Leznoff, *J. Am. Chem. Soc.* **2009**, *131*, 4866–4871; c) A. L. Goodwin, M. Calleja, M. J. Conterio, M. T. Dove, J. S. O. Evans, D. A. Keen, L. Peters, M. G. Tucker, *Science* **2008**, *319*, 794–797; d) A. L. Goodwin, D. A. Keen, M. G. Tucker, M. T. Dove, L. Peters, J. S. O. Evans, *J. Am. Chem. Soc.* **2008**, *130*, 9660–9661;
- [26] For details of the energetics of the formation of this tetrameric unit, cf. supporting information section 4.5.7.
- [27] C. Yang, M. Messerschmidt, P. Coppens, M. A. Omary, *Inorg. Chem.* **2006**, *45*, 6592–6594.
- [28] H. Yersin, U. Riedl, *Inorg. Chem.* **1995**, *34*, 1642–1645.
- [29] H. Yersin, D. Trümbach, J. Strasser, H. H. Patterson, Z. Assefa, *Inorg. Chem.* **1998**, *37*, 3209–3216.
- [30] T. Tanase, M. Chikanishi, K. Morita, K. Nakamae, B. Kure, T. Nakajima, *Chem. Asian. J.* **2015**, *10*, 2619–2623.
- [31] a) S. Y. Ho, E. C.-C. Cheng, E. R. T. Tiekink, V. W.-W. Yam, *Inorg. Chem.* **2006**, *45*, 8165–8174; b) C.-M. Che, H.-L. Kwong, C.-K. Poon, V. W.-W. Yam, *Dalton Trans.* **1990**, 3215–3219; c) Y. Chen, G. Cheng, K. Li, D. P. Shelar, W. Lu, C.-M. Che, *Chem. Sci.* **2014**, *5*, 1348–1353; d) R. J. Roberts, N. Bélanger-Desmarais, C. Reber, D. B. Leznoff; *Chem. Commun.* **2014**, *50*, 3148–3150.
- [32] R. Czerwieniec, T. Hofbeck, O. Crespo, A. Laguna, M. C. Gimeno, H. Yersin, *Inorg. Chem.* **2010**, *49*, 3764–3767.
- [33] Also see supporting information section 4.5.8.
- [34] J.-G. Kang, Y.-K. Jeong, S.-I. Oh, H.-J. Kim, Ch. Park, E. R. R. Tiekink, *Bull. Korean. Soc.* **2010**, *31*, 2151–2157.
- [35] a) H. Yersin, G. Gliemann, *Ann. N. Y. Acad. Sci.* **1978**, *313*, 539–559; b) G. Gliemann, H. Yersin, *Clusters. Structure and Bonding* **1985**, *62*, 87–153; c) U. Rössler, H. Yersin, *Phys. Rev. B* **1982**, *26*, 3187–3191.
- [36] R. K. Arvapally, P. Sinha, S. R. Hettiarachchi, N. L. Coker, Ch. E. Bedel, H. H. Patterson, R. C. Elder, A. K. Wilson, M. A. Omary, *J. Phys. Chem.* **2007**, *111*, 10689–10699.
- [37] a) Q.-J. Pan, H.-X. Zhang, *Inorg. Chem.* **2004**, *43*, 593–601; b) R. K. Arvapally, P. Sinha, S. R. Hettiarachchi, N. L. Coker, C. E. Bedel, H. H. Patterson, R. Elder, A. K. Wilson, M. A. Omary, *J. Phys. Chem. C* **2007**, *111*, 10689–10691; c) G. Cui, X. Y. Cao, W. H. Fang, M. Dolg, W. Thiel, *Angew. Chem. Int. Ed.* **2013**, *52*, 10281–10285.
- [38] W. Daniels, H. Yersin, H. v. Philipsborn, G. Gliemann, *Solid State Commun.* **1979**, *30*, 353–355.

4.5 Supporting Information

4.5.1 General information

All manipulations were performed under an atmosphere of dry argon using standard glovebox and Schlenk techniques. All solvents are degassed and purified by standard procedures.

The compounds $RR'EBH_2 \cdot NMe_3$ (**1a**: E = P; R,R' = H; **1b**: E = As; R,R' = H; **1c**: E = P; R = H, R' = *t*Bu, **1d**: E = P, R,R' = Ph),^[1] were prepared according to literature procedures.

The NMR spectra were recorded on an Avance 400 spectrometer (1H : 400.13 MHz, ^{31}P : 161.976 MHz, ^{11}B : 128.378 MHz, $^{13}C\{^1H\}$: 100.623 MHz with δ [ppm] referenced to external $SiMe_4$ (1H , ^{13}C), H_3PO_4 (^{31}P) or $BF_3 \cdot Et_2O$ (^{11}B).

IR spectra were measured on a DIGILAB (FTS 800) FT-IR spectrometer and on a Thermo Scientific Nicolet iS5. All mass spectra were recorded on a Finnigan MAT 95 (FDMS and EI-MS) and a Jeol AccuTOF GCX (LIFDI).

The C, H, N analyses were measured on an Elementar Vario EL III apparatus.

4.5.2 Syntheses of described compounds

Synthesis of $[AuCl(H_2PBH_2NMe_3)]$ (2a**):** A solution of 21 mg (0.2 mmol) $H_2PBH_2NMe_3$ (**1a**) in 0.4 mL toluene is added to a stirred solution of 64 mg (0.2 mmol) $AuCl(tht)$ in cold 10 mL CH_2Cl_2 ($-80^\circ C$). The solution was warmed to room temperature and stirred for 1 hour. Addition of 100 mL *n*-hexane leads to precipitation of **2a**. The supernatant is decanted off, the remaining solid is washed two times with small amounts of *n*-hexane and dried under reduced pressure. Single Crystals suitable for X-ray structure analysis are obtained by layering of concentrated CH_2Cl_2 solution with *n*-hexane. **2a** crystallizes as colourless blocks.

Yield of **2a**: 49 mg (73%). 1H -NMR (CD_2Cl_2 , $25^\circ C$): δ [ppm] = 2.25 (br, 2H, BH_2), 2.84 (s, 9H, $N(CH_3)_3$), 3.69 (dm, $^1J_{H,P}$ = 328 Hz, 2H, PH_2). ^{11}B -NMR (CD_2Cl_2 , $25^\circ C$): δ [ppm] = -9.41 (br). $^{11}B\{^1H\}$ -NMR (CD_2Cl_2 , $25^\circ C$): δ [ppm] = -9.41 (d, $^1J_{B,P}$ = 59 Hz). ^{31}P -NMR (CD_2Cl_2 , $25^\circ C$): δ [ppm] = -138.5 (br). $^{31}P\{^1H\}$ -NMR (CD_2Cl_2 , $25^\circ C$): δ [ppm] = -138.5 (br). IR(KBr) : $\tilde{\nu}$ [cm^{-1}] = 3002 (w, CH), 2990 (w, CH), 2967 (w, CH), 2432 (m, BH), 2397 (m, BH), 2392 (m, BH), 2343 (w, PH), 2295 (w, PH), 1479 (m), 1471 (m), 1466 (m), 1406 (w), 1251 (w), 1242 (m), 1152 (m), 1128 (s), 1094 (m), 1073 (s), 1066 (vs), 1049 (vs), 1009 (s), 975(m), 950 (w), 863 (m), 846 (s), 790 (vs), 705 (m), 682 (w), 667 (w), 474 (w), 410 (w). EI-MS (70eV): m/z = 337 (100%, $[AuCl(PH_2BH_2NMe_3)]^+$). Elemental analysis

(%) calculated for $C_3H_{13}AuBCINP$ (**2a**): C: 10.68, H: 3.88, N: 4.15; found: C: 10.89, H: 3.81, N: 4.22.

Synthesis of $[AuCl(H_2AsBH_2NMe_3)]$ (**2b**): A solution of 37 mg (0.25 mmol) $H_2AsBH_2NMe_3$ (**1b**) in 0.25 mL toluene is added to a stirred solution of 80 mg (0.25 mmol) $AuCl(tht)$ in cold 10 mL CH_2Cl_2 ($-80^\circ C$). The solution was warmed shortly to room temperature before cooling the solution again to $-80^\circ C$. The solution is filtered off into 100 mL cold *n*-hexane ($-80^\circ C$), which leads to precipitation of **2b**. The supernatant is decanted off, the remaining solid is washed once with 5 mL toluene and two times with small amounts of *n*-hexane and dried under reduced pressure. Single Crystals suitable for X-ray structure analysis are obtained by layering of concentrated CH_2Cl_2 solution with *n*-hexane. **2b** crystallizes as colourless blocks.

Yield of **2b**: 61 mg (64%). 1H -NMR (CD_2Cl_2 , $25^\circ C$): δ [ppm] = 2.55 (q, 2H, $^1J_{H,B} = 122$ Hz, BH_2), 2.66 (s, 9H, $N(CH_3)_3$), 2.66 (s, 2H, AsH_2). ^{11}B -NMR (CD_2Cl_2 , $25^\circ C$): δ [ppm] = -0.41 (t, $^1J_{H,B} = 122$ Hz). $^{11}B\{^1H\}$ -NMR (CD_2Cl_2 , $25^\circ C$): δ [ppm] = -0.41 (s). IR(ATR) : $\tilde{\nu}$ [cm^{-1}] = 3021 (w, CH), 3005 (w, CH), 3958 (m, CH), , 2928 (w, CH), 2899 (w, CH), 2446 (m, BH), 2413 (s, BH), 2347 (m, BH), 2261 (w, AsH), 2220 (w, AsH), 2194 (w, AsH), 1479 (m), 1470 (s), 1457 (m), 1446 (w), 1403 (m), 1256 (s), 1184 (s), 1129 (vs), 1092 (vs), 1005 (s), 982 (vs), 948 (m), 797 (s), 696 (m), 662 (w), 637 (s). ESI-MS (MeOH): cation: $m/z = 382$ (100%, $[AuCl(H_2AsBH_2NMe_3)H]^+$). Elemental analysis for Au(I)-arsine compounds could not be carried out without formation of black byproduct.

Synthesis of $[AuCl(^tBuHPBH_2NMe_3)]$ (**2c**): 40 mg (0.25 mmol) tBuHPBH_2NMe_3 (**1c**) is added to a stirred solution of 80 mg (0.25 mmol) $AuCl(tht)$ in cold 2.5 mL CH_2Cl_2 ($-80^\circ C$). The solution was warmed to room temperature and stirred for 1 hour. Addition of 50 mL cold *n*-pentane leads to precipitation of **2c**. The supernatant is decanted off, the remaining solid is washed two times with small amounts of cold *n*-pentane and dried under reduced pressure. Single Crystals suitable for X-ray structure analysis are obtained by layering of concentrated CH_2Cl_2 solution with *n*-hexane at $0^\circ C$. **2c** crystallizes as colourless blocks.

Yield of **2c**: 91 mg (93%). 1H -NMR (CD_2Cl_2 , $25^\circ C$): δ [ppm] = 1.24 (d, $^3J_{H,P} = 16$ Hz, 9H, $C(CH_3)_3$), 2.15 (q, $^1J_{H,B} = 106$ Hz, 2H, BH_2), 2.86 (s, 9H, $N(CH_3)_3$), 4.05 (ddd, 1H, $^1J_{H,P} = 333$ Hz, $^3J_{H,H} = 10$ Hz, $^3J_{H,H} = 5$ Hz, PH). ^{11}B -NMR (CD_2Cl_2 , $25^\circ C$): δ [ppm] = -9.64 (m, $^1J_{H,B} = 106$ Hz, $^1J_{B,P} = 75$ Hz, BH_2). $^{11}B\{^1H\}$ -NMR (CD_2Cl_2 , $25^\circ C$): δ [ppm] = -9.64 (d, $^1J_{B,P} = 75$ Hz). ^{31}P -NMR (CD_2Cl_2 , $25^\circ C$): δ [ppm] = -32.1 (d, br $^1J_{H,P} = 333$ Hz, PH).

$^{31}\text{P}\{^1\text{H}\}$ -NMR (CD_2Cl_2 , 25°C): δ [ppm] = -32.1 (q, $^1J_{\text{B,P}} = 80$ Hz, PH). IR(ATR) : $\tilde{\nu}$ [cm^{-1}] = 2972 (w, CH), 2950 (w, CH), 2899 (w, CH), 2862 (w, CH), 2423 (m, BH), 2392 (m, BH), 2326 (w, PH), 2305 (w, PH), 1469 (m), 1458 (m), 1408 (w), 1402 (w), 1392 (w), 1363 (m), 1253 (w), 1244 (w), 1209 (w), 1182 (w), 1158 (m), 1124 (s), 1074 (s), 1034 (w), 1025 (w), 1014 (m), 973 (m), 956 (w), 878 (w), 857 (s), 846 (s), 822 (m), 731 (w), 688 (m), 662 (w), 646 (m), 604 (w), 524 (w), 514(w), 479 (m), 465 (w), 442(m), 422(w), 414 (w). EI-MS (70eV): $m/z = 393$ (100%, $[\text{AuCl}(\text{t}^i\text{BuHPBH}_2\text{NMe}_3)]^+$). Elemental analysis (%) calculated for $\text{C}_7\text{H}_{21}\text{AuBCINP}$ (**2c**): C: 21.37, H: 5.38, N: 3.56; found: C: 22.17, H: 5.21, N: 3.44.

Synthesis of $[\text{AuCl}(\text{Ph}_2\text{PBH}_2\text{NMe}_3)]$ (**2d**): A solution of 257 mg (1 mmol) $\text{Ph}_2\text{PBH}_2\text{NMe}_3$ (**1d**) in 3 mL CH_2Cl_2 is added to a stirred solution of 321 mg (1 mmol) $\text{AuCl}(\text{tht})$ in cold 7 mL CH_2Cl_2 (-80°C). The solution was warmed to room temperature and stirred for 1 hour. Addition of 100 mL *n*-hexane leads to precipitation of **2d**. The supernatant is decanted off, the remaining solid is washed two times with small amounts of *n*-hexane and dried under reduced pressure. Single Crystals suitable for X-ray structure analysis are obtained by layering of concentrated CH_2Cl_2 solution with *n*-hexane. **2d** crystallizes as colourless rods.

Yield of **2d**: 380 mg (78%). ^1H -NMR (CD_2Cl_2 , 25°C): δ [ppm] = 2.76 (q, 2H, $^1J_{\text{H,B}} = 80$ Hz, BH_2), 2.82 (s, 9H, $\text{N}(\text{CH}_3)_3$), 7.37 (m, 6H, *m*-/*p*-H Ph), 7.77 (m, 4H, *o*-H Ph). ^{11}B -NMR (CD_2Cl_2 , 25°C): δ [ppm] = -6.36 (m, br $^1J_{\text{H,B}} = 80$ Hz, $^1J_{\text{B,P}} = 75$ Hz, BH_2). $^{11}\text{B}\{^1\text{H}\}$ -NMR (CD_2Cl_2 , 25°C): δ [ppm] = -6.36 (d, br $^1J_{\text{B,P}} = 75$ Hz). ^{31}P -NMR (CD_2Cl_2 , 25°C): δ [ppm] = -5.70 (m, br). $^{31}\text{P}\{^1\text{H}\}$ -NMR (CD_2Cl_2 , 25°C): δ [ppm] = -5.70 (m, br $^1J_{\text{B,P}} = 95$ Hz). IR(ATR) : $\tilde{\nu}$ [cm^{-1}] = 3067 (w, CH), 3050 (w, CH), 3017 (w, CH), 2995 (w, CH), 2935 (w, CH), 2910 (w, CH), 2436 (m, BH), 2406 (m, BH), 1475 (m), 1459 (m), 1442 (s), 1431 (m), 1407 (w), 1400 (w), 1304 (w), 1247 (m), 1241 (m), 1146 (m), 1156 (m), 1121 (s), 1099 (m), 1066 (s), 1030 (w), 1009 (m), 999(w), 971 (w), 949 (w), 926 (w), 912 (w), 859 (s), 764 (w), 752 (s), 741 (w), 691 (s), 650 (m), 636 (s), 615 (w), 512 (s), 488 (m), 479 (w), 457 (m), 430 (m), 416 (w), 405 (w). EI-MS (70eV): $m/z = 489$ (100%, $[\text{AuCl}(\text{Ph}_2\text{PBH}_2\text{NMe}_3)]^+$). Elemental analysis (%) calculated for $\text{C}_{15}\text{H}_{21}\text{AuBCINP}$ (**2d**): C: 36.80, H: 4.32, N: 2.86; found: C: 36.84, H: 4.35, N: 2.85.

Synthesis of $[\text{Au}(\text{H}_2\text{PBH}_2\text{NMe}_3)_2][\text{AlCl}_4]$ (**3a**): A solution of 26 mg (0.25 mmol) $\text{H}_2\text{PBH}_2\text{NMe}_3$ (**1a**) in 0.5 mL toluene is added to a stirred solution of 80 mg (0.25 mmol) $\text{AuCl}(\text{tht})$ in cold 7 mL CH_2Cl_2 (-80°C). A cooled solution of 34mg (0.25mmol) AlCl_3 and 26 mg (0.25 mmol) $\text{H}_2\text{PBH}_2\text{NMe}_3$ in 5 mL CH_2Cl_2 (-80°C) is added to the reaction

mixture. The solution is stirred for 1 hour and was warmed to room temperature. Addition of 100 mL *n*-hexane leads to precipitation of **3a**. The supernatant is decanted off, the remaining solid is washed two times with small amounts of *n*-hexane and dried under reduced pressure. Single Crystals suitable for X-ray structure analysis are obtained by storing a concentrated solution of **3a** in 1,2-Difluorobenzene at -30°C. **3a** crystallizes as colourless rods.

Yield of **3a**: 121 mg (82%). ¹H-NMR (CD₂Cl₂, 25°C): δ [ppm] = 2.29 (q, 4H, ¹J_{H,B} = 116 Hz, BH₂), 2.82 (s, 18H, N(CH₃)₃); 3.88 (d, 4H, ¹J_{H,P} = 333 Hz, PH₂). ¹¹B-NMR (CD₂Cl₂, 25°C): δ [ppm] = -9.68 (m, br ¹J_{H,B} = 116 Hz, ¹J_{B,P} = 58 Hz, BH₂). ¹¹B{¹H}-NMR (CD₂Cl₂, 25°C): δ [ppm] = -9.68 (d, br ¹J_{B,P} = 58 Hz). ³¹P-NMR (CD₂Cl₂, 25°C): δ [ppm] = -133.00 (br). ³¹P{¹H}-NMR (CD₂Cl₂, 25°C): δ [ppm] = -133.00 (br). IR(KBr) : $\tilde{\nu}$ [cm⁻¹] = 3064 (w, CH), 3015 (w, CH), 2953 (w, CH), 2425 (s, BH), 2387 (s, BH), 2294 (m, PH), 2139 (w), 1645 (m), 1483 (s), 1455 (s), 1409 (m), 1244 (m). ESI-MS (CH₂Cl₂): cation: *m/z* = 407 (100%, [Au(PH₂BH₂NMe₃)₂]⁺). Elemental analysis (%) calculated for C₆H₂₆AuP₂B₂N₂AlCl₄ (**3a**): C: 12.52, H: 4.55, N: 4.87; found: C: 12.26, H: 5.01, N: 4.75.

Synthesis of [Au(H₂AsBH₂NMe₃)₂][AlCl₄] (**3b**): A solution of 37 mg (0.25 mmol) H₂AsBH₂NMe₃ (**1b**) in 0.25 mL toluene is added to a stirred solution of 80 mg (0.25 mmol) AuCl(tht) in cold 7 mL CH₂Cl₂ (-80°C). A cooled solution of 34mg (0.25mmol) AlCl₃ and 37 mg (0.25 mmol) H₂AsBH₂NMe₃ in 5 mL CH₂Cl₂ (-80°C) is added to the reaction mixture. The solution is stirred for 1 hour and was slowly warmed to room temperature. Addition of 100 mL *n*-hexane leads to precipitation of **3b**. The supernatant is decanted off, the remaining solid is washed two times with small amounts of *n*-hexane and dried under reduced pressure. Single Crystals suitable for X-ray structure analysis are obtained by storing a concentrated solution of **3b** in 1,2-Difluorobenzene at -30°C. **3b** crystallizes as colourless rods.

Yield of **3b**: 98 mg (59%). ¹H-NMR (CD₂Cl₂, 25°C): δ [ppm] = 2.51 (q, 4H, ¹J_{H,B} = 123 Hz, BH₂), 2.82 (s, 4H, AsH₂); 2.86 (s, 18H, N(CH₃)₃). ¹¹B-NMR (CD₂Cl₂, 25°C): δ [ppm] 0.67 (t, ¹J_{H,B} = 123 Hz, BH₂). ¹¹B{¹H}-NMR (CD₂Cl₂, 25°C): δ [ppm] = 0.67 (s). IR(ATR) : $\tilde{\nu}$ [cm⁻¹] = 3037 (m, CH), 2950 (w, CH), 2439 (m, BH), 2402 (s, BH), 2308 (w), 2143 (m, AsH), 2076 (w), 1636 (s), 1480 (s), 1465 (s), 1407 (m), 1242 (m), 1185 (w), 1154 (m), 1116 (s), 1065 (s), 1049 (vs), 1007 (m), 974 (m), 951 (m), 852 (s), 800 (m), 723 (w). ESI-MS (MeCN): cation: *m/z* = 496 (100%, [Au(AsH₂BH₂NMe₃)₂H]⁺). Elemental analysis for Au(I)-arsine compounds could not be carried out without formation of black byproduct.

Synthesis of $[\text{Au}(\text{}^t\text{BuHPBH}_2\text{NMe}_3)_2][\text{AlCl}_4]$ (3c**):** 40 mg (0.25 mmol) $\text{}^t\text{BuHPBH}_2\text{NMe}_3$ (**1c**) is added to a stirred solution of 80 mg (0.25 mmol) $\text{AuCl}(\text{tht})$ in cold 7 mL CH_2Cl_2 (-80°C). A cooled solution of 34mg (0.25mmol) AlCl_3 and 40 mg (0.25 mmol) $\text{}^t\text{BuHPBH}_2\text{NMe}_3$ in 5 mL CH_2Cl_2 (-80°C) is added to the reaction mixture. The solution is stirred for 1 hour and was warmed to room temperature. Addition of 100 mL *n*-pentane leads to precipitation of **3c** as an oily viscous liquid. The supernatant is decanted off, the remaining oil is washed two times with small amounts of *n*-pentane and dried under reduced pressure to give a white solid. Single Crystals suitable for X-ray structure analysis are obtained by storing a concentrated solution of **3c** in 1,2-Difluorobenzene at -30°C. **3c** crystallizes as colourless blocks.

Yield of **3c**: 157 mg (91%). $^1\text{H-NMR}$ (CD_2Cl_2 , 25°C): δ [ppm] = 1.27 (m, $^3J_{\text{H,P}} = 8$ Hz, 18H, $\text{C}(\text{CH}_3)_3$), 2.28 (q, $^1J_{\text{H,B}} = 93$ Hz, 4H, BH_2), 2.86 (s, 18H, $\text{N}(\text{CH}_3)_3$), 4.26 (ddd, 2H, $^1J_{\text{H,P}} = 322$ Hz, $^3J_{\text{H,H}} = 10$ Hz, $^3J_{\text{H,H}} = 5$ Hz, PH). $^{11}\text{B-NMR}$ (CD_2Cl_2 , 25°C): δ [ppm] = -9.03 (m, br, BH_2). $^{11}\text{B}\{^1\text{H}\}$ -NMR (CD_2Cl_2 , 25°C): δ [ppm] = -9.03 (br). $^{31}\text{P-NMR}$ (CD_2Cl_2 , 25°C): δ [ppm] = -19.3 (d, br $^1J_{\text{H,P}} = 290$ Hz, PH). $^{31}\text{P}\{^1\text{H}\}$ -NMR (CD_2Cl_2 , 25°C): δ [ppm] = -19.3 (br, PH). IR(CH_2Cl_2) : $\tilde{\nu}$ [cm^{-1}] = 2996 (w, CH), 2954 (m, CH), 2899 (w, CH), 2864 (w, CH), 2436 (m, BH), 2407 (m, BH), 2332 (w, PH), 1464 (m), 1407 (w), 1394 (w), 1366 (m), 1263 (m), 1243 (w), 1178 (w), 1159 (w), 1263 (s), 1077 (s), 1015 (m), 976 (m), 856 (m), 812 (w), 639 (w), 492 (s), 465 (m), 445 (s). ESI-MS (CH_2Cl_2): cation: $m/z = 519$ (100%, $[\text{Au}(\text{}^t\text{BuHPBH}_2\text{NMe}_3)_2]^+$). Elemental analysis (%) calculated for $\text{C}_{14}\text{H}_{42}\text{AuB}_2\text{N}_2\text{P}_2\text{AlCl}_4$ (**3c**): C: 21.37, H: 5.38, N: 3.56; found: C: 22.17, H: 5.21, N: 3.44.

Synthesis of $[\text{Au}(\text{Ph}_2\text{PBH}_2\text{NMe}_3)_2][\text{AlCl}_4]$ (3d**):** 64 mg (0.25 mmol) $\text{Ph}_2\text{PBH}_2\text{NMe}_3$ (**1d**) is added to a stirred solution of 80 mg (0.25 mmol) $\text{AuCl}(\text{tht})$ in cold 7 mL CH_2Cl_2 (-80°C). A cooled solution of 34mg (0.25mmol) AlCl_3 and 64 mg (0.25 mmol) $\text{Ph}_2\text{PBH}_2\text{NMe}_3$ in 5 mL CH_2Cl_2 (-80°C) is added to the reaction mixture. The solution is stirred for 1 hour and was warmed to room temperature. Addition of 100 mL *n*-hexane leads to precipitation of **3d**. The supernatant is decanted off, the remaining solid is washed two times with small amounts of *n*-hexane and dried under reduced pressure to give a white solid. Single Crystals suitable for X-ray structure analysis could not be obtained. Storing a concentrated solution of **3d** in 1,2-Difluorobenzene at -30°C gives repeatedly single crystals of **2d**.

Yield of **3d**: 150 mg (68%). $^1\text{H-NMR}$ (CD_2Cl_2 , 25°C): δ [ppm] = 2.76 (br, 4H, BH_2), 2.79 (s, 18H, $\text{N}(\text{CH}_3)_3$), 7.44 (m, 12H, *m*-/*p*-H Ph), 7.70 (m, 8H, *o*-H Ph). $^{11}\text{B-NMR}$ (CD_2Cl_2 , 25°C): δ [ppm] = -5.79 (m, br). $^{11}\text{B}\{^1\text{H}\}$ -NMR (CD_2Cl_2 , 25°C): δ [ppm] = -5.79 (m,

br). ^{31}P -NMR (CD_2Cl_2 , 25°C): δ [ppm] = 6.02 (br). $^{31}\text{P}\{^1\text{H}\}$ -NMR (CD_2Cl_2 , 25°C): δ [ppm] = 6.02 (br). IR(ATR) : $\tilde{\nu}$ [cm^{-1}] = 3049 (w, CH), 3013 (w, CH), 2995 (w, CH), 2944 (w, CH), 2435 (m, BH), 2406 (m, BH), 1644 (w), 1584 (w), 1571 (w), 1506 (w), 1478 (s), 1462 (m), 1432 (s), 1407 (w), 1331 (w), 1305 (w), 1266 (w), 1241 (m), 1183 (w), 1156 (m), 1121 (s), 1098 (m), 1066 (s), 1026 (w), 1010 (m), 999 (w), 971 (w), 911 (w), 859 (s), 741 (s), 691 (s), 649 (w), 636 (m), 615 (m), 512 (s), 478 (s), 457 (m), 430 (m). ESI-MS (CH_2Cl_2): cation: m/z = 711 (100%, $[\text{Au}(\text{Ph}_2\text{PBH}_2\text{NMe}_3)_2]^+$). Elemental analysis (%) calculated for $\text{C}_{30}\text{H}_{42}\text{AuB}_2\text{N}_2\text{P}_2\text{AlCl}_4$ (**3d**): C: 40.95, H: 4.81, N: 3.18; found: C: 41.07, H: 4.95, N: 2.98.

4.5.3 Details of Crystal Structure Solution and Refinement

The X-ray diffraction experiments were performed on either an Rigaku Oxford Diffraction Gemini R Ultra diffractometer with Cu- $K\alpha$ radiation ($\lambda = 1.54178$ Å) (**2a**, **2b**, **2d**, **3a**, **3c**) and Mo- $K\alpha$ radiation ($\lambda = 0.71073$) (**2c**, **3b**). The experiments were performed at 273K (**3a**) and 123 K (**2a-d**, **3b-c**). Additionally unit cell determinations were performed at 90, 160, 230 and 300 K for **3a** and **3b**. Crystallographic data together with the details of the experiments are given below. Absorption corrections were applied semi-empirically from equivalent reflections or analytically (SCALE3/ABSPACK algorithm implemented in CrysAlisPro software by Rigaku Oxford Diffraction).^[2]

All structures were solved using SIR97^[3], SHELXT^[4] and olex2.solve.^[5] Least square refinements against F^2 in anisotropic models were done using SHELXL.^[4] All images were created with Olex2.^[5]

The hydrogen positions of the methyl groups were located geometrically and refined riding on the carbon atoms. Hydrogen atoms at BH_2 , PH_2 and AsH_2 have been located from the difference Fourier map and refined without constraints (**2c**, **2d**, **3c**) or with restrained E–H distances (**2a-b**, **3a**). All crystals of **2a-b** showed twinning, they were refined applying HKLF5 refinement. The crystals of **3b** turned out to be modulated and a full refinement was not possible even from different crystallization efforts. Details are given below (c.f. 4.5.4).

The fluorescent compounds **3a** and **3b** revealed the Au–Au contacts along the crystallographic b (**3a**) and c (**3b**) axis, with gold distances of one-half of the corresponding unit cell axis. Therefore, the unit cell parameters were determined for different temperatures and are given below together with the Au–Au- distances of the structure determination (**3a**) and average structure (**3b**), respectively (Table S1 and S2).

Table S1 Compound **3a** [Au(H₂PBH₂NMe₃)₂][AlCl₄].

T [K]	b-axis (Å)	1/2 b-axis (Å)	Au-Au distance (Å)
300	6.4270(2)	3.2135(1)	3.2135(1)
273	6.4165(2)	3.2083(1)	3.2083(1)
230	6.3913(1)	3.1957(1)	3.1957(1)
160	6.3545(1)	3.1772(1)	3.1772(1)
90	6.3190(7)	3.1595(4)	3.1596(4)

Table S2 Compound **3b** [Au(H₂AsBH₂NMe₃)₂][AlCl₄].

T [K]	c-axis (Å)	1/2 c-axis (Å)	Av. str. Au-Au distance (Å)
300	6.339(8)	3.170(4)	3.169(4)
230	6.3191(18)	3.1596(9)	3.1596(9)
160	6.2499(4)	3.1250(2)	3.1250(2)
123	6.2263(2)	3.1132(1)	3.1132(1)
90	6.2073(8)	3.1037(4)	3.1037(4)

CCDC-1838755 (**2a**), CCDC-1838756 (**2b**), CCDC-1838757 (**2c**), CCDC-1838758 (**2d**), CCDC-1838759 (**3a**), and CCDC-1838761 (**3c**) contain the supplementary crystallographic data for this paper. These data can be obtained free of charge at www.ccdc.cam.ac.uk/conts/retrieving.html (or from the Cambridge Crystallographic Data Centre, 12 Union Road, Cambridge CB2 1EZ, UK; Fax: +44-1223-336-033; e-mail: deposit@ccdc.cam.ac.uk).

4.5.4 Crystal Structures

[AuCl(H₂PBH₂NMe₃)]

2a crystallizes by layering of a concentrated CH₂Cl₂ solution with *n*-hexane as colourless blocks in the triclinic space group *P*-1. Figure S1 shows the structure of **2a** in the solid state.

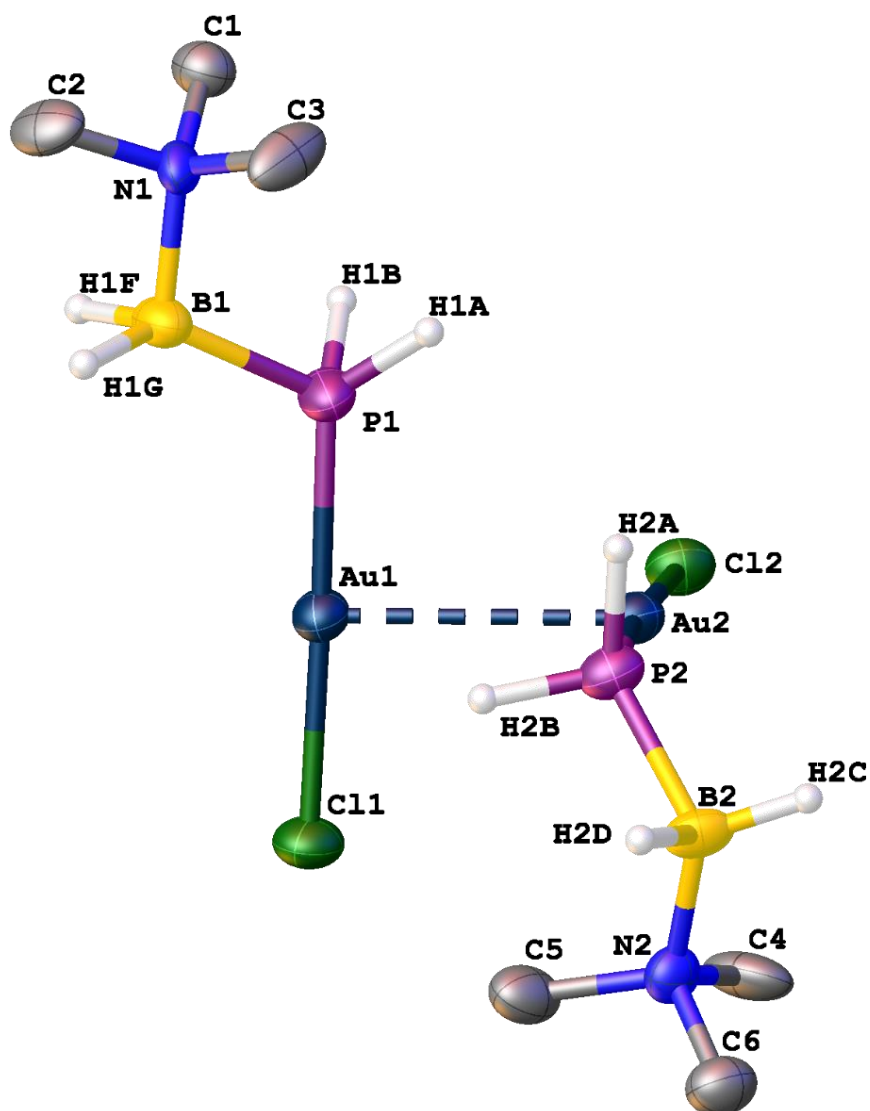


Figure S1: Molecular structure of **2a** in the solid state. Hydrogen atoms bonded to carbon are omitted for clarity. Thermal ellipsoids are drawn with 50% probability. Selected bond lengths [Å] and angles [°]: Au1–Au2 3.1031(8), Au1–P1 2.237(4), P1–B1 1.948(2), 1.947(2), N1–B1 1.619(2), P1–Au1–Cl1 178.10(14), P1–Au1–Au2–P2 89.69(16)

[AuCl(H₂AsBH₂NMe₃)]

2b crystallizes by layering of a concentrated CH₂Cl₂ solution with *n*-hexane as colourless blocks in the monoclinic space group *P*2₁/*c*. Figure S2 shows the structure of **2b** in the solid state.

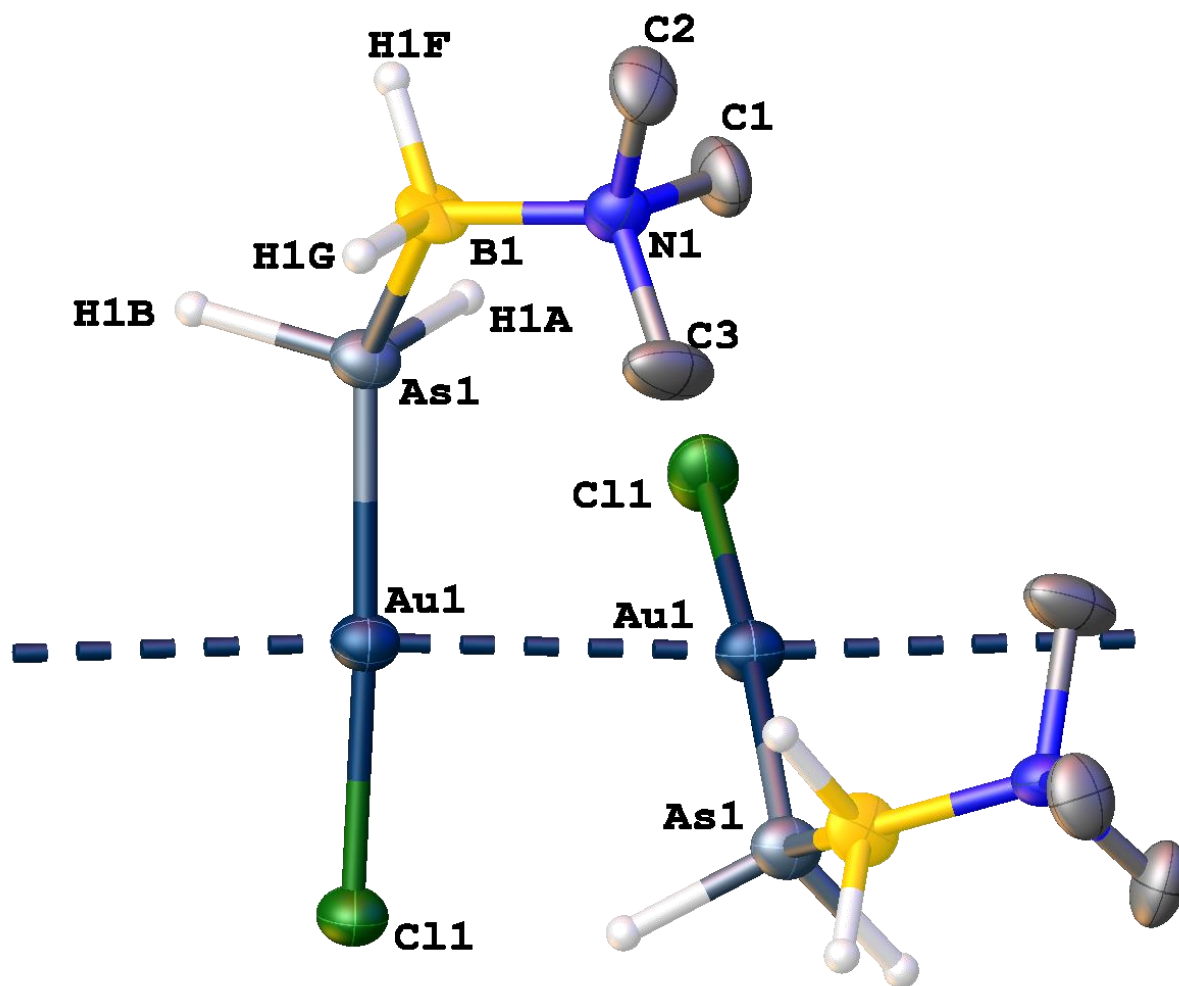


Figure S2: Molecular structure of **2b** in the solid state. Hydrogen atoms bonded to carbon are omitted for clarity. Thermal ellipsoids are drawn with 50% probability. Selected bond lengths [Å] and angles [°]: Au1–Au1' 3.251(1), Au1–As1 2.361 (1), As1–B1 2.091(18), N1–B1 1.57(3), P1–Au1–Cl1 175.65(14), Au1–Au1'–Au'' 176.61(4), As1–Au1–Au1'–As1' 127.18(10)

[AuCl('BuHPBH₂NMe₃)]

2c crystallizes by layering of a concentrated CH₂Cl₂ solution with *n*-hexane at 0°C as colourless blocks in the monoclinic space group *Cc*. Figure S3 shows the structure of **2c** in the solid state.

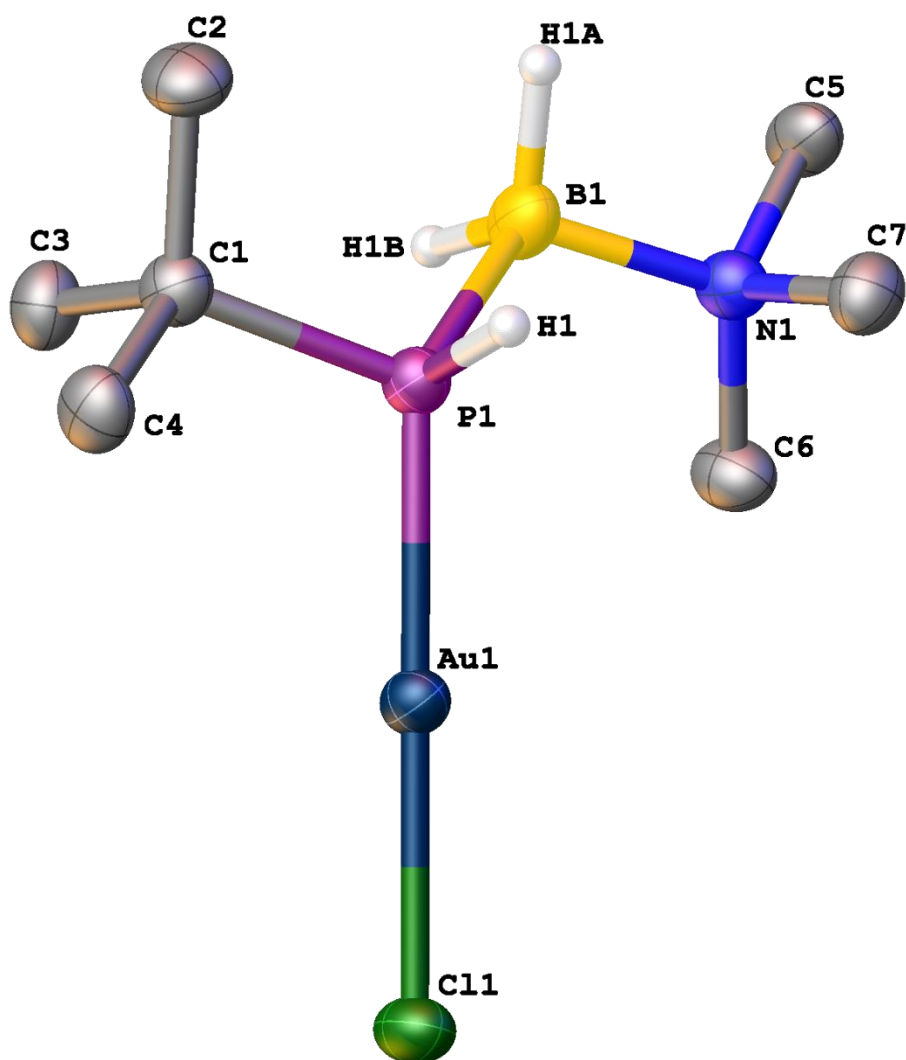


Figure S3: Molecular structure of **2c** in the solid state. Hydrogen atoms bonded to carbon are omitted for clarity. Thermal ellipsoids are drawn with 50% probability. Selected bond lengths [Å] and angles Au1-P1 2.250(2), P1-B1 1.978(10), N1-B1 1.597(11), P1-Au1-Cl1 179.62(9)

[AuCl(Ph₂PBH₂NMe₃)]

2d crystallizes by layering of a concentrated CH₂Cl₂ solution with *n*-hexane as colourless rods in the orthorhombic space group *Pna*2₁. Figure S4 shows the structure of **2d** in the solid state.

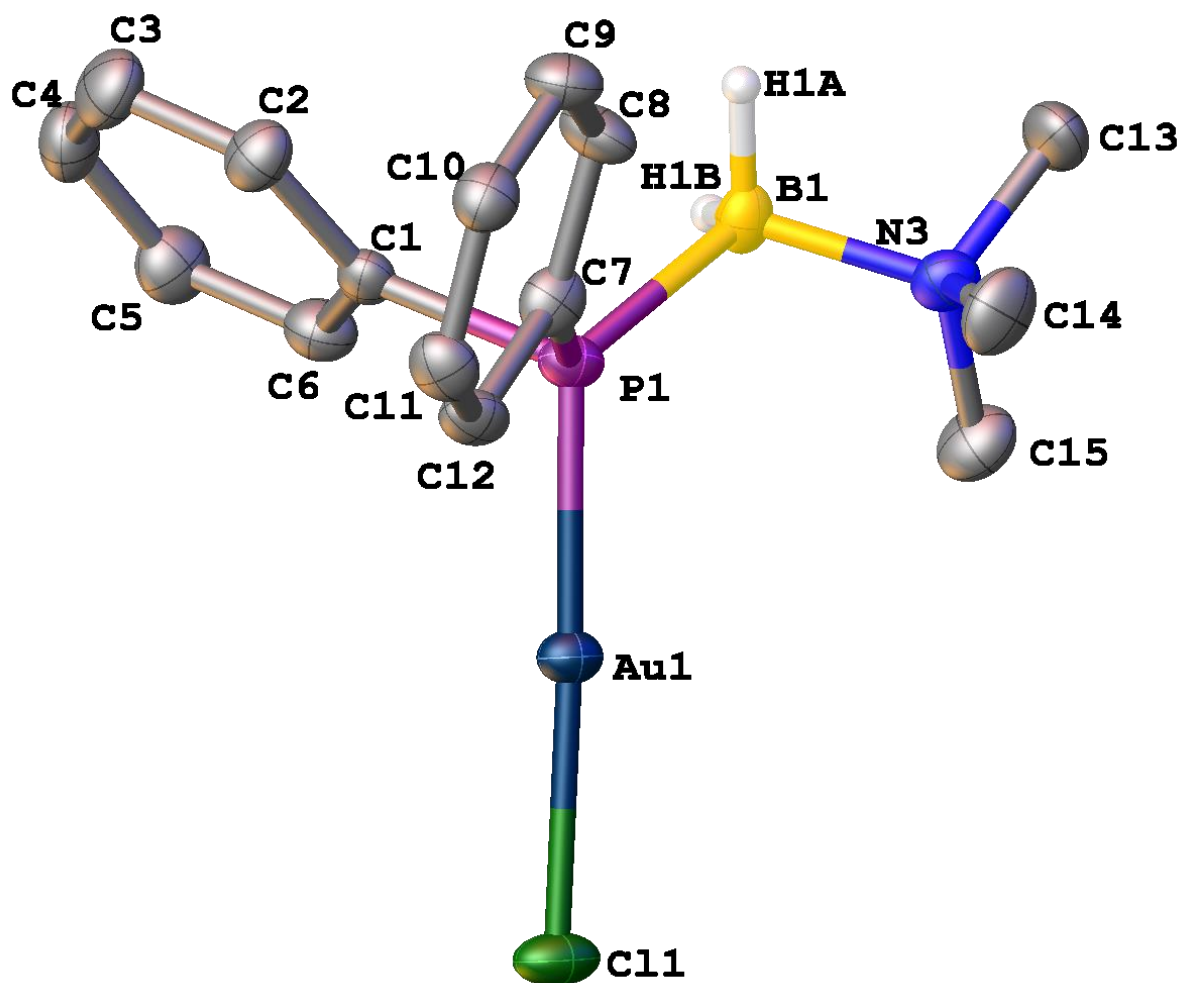


Figure S4: Molecular structure of **2d** in the solid state. Hydrogen atoms bonded to carbon are omitted for clarity. Thermal ellipsoids are drawn with 50% probability. Selected bond lengths [Å] and angles [°]: Au1-P1 2.252(1), P1-B1 1.962(9), N1-B1 1.603(9), P1-Au1-Cl1 177.57(9)

[Au(H₂PBH₂NMe₃)₂][AlCl₄]

3a crystallizes by storing a concentrated solution of **3a** in 1,2-Difluorobenzene at -30°C as colourless rods in the orthorhombic space group *Pb2n*. Figure S5 shows the structure of **3a** in the solid state.

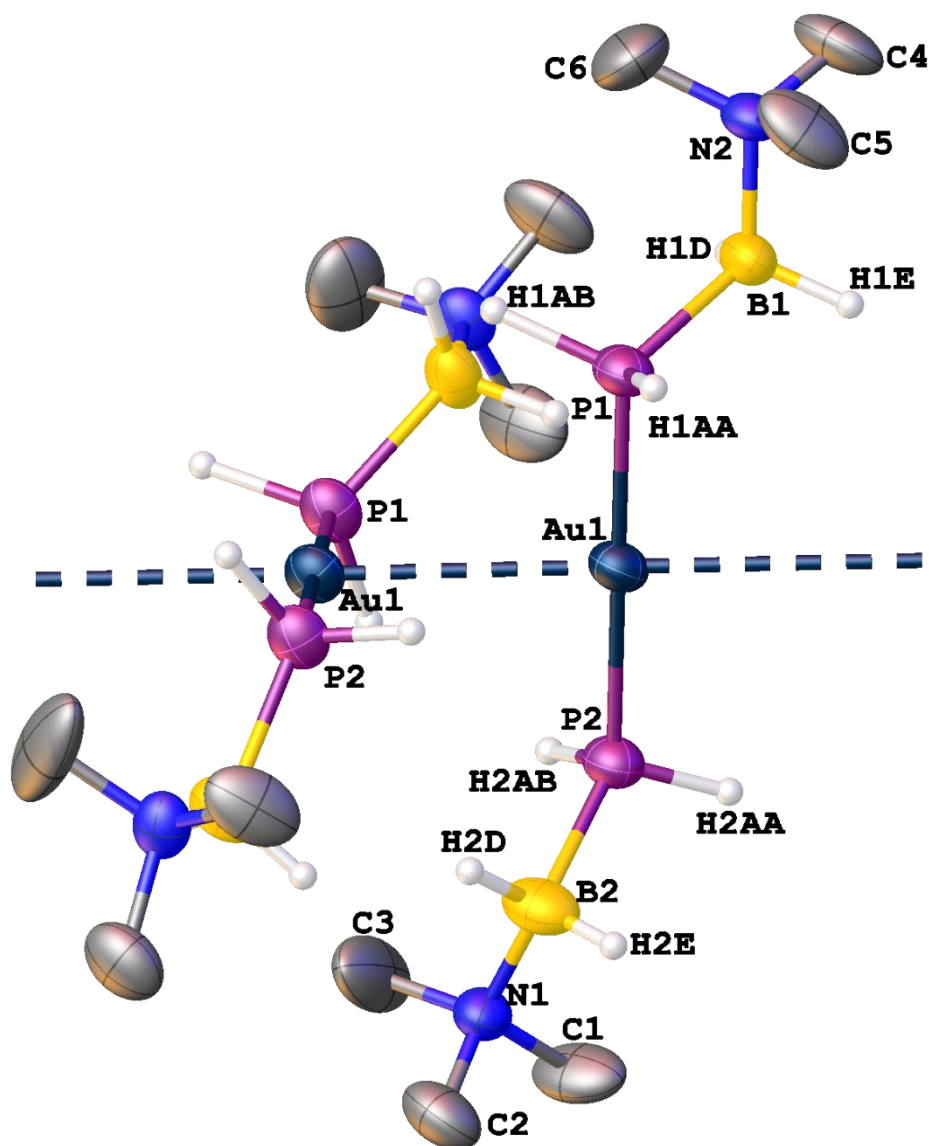


Figure S5: Molecular structure of **3a** in the solid state. [AlCl₄]⁻ counter ions not shown. Hydrogen atoms bonded to carbon are omitted for clarity. Thermal ellipsoids are drawn with 30% probability. Selected bond lengths [Å] and angles [°]: Au1-Au1' 3.168(1), Au1-P1 2.305(1), P1-B1 1.94(4), N1-B1 1.61(4), P1-Au1-P2 179.9(1), Au1-Au1'-Au1'' 179.4(1), P1-Au1-Au1'-P1' 99.3(1)

[Au(H₂AsBH₂NMe₃)₂][AlCl₄]

3b crystallizes by storing a concentrated solution of **3b** in 1,2-Difluorobenzene at -30°C. **3b** crystallizes as colourless rods. The diffraction pattern with diffuse scattering intensities revealed a 2D incommensurate structure and no satisfying model for the atoms besides gold and arsenic could be refined. Figure S7 shows the average structure and provides the connectivity model of **3b** in the solid state.

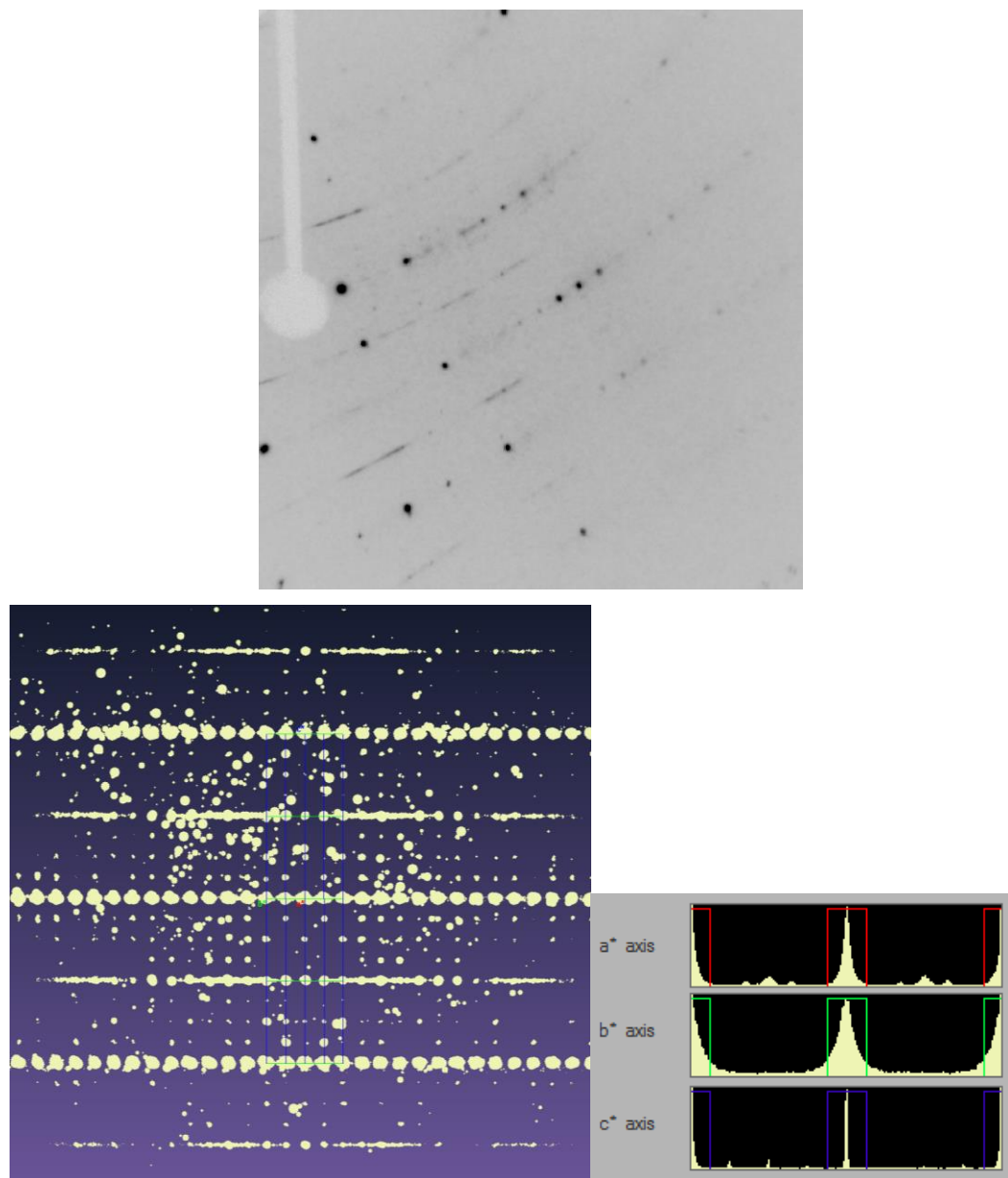


Figure S6: Diffraction pattern (top left), reciprocal space view (top right) and intensity distribution histogram (bottom) of **3b**.

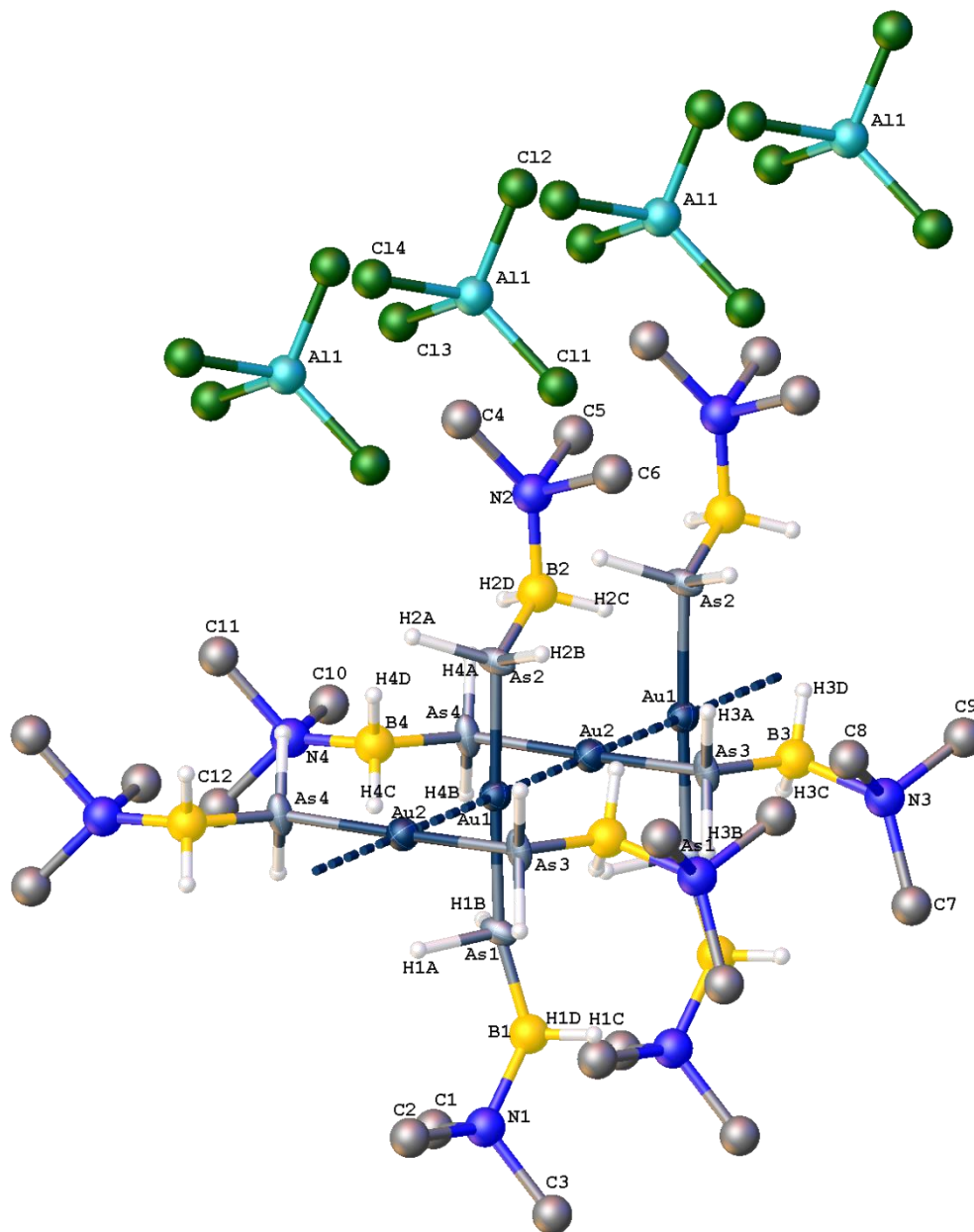


Figure S7: Average structure of **3b** in the solid state. Hydrogen atoms bonded to carbon are omitted for clarity. Thermal ellipsoids of Au and As are drawn with 50% probability. Selected bond lengths [Å] and angles [°]: Au1–Au2 3.088(2), Au1–Au2' 3.139(2), Au1–As1 2.397(4), As1–B1 1.835(15), N1–B1 1.862(15), As1–Au1–As2 177.33(15), Au2–Au1–Au2' 179.62(9), As1–Au1–Au2–As4 92.58(13)

[Au('BuHPBH₂NMe₃)₂][AlCl₄]

3c crystallizes by storing a concentrated solution of **3c** in 1,2-Difluorobenzene at -30°C as colourless blocks in the triclinic space group *P*-1. Figure S8 shows the structure of **3c** in the solid state.

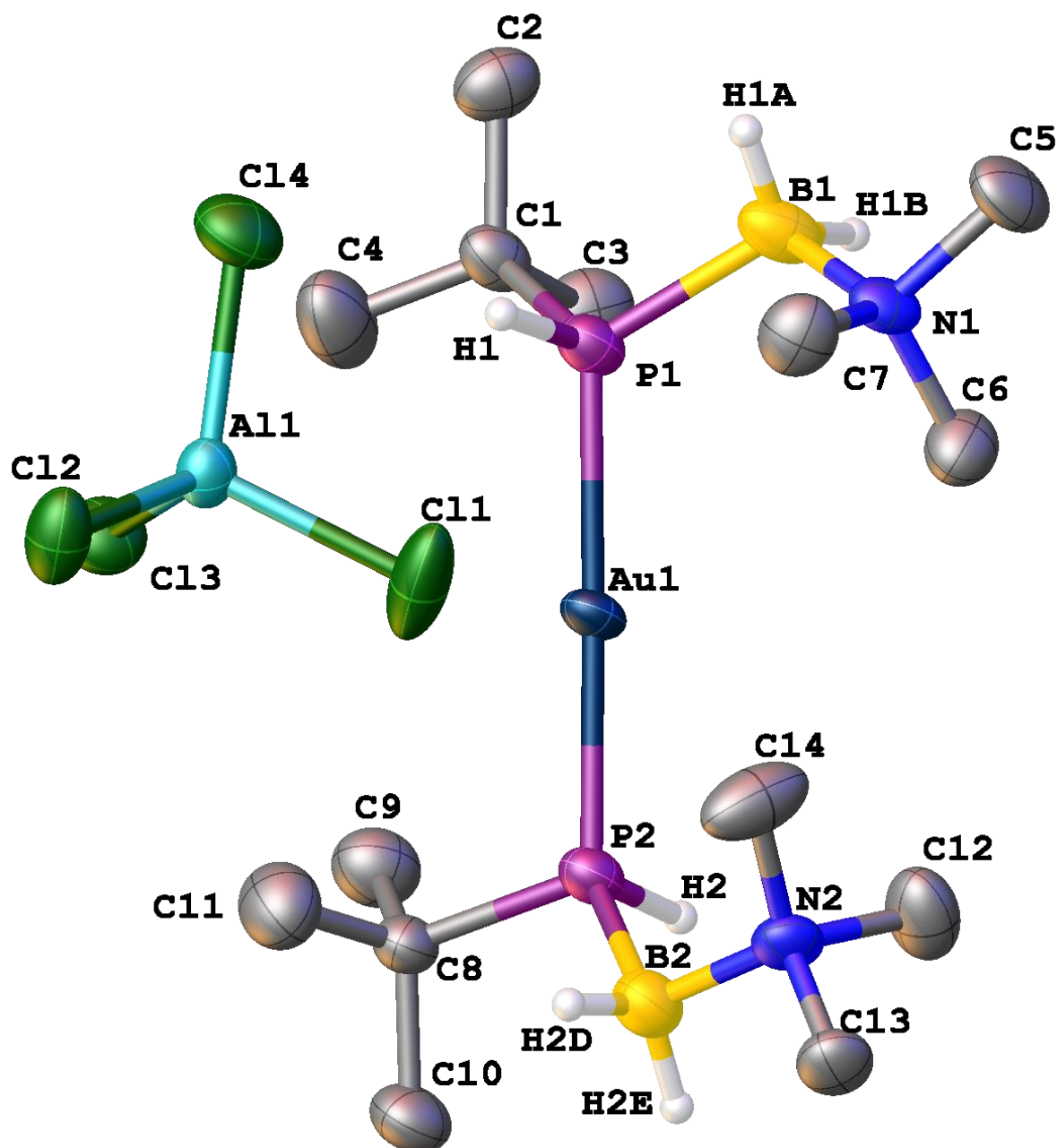


Figure S8: Molecular structure of **3c** in the solid state. Hydrogen atoms bonded to carbon are omitted for clarity. Thermal ellipsoids are drawn with 50% probability. Selected bond lengths [Å] and angles [°]: Au1-P1 2.363(2), P1-B1 1.963(7), N1-B1 1.608(8), P1-Au1-P2 179.07(9)

4.5.5 Crystallographic Information

Table S3: Crystallographic data for compounds **2a**

Formula	C ₆ H ₂₆ Au ₂ B ₂ Cl ₂ N ₂ P ₂
<i>D</i> _{calc.} / g cm ⁻³	2.449
μ /mm ⁻¹	33.889
Formula Weight	674.68
Colour	clear colourless
Shape	block
Size/mm ³	0.14×0.04×0.04
<i>T</i> /K	122.8(7)
Crystal System	triclinic
Space Group	P-1
<i>a</i> /Å	9.4692(6)
<i>b</i> /Å	9.7236(5)
<i>c</i> /Å	11.1025(5)
α /°	66.915(5)
β /°	85.150(4)
γ /°	76.630(5)
<i>V</i> /Å ³	914.89(9)
<i>Z</i>	2
<i>Z'</i>	1
Wavelength/Å	1.54184
Radiation type	CuK α
θ_{min} /°	4.329
θ_{max} /°	73.969
Measured Refl.	6330
Independent Refl.	6330
Reflections Used	5316
<i>R</i> _{int}	.
Parameters	176
Restraints	4
Largest Peak	4.324
Deepest Hole	-1.909
GooF	1.083
<i>wR</i> ₂ (all data)	0.1789
<i>wR</i> ₂	0.1655
<i>R</i> ₁ (all data)	0.0612
<i>R</i> ₁	0.0539

Table S4: Crystallographic data for compounds **2b**

Formula	C ₃ H ₁₃ AsAuBCIN
<i>D</i> _{calc.} / g cm ⁻³	2.843
μ /mm ⁻¹	37.231
Formula Weight	381.29
Colour	clear colourless
Shape	block
Size/mm ³	0.20×0.07×0.04
<i>T</i> /K	123.00(14)
Crystal System	monoclinic
Space Group	P2 ₁ /c
<i>a</i> /Å	7.9616(6)
<i>b</i> /Å	17.5813(8)
<i>c</i> /Å	6.4999(5)
α [°]	90
β [°]	101.707(7)
γ [°]	90
<i>V</i> /Å ³	890.90(10)
<i>Z</i>	4
<i>Z</i> '	1
Wavelength/Å	1.54184
Radiation type	CuK α
θ_{min} [°]	5.031
θ_{max} [°]	66.784
Measured Refl.	2337
Independent Refl.	2337
Reflections Used	1669
<i>R</i> _{int}	.
Parameters	79
Restraints	3
Largest Peak	6.323
Deepest Hole	-7.312
Goof	0.996
<i>wR</i> ₂ (all data)	0.2515
<i>wR</i> ₂	0.2397
<i>R</i> ₁ (all data)	0.0992
<i>R</i> ₁	0.0883

Table S5: Crystallographic data for compounds **2c**

Formula	C ₇ H ₂₁ AuBCINP
<i>D</i> _{calc.} / g cm ⁻³	2.046
μ /mm ⁻¹	11.808
Formula Weight	393.44
Colour	clear colourless
Shape	block
Size/mm ³	0.31×0.29×0.21
<i>T</i> /K	122.95(10)
Crystal System	monoclinic
Flack Parameter	0.000(8)
Space Group	Cc
<i>a</i> /Å	9.8373(3)
<i>b</i> /Å	18.9084(6)
<i>c</i> /Å	6.9888(3)
α [°]	90
β [°]	100.698(3)
γ [°]	90
<i>V</i> /Å ³	1277.39(8)
<i>Z</i>	4
<i>Z</i> '	1
Wavelength/Å	0.71073
Radiation type	MoK _α
θ_{min} [°]	3.476
θ_{max} [°]	41.093
Measured Refl.	23493
Independent Refl.	8211
Reflections Used	7158
<i>R</i> _{int}	0.0528
Parameters	125
Restraints	2
Largest Peak	4.473
Deepest Hole	-1.868
Goof	1.043
<i>wR</i> ₂ (all data)	0.1087
<i>wR</i> ₂	0.1029
<i>R</i> ₁ (all data)	0.0540
<i>R</i> ₁	0.0459

Table S6: Crystallographic data for compounds **2d**

Formula	C ₁₅ H ₂₁ BNPClAu
<i>D</i> _{calc.} / g cm ⁻³	1.915
μ /mm ⁻¹	18.516
Formula Weight	489.52
Colour	clear colourless
Shape	rod
Size/mm ³	0.14×0.05×0.03
<i>T</i> /K	123.1(7)
Crystal System	orthorhombic
Flack Parameter	-0.052(10)
Space Group	Pna2 ₁
<i>a</i> /Å	11.1992(2)
<i>b</i> /Å	13.3982(2)
<i>c</i> /Å	11.3156(2)
α /°	90
β /°	90
γ /°	90
<i>V</i> /Å ³	1697.90(5)
<i>Z</i>	4
<i>Z'</i>	1
Wavelength/Å	1.54178
Radiation type	CuK α
θ_{min} /°	5.116
θ_{max} /°	73.921
Measured Refl.	8623
Independent Refl.	2811
Reflections Used	2666
<i>R</i> _{int}	0.0254
Parameters	192
Restraints	1
Largest Peak	1.188
Deepest Hole	-0.379
GooF	1.076
<i>wR</i> ₂ (all data)	0.0452
<i>wR</i> ₂	0.0442
<i>R</i> ₁ (all data)	0.0212
<i>R</i> ₁	0.0191

Table S7: Crystallographic data for compounds **3a** at 273K

Formula	C ₆ H ₂₆ AlAuB ₂ Cl ₄ N ₂ P ₂
<i>D</i> _{calc.} / g cm ⁻³	1.719
μ /mm ⁻¹	18.493
Formula Weight	575.59
Colour	clear colourless
Shape	rod
Size/mm ³	0.12x0.10x0.06
<i>T</i> /K	123(2)
Crystal System	orthorhombic
Space Group	Pbcn
<i>a</i> /Å	22.4027(7)
<i>b</i> /Å	6.4165(2)
<i>c</i> /Å	30.9447(11)
α °	90
β °	90
γ °	90
<i>V</i> /Å ³	4448.2(3)
<i>Z</i>	8
<i>Z</i> '	1
Wavelength/Å	1.54184
Radiation type	CuK α
θ_{min} °	3.472
θ_{max} °	66.828
Measured Refl.	29023
Independent Refl.	3939
Reflections Used	2737
<i>R</i> _{int}	0.0521
Parameters	257
Restraints	39
Largest Peak	0.607
Deepest Hole	-0.738
Goof	1.146
<i>wR</i> ₂ (all data)	0.1149
<i>wR</i> ₂	0.1041
<i>R</i> ₁ (all data)	0.0764
<i>R</i> ₁	0.0508

Table S8: Crystallographic data for compounds **3a** at 300K

Formula	C ₆ H ₂₆ AlAuB ₂ Cl ₄ N ₂ P ₂
<i>D</i> _{calc.} / g cm ⁻³	1.709
<i>μ</i> /mm ⁻¹	18.389
Formula Weight	575.59
Colour	clear colourless
Shape	rod
Size/mm ³	0.22×0.20×0.14
<i>T</i> /K	300.0(1)
Crystal System	orthorhombic
Space Group	Pbcn
<i>a</i> /Å	22.4674(8)
<i>b</i> /Å	6.4270(2)
<i>c</i> /Å	30.9792(10)
<i>α</i> [°]	90
<i>β</i> [°]	90
<i>γ</i> [°]	90
<i>V</i> /Å ³	4473.3(3)
<i>Z</i>	8
<i>Z</i> '	1
Wavelength/Å	1.54184
Radiation type	CuK _α
<i>θ</i> _{min} [°]	3.466
<i>θ</i> _{max} [°]	73.555
Measured Refl.	17527
Independent Refl.	4409
Reflections Used	2182
<i>R</i> _{int}	0.0391
Parameters	173
Restraints	44
Largest Peak	2.309
Deepest Hole	-0.789
GooF	0.828
<i>wR</i> ₂ (all data)	0.1325
<i>wR</i> ₂	0.1180
<i>R</i> ₁ (all data)	0.0839
<i>R</i> ₁	0.0476

Table S9: Crystallographic data for compounds **3a** at 230K

Formula	C ₆ H ₂₆ AlAuB ₂ Cl ₄ N ₂ P ₂
<i>D</i> _{calc.} / g cm ⁻³	1.737
μ /mm ⁻¹	18.692
Formula Weight	575.59
Colour	clear colourless
Shape	rod
Size/mm ³	0.22x0.20x0.14
<i>T</i> /K	230.0(1)
Crystal System	orthorhombic
Space Group	Pbcn
<i>a</i> /Å	22.2949(6)
<i>b</i> /Å	6.39132(10)
<i>c</i> /Å	30.8844(7)
α [°]	90
β [°]	90
γ [°]	90
<i>V</i> /Å ³	4400.84(17)
<i>Z</i>	8
<i>Z'</i>	1
Wavelength/Å	1.54184
Radiation type	CuK α
θ_{min} [°]	3.482
θ_{max} [°]	73.455
Measured Refl.	17231
Independent Refl.	4348
Reflections Used	2577
<i>R</i> _{int}	0.0366
Parameters	173
Restraints	32
Largest Peak	2.801
Deepest Hole	-1.154
GooF	0.909
<i>wR</i> ₂ (all data)	0.1326
<i>wR</i> ₂	0.1225
<i>R</i> ₁ (all data)	0.0703
<i>R</i> ₁	0.0464

Table S10: Crystallographic data for compounds **3a** at 160K

Formula	C ₆ H ₂₆ AlAuB ₂ Cl ₄ N ₂ P ₂
$D_{calc.}/g\text{ cm}^{-3}$	1.769
μ/mm^{-1}	19.029
Formula Weight	575.59
Colour	clear colourless
Shape	rod
Size/mm ³	0.22x0.20x0.14
T/K	160.0(1)
Crystal System	orthorhombic
Space Group	Pbcn
$a/\text{\AA}$	22.1169(7)
$b/\text{\AA}$	6.35448(10)
$c/\text{\AA}$	30.7581(7)
α°	90
β°	90
γ°	90
$V/\text{\AA}^3$	4322.79(17)
Z	8
Z'	1
Wavelength/ \AA	1.54184
Radiation type	CuK α
θ_{min}°	3.500
θ_{max}°	73.724
Measured Refl.	16861
Independent Refl.	4282
Reflections Used	2944
R_{int}	0.0341
Parameters	173
Restraints	26
Largest Peak	3.562
Deepest Hole	-0.790
GooF	0.939
wR_2 (all data)	0.1178
wR_2	0.1111
R_1 (all data)	0.0584
R_1	0.0427

Table S11: Crystallographic data for compounds **3a** at 90K

Formula	C ₆ H ₂₆ AlAuB ₂ Cl ₄ N ₂ P ₂
$D_{calc.}/\text{g cm}^{-3}$	1.791
μ/mm^{-1}	19.238
Formula Weight	575.59
Colour	clear colourless
Shape	rod
Size/mm ³	0.22x0.20x0.14
T/K	89.9(3)
Crystal System	orthorhombic
Space Group	Pbcn
$a/\text{\AA}$	21.951(3)
$b/\text{\AA}$	6.3190(7)
$c/\text{\AA}$	30.726(4)
α°	90
β°	90
γ°	90
$V/\text{\AA}^3$	4261.9(9)
Z	8
Z'	1
Wavelength/ \AA	1.54184
Radiation type	CuK α
θ_{min}°	3.512
θ_{max}°	74.761
Measured Refl.	15789
Independent Refl.	4229
Reflections Used	3390
R_{int}	0.0944
Parameters	174
Restraints	38
Largest Peak	11.307
Deepest Hole	-6.436
GooF	1.083
wR_2 (all data)	0.3167
wR_2	0.3104
R_1 (all data)	0.1332
R_1	0.1222

Table S12: Crystallographic data for compounds **3b**

Formula	C ₆ H ₂₆ B ₂ N ₂ AlCl ₄ As ₂ Au
<i>D</i> _{calc.} / g cm ⁻³	2.759
μ /mm ⁻¹	14.027
Formula Weight	663.49
Colour	clear colourless
Shape	rod
Size/mm ³	0.45x0.23x0.04
<i>T</i> /K	123(2)
Crystal System	orthorhombic
<i>a</i> /Å	14.3566(4)
<i>b</i> /Å	26.8056(9)
<i>c</i> /Å	6.2263(2)
α [°]	90
β [°]	90
γ [°]	90
<i>V</i> /Å ³	2396.11(13)
Wavelength/Å	0.71073
Radiation type	MoK α
θ_{min} [°]	3.219
θ_{max} [°]	34.779
Measured Refl.	63309
Independent Refl.	19396
Reflections Used	11539
<i>R</i> _{int}	0.0653

Table S13: Crystallographic data for compounds **3c**

Formula	C ₁₄ H ₄₂ AlAuB ₂ Cl ₄ N ₂ P ₂
<i>D</i> _{calc.} / g cm ⁻³	1.559
μ /mm ⁻¹	14.139
Formula Weight	687.80
Colour	clear colourless
Shape	block
Size/mm ³	0.16×0.11×0.08
<i>T</i> /K	123(2)
Crystal System	triclinic
Space Group	P-1
<i>a</i> /Å	10.5572(4)
<i>b</i> /Å	11.3638(4)
<i>c</i> /Å	14.2359(5)
α /°	105.204(3)
β /°	102.846(3)
γ /°	109.172(3)
<i>V</i> /Å ³	1464.84(10)
<i>Z</i>	2
<i>Z'</i>	1
Wavelength/Å	1.54184
Radiation type	CuK α
θ _{min} /°	4.423
θ _{max} /°	66.276
Measured Refl.	15617
Independent Refl.	5113
Reflections Used	4139
<i>R</i> _{int}	0.0458
Parameters	304
Restraints	5
Largest Peak	1.622
Deepest Hole	-0.906
GooF	1.013
<i>wR</i> ₂ (all data)	0.0824
<i>wR</i> ₂	0.0787
<i>R</i> ₁ (all data)	0.0532
<i>R</i> ₁	0.0373

4.5.6 NMR Spectroscopy

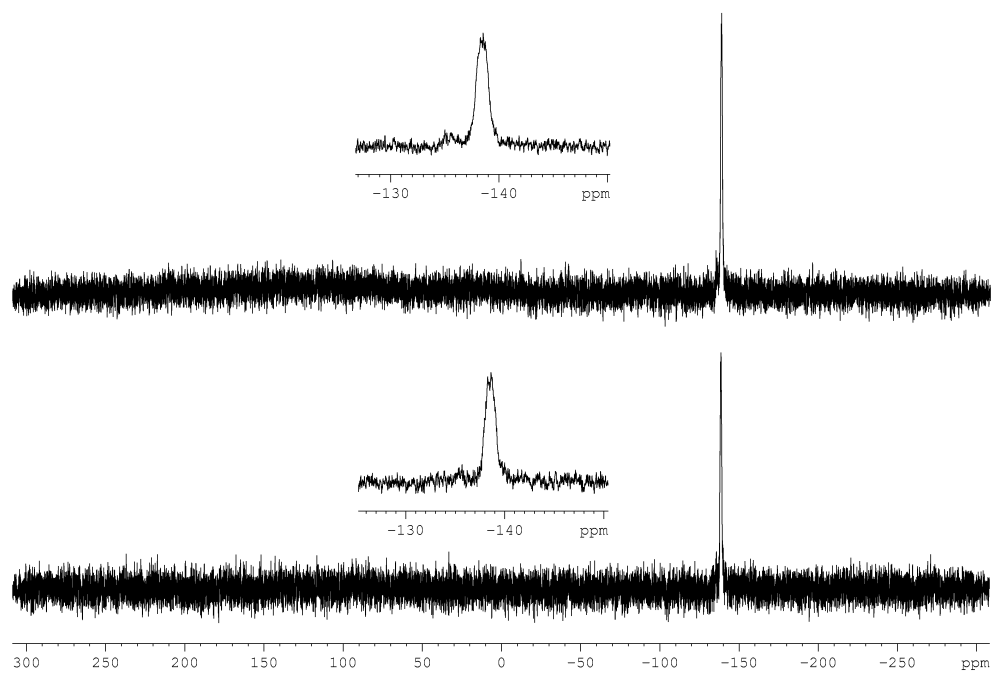
[AuCl(H₂PBH₂NMe₃)] (2a)

Figure S9: ³¹P (top) and ³¹P{¹H} NMR spectrum (bottom) of **2a** in CD₂Cl₂.

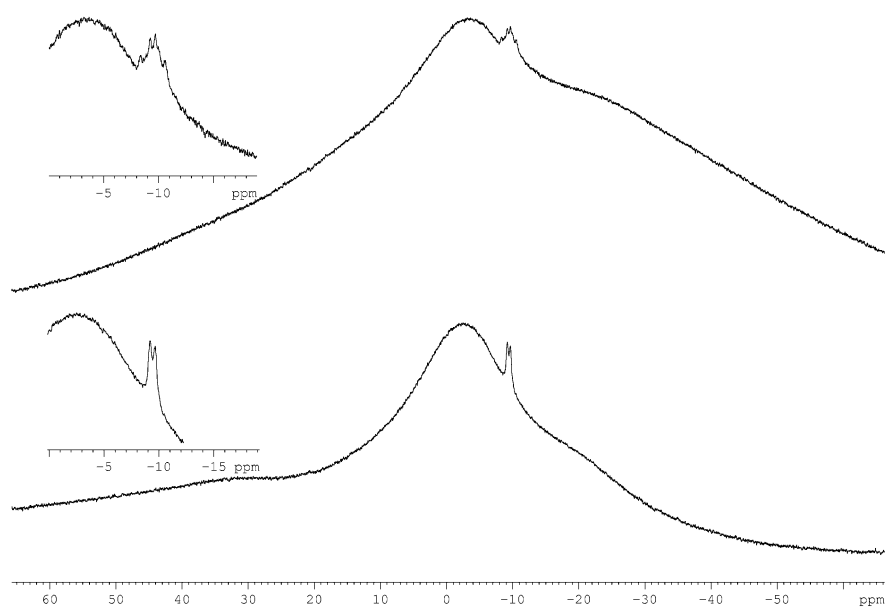


Figure S10: ¹¹B (top) and ¹¹B{¹H} NMR spectrum (bottom) of **2a** in CD₂Cl₂.

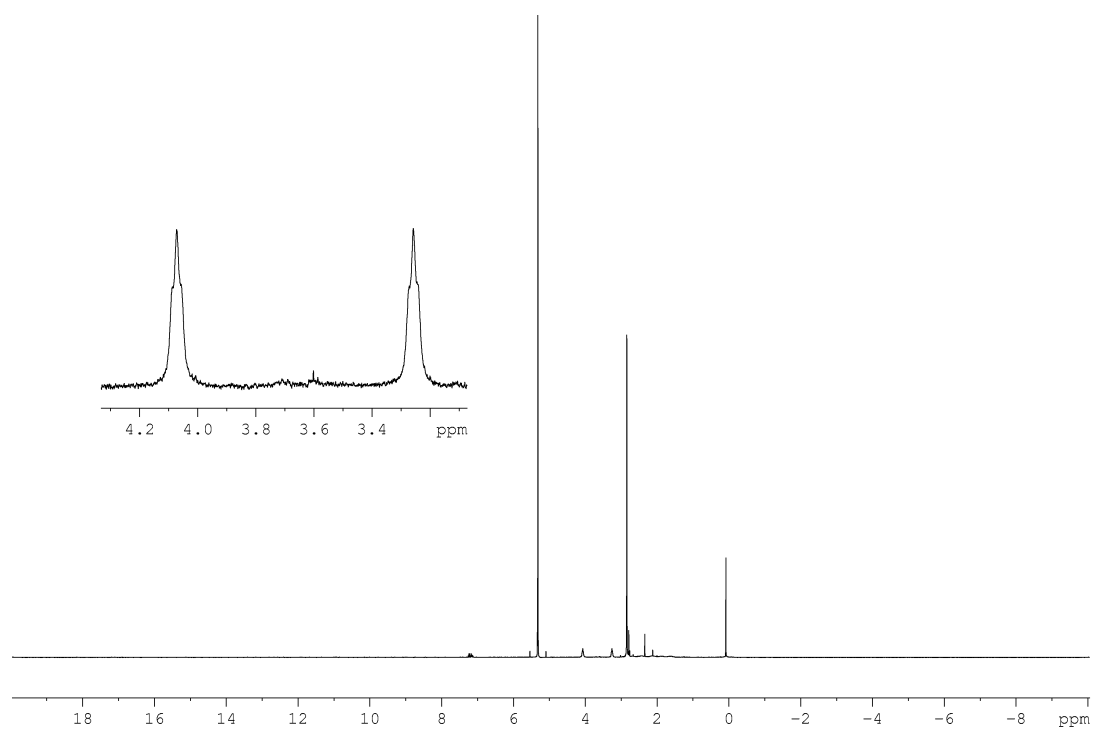


Figure S11: ^1H NMR spectrum of **2a** in CD_2Cl_2 .

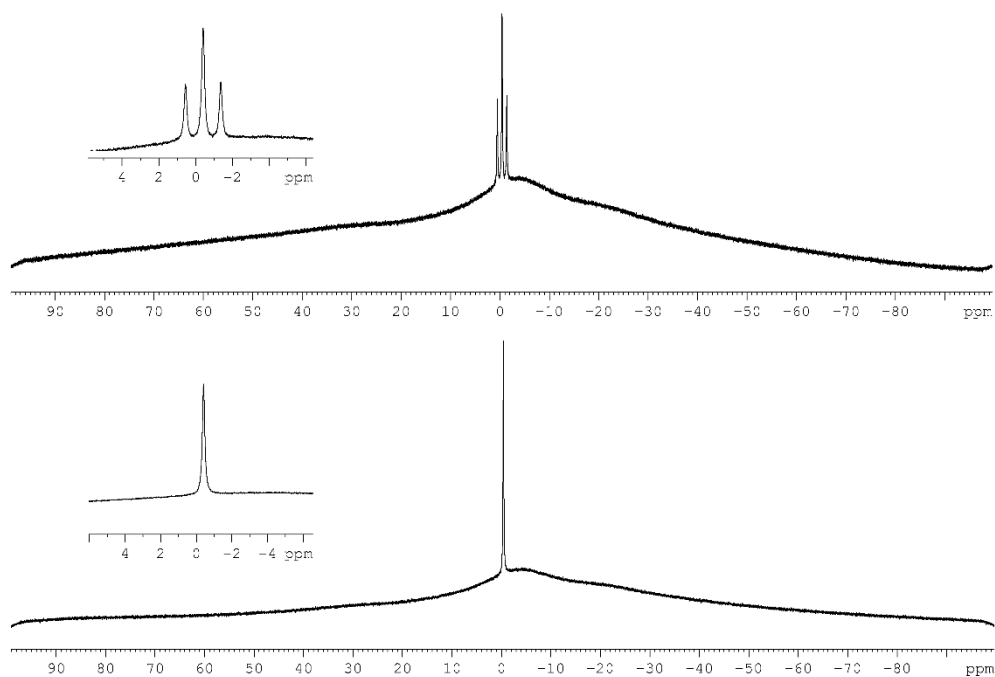
[AuCl(H₂AsBH₂NMe₃)] (2b)

Figure S12: ¹¹B (top) and ¹¹B{¹H} NMR spectrum (bottom) of **2b** in CD₂Cl₂.

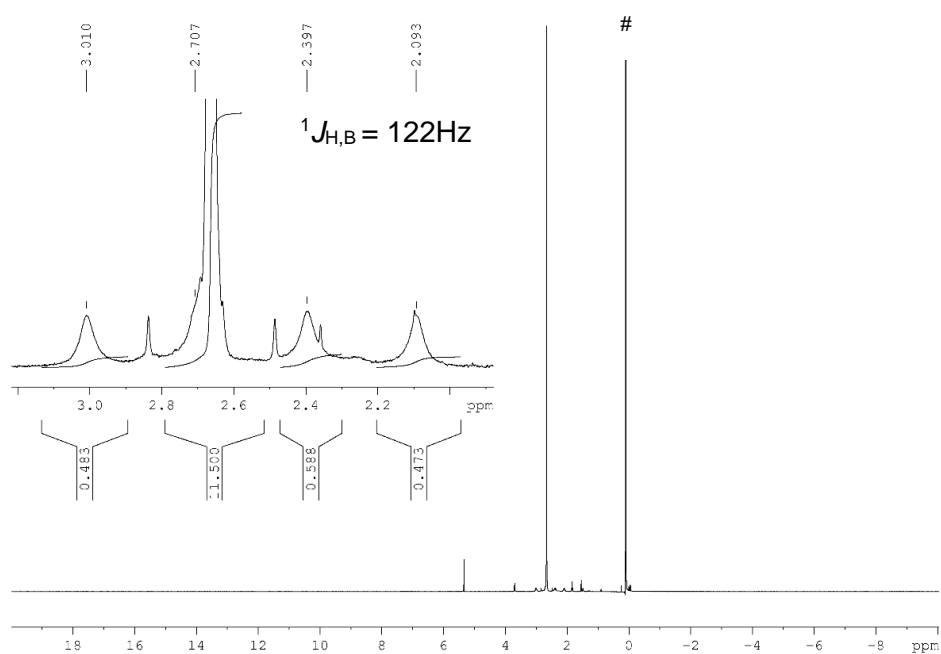


Figure S13: ¹H NMR spectrum of **2b** in CD₂Cl₂. Overlap of signals from N(CH₃)₃ (9H), AsH₂ (2H) and BH₂ (quartet: 0.5 H) at 2.66ppm. Impurities of silicon grease (#).

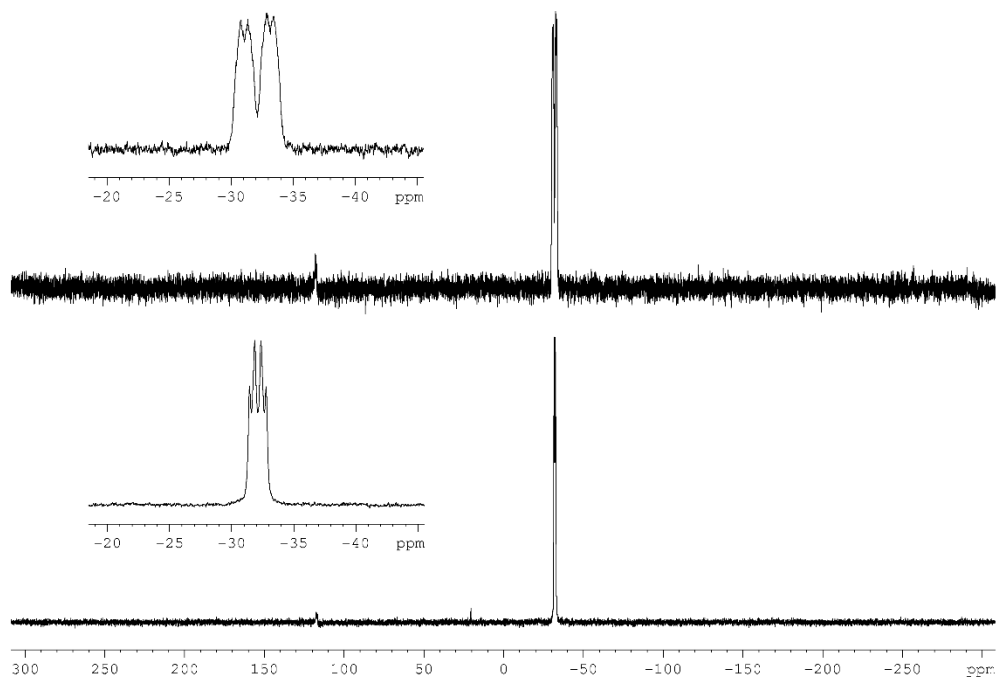
[AuCl('BuHPBH₂NMe₃)] (2c)

Figure S14: ³¹P (top) and ³¹P{¹H} NMR spectrum (bottom) of 2c in CD₂Cl₂.

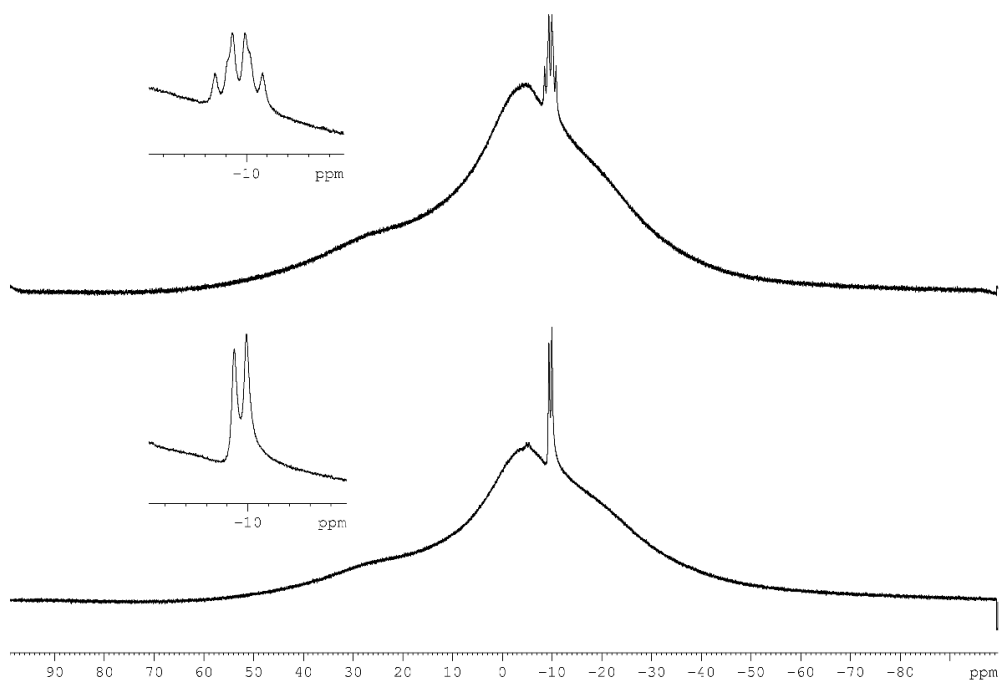


Figure S15: ¹¹B (top) and ¹¹B{¹H} NMR spectrum (bottom) of 2c in CD₂Cl₂.

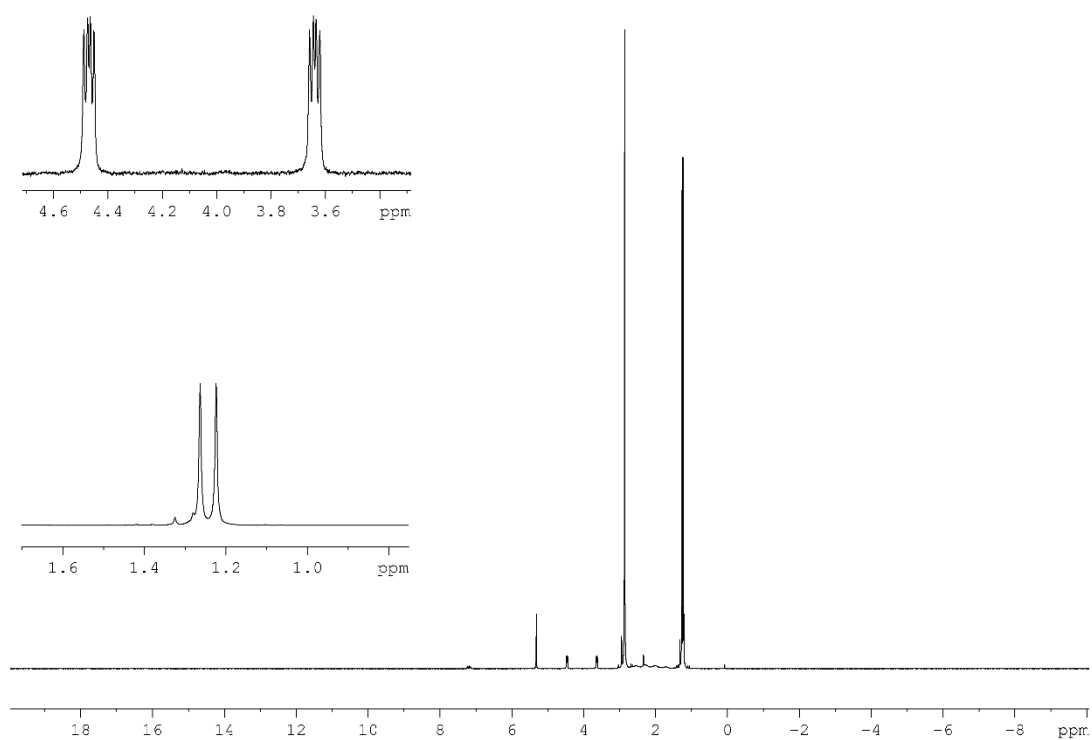


Figure S16: ^1H NMR spectrum of **2c** in CD_2Cl_2 .

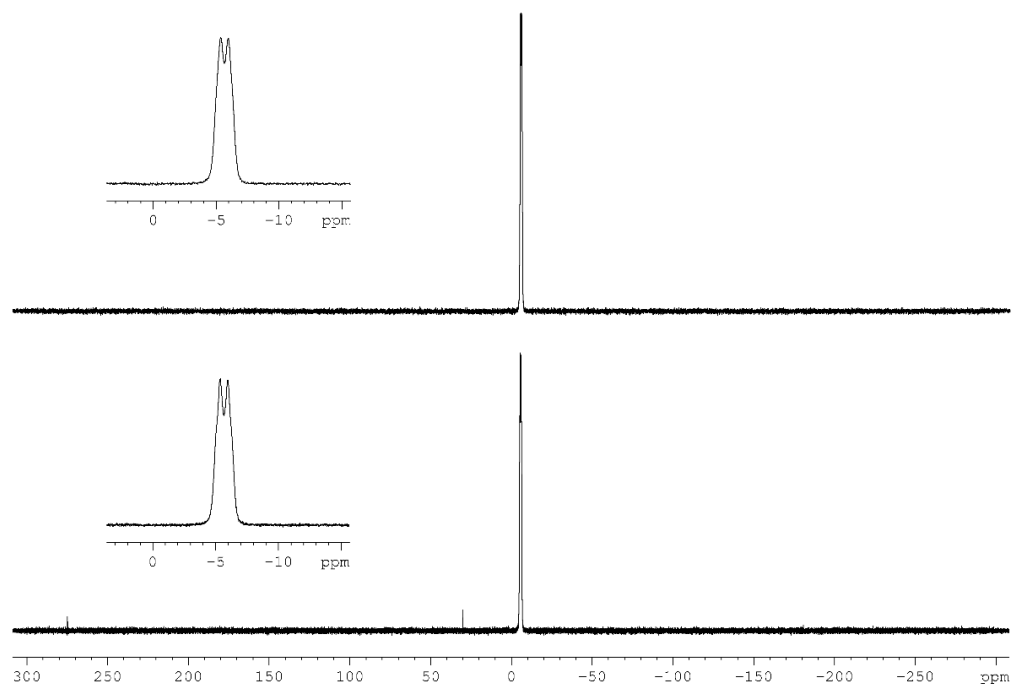
[AuCl(Ph₂PBH₂NMe₃)] (2d)

Figure S17: ³¹P (top) and ³¹P{¹H} NMR spectrum (bottom) of 2d in CD₂Cl₂.

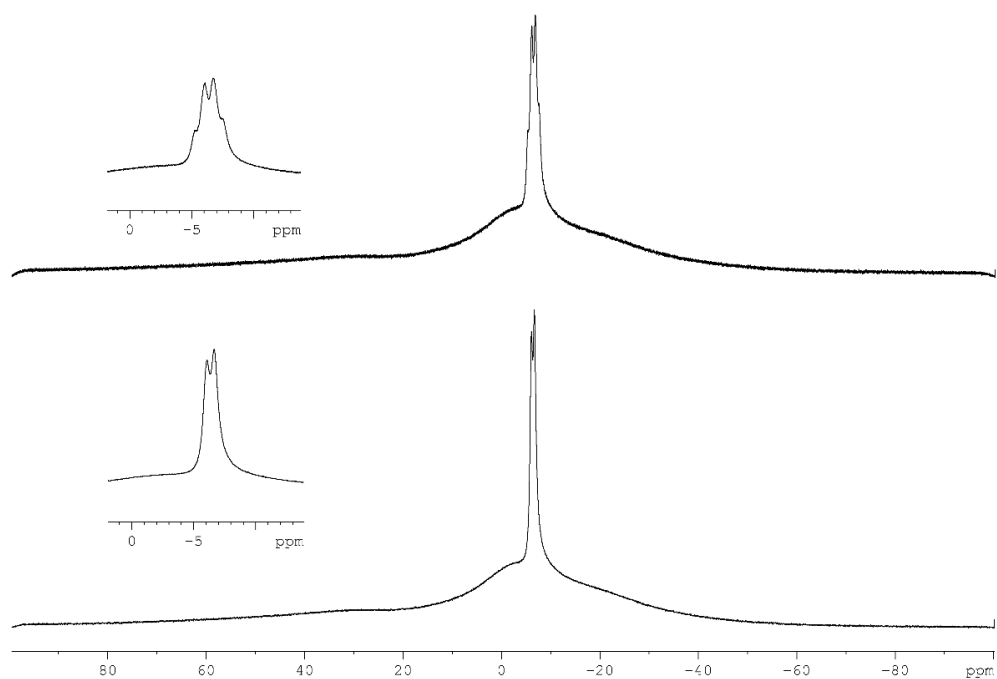


Figure S18: ¹¹B (top) and ¹¹B{¹H} NMR spectrum (bottom) of 2d in CD₂Cl₂.

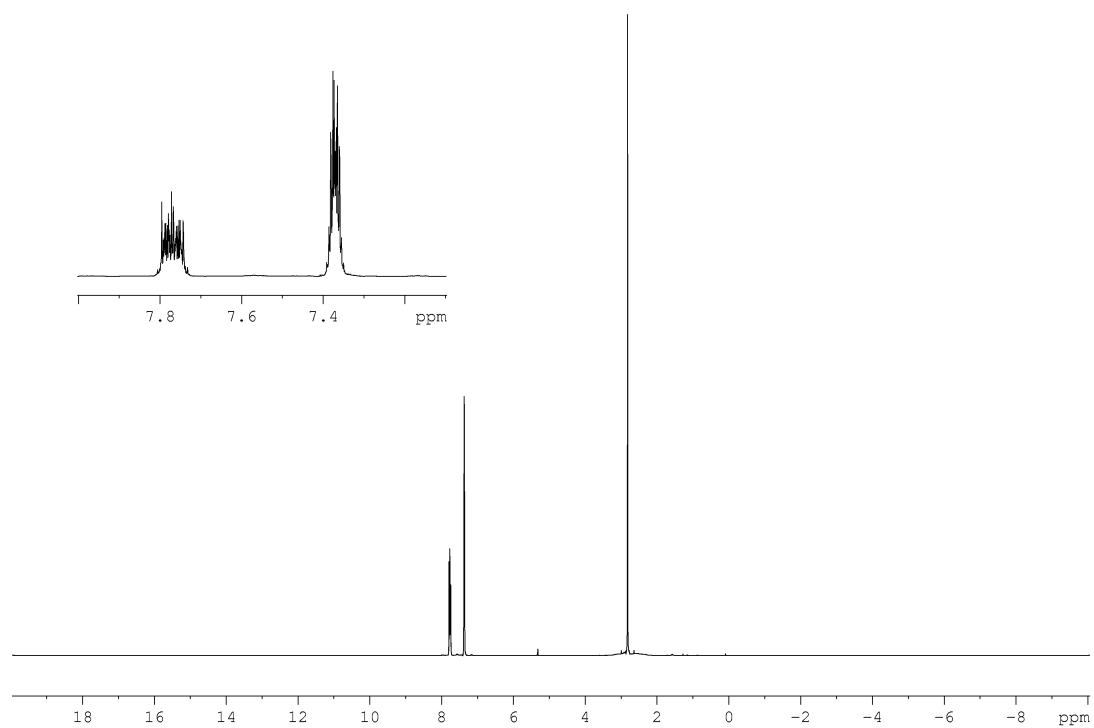


Figure S19: ^1H NMR spectrum of **2d** in CD_2Cl_2 .

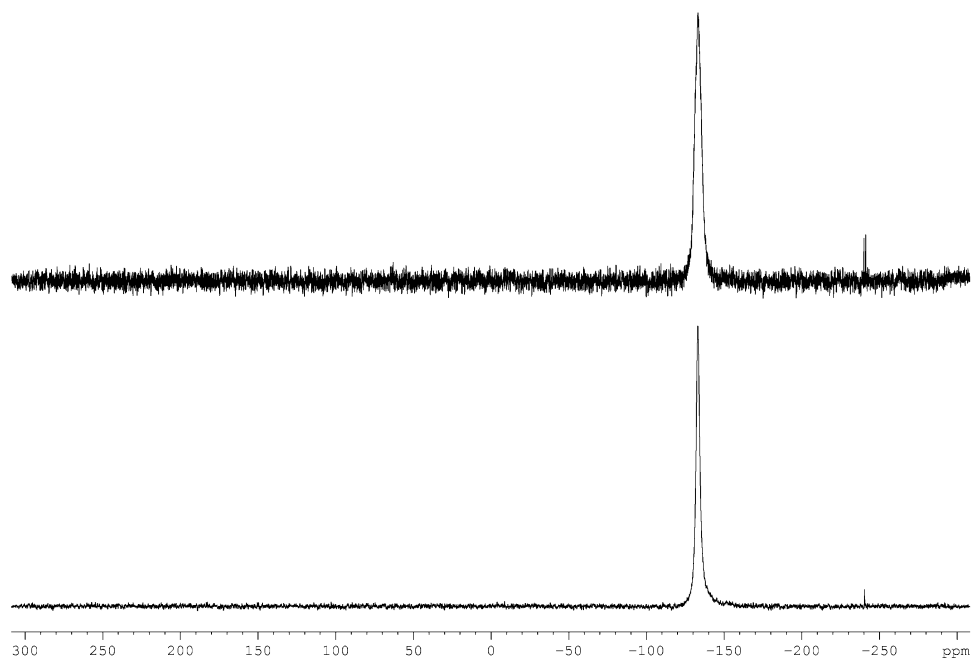
[Au(H₂PBH₂NMe₃)₂][AlCl₄] (3a)

Figure S20: ³¹P (top) and ³¹P{¹H} NMR spectrum (bottom) of 3a in CD₂Cl₂.

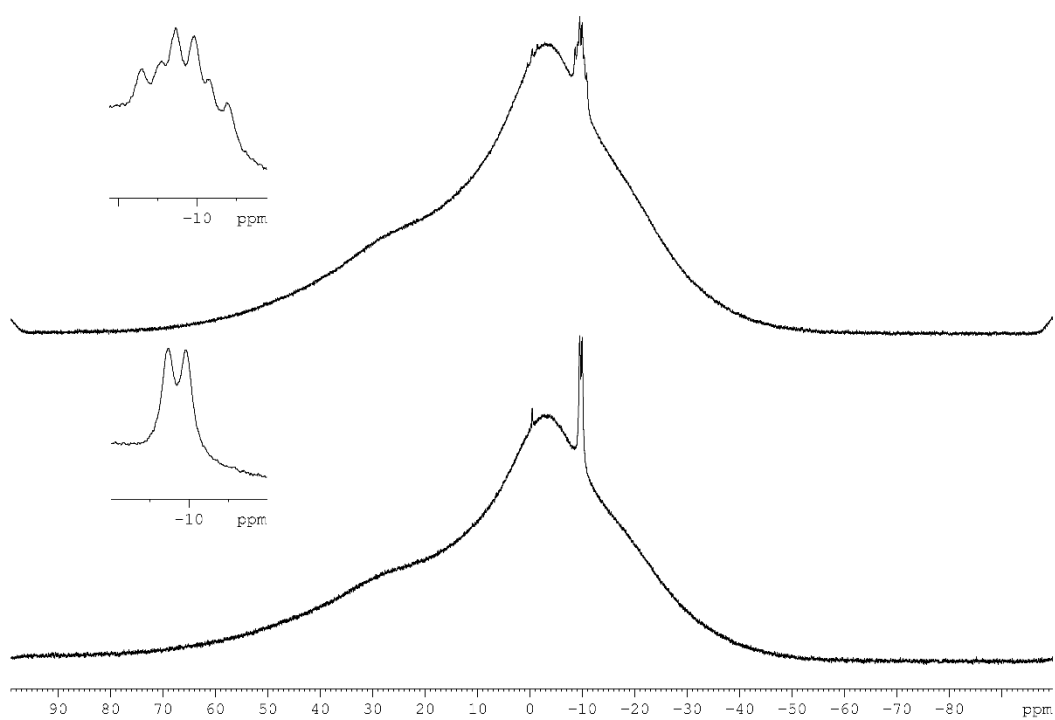


Figure S21: ¹¹B (top) and ¹¹B{¹H} NMR spectrum (bottom) of 3a in CD₂Cl₂.

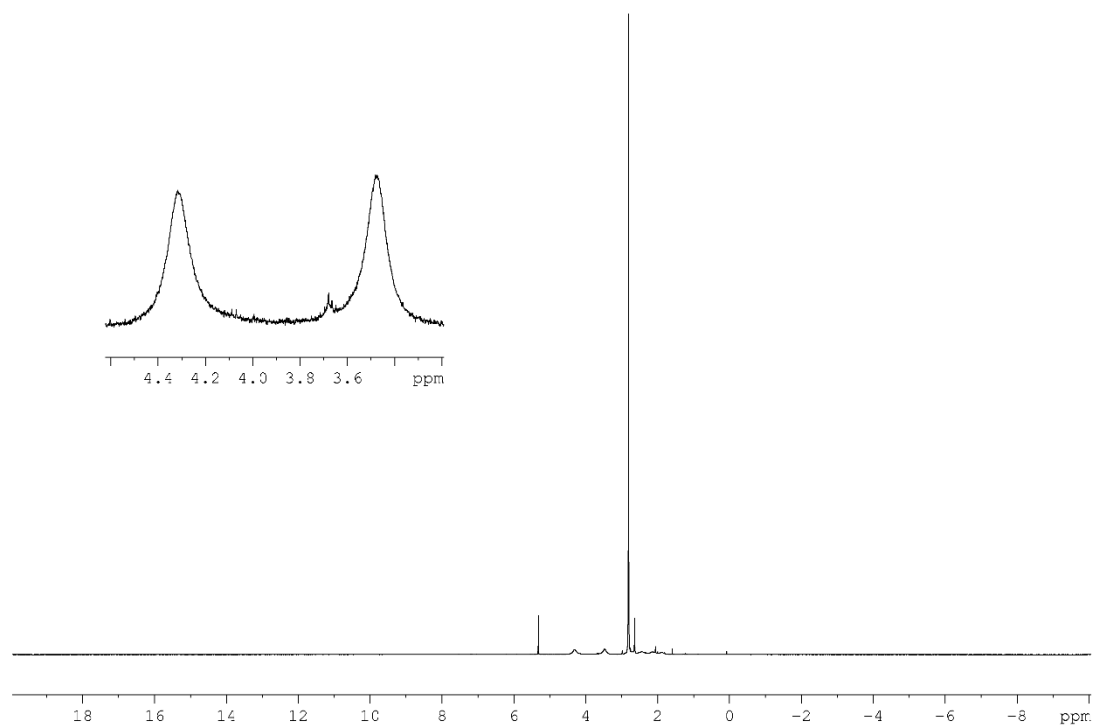


Figure S22: ^1H NMR spectrum of **3a** in CD_2Cl_2 .

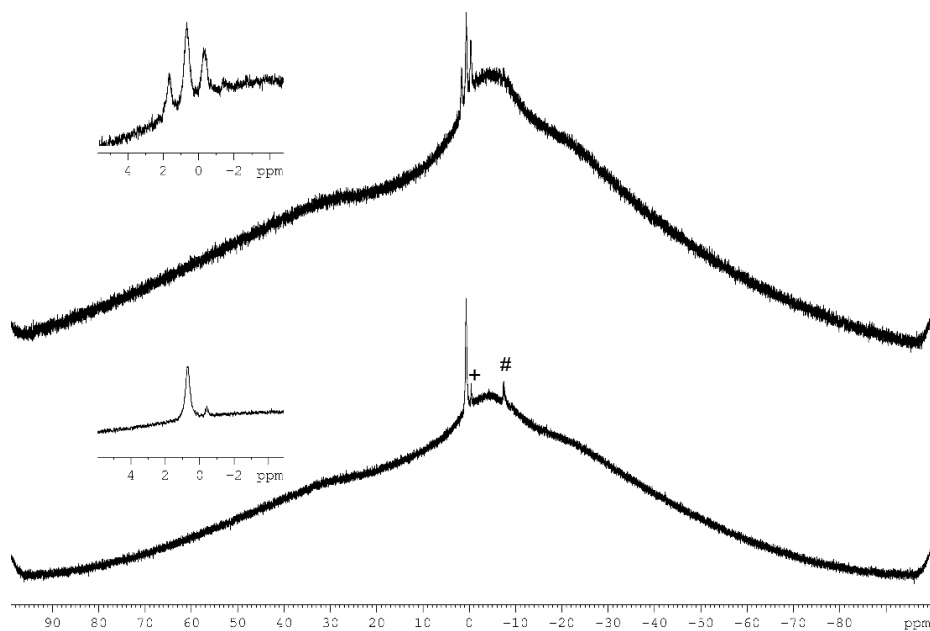
[Au(H₂AsBH₂NMe₃)₂][AlCl₄] (3b)

Figure S23: ¹¹B (top) and ¹¹B{¹H} NMR spectrum (bottom) of **3b** in CD₂Cl₂. Traces of starting material **1b**(#) and **2b**(+).

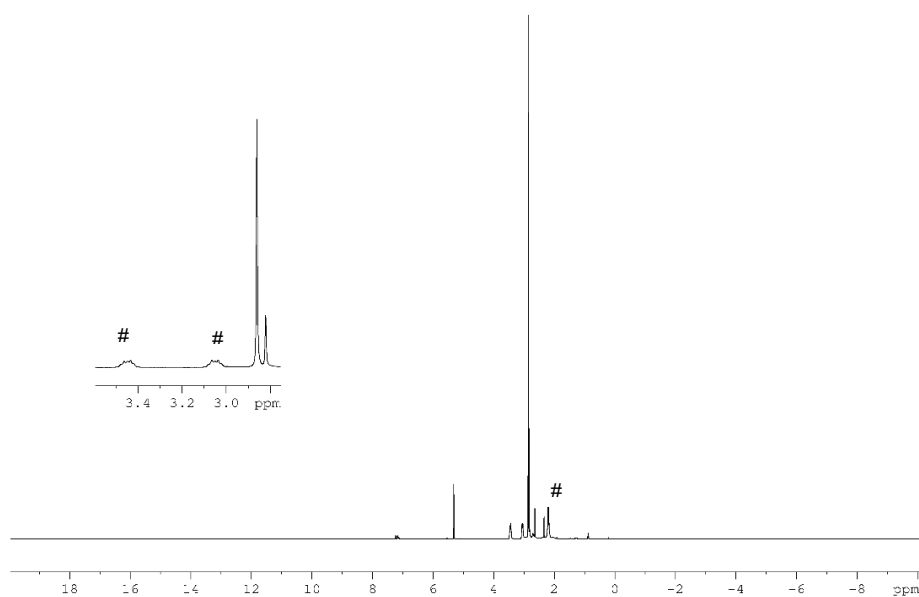


Figure S24: ¹H NMR spectrum of **3b** in CD₂Cl₂. Traces if starting material [AuCl(tht)](#).

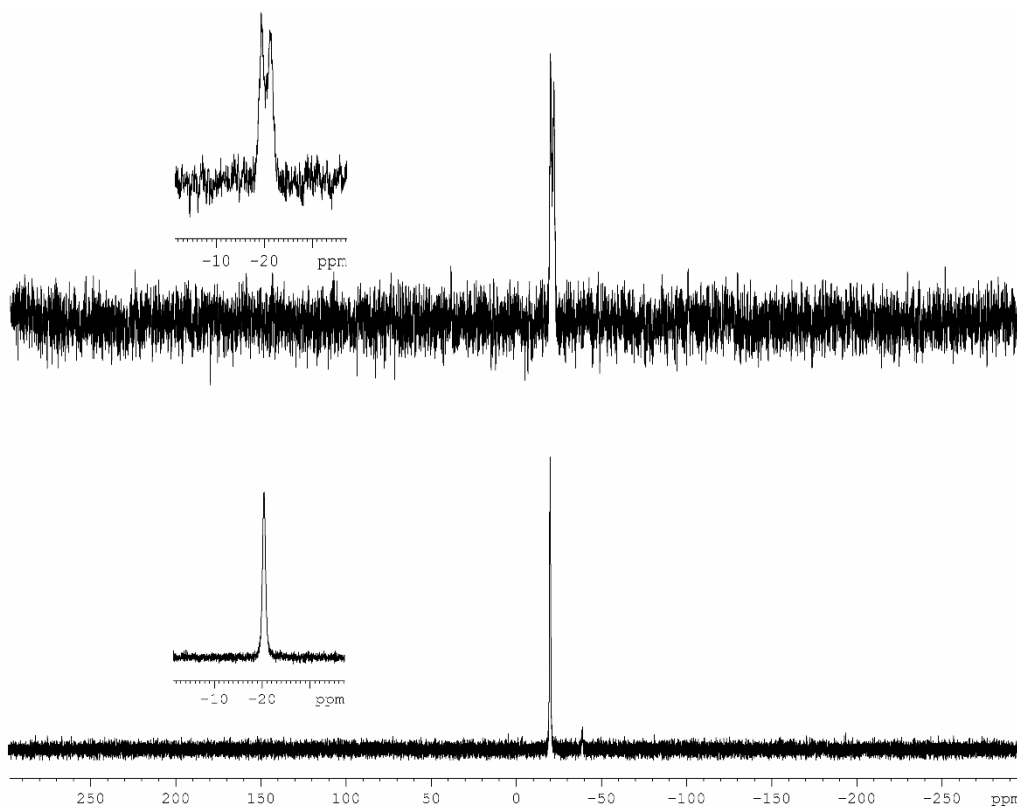
[Au(^tBuHPBH₂NMe₃)₂][AlCl₄] (3c)

Figure S25: ³¹P (top) and ³¹P{¹H} NMR spectrum (bottom) of 3c in CD₂Cl₂.

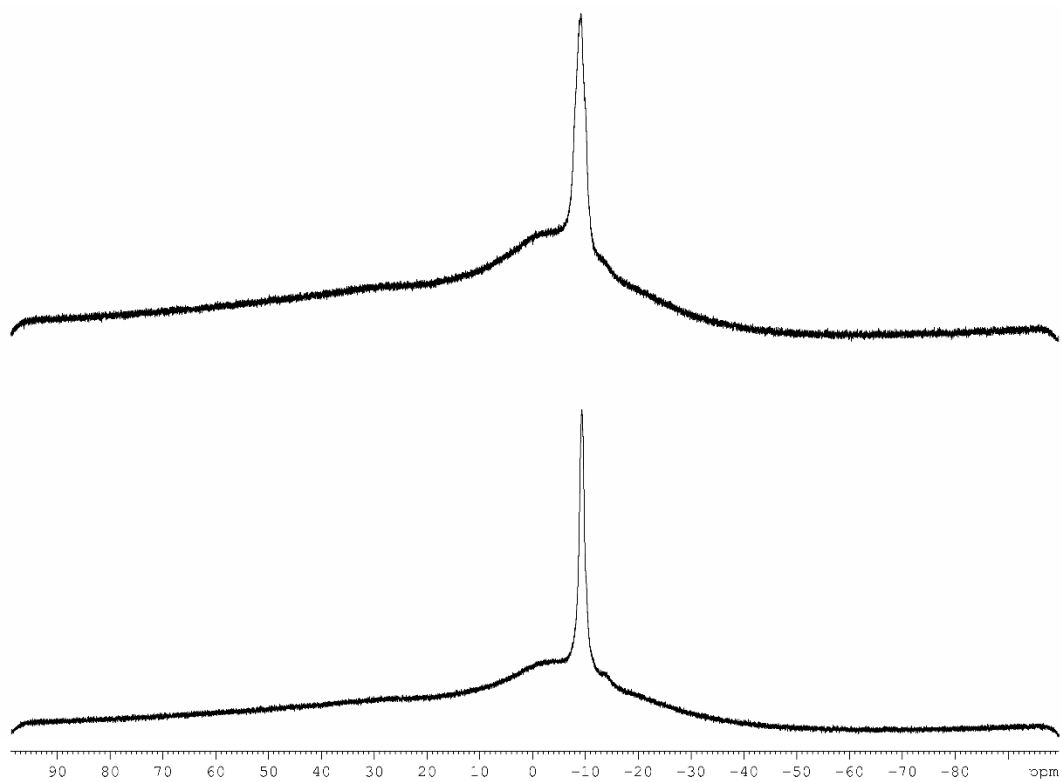


Figure S26: ¹¹B (top) and ¹¹B{¹H} NMR spectrum (bottom) of 3c in CD₂Cl₂.

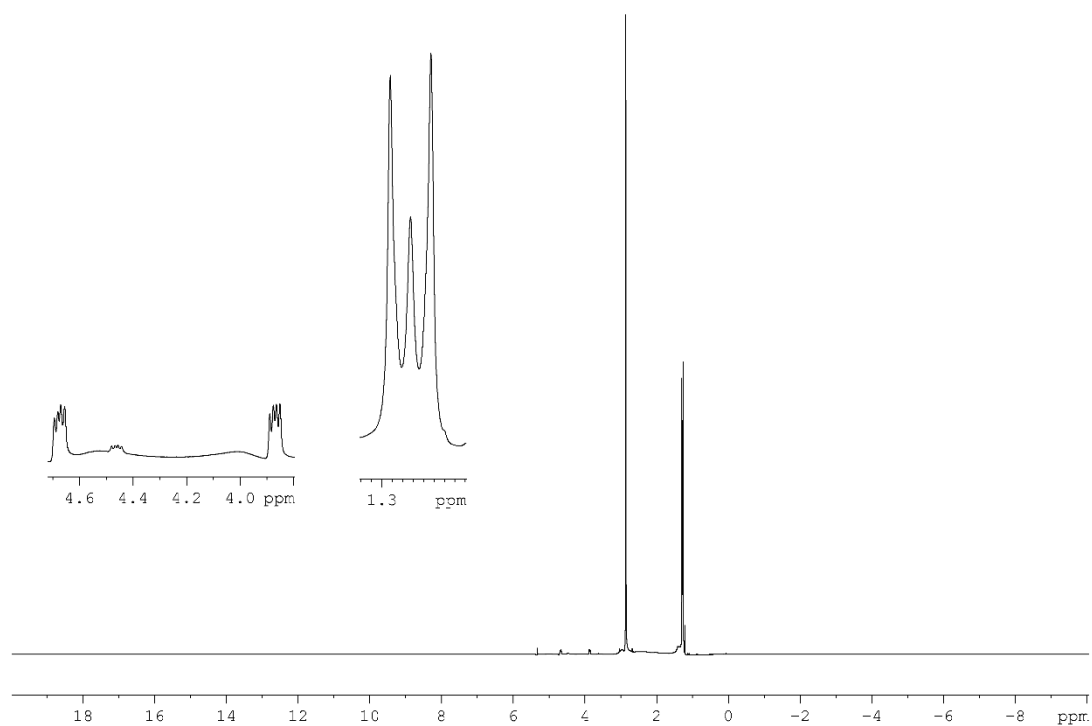


Figure S27: ^1H NMR spectrum of **3c** in CD_2Cl_2 .

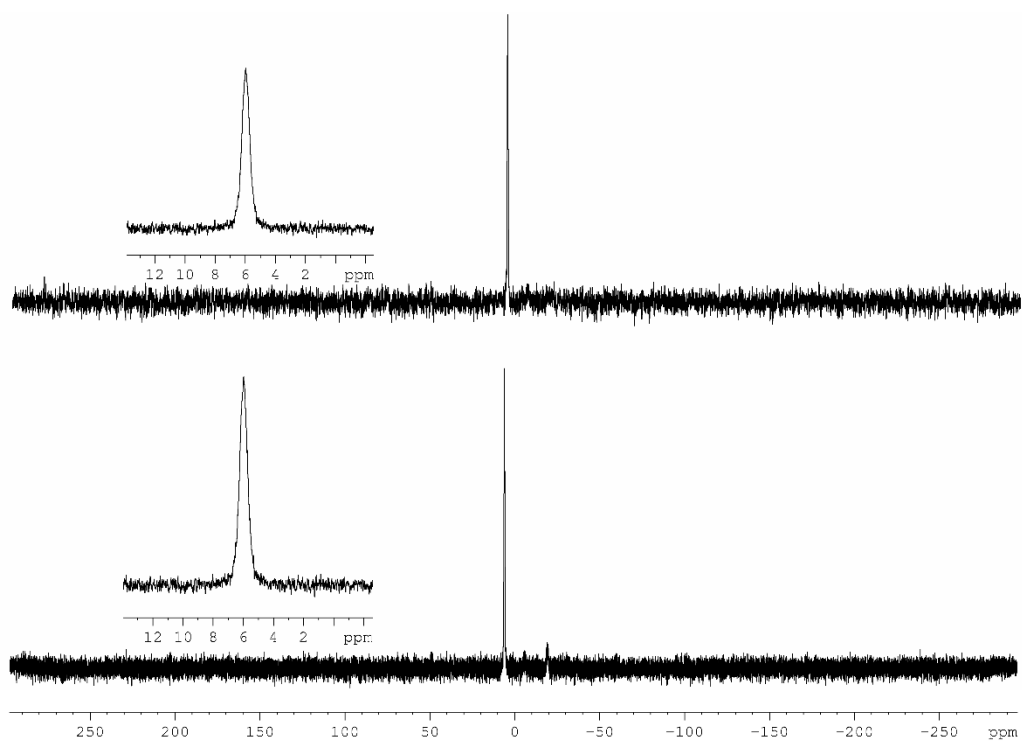
[AuCl(Ph₂PBH₂NMe₃)₂][AlCl₄] (3d)

Figure 28 ³¹P (top) and ³¹P{¹H} NMR spectrum (bottom) of 3d in CD₂Cl₂.

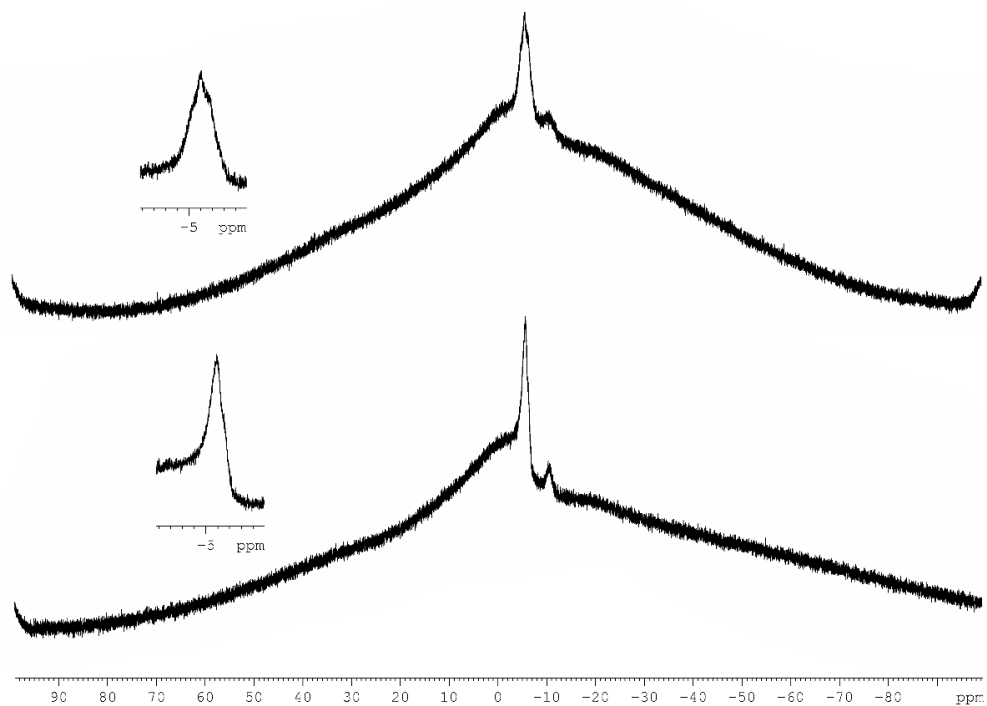


Figure S29: ¹¹B (top) and ¹¹B{¹H} NMR spectrum (bottom) of 3d in CD₂Cl₂.

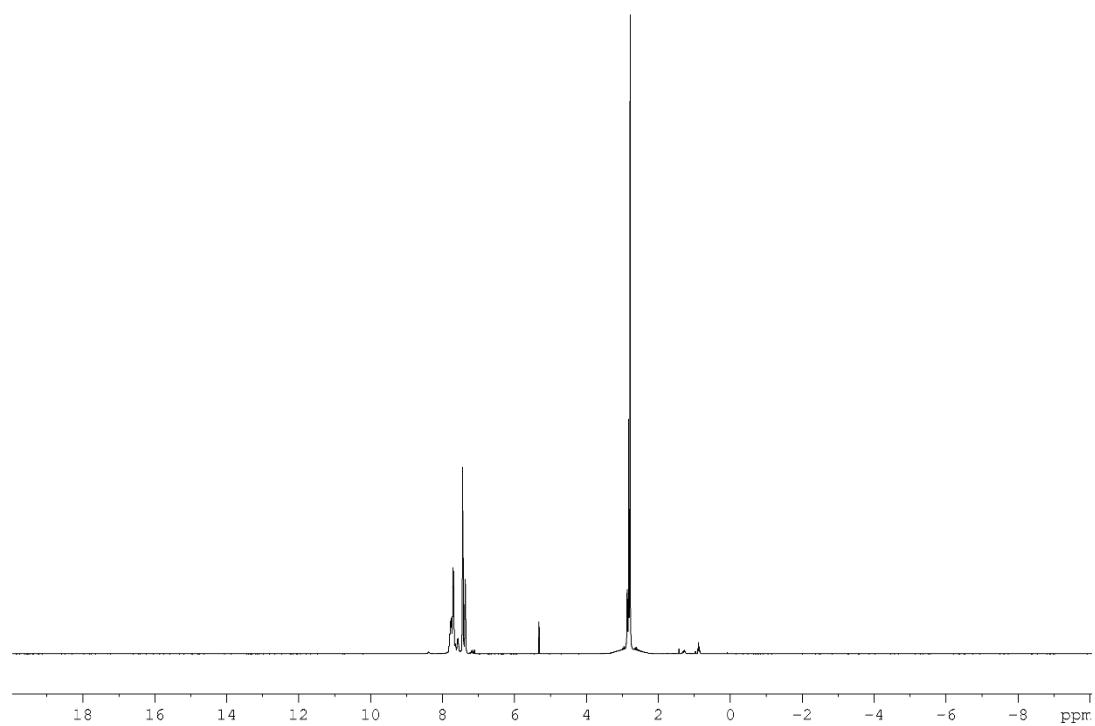


Figure S30: ^1H NMR spectrum of **3d** in CD_2Cl_2 .

4.5.7 Computational Details

Quantum chemical computations have been performed with gradient-corrected density functional theory (DFT) in form of M06-2X^[6] functional, which includes dispersion corrections, in conjunction with def2-TZVPP basis set (ECP for Au).^[7] Basis set was obtained from the EMSL basis set exchange database.^[8] Gaussian 09 program package^[9] was used throughout. Both single point energy computations on experimental solid state geometries and geometry optimization have been performed. Optimized geometry structures correspond to minima on their respective potential energy surfaces as was verified by subsequent vibrational analysis. Natural bond orbital analysis (NBO Version 3.1, E. D. Glendening, A. E. Reed, J. E. Carpenter, and F. Weinhold) was performed as implemented in Gaussian 09.

Results of Computational Studies for **2a** and **2b**

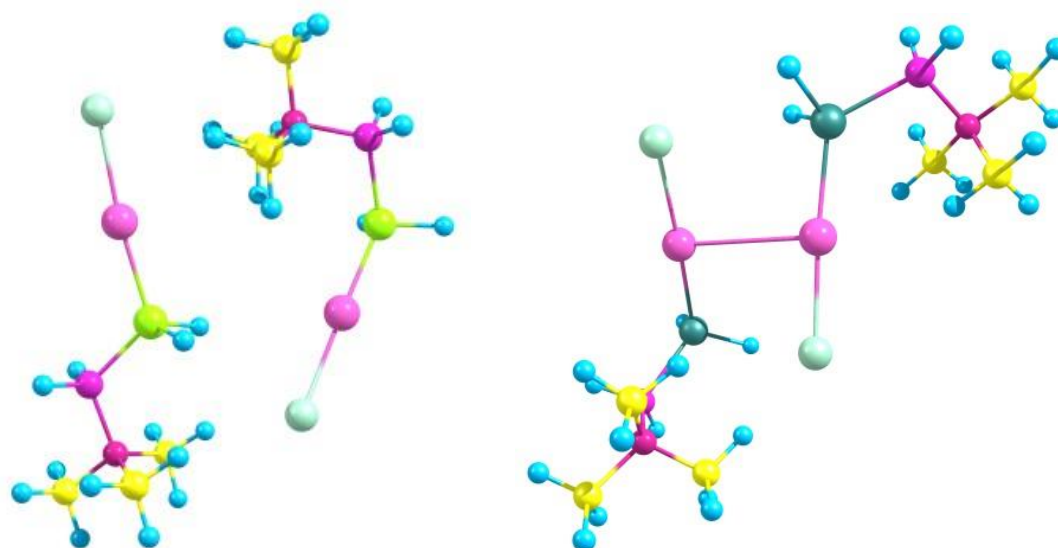


Figure S31: Optimized gas phase structures of dimer **2a** (left) and dimer **2b** (right).

Optimization of dimer of **2a** results in breaking the Au-Au bond (Au-Au distance is 5.12 Å), nevertheless the dimerization energy is exothermic (-83.3 kJ mol⁻¹) due to additional interactions (Figure S31). In contrast, optimization of **2b** dimer yielded the structure with Au-Au distance of 3.371 Å, which is longer than experimental value of 3.251 Å in the solid **2b** polymer. Gas phase dimerization energy of **2b** is -67.2 kJ mol⁻¹.

Energetics of the interactions based on the single point energy computations at experimental solid state geometries of **2a** and **2b** are given in Table S14. The values are exothermic, for **2b** the energy gain upon formation of Au-Au bond is about -42 kJ mol⁻¹.

MOs of **2b** tetramer (left) and **2b** dimer (right) at experimental geometries are presented in Figure S32. The HOMO-LUMO gap for **2b** tetramer is 6.29 eV and for **2b** dimer is 7.43 eV. HOMO is essentially Au orbital (with some contribution of Cl), and LUMO is ligand-based. WBI of the middle Au-Au bond in **2b** tetramer is 0.146, corresponding Au-Cl and Au-As WBI are 0.554 and 0.623. According to NBO analysis, the electronic configuration of middle Au atoms in **2b** tetramer is $6s^{0.74} 5d^{9.78} 6p^{0.34}$.

Table S14. Energetics for the complexation processes, kJ mol^{-1} . M06-2X/def2-TZVPP (ECP on Au) level of theory (single point energy computation at experimental geometries).

Process	ΔE	ΔE per Au-Au bond
2 [2a] = [2a _dimer]	-39.1	-39.1
2 [2b] = [2b _dimer]	-45.3	-45.3
2 [2b _dimer] = [2b _tetramer]	-36.8	-36.8
3 [2b] = [2b _trimer]	-84.5	-42.3
4 [2b] = [2b _tetramer]	-127.4	-42.5

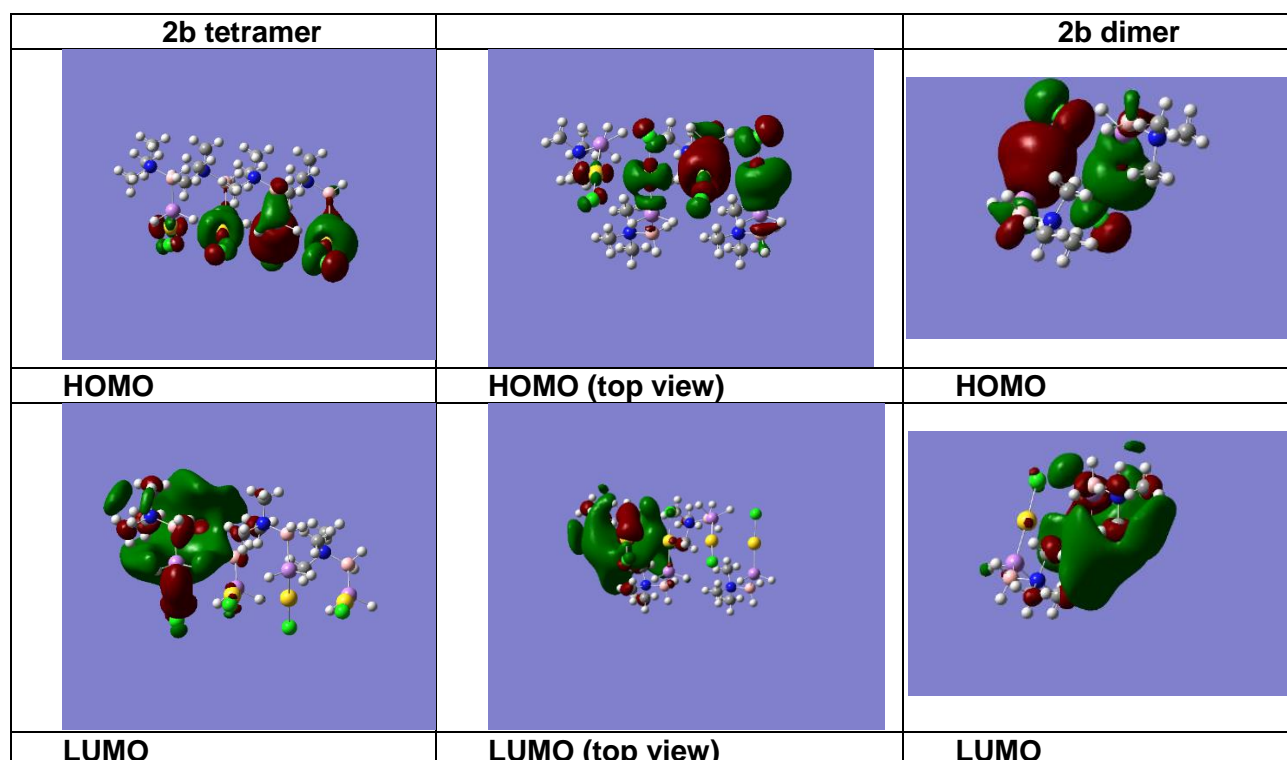


Figure S32. MOs of tetramer (left) and dimer (right) of **2b** at experimental solid state geometries.

Table S15. Total energies E^0 (Hartree) for single point computations at experimental geometries. M06-2X/def2-TZVPP (ECP on Au) level of theory.

Compound	E^0
2a_monomer1	-1138.838211
2a_monomer2	-1138.820419
2a_dimer	-2277.673535
2b_monomer	-3033.397935
2b_dimer	-6066.81312
2b_trimer	-9100.225998
2b_tetramer	-12133.64027
3a_monomer_90 [Au(PH ₂ BH ₂ Nme ₃) ₂] ⁺	-1221.385138
3a_monomer_300 [Au(PH ₂ BH ₂ Nme ₃) ₂] ⁺	-1221.350719
[3a_dimer] ²⁺ _90	-2442.724326
[3a_dimer] ²⁺ _300	-2442.654701
[3a_tetramer] ⁴⁺ _90	-4885.245132
[3a_tetramer] ⁴⁺ _300	-4885.104208

Table S16. Total energies E^0 (Hartree) for optimized gas phase geometries. M06-2X/def2-TZVPP (ECP on Au) level of theory.

Compound	E^0
2a_monomer	-1138.99581
2a_dimer	-2278.02334
2b_monomer	-3033.529433
2b_dimer	-6067.084466
3a_monomer [Au(PH ₂ BH ₂ Nme ₃) ₂] ⁺	-1221.667384
[3a_dimer] ²⁺	-2443.292068

Table S17. Geometries of compounds used for the single point computations. Xyz coordinates in angstroms. M06-2X/def2-TZVPP (ECP on Au) level of theory.

2a_monomer1			
79	1.104601000	-0.193925000	0.021949000
17	2.920339000	1.227049000	-0.051713000
15	-0.716214000	-1.500726000	-0.081851000
1	-0.124721000	-2.575867000	-0.519446000
1	-0.990115000	-1.847387000	1.138047000
7	-3.001508000	0.481486000	-0.015836000
6	-2.929411000	0.366440000	1.466919000
1	-3.184953000	-0.515696000	1.732320000
1	-3.521374000	1.009750000	1.864503000
1	-2.028865000	0.542939000	1.754687000
5	-2.479027000	-0.868241000	-0.726904000
1	-2.283920000	-0.806091000	-1.818636000
1	-3.275129000	-1.849930000	-0.399114000
6	-2.183698000	1.651979000	-0.458344000

1	-2.591943000	2.463433000	-0.148505000
1	-2.134119000	1.663762000	-1.416857000
1	-1.298255000	1.579663000	-0.093241000
6	-4.414409000	0.672062000	-0.418725000
1	-4.910103000	-0.131322000	-0.234669000
1	-4.457636000	0.865077000	-1.357196000
1	-4.794069000	1.400719000	0.077258000

2a_monomer2

79	-1.357026000	-0.097453000	0.000658000
15	0.791836000	-0.719892000	0.011647000
1	1.356689000	-1.556504000	0.828129000
1	1.269112000	-1.511092000	-0.903697000
17	-3.539696000	0.613813000	-0.000765000
7	3.626356000	0.227967000	0.003511000
6	4.044270000	-0.738168000	-1.058757000
1	3.644292000	-1.594119000	-0.888379000
1	5.000488000	-0.825380000	-1.053604000
1	3.757129000	-0.415543000	-1.915979000
5	2.092567000	0.711462000	-0.193865000
1	2.129871000	1.105385000	-1.299426000
1	2.272044000	1.915647000	0.474324000
6	3.859663000	-0.338915000	1.362183000
1	3.298672000	-1.101571000	1.494149000
1	3.656319000	0.329433000	2.024862000
1	4.781760000	-0.596050000	1.446605000
6	4.500092000	1.427730000	-0.134127000
1	5.420433000	1.163263000	-0.060425000
1	4.291641000	2.057164000	0.559682000
1	4.352415000	1.834765000	-0.990980000

2a_dimer

79	0.775331000	-0.346520000	1.329694000
79	-1.115800000	1.192548000	-0.589775000
15	2.455139000	0.189651000	-0.047232000
1	2.356793000	0.578291000	-1.282104000
1	3.119409000	1.298176000	0.099610000
17	-0.937326000	3.217543000	0.500657000
15	-1.445060000	-0.700928000	-1.747446000
1	-0.539938000	-0.496439000	-2.661898000
1	-0.892768000	-1.652852000	-1.060306000
17	-0.917763000	-0.966416000	2.750647000
7	5.079920000	-0.682594000	-1.179802000
7	-4.169621000	-1.625802000	-0.810717000
6	5.724535000	0.648093000	-0.955694000
1	5.110797000	1.345839000	-1.196813000
1	6.514620000	0.716056000	-1.497111000
1	5.962511000	0.736805000	-0.030024000
6	-3.444799000	-2.343715000	0.273823000
1	-2.915840000	-3.044579000	-0.104193000
1	-4.081440000	-2.713506000	0.890494000
1	-2.875606000	-1.723320000	0.738663000
5	3.980239000	-1.017367000	-0.037934000
1	4.628393000	-0.886507000	0.932429000
1	4.084745000	-2.394110000	-0.187619000
5	-3.238096000	-1.457674000	-2.116228000

1	-3.600176000	-0.749812000	-2.891882000
1	-2.959342000	-2.642953000	-2.587764000
6	4.501845000	-0.771416000	-2.550830000
1	3.790686000	-0.139272000	-2.642582000
1	4.163212000	-1.661012000	-2.696178000
1	5.186856000	-0.585264000	-3.198607000
6	-4.605981000	-0.287358000	-0.307885000
1	-5.273323000	-0.402663000	0.372175000
1	-4.972490000	0.223204000	-1.033379000
1	-3.850609000	0.177509000	0.060694000
6	6.157813000	-1.707669000	-1.084089000
1	6.844800000	-1.510211000	-1.725543000
1	5.791220000	-2.575917000	-1.265103000
1	6.533069000	-1.696153000	-0.200498000
6	-5.351472000	-2.423178000	-1.213644000
1	-5.059230000	-3.233489000	-1.641438000
1	-5.888056000	-1.915615000	-1.825452000
1	-5.870364000	-2.642940000	-0.436768000

2b_monomer

33	-0.725985000	-1.147930000	-0.002671000
1	-0.978684000	-1.459121000	1.464952000
1	-0.422861000	-2.485894000	-0.662327000
79	1.339838000	-0.006004000	-0.009784000
17	3.437453000	0.957205000	0.019591000
7	-3.312322000	0.572021000	-0.006775000
6	-2.634813000	1.881657000	-0.314013000
1	-1.762620000	1.892855000	0.078185000
1	-2.561576000	1.986356000	-1.267428000
1	-3.159688000	2.603309000	0.043860000
6	-3.380759000	0.375517000	1.486870000
1	-3.792753000	1.140523000	1.891289000
1	-3.899691000	-0.409389000	1.681831000
1	-2.493140000	0.265620000	1.835357000
5	-2.609666000	-0.619187000	-0.749026000
1	-3.308059000	-1.570698000	-0.688166000
1	-2.490628000	-0.339405000	-1.888425000
6	-4.692887000	0.661279000	-0.538966000
1	-4.664914000	0.654342000	-1.501404000
1	-5.205523000	-0.089072000	-0.231481000
1	-5.100890000	1.475118000	-0.238963000

2b_dimer

33	2.102440000	-1.216288000	-0.456478000
1	3.047394000	-2.242706000	0.150074000
1	1.280707000	-1.972171000	-1.491164000
79	0.572067000	-0.736720000	1.275470000
17	-0.994238000	-0.426822000	2.942693000
7	4.522659000	0.699979000	-0.799443000
6	4.009194000	1.775021000	0.122233000
1	3.498353000	1.378398000	0.826577000
1	3.454859000	2.383365000	-0.375789000
1	4.753037000	2.257529000	0.493983000
6	5.347547000	-0.288505000	-0.014042000
1	6.029764000	0.178364000	0.470678000
1	5.754535000	-0.915362000	-0.618208000

1	4.780799000	-0.760156000	0.600472000
5	3.349428000	0.023889000	-1.593024000
1	3.806376000	-0.621926000	-2.471193000
1	2.685821000	0.867414000	-2.081845000
6	5.396105000	1.362820000	-1.796663000
1	4.856315000	1.896801000	-2.388936000
1	5.863820000	0.698537000	-2.306897000
1	6.027064000	1.926999000	-1.346852000
33	-2.688694000	1.280319000	-0.184141000
1	-2.632892000	1.250627000	1.335931000
1	-4.167686000	1.261229000	-0.543519000
79	-1.895739000	-0.844366000	-0.838822000
17	-1.272017000	-2.989240000	-1.421153000
7	-0.645541000	3.619444000	-0.139605000
6	0.450563000	2.890295000	-0.871352000
1	0.416752000	1.958963000	-0.657035000
1	0.333806000	3.008015000	-1.818893000
1	1.302442000	3.251568000	-0.610601000
6	-0.500847000	3.393337000	1.344380000
1	0.386185000	3.630551000	1.618827000
1	-1.138687000	3.937705000	1.813651000
1	-0.663307000	2.468440000	1.543714000
5	-2.060347000	3.214076000	-0.685171000
1	-2.861269000	3.978153000	-0.271075000
1	-2.055407000	3.308143000	-1.860632000
6	-0.469653000	5.064126000	-0.420403000
1	-0.689341000	5.239225000	-1.341378000
1	-1.050623000	5.575329000	0.146620000
1	0.441294000	5.314388000	-0.258086000
2b_trimer			
33	-2.893661000	0.984889000	-1.453283000
1	-3.818801000	0.987964000	-2.661058000
1	-1.543576000	1.466171000	-1.965940000
79	-2.561908000	-1.303308000	-0.978134000
17	-2.137411000	-3.549575000	-0.657655000
7	-5.099883000	2.474051000	0.147457000
6	-5.321135000	1.387424000	1.166695000
1	-5.176734000	0.532669000	0.762702000
1	-4.707558000	1.506874000	1.897844000
1	-6.222055000	1.440474000	1.498174000
6	-6.020620000	2.261017000	-1.027758000
1	-6.923972000	2.186111000	-0.716514000
1	-5.948785000	3.007481000	-1.628599000
1	-5.770434000	1.456392000	-1.487512000
5	-3.588894000	2.564714000	-0.267674000
1	-3.417121000	3.571784000	-0.861925000
1	-2.929052000	2.612459000	0.708546000
6	-5.448932000	3.758924000	0.798933000
1	-4.786986000	3.968627000	1.465992000
1	-5.469234000	4.457809000	0.142034000
1	-6.308347000	3.684235000	1.216820000
33	0.576739000	-1.808530000	1.615031000
1	-0.234401000	-3.077605000	1.400840000
1	2.011027000	-2.267663000	1.836827000

79	0.610873000	-0.772799000	-0.505763000
17	0.754927000	0.114086000	-2.632183000
7	-1.581075000	-0.858964000	3.637241000
6	-2.008563000	0.357095000	2.857944000
1	-1.925220000	0.184899000	1.921050000
1	-1.451087000	1.102705000	3.100187000
1	-2.923279000	0.564869000	3.068753000
6	-2.414779000	-2.045071000	3.221931000
1	-3.344275000	-1.826941000	3.304370000
1	-2.208961000	-2.793533000	3.788544000
1	-2.216289000	-2.271281000	2.310494000
5	-0.039240000	-1.113853000	3.491930000
1	0.293668000	-1.906405000	4.303159000
1	0.535055000	-0.109624000	3.721200000
6	-1.840826000	-0.572061000	5.067950000
1	-1.219833000	0.095670000	5.377463000
1	-1.726791000	-1.373502000	5.582787000
1	-2.736055000	-0.246112000	5.173113000
33	3.438476000	2.197298000	-0.626840000
1	2.513336000	2.200373000	-1.834615000
1	4.788469000	2.678550000	-1.139526000
79	3.770229000	-0.090899000	-0.151692000
17	4.194726000	-2.337166000	0.168788000
7	1.232214000	3.686514000	0.973974000
6	1.010911000	2.599803000	1.993110000
1	1.155362000	1.745133000	1.589219000
1	1.624488000	2.719253000	2.724259000
1	0.110082000	2.652883000	2.324617000
6	0.311476000	3.473480000	-0.201242000
1	-0.591835000	3.398521000	0.109929000
1	0.383352000	4.219890000	-0.802156000
1	0.561703000	2.668801000	-0.661069000
5	2.743202000	3.777177000	0.558843000
1	2.914925000	4.784163000	-0.035511000
1	3.403085000	3.824868000	1.534989000
6	0.883205000	4.971333000	1.625376000
1	1.545151000	5.181036000	2.292435000
1	0.862903000	5.670219000	0.968477000
1	0.023790000	4.896644000	2.043263000

2b_tetramer

33	-4.668324000	-1.519037000	0.580921000
1	-5.741176000	-2.548202000	0.258144000
1	-3.382182000	-2.309994000	0.774326000
79	-4.345692000	-0.356366000	-1.447766000
17	-3.949716000	0.637054000	-3.493623000
7	-6.604211000	-0.261619000	2.659138000
6	-6.723949000	1.076962000	1.978909000
1	-6.658207000	0.963875000	1.031672000
1	-6.017814000	1.654030000	2.285114000
1	-7.572440000	1.471348000	2.199611000
6	-7.675050000	-1.189429000	2.142545000
1	-8.532315000	-0.771601000	2.236054000
1	-7.659333000	-2.006977000	2.647496000
1	-7.510122000	-1.383313000	1.216981000

5	-5.157599000	-0.850361000	2.504106000
1	-5.034375000	-1.758902000	3.250043000
1	-4.375904000	-0.025234000	2.818556000
6	-6.828024000	-0.035375000	4.106717000
1	-6.079546000	0.446283000	4.473929000
1	-6.912391000	-0.879295000	4.555104000
1	-7.628107000	0.477513000	4.231967000
33	-0.914460000	1.888202000	-1.306214000
1	-1.783685000	2.197038000	-2.516041000
1	0.522276000	2.086322000	-1.768509000
79	-1.124079000	-0.445103000	-1.017392000
17	-1.229953000	-2.746877000	-0.878653000
7	-2.763999000	3.713107000	0.395643000
6	-3.252428000	2.629826000	1.321114000
1	-3.296041000	1.798888000	0.849619000
1	-2.646526000	2.548335000	2.063789000
1	-4.125778000	2.861564000	1.649606000
6	-3.678924000	3.808695000	-0.799367000
1	-4.583234000	3.918407000	-0.501515000
1	-3.423944000	4.563452000	-1.336680000
1	-3.606741000	3.006548000	-1.321609000
5	-1.261962000	3.487772000	-0.000271000
1	-0.850583000	4.472029000	-0.509030000
1	-0.633554000	3.307003000	0.981108000
6	-2.828044000	4.988927000	1.147530000
1	-2.152900000	4.988946000	1.834041000
1	-2.672155000	5.722967000	0.549825000
1	-3.692241000	5.080480000	1.551986000
33	1.750501000	-1.855656000	1.547366000
1	0.677649000	-2.884822000	1.224589000
1	3.036643000	-2.646614000	1.740770000
79	2.073162000	-0.693041000	-0.481398000
17	2.469109000	0.300435000	-2.527178000
7	-0.185357000	-0.598295000	3.625505000
6	-0.305095000	0.740287000	2.945276000
1	-0.239353000	0.627200000	1.998040000
1	0.401040000	1.317355000	3.251481000
1	-1.153616000	1.134729000	3.166056000
6	-1.256196000	-1.526105000	3.108912000
1	-2.113490000	-1.108220000	3.202498000
1	-1.240479000	-2.343652000	3.613863000
1	-1.091297000	-1.719933000	2.183426000
5	1.261255000	-1.187037000	3.470473000
1	1.384450000	-2.095521000	4.216488000
1	2.042920000	-0.361854000	3.785001000
6	-0.409265000	-0.372057000	5.073053000
1	0.339279000	0.109664000	5.440374000
1	-0.493632000	-1.215977000	5.521440000
1	-1.209253000	0.140838000	5.198334000
33	5.504394000	1.551527000	-0.339847000
1	4.635169000	1.860363000	-1.549674000
1	6.941035000	1.749641000	-0.802173000
79	5.294775000	-0.781778000	-0.051025000
17	5.188901000	-3.083552000	0.087714000
7	3.654826000	3.376488000	1.362088000

6	3.166331000	2.293144000	2.287450000
1	3.122784000	1.462269000	1.816064000
1	3.772233000	2.211653000	3.030125000
1	2.293077000	2.524889000	2.615973000
6	2.739901000	3.472076000	0.167078000
1	1.835620000	3.581731000	0.464852000
1	2.994910000	4.226776000	-0.370313000
1	2.812113000	2.669872000	-0.355241000
5	5.156863000	3.151152000	0.966174000
1	5.568176000	4.135347000	0.457306000
1	5.785300000	2.970328000	1.947475000
6	3.590810000	4.652252000	2.113898000
1	4.265954000	4.652271000	2.800408000
1	3.746699000	5.386292000	1.516192000
1	2.726613000	4.743804000	2.518353000

Table S18. Optimized geometries of computationally studied compounds. Xyz coordinates in angstroms. M06-2X/def2-TZVPP (ECP on Au) level of theory.

2a monomer

79	1.047936000	-0.219932000	-0.005292000
17	2.774134000	1.335056000	0.007182000
15	-0.704308000	-1.604067000	-0.001219000
1	-0.533779000	-2.724137000	-0.824104000
1	-0.818107000	-2.268136000	1.230020000
7	-2.817501000	0.519171000	-0.005882000
6	-2.499528000	0.705771000	1.428928000
1	-3.000248000	-0.072766000	2.000212000
1	-2.839553000	1.688074000	1.757227000
1	-1.422311000	0.633875000	1.567990000
5	-2.516166000	-0.997656000	-0.487499000
1	-2.601792000	-1.011989000	-1.683910000
1	-3.313349000	-1.704074000	0.066495000
6	-2.070418000	1.519582000	-0.808688000
1	-2.341685000	2.522712000	-0.479243000
1	-2.328799000	1.385823000	-1.855517000
1	-1.002048000	1.368800000	-0.675667000
6	-4.268310000	0.752191000	-0.208481000
1	-4.827570000	0.071345000	0.426808000
1	-4.510665000	0.553306000	-1.249371000
1	-4.509810000	1.785674000	0.041410000

2a_dimer

79	0.827321000	-2.341520000	-0.007965000
79	-1.235502000	2.348677000	0.009802000
15	1.850303000	-0.354135000	-0.018176000
1	1.248059000	0.494088000	-0.961587000
1	1.492907000	0.357610000	1.137187000
17	0.863525000	3.199680000	0.688288000
15	-3.238432000	1.604832000	-0.664573000
1	-4.202107000	2.610994000	-0.509466000
1	-3.252293000	1.524207000	-2.066088000
17	-0.472012000	-4.310973000	0.075568000
7	4.426834000	1.180592000	-0.157054000

7	-3.257609000	-1.269596000	0.131268000
6	4.230032000	1.774416000	1.188439000
1	3.169126000	1.943361000	1.355017000
1	4.754559000	2.728755000	1.241787000
1	4.626335000	1.086971000	1.931581000
6	-2.530986000	-1.517745000	-1.140798000
1	-3.252040000	-1.498731000	-1.955828000
1	-2.027825000	-2.482695000	-1.092898000
1	-1.787949000	-0.733135000	-1.284972000
5	3.792146000	-0.302165000	-0.254153000
1	4.278456000	-0.958570000	0.625079000
1	4.025997000	-0.723045000	-1.354086000
5	-4.198316000	0.021564000	0.022733000
1	-4.599129000	0.296314000	1.119554000
1	-5.067704000	-0.215351000	-0.771097000
6	3.856406000	2.095133000	-1.176457000
1	2.813566000	2.293711000	-0.939552000
1	3.943918000	1.623995000	-2.152719000
1	4.407256000	3.036067000	-1.164634000
6	-2.285717000	-1.151603000	1.248739000
1	-1.725700000	-2.081747000	1.336207000
1	-2.838120000	-0.948128000	2.162597000
1	-1.604038000	-0.327427000	1.045480000
6	5.880576000	1.035729000	-0.405190000
1	6.362111000	2.010838000	-0.327643000
1	6.027508000	0.623046000	-1.399756000
1	6.295600000	0.352952000	0.331561000
6	-4.123302000	-2.446147000	0.406463000
1	-4.817121000	-2.571352000	-0.420220000
1	-4.680733000	-2.259169000	1.321186000
1	-3.493915000	-3.330082000	0.514279000
2b_monomer			
33	-0.739571000	-1.505412000	0.000799000
1	-0.760874000	-2.367769000	1.239092000
1	-0.647010000	-2.602207000	-1.027481000
79	1.153146000	-0.093477000	-0.003857000
17	2.905814000	1.425068000	0.006458000
7	-2.740340000	0.853718000	-0.002587000
6	-2.014737000	1.590262000	-1.067605000
1	-0.955077000	1.351518000	-1.016821000
1	-2.414485000	1.286826000	-2.031671000
1	-2.151406000	2.662003000	-0.923892000
6	-2.209433000	1.258462000	1.321723000
1	-2.383680000	2.323626000	1.473937000
1	-2.718726000	0.683105000	2.091199000
1	-1.140061000	1.061540000	1.356646000
5	-2.678507000	-0.746408000	-0.218498000
1	-3.368643000	-1.245106000	0.623792000
1	-3.026672000	-0.965928000	-1.343243000
6	-4.174917000	1.228819000	-0.070532000
1	-4.574089000	0.907209000	-1.028788000
1	-4.707772000	0.723590000	0.730073000
1	-4.273575000	2.309488000	0.034793000

2b_dimer

33	2.828776000	-0.928370000	-0.500072000
1	2.507607000	-2.031328000	0.472205000
1	2.775651000	-1.704864000	-1.783563000
79	1.131567000	0.717455000	-0.416588000
17	-0.454375000	2.472061000	-0.309413000
7	5.083154000	0.819935000	0.684899000
6	4.628109000	2.078888000	0.046174000
1	3.557294000	2.024540000	-0.135512000
1	5.151100000	2.196675000	-0.899060000
1	4.846917000	2.919971000	0.704662000
6	4.399084000	0.658175000	1.989149000
1	4.688071000	1.469241000	2.658088000
1	4.686767000	-0.299931000	2.415982000
1	3.322265000	0.685887000	1.834290000
5	4.846389000	-0.461883000	-0.274905000
1	5.389302000	-1.394172000	0.248018000
1	5.282666000	-0.177762000	-1.354812000
6	6.543866000	0.915217000	0.921375000
1	7.047255000	0.984725000	-0.039446000
1	6.875276000	0.018066000	1.436621000
1	6.760288000	1.798155000	1.523831000
33	-2.764733000	-0.058976000	1.492865000
1	-2.018628000	1.074425000	2.154330000
1	-3.234758000	-0.771733000	2.737628000
79	-1.369289000	-1.457995000	0.196861000
17	-0.077773000	-2.885901000	-1.147870000
7	-4.472515000	1.563926000	-0.522386000
6	-3.605251000	0.988240000	-1.582126000
1	-2.571526000	0.994219000	-1.245214000
1	-3.926978000	-0.031607000	-1.781797000
1	-3.689700000	1.595883000	-2.483349000
6	-3.947293000	2.894466000	-0.127926000
1	-3.877759000	3.531860000	-1.009799000
1	-4.626582000	3.330052000	0.600303000
1	-2.956315000	2.776002000	0.301591000
5	-4.604244000	0.598417000	0.754324000
1	-5.175634000	1.205716000	1.615334000
1	-5.158293000	-0.406552000	0.404074000
6	-5.839005000	1.737397000	-1.070477000
1	-6.201603000	0.775175000	-1.421475000
1	-6.490347000	2.102592000	-0.280387000
1	-5.811473000	2.451154000	-1.894154000

Results of Computational Studies for **3a**

Optimization of a dimer of cationic compound **3a** in the gas phase yielded structure with Au-Au bond distance of 3.338 Å, considerably longer than experimental value of 3.168(1) Å in the solid polymer. The computed gas phase dimerization energy is endothermic, 112 kJ mol⁻¹, due to Coulomb repulsion of positively charged monomers.

In order to get insight how the energetics of interaction changes upon the changing the temperature, the single point energy computations using experimentally determined geometries of **3a** at 90K and 300 K were performed. In case of the **3a** polymers, the geometry of the cationic tetrameric unit was extracted from experimental data, the tetramer was subsequently divided into the two dimers and four monomers. The counter anions were not included in the computation. The energetics of the complex formation are given in Table S19. The interaction energies between positively charged monomers are highly endothermic. Nevertheless, one can compare the energetic data for **3a** at the geometries determined at temperatures 90 and 300 K. The energy difference $\Delta(\Delta E_{300} - \Delta E_{90})$ indicate that the Au-Au bond is by 2-4 kJ mol⁻¹ stronger for the structure at 90 K than those at 300 K. This conclusion is in accord with the Wiberg bond index (WBI) trends, Table S20. WBI of the Au-Au bonds in the **3a** dimer and middle Au-Au bond in the tetrameric unit decrease by ~7% on going from the 90 to 300 K, while WBI of Au-P bond does not show significant changes. These results are in accord with experimentally observed shorter Au-Au distances at 90 K.

A cationic tetrameric unit of the polymer **3a** has been extracted from the solid state structure as a simplified model. This might not account for all effects present in the crystalline material (e.g. formal infinite chain, anion effects, dielectric constant). Thus, a lifelike picture is not possible and the findings from the photoluminescence part have also been explained by comparison with approved literature. Analysis of the molecular orbitals of [**3a**_tetramer]⁴⁺ (Figure S33/34, Table S21) reveals that the HOMO-LUMO gap is 6.86 and 7.03 eV at 90 and 300 K, respectively. The largest contributions to HOMO and LUMO of [**3a**_tetramer]⁴⁺ are from the Au atoms (72% for HOMO and 77% for LUMO). The HOMO is essentially formed by mixing 5d and 6s orbitals of Au atoms, while LUMO is formed by overlapping of 6p orbitals of Au atoms. The major contributions to HOMO and LUMO are given in Table S21. According to NBO analysis, overall electronic configuration of gold atoms is the same for structures at 90 and 300K: 6s^{0.81}5d^{9.79}6p^{0.33} for terminal and 6s^{0.85}5d^{9.79}6p^{0.14} for the middle Au atoms in [**3a**_tetramer]⁴⁺.

Table S19. Energetics for the complexation processes, kJ mol⁻¹. M06-2X/def2-TZVPP (ECP on Au) level of theory.

Process	ΔE_{90}	ΔE_{300}	$\Delta(\Delta E_{300} - \Delta E_{90})$
2 [Au(PH ₂ BH ₂ NMe ₃) ₂] ⁺ = [3a_dimer] ²⁺	120.6	122.7	2.1
2 [3a_dimer] ²⁺ = [3a_tetramer] ⁴⁺	534.3	538.7	4.4
4 [Au(PH ₂ BH ₂ NMe ₃) ₂] ⁺ = [3a_tetramer] ⁴⁺	775.6	784.1	8.5

Table S20. Wiberg bond indexes. M06-2X/def2-TZVPP (ECP on Au) level of theory.

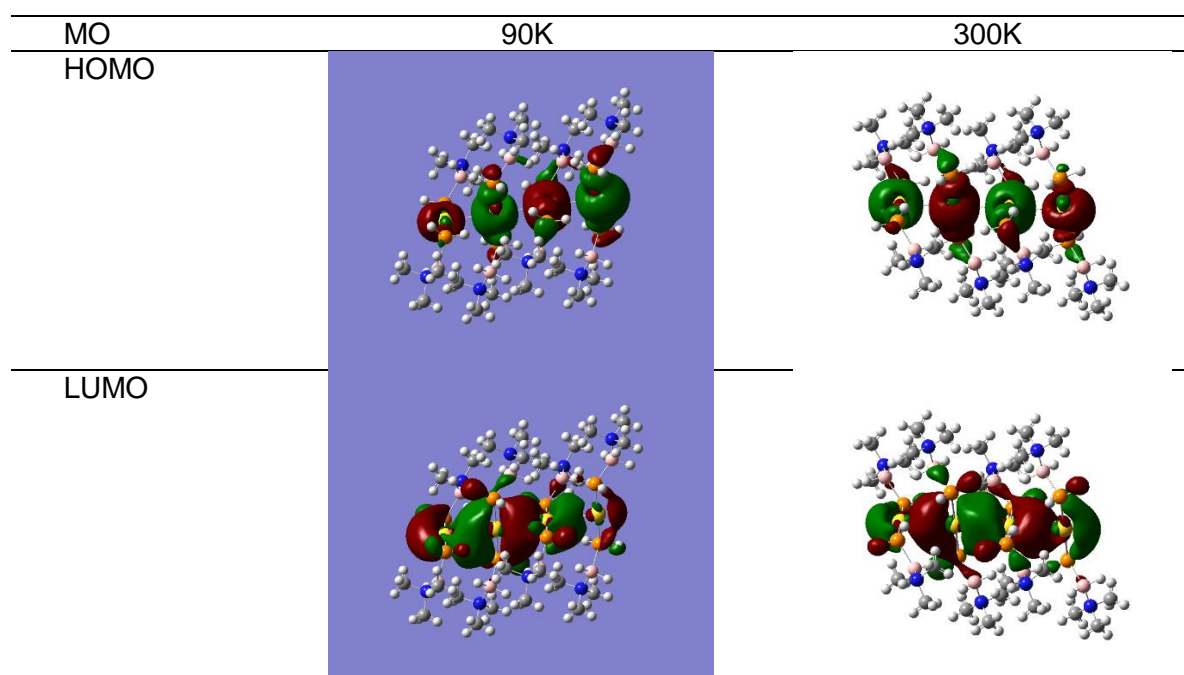
Compound	Bond	WBI ₉₀	WBI ₃₀₀	$\Delta(\text{WBI}_{300} - \text{WBI}_{90})$
[3a_dimer] ²⁺	Au-Au	0.139	0.129	-0.010
	Au-P ^{b)}	0.553	0.553	0.000
[3a_tetramer] ⁴⁺	Au-Au ^{a)}	0.183	0.170	-0.013
	Au-P ^{b)}	0.546	0.547	0.001

a) The central Au-Au bond in the 3a tetramer; b) Average value.

Table S21. Major atomic orbital contributions to HOMO and LUMO for [3a_tetramer]⁴⁺. M06-2X/def2-TZVPP (ECP on Au) level of theory.

Atom ^{a)}	HOMO ₉₀	HOMO ₃₀₀	LUMO ₉₀	LUMO ₃₀₀
Au1	0.04d + 0.04s	0.08d + 0.08s	0.11p _z	0.05p _z
Au40	0.09d + 0.08s	0.12d + 0.11s	0.39p _z	0.33p _z
Au78	0.13d + 0.12s	0.11d + 0.10s	0.21p _z	0.35p _z
Au118	0.11d + 0.13s	0.06d + 0.06s		

a) Contributions from p-orbitals of neighboring P atoms are smaller than 0.04.

**Figure S33.** HOMO and LUMO of [3a_tetramer]⁴⁺ at 90K and 300K.

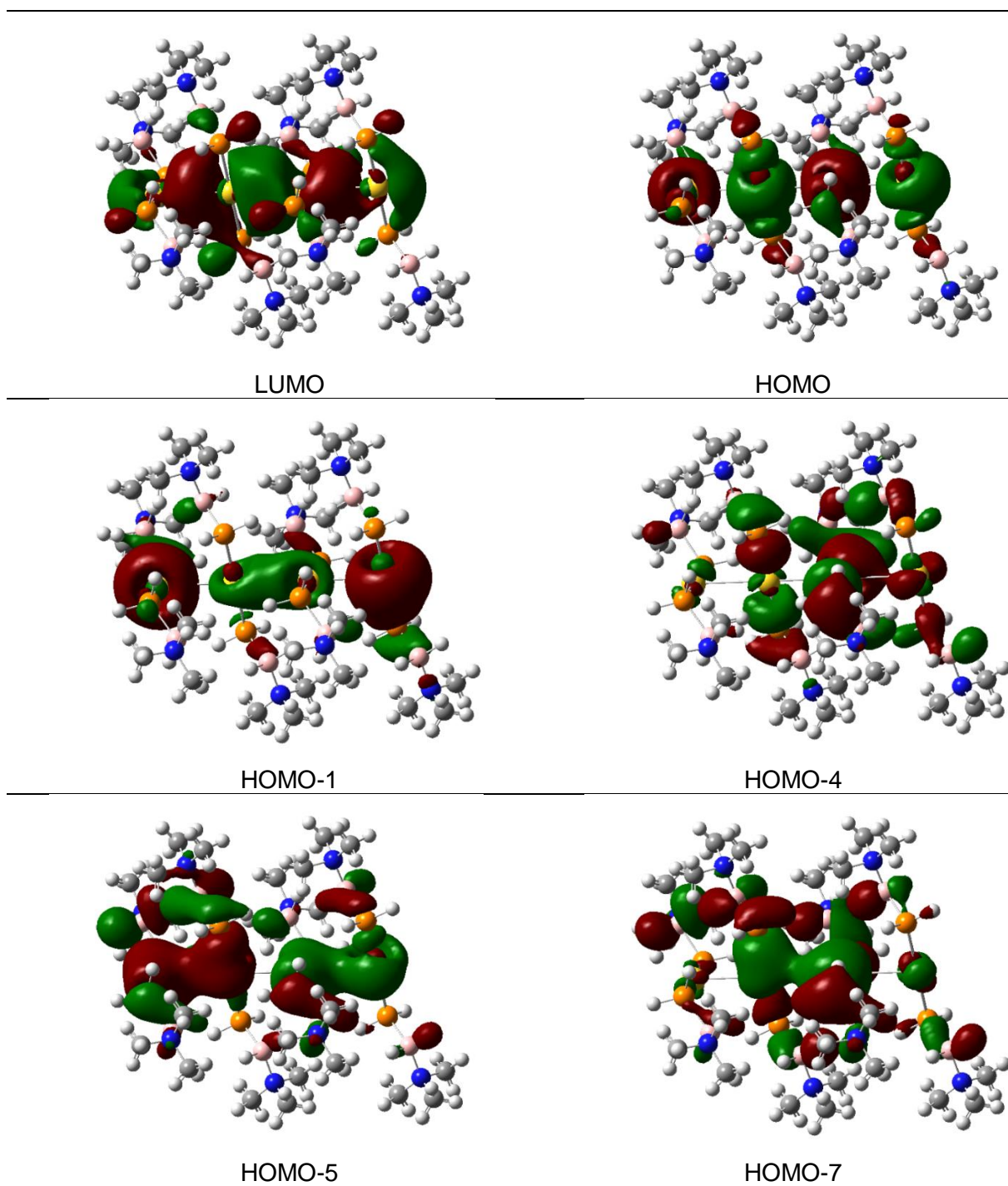


Figure S34. Selected MOs of $[3a_tetramer]^{4+}$ at 300K.

Table S22. Geometries of compounds used for the single point computations. xyz coordinates in angstroms. M06-2X/def2-TZVPP (ECP on Au) level of theory.

3a monomer [Au(PH₂BH₂NMe₃)₂]⁺ 90K			
79	5.500900000	4.877500000	11.403300000
15	3.738300000	4.990100000	12.900300000
1	2.667000000	5.363600000	12.262700000
1	3.518700000	3.804000000	13.384200000
15	7.281100000	4.708900000	9.933400000
1	7.799200000	5.895600000	9.787800000
1	8.187700000	3.954400000	10.480600000
7	8.005500000	3.197400000	7.426500000
7	2.897500000	6.407500000	15.402900000
5	4.060900000	6.230500000	14.382800000
1	5.022400000	5.857700000	14.975900000
1	4.320000000	7.298400000	13.925000000
6	7.570900000	2.818300000	6.043800000
1	7.615400000	3.586200000	5.470300000
1	6.667600000	2.491100000	6.070100000
1	8.148400000	2.130400000	5.703200000
6	2.355300000	5.181600000	15.962200000
1	2.130700000	4.580900000	15.249500000
1	1.567900000	5.385800000	16.471400000
1	3.010500000	4.775300000	16.532400000
6	9.280900000	3.911500000	7.337400000
1	9.892100000	3.405200000	6.797200000
1	9.646800000	4.018600000	8.218900000
1	9.138600000	4.772300000	6.941600000
6	3.358500000	7.279500000	16.499900000
1	4.047000000	6.831600000	16.995300000
1	2.621500000	7.478300000	17.080900000
1	3.706800000	8.095900000	16.133100000
6	1.716600000	7.102600000	14.745400000
1	2.016600000	7.912300000	14.323800000
1	1.058400000	7.314400000	15.411000000
1	1.331700000	6.522400000	14.086000000
5	6.881600000	3.981000000	8.124000000
1	5.935600000	3.266900000	8.216100000
1	6.574300000	4.890900000	7.423400000
6	8.143800000	1.895700000	8.105500000
1	7.628700000	1.234400000	7.646500000
1	7.851000000	1.971400000	9.012200000
1	9.076800000	1.633100000	8.095400000
[3a_dimer]²⁺ 90 K			
79	5.500900000	4.877500000	11.403300000
15	3.738300000	4.990100000	12.900300000
1	2.667000000	5.363600000	12.262700000
1	3.518700000	3.804000000	13.384200000
15	7.281100000	4.708900000	9.933400000
1	7.799200000	5.895600000	9.787800000
1	8.187700000	3.954400000	10.480600000
7	8.005500000	3.197400000	7.426500000
7	2.897500000	6.407500000	15.402900000
5	4.060900000	6.230500000	14.382800000

1	5.022400000	5.857700000	14.975900000
1	4.320000000	7.298400000	13.925000000
6	7.570900000	2.818300000	6.043800000
1	7.615400000	3.586200000	5.470300000
1	6.667600000	2.491100000	6.070100000
1	8.148400000	2.130400000	5.703200000
6	2.355300000	5.181600000	15.962200000
1	2.130700000	4.580900000	15.249500000
1	1.567900000	5.385800000	16.471400000
1	3.010500000	4.775300000	16.532400000
6	9.280900000	3.911500000	7.337400000
1	9.892100000	3.405200000	6.797200000
1	9.646800000	4.018600000	8.218900000
1	9.138600000	4.772300000	6.941600000
6	3.358500000	7.279500000	16.499900000
1	4.047000000	6.831600000	16.995300000
1	2.621500000	7.478300000	17.080900000
1	3.706800000	8.095900000	16.133100000
6	1.716600000	7.102600000	14.745400000
1	2.016600000	7.912300000	14.323800000
1	1.058400000	7.314400000	15.411000000
1	1.331700000	6.522400000	14.086000000
5	6.881600000	3.981000000	8.124000000
1	5.935600000	3.266900000	8.216100000
1	6.574300000	4.890900000	7.423400000
6	8.143800000	1.895700000	8.105500000
1	7.628700000	1.234400000	7.646500000
1	7.851000000	1.971400000	9.012200000
1	9.076800000	1.633100000	8.095400000
79	5.474600000	8.037000000	11.403300000
15	7.237200000	8.149600000	12.900300000
1	8.308500000	8.523100000	12.262700000
1	7.456800000	6.963500000	13.384200000
15	3.694400000	7.868400000	9.933400000
1	3.176300000	9.055100000	9.787800000
1	2.787800000	7.113900000	10.480600000
7	2.970000000	6.356900000	7.426500000
7	8.078000000	9.567000000	15.402900000
5	6.914600000	9.390000000	14.382800000
1	5.953100000	9.017200000	14.975900000
1	6.655500000	10.457900000	13.925000000
6	3.404600000	5.977800000	6.043800000
1	3.360100000	6.745700000	5.470300000
1	4.307900000	5.650600000	6.070100000
1	2.827100000	5.289900000	5.703200000
6	8.620200000	8.341100000	15.962200000
1	8.844800000	7.740400000	15.249500000
1	9.407600000	8.545300000	16.471400000
1	7.965000000	7.934800000	16.532400000
6	1.694600000	7.071000000	7.337400000
1	1.083400000	6.564700000	6.797200000
1	1.328700000	7.178100000	8.218900000
1	1.836900000	7.931800000	6.941600000
6	7.617000000	10.439000000	16.499900000
1	6.928500000	9.991100000	16.995300000

1	8.35400000	10.63780000	17.08090000
1	7.26870000	11.25540000	16.13310000
6	9.25890000	10.26210000	14.74540000
1	8.95890000	11.07180000	14.32380000
1	9.91710000	10.47390000	15.41100000
1	9.64380000	9.68190000	14.08600000
5	4.09390000	7.14050000	8.12400000
1	5.03990000	6.42640000	8.21610000
1	4.40120000	8.05040000	7.42340000
6	2.83170000	5.05520000	8.10550000
1	3.34680000	4.39390000	7.64650000
1	3.12450000	5.13090000	9.01220000
1	1.89870000	4.79260000	8.09540000
[3a_tetramer]⁴⁺ 90 K			
79	5.50090000	4.87750000	11.40330000
15	3.73830000	4.99010000	12.90030000
1	2.66700000	5.36360000	12.26270000
1	3.51870000	3.80400000	13.38420000
15	7.28110000	4.70890000	9.93340000
1	7.79920000	5.89560000	9.78780000
1	8.18770000	3.95440000	10.48060000
7	8.00550000	3.19740000	7.42650000
7	2.89750000	6.40750000	15.40290000
5	4.06090000	6.23050000	14.38280000
1	5.02240000	5.85770000	14.97590000
1	4.32000000	7.29840000	13.92500000
6	7.57090000	2.81830000	6.04380000
1	7.61540000	3.58620000	5.47030000
1	6.66760000	2.49110000	6.07010000
1	8.14840000	2.13040000	5.70320000
6	2.35530000	5.18160000	15.96220000
1	2.13070000	4.58090000	15.24950000
1	1.56790000	5.38580000	16.47140000
1	3.01050000	4.77530000	16.53240000
6	9.28090000	3.91150000	7.33740000
1	9.89210000	3.40520000	6.79720000
1	9.64680000	4.01860000	8.21890000
1	9.13860000	4.77230000	6.94160000
6	3.35850000	7.27950000	16.49990000
1	4.04700000	6.83160000	16.99530000
1	2.62150000	7.47830000	17.08090000
1	3.70680000	8.09590000	16.13310000
6	1.71660000	7.10260000	14.74540000
1	2.01660000	7.91230000	14.32380000
1	1.05840000	7.31440000	15.41100000
1	1.33170000	6.52240000	14.08600000
5	6.88160000	3.98100000	8.12400000
1	5.93560000	3.26690000	8.21610000
1	6.57430000	4.89090000	7.42340000
6	8.14380000	1.89570000	8.10550000
1	7.62870000	1.23440000	7.64650000
1	7.85100000	1.97140000	9.01220000
1	9.07680000	1.63310000	8.09540000
79	5.47460000	8.03700000	11.40330000

15	7.237200000	8.149600000	12.900300000
1	8.308500000	8.523100000	12.262700000
1	7.456800000	6.963500000	13.384200000
15	3.694400000	7.868400000	9.933400000
1	3.176300000	9.055100000	9.787800000
1	2.787800000	7.113900000	10.480600000
7	2.970000000	6.356900000	7.426500000
7	8.078000000	9.567000000	15.402900000
5	6.914600000	9.390000000	14.382800000
1	5.953100000	9.017200000	14.975900000
1	6.655500000	10.457900000	13.925000000
6	3.404600000	5.977800000	6.043800000
1	3.360100000	6.745700000	5.470300000
1	4.307900000	5.650600000	6.070100000
1	2.827100000	5.289900000	5.703200000
6	8.620200000	8.341100000	15.962200000
1	8.844800000	7.740400000	15.249500000
1	9.407600000	8.545300000	16.471400000
1	7.965000000	7.934800000	16.532400000
6	1.694600000	7.071000000	7.337400000
1	1.083400000	6.564700000	6.797200000
1	1.328700000	7.178100000	8.218900000
1	1.836900000	7.931800000	6.941600000
6	7.617000000	10.439000000	16.499900000
1	6.928500000	9.991100000	16.995300000
1	8.354000000	10.637800000	17.080900000
1	7.268700000	11.255400000	16.133100000
6	9.258900000	10.262100000	14.745400000
1	8.958900000	11.071800000	14.323800000
1	9.917100000	10.473900000	15.411000000
1	9.643800000	9.681900000	14.086000000
5	4.093900000	7.140500000	8.124000000
1	5.039900000	6.426400000	8.216100000
1	4.401200000	8.050400000	7.423400000
6	2.831700000	5.055200000	8.105500000
1	3.346800000	4.393900000	7.646500000
1	3.124500000	5.130900000	9.012200000
1	1.898700000	4.792600000	8.095400000
79	5.500900000	11.196500000	11.403300000
15	3.738300000	11.309100000	12.900300000
1	2.667000000	11.682600000	12.262700000
1	3.518700000	10.123000000	13.384200000
15	7.281100000	11.027900000	9.933400000
1	7.799200000	12.214600000	9.787800000
1	8.187700000	10.273400000	10.480600000
7	8.005500000	9.516400000	7.426500000
7	2.897500000	12.726500000	15.402900000
5	4.060900000	12.549500000	14.382800000
1	5.022400000	12.176700000	14.975900000
1	4.320000000	13.617400000	13.925000000
6	7.570900000	9.137300000	6.043800000
1	7.615400000	9.905200000	5.470300000
1	6.667600000	8.810100000	6.070100000
1	8.148400000	8.449400000	5.703200000
6	2.355300000	11.500600000	15.962200000

1	2.130700000	10.899900000	15.249500000
1	1.567900000	11.704800000	16.471400000
1	3.010500000	11.094300000	16.532400000
6	9.280900000	10.230500000	7.337400000
1	9.892100000	9.724200000	6.797200000
1	9.646800000	10.337600000	8.218900000
1	9.138600000	11.091300000	6.941600000
6	3.358500000	13.598500000	16.499900000
1	4.047000000	13.150600000	16.995300000
1	2.621500000	13.797300000	17.080900000
1	3.706800000	14.414900000	16.133100000
6	1.716600000	13.421600000	14.745400000
1	2.016600000	14.231300000	14.323800000
1	1.058400000	13.633400000	15.411000000
1	1.331700000	12.841400000	14.086000000
5	6.881600000	10.300000000	8.124000000
1	5.935600000	9.585900000	8.216100000
1	6.574300000	11.209900000	7.423400000
6	8.143800000	8.214700000	8.105500000
1	7.628700000	7.553400000	7.646500000
1	7.851000000	8.290400000	9.012200000
1	9.076800000	7.952100000	8.095400000
79	5.474600000	14.356000000	11.403300000
15	7.237200000	14.468600000	12.900300000
1	8.308500000	14.842100000	12.262700000
1	7.456800000	13.282500000	13.384200000
15	3.694400000	14.187400000	9.933400000
1	3.176300000	15.374100000	9.787800000
1	2.787800000	13.432900000	10.480600000
7	2.970000000	12.675900000	7.426500000
7	8.078000000	15.886000000	15.402900000
5	6.914600000	15.709000000	14.382800000
1	5.953100000	15.336200000	14.975900000
1	6.655500000	16.776900000	13.925000000
6	3.404600000	12.296800000	6.043800000
1	3.360100000	13.064700000	5.470300000
1	4.307900000	11.969600000	6.070100000
1	2.827100000	11.608900000	5.703200000
6	8.620200000	14.660100000	15.962200000
1	8.844800000	14.059400000	15.249500000
1	9.407600000	14.864300000	16.471400000
1	7.965000000	14.253800000	16.532400000
6	1.694600000	13.390000000	7.337400000
1	1.083400000	12.883700000	6.797200000
1	1.328700000	13.497100000	8.218900000
1	1.836900000	14.250800000	6.941600000
6	7.617000000	16.758000000	16.499900000
1	6.928500000	16.310100000	16.995300000
1	8.354000000	16.956800000	17.080900000
1	7.268700000	17.574400000	16.133100000
6	9.258900000	16.581100000	14.745400000
1	8.958900000	17.390800000	14.323800000
1	9.917100000	16.792900000	15.411000000
1	9.643800000	16.000900000	14.086000000
5	4.093900000	13.459500000	8.124000000

1	5.039900000	12.745400000	8.216100000
1	4.401200000	14.369400000	7.423400000
6	2.831700000	11.374200000	8.105500000
1	3.346800000	10.712900000	7.646500000
1	3.124500000	11.449900000	9.012200000
1	1.898700000	11.111600000	8.095400000

3a monomer [Au(PH₂BH₂NMe₃)₂]⁺ 300K

79	16.844000000	4.691200000	11.579100000
15	18.594000000	4.811900000	10.091200000
1	19.629800000	5.297800000	10.712600000
1	18.896900000	3.599100000	9.716000000
15	15.086000000	4.570200000	13.057400000
1	14.806500000	5.777900000	13.480300000
1	14.030900000	4.117100000	12.422700000
7	14.230900000	3.156300000	15.579400000
7	19.441000000	6.204600000	7.586800000
6	14.689200000	2.410100000	16.735000000
1	15.637100000	2.270300000	16.672200000
1	14.242900000	1.559800000	16.766400000
1	14.491500000	2.903200000	17.535200000
5	15.426100000	3.425600000	14.603600000
1	15.817000000	2.384400000	14.207100000
1	16.306800000	3.914000000	15.232500000
6	19.038900000	6.761200000	6.350700000
1	18.813900000	6.054400000	5.739500000
1	19.756200000	7.283100000	5.984300000
1	18.271500000	7.321700000	6.486100000
5	18.277200000	5.880700000	8.506900000
1	17.457200000	5.328000000	7.859400000
1	17.805400000	6.909000000	8.857000000
6	13.222100000	2.390800000	14.910300000
1	13.607900000	1.585000000	14.566500000
1	12.859400000	2.908800000	14.185900000
1	12.521900000	2.176300000	15.530200000
6	13.574800000	4.280400000	16.047200000
1	12.737200000	4.020700000	16.438000000
1	13.415900000	4.883600000	15.318900000
1	14.117300000	4.712500000	16.710400000
6	20.436300000	5.218700000	7.345200000
1	20.068600000	4.518600000	6.798800000
1	20.732200000	4.848400000	8.180200000
1	21.182200000	5.618200000	6.890800000
6	20.249900000	7.256100000	8.243600000
1	21.181700000	7.083500000	8.094600000
1	20.069600000	7.255800000	9.186000000
1	20.019900000	8.112600000	7.874100000

[3a_dimer]²⁺ 300 K

79	16.844000000	4.691200000	11.579100000
15	18.594000000	4.811900000	10.091200000
1	19.629800000	5.297800000	10.712600000
1	18.896900000	3.599100000	9.716000000
15	15.086000000	4.570200000	13.057400000
1	14.806500000	5.777900000	13.480300000
1	14.030900000	4.117100000	12.422700000

7	14.230900000	3.156300000	15.579400000
7	19.441000000	6.204600000	7.586800000
6	14.689200000	2.410100000	16.735000000
1	15.637100000	2.270300000	16.672200000
1	14.242900000	1.559800000	16.766400000
1	14.491500000	2.903200000	17.535200000
5	15.426100000	3.425600000	14.603600000
1	15.817000000	2.384400000	14.207100000
1	16.306800000	3.914000000	15.232500000
6	19.038900000	6.761200000	6.350700000
1	18.813900000	6.054400000	5.739500000
1	19.756200000	7.283100000	5.984300000
1	18.271500000	7.321700000	6.486100000
5	18.277200000	5.880700000	8.506900000
1	17.457200000	5.328000000	7.859400000
1	17.805400000	6.909000000	8.857000000
6	13.222100000	2.390800000	14.910300000
1	13.607900000	1.585000000	14.566500000
1	12.859400000	2.908800000	14.185900000
1	12.521900000	2.176300000	15.530200000
6	13.574800000	4.280400000	16.047200000
1	12.737200000	4.020700000	16.438000000
1	13.415900000	4.883600000	15.318900000
1	14.117300000	4.712500000	16.710400000
6	20.436300000	5.218700000	7.345200000
1	20.068600000	4.518600000	6.798800000
1	20.732200000	4.848400000	8.180200000
1	21.182200000	5.618200000	6.890800000
6	20.249900000	7.256100000	8.243600000
1	21.181700000	7.083500000	8.094600000
1	20.069600000	7.255800000	9.186000000
1	20.019900000	8.112600000	7.874100000
79	16.857100000	7.904700000	11.579100000
15	15.107100000	8.025400000	10.091200000
1	14.071300000	8.511300000	10.712600000
1	14.804200000	6.812600000	9.716000000
15	18.615100000	7.783700000	13.057400000
1	18.894600000	8.991400000	13.480300000
1	19.670200000	7.330600000	12.422700000
7	19.470200000	6.369800000	15.579400000
7	14.260100000	9.418100000	7.586800000
6	19.011900000	5.623600000	16.735000000
1	18.064000000	5.483800000	16.672200000
1	19.458200000	4.773300000	16.766400000
1	19.209600000	6.116700000	17.535200000
5	18.275000000	6.639100000	14.603600000
1	17.884100000	5.597900000	14.207100000
1	17.394300000	7.127500000	15.232500000
6	14.662200000	9.974700000	6.350700000
1	14.887200000	9.267900000	5.739500000
1	13.944900000	10.496600000	5.984300000
1	15.429600000	10.535200000	6.486100000
5	15.423900000	9.094200000	8.506900000
1	16.243900000	8.541500000	7.859400000
1	15.895700000	10.122500000	8.857000000

6	20.47900000	5.60430000	14.91030000
1	20.09320000	4.79850000	14.56650000
1	20.84170000	6.12230000	14.18590000
1	21.17920000	5.38980000	15.53020000
6	20.12630000	7.49390000	16.04720000
1	20.96390000	7.23420000	16.43800000
1	20.28520000	8.09710000	15.31890000
1	19.58380000	7.92600000	16.71040000
6	13.26480000	8.43220000	7.34520000
1	13.63250000	7.73210000	6.79880000
1	12.96890000	8.06190000	8.18020000
1	12.51890000	8.83170000	6.89080000
6	13.45120000	10.46960000	8.24360000
1	12.51940000	10.29700000	8.09460000
1	13.63150000	10.46930000	9.18600000
1	13.68120000	11.32610000	7.87410000
[3a_tetramer] ⁴⁺ 300 K			
79	16.84400000	4.69120000	11.57910000
15	18.59400000	4.81190000	10.09120000
1	19.62980000	5.29780000	10.71260000
1	18.89690000	3.59910000	9.71600000
15	15.08600000	4.57020000	13.05740000
1	14.80650000	5.77790000	13.48030000
1	14.03090000	4.11710000	12.42270000
7	14.23090000	3.15630000	15.57940000
7	19.44100000	6.20460000	7.58680000
6	14.68920000	2.41010000	16.73500000
1	15.63710000	2.27030000	16.67220000
1	14.24290000	1.55980000	16.76640000
1	14.49150000	2.90320000	17.53520000
5	15.42610000	3.42560000	14.60360000
1	15.81700000	2.38440000	14.20710000
1	16.30680000	3.91400000	15.23250000
6	19.03890000	6.76120000	6.35070000
1	18.81390000	6.05440000	5.73950000
1	19.75620000	7.28310000	5.98430000
1	18.27150000	7.32170000	6.48610000
5	18.27720000	5.88070000	8.50690000
1	17.45720000	5.32800000	7.85940000
1	17.80540000	6.90900000	8.85700000
6	13.22210000	2.39080000	14.91030000
1	13.60790000	1.58500000	14.56650000
1	12.85940000	2.90880000	14.18590000
1	12.52190000	2.17630000	15.53020000
6	13.57480000	4.28040000	16.04720000
1	12.73720000	4.02070000	16.43800000
1	13.41590000	4.88360000	15.31890000
1	14.11730000	4.71250000	16.71040000
6	20.43630000	5.21870000	7.34520000
1	20.06860000	4.51860000	6.79880000
1	20.73220000	4.84840000	8.18020000
1	21.18220000	5.61820000	6.89080000
6	20.24990000	7.25610000	8.24360000
1	21.18170000	7.08350000	8.09460000

1	20.069600000	7.255800000	9.186000000
1	20.019900000	8.112600000	7.874100000
79	16.857100000	7.904700000	11.579100000
15	15.107100000	8.025400000	10.091200000
1	14.071300000	8.511300000	10.712600000
1	14.804200000	6.812600000	9.716000000
15	18.615100000	7.783700000	13.057400000
1	18.894600000	8.991400000	13.480300000
1	19.670200000	7.330600000	12.422700000
7	19.470200000	6.369800000	15.579400000
7	14.260100000	9.418100000	7.586800000
6	19.011900000	5.623600000	16.735000000
1	18.064000000	5.483800000	16.672200000
1	19.458200000	4.773300000	16.766400000
1	19.209600000	6.116700000	17.535200000
5	18.275000000	6.639100000	14.603600000
1	17.884100000	5.597900000	14.207100000
1	17.394300000	7.127500000	15.232500000
6	14.662200000	9.974700000	6.350700000
1	14.887200000	9.267900000	5.739500000
1	13.944900000	10.496600000	5.984300000
1	15.429600000	10.535200000	6.486100000
5	15.423900000	9.094200000	8.506900000
1	16.243900000	8.541500000	7.859400000
1	15.895700000	10.122500000	8.857000000
6	20.479000000	5.604300000	14.910300000
1	20.093200000	4.798500000	14.566500000
1	20.841700000	6.122300000	14.185900000
1	21.179200000	5.389800000	15.530200000
6	20.126300000	7.493900000	16.047200000
1	20.963900000	7.234200000	16.438000000
1	20.285200000	8.097100000	15.318900000
1	19.583800000	7.926000000	16.710400000
6	13.264800000	8.432200000	7.345200000
1	13.632500000	7.732100000	6.798800000
1	12.968900000	8.061900000	8.180200000
1	12.518900000	8.831700000	6.890800000
6	13.451200000	10.469600000	8.243600000
1	12.519400000	10.297000000	8.094600000
1	13.631500000	10.469300000	9.186000000
1	13.681200000	11.326100000	7.874100000
79	16.844000000	11.118200000	11.579100000
15	18.594000000	11.238900000	10.091200000
1	19.629800000	11.724800000	10.712600000
1	18.896900000	10.026100000	9.716000000
15	15.086000000	10.997200000	13.057400000
1	14.806500000	12.204900000	13.480300000
1	14.030900000	10.544100000	12.422700000
7	14.230900000	9.583300000	15.579400000
7	19.441000000	12.631600000	7.586800000
6	14.689200000	8.837100000	16.735000000
1	15.637100000	8.697300000	16.672200000
1	14.242900000	7.986800000	16.766400000
1	14.491500000	9.330200000	17.535200000
5	15.426100000	9.852600000	14.603600000

1	15.81700000	8.81140000	14.20710000
1	16.30680000	10.34100000	15.23250000
6	19.03890000	13.18820000	6.35070000
1	18.81390000	12.48140000	5.73950000
1	19.75620000	13.71010000	5.98430000
1	18.27150000	13.74870000	6.48610000
5	18.27720000	12.30770000	8.50690000
1	17.45720000	11.75500000	7.85940000
1	17.80540000	13.33600000	8.85700000
6	13.22210000	8.81780000	14.91030000
1	13.60790000	8.01200000	14.56650000
1	12.85940000	9.33580000	14.18590000
1	12.52190000	8.60330000	15.53020000
6	13.57480000	10.70740000	16.04720000
1	12.73720000	10.44770000	16.43800000
1	13.41590000	11.31060000	15.31890000
1	14.11730000	11.13950000	16.71040000
6	20.43630000	11.64570000	7.34520000
1	20.06860000	10.94560000	6.79880000
1	20.73220000	11.27540000	8.18020000
1	21.18220000	12.04520000	6.89080000
6	20.24990000	13.68310000	8.24360000
1	21.18170000	13.51050000	8.09460000
1	20.06960000	13.68280000	9.18600000
1	20.01990000	14.53960000	7.87410000
79	16.85710000	14.33170000	11.57910000
15	15.10710000	14.45240000	10.09120000
1	14.07130000	14.93830000	10.71260000
1	14.80420000	13.23960000	9.71600000
15	18.61510000	14.21070000	13.05740000
1	18.89460000	15.41840000	13.48030000
1	19.67020000	13.75760000	12.42270000
7	19.47020000	12.79680000	15.57940000
7	14.26010000	15.84510000	7.58680000
6	19.01190000	12.05060000	16.73500000
1	18.06400000	11.91080000	16.67220000
1	19.45820000	11.20030000	16.76640000
1	19.20960000	12.54370000	17.53520000
5	18.27500000	13.06610000	14.60360000
1	17.88410000	12.02490000	14.20710000
1	17.39430000	13.55450000	15.23250000
6	14.66220000	16.40170000	6.35070000
1	14.88720000	15.69490000	5.73950000
1	13.94490000	16.92360000	5.98430000
1	15.42960000	16.96220000	6.48610000
5	15.42390000	15.52120000	8.50690000
1	16.24390000	14.96850000	7.85940000
1	15.89570000	16.54950000	8.85700000
6	20.47900000	12.03130000	14.91030000
1	20.09320000	11.22550000	14.56650000
1	20.84170000	12.54930000	14.18590000
1	21.17920000	11.81680000	15.53020000
6	20.12630000	13.92090000	16.04720000
1	20.96390000	13.66120000	16.43800000
1	20.28520000	14.52410000	15.31890000

1	19.583800000	14.353000000	16.710400000
6	13.264800000	14.859200000	7.345200000
1	13.632500000	14.159100000	6.798800000
1	12.968900000	14.488900000	8.180200000
1	12.518900000	15.258700000	6.890800000
6	13.451200000	16.896600000	8.243600000
1	12.519400000	16.724000000	8.094600000
1	13.631500000	16.896300000	9.186000000
1	13.681200000	17.753100000	7.874100000

Table S23. Optimized geometries of computationally studied compounds. xyz coordinates in angstroms. M06-2X/def2-TZVPP (ECP on Au) level of theory.

3a monomer [Au(PH₂BH₂NMe₃)₂]⁺			
79	0.000013000	0.000018000	0.175341000
15	-2.207497000	-0.760887000	0.170655000
1	-2.339796000	-1.850238000	-0.703488000
1	-2.488378000	-1.421512000	1.376608000
15	2.207493000	0.761001000	0.170597000
1	2.339791000	1.850015000	-0.703968000
1	2.488261000	1.422106000	1.376314000
7	5.069880000	-0.140900000	-0.235323000
7	-5.069899000	0.140830000	-0.235340000
5	-3.535559000	0.629652000	-0.213660000
1	-3.421445000	1.447456000	0.655669000
1	-3.268455000	1.047799000	-1.305320000
6	5.893294000	-1.338434000	-0.550924000
1	5.585369000	-1.728468000	-1.517031000
1	5.723730000	-2.091347000	0.213653000
1	6.946060000	-1.058270000	-0.575698000
6	-5.497802000	-0.392604000	1.079751000
1	-4.929031000	-1.290577000	1.307101000
1	-6.559610000	-0.635428000	1.048516000
1	-5.311202000	0.360253000	1.841153000
6	5.307534000	0.882982000	-1.280574000
1	6.370900000	1.114977000	-1.330774000
1	4.752957000	1.784385000	-1.033157000
1	4.964982000	0.494628000	-2.236249000
6	-5.893406000	1.338236000	-0.551178000
1	-5.723713000	2.091408000	0.213108000
1	-6.946167000	1.058028000	-0.575670000
1	-5.585678000	1.727954000	-1.517481000
6	-5.307543000	-0.883323000	-1.280336000
1	-4.965070000	-0.495177000	-2.236119000
1	-6.370897000	-1.115406000	-1.330417000
1	-4.752893000	-1.784632000	-1.032722000
5	3.535523000	-0.629660000	-0.213438000
1	3.421494000	-1.447386000	0.655960000
1	3.268260000	-1.047843000	-1.305052000
6	5.497876000	0.392816000	1.079628000
1	5.311248000	-0.359831000	1.841214000
1	4.929174000	1.290876000	1.306778000

1	6.559701000	0.635552000	1.048292000
[3a_dimer]²⁺			
79	-0.801645000	-0.006507000	-1.472025000
15	0.721948000	-1.596245000	-2.265012000
1	0.195005000	-2.889558000	-2.122861000
1	0.761203000	-1.536439000	-3.665786000
15	-2.350495000	1.626222000	-0.822140000
1	-2.214966000	1.937574000	0.539594000
1	-1.956692000	2.861953000	-1.360934000
7	-5.249718000	2.447113000	-1.058857000
7	3.594787000	-2.537824000	-2.117172000
5	2.529366000	-1.500206000	-1.505332000
1	2.928863000	-0.386731000	-1.722038000
1	2.410662000	-1.740986000	-0.333127000
6	-6.615380000	1.909598000	-1.306074000
1	-6.825460000	1.136840000	-0.571895000
1	-6.647593000	1.480785000	-2.303940000
1	-7.344044000	2.714879000	-1.220590000
6	3.806895000	-2.325575000	-3.570731000
1	2.890444000	-2.556248000	-4.107307000
1	4.604491000	-2.978995000	-3.922237000
1	4.076481000	-1.286097000	-3.738929000
6	-5.198575000	2.999611000	0.315201000
1	-5.985439000	3.741924000	0.443261000
1	-4.231357000	3.469059000	0.477718000
1	-5.333892000	2.188142000	1.026520000
6	4.882522000	-2.296952000	-1.412248000
1	5.192817000	-1.271846000	-1.596462000
1	5.635578000	-2.990030000	-1.785595000
1	4.732149000	-2.442512000	-0.345863000
6	3.189516000	-3.946273000	-1.884909000
1	3.027706000	-4.093852000	-0.820169000
1	3.973311000	-4.615195000	-2.238076000
1	2.270468000	-4.151301000	-2.427891000
5	-4.224761000	1.222302000	-1.257807000
1	-4.249320000	0.903726000	-2.411707000
1	-4.540277000	0.339935000	-0.505908000
6	-4.995921000	3.537328000	-2.034152000
1	-5.053769000	3.128085000	-3.039005000
1	-4.005427000	3.950764000	-1.863998000
1	-5.742414000	4.320365000	-1.907076000
79	0.803608000	0.021941000	1.454848000
15	2.344675000	1.650432000	0.776255000
1	1.922827000	2.902454000	1.252444000
1	2.240998000	1.902933000	-0.600270000
15	-0.710871000	-1.563265000	2.272604000
1	-0.711463000	-1.521430000	3.674375000
1	-0.199097000	-2.858852000	2.099837000
7	-3.594558000	-2.477584000	2.189914000
7	5.242970000	2.484191000	1.034475000
5	4.205473000	1.281551000	1.291422000
1	4.543960000	0.342589000	0.623008000
1	4.188690000	1.053728000	2.467325000
6	-4.895912000	-2.225172000	1.514764000

1	-5.194370000	-1.198388000	1.709200000
1	-4.770063000	-2.368371000	0.444829000
1	-5.645382000	-2.914167000	1.902641000
6	5.287492000	2.883103000	-0.391998000
1	4.326428000	3.303029000	-0.678886000
1	6.066917000	3.629281000	-0.541374000
1	5.495756000	2.002891000	-0.995654000
6	-3.773458000	-2.270081000	3.648717000
1	-4.564094000	-2.923417000	4.015723000
1	-2.845506000	-2.504048000	4.163636000
1	-4.037396000	-1.230761000	3.826395000
6	6.587246000	1.982832000	1.430882000
1	6.837248000	1.122495000	0.816364000
1	7.325279000	2.771369000	1.289046000
1	6.555692000	1.684319000	2.475182000
6	4.925986000	3.672453000	1.865703000
1	4.889297000	3.370766000	2.909037000
1	5.693770000	4.432096000	1.724417000
1	3.961706000	4.073835000	1.565954000
5	-2.535702000	-1.444336000	1.559586000
1	-2.447267000	-1.677385000	0.383035000
1	-2.919801000	-0.329047000	1.793241000
6	-3.203619000	-3.887478000	1.942952000
1	-3.063340000	-4.030787000	0.874516000
1	-2.275579000	-4.100937000	2.467072000
1	-3.984729000	-4.553073000	2.308098000

4.5.8 Photoluminescence

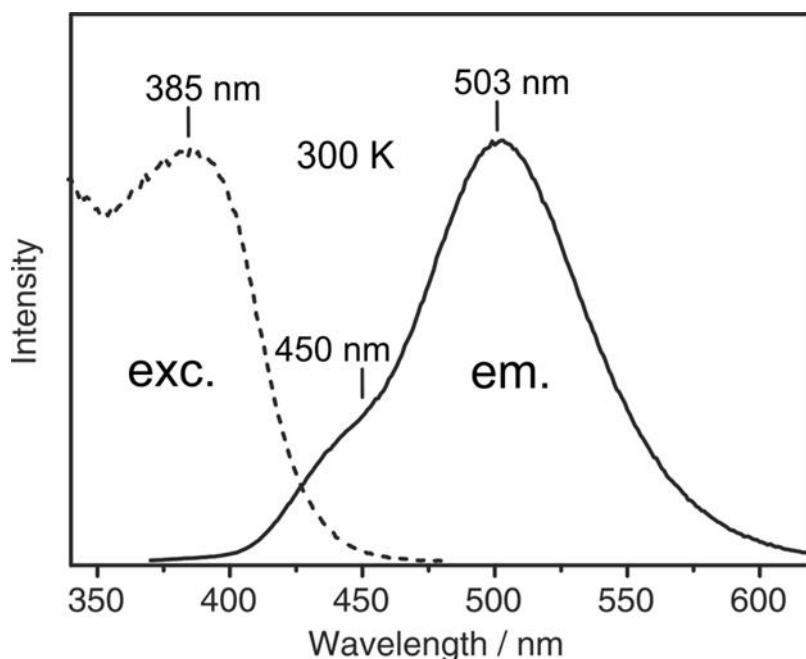


Figure S35: Emission and excitation spectra of compound **3a** measured at $T = 300$ K. Excitation wavelength $\lambda_{\text{exc}} = 330$ nm, detection wavelength $\lambda_{\text{det}} = 540$ nm.

4.5.9 References

- [1] a) C. Marquardt, A. Adolf, A. Stauber, M. Bodensteiner, A. V. Virovets, A. Y. Timoshkin, M. Scheer, *Chem. Eur. J.* **2013**, *19*, 11887 – 11891; b) C. Marquardt, T. Jurca, K.-C. Schwan, A. Stauber, A. V. Virovets, G. R. Whittell, I. Manners, M. Scheer, *Angew. Chem. Int. Ed.* **2015**, *54*, 13782-13786.
- [2] Rigaku Oxford Diffraction **2017**, CrysAlisPro Software system, different versions, Agilent Technologies UK Ltd, Oxford, UK.
- [3] A. Altomare, M. C. Burla, M. Camalli, G. L. Cascarano, C. Giacovazzo, A. Guagliardi, A. G. G. Moliterni, G. Polidori, R. Spagna, *J. Appl. Cryst.* (1999) *32*, 115-119.
- [4] G. M. Sheldrick, *Acta Cryst.* **2008**, *A64*, 112–122.
- [5] O.V. Dolomanov, L. J. Bourhis, R. J. Gildea, J. A. K. Howard, H. Puschmann, OLEX2: A complete structure solution, refinement and analysis program, **2009**. *J. Appl. Cryst.*, *42*, 339-341.
- [6] Y. Zhao, D.G. Truhlar, *Theor. Chem. Account.* **2006**, *120*, 215–241.
- [7] F. Weigend, R. Ahlrichs, *Phys.Chem.Chem.Phys.*, **2005**, *7*, 3297-3305.
- [8] a) D. Feller, *J. Comp. Chem.* **1996**, *17*, 1571-1586; b) K. L. Schuchardt, B. T. Didier, T. Elsethagen, L. Sun, V. Gurumoorthi, J. Chase, J. Li, T. L. Windus, *J. Chem. Inf. Model.* **2007**, *47*, 1045-1052.
- [9] M. J. Frisch, G. W. Trucks, H. B. Schlegel, G. E. Scuseria, M. A. Robb, J. R. Cheeseman, G. Scalmani, V. Barone, B. Mennucci, G. A. Petersson, H. Nakatsuji, M. Caricato, X. Li, H. P. Hratchian, A. F. Izmaylov, J. Bloino, G. Zheng, J. L. Sonnenberg, M. Hada, M. Ehara, K. Toyota, R. Fukuda, J. Hasegawa, M. Ishida, T.

Nakajima, Y. Honda, O. Kitao, H. Nakai, T. Vreven, J. A. Montgomery, Jr., J. E. Peralta, F. Ogliaro, M. Bearpark, J. J. Heyd, E. Brothers, K. N. Kudin, V. N. Staroverov, T. Keith, R. Kobayashi, J. Normand, K. Raghavachari, A. Rendell, J. C. Burant, S. S. Iyengar, J. Tomasi, M. Cossi, N. Rega, J. M. Millam, M. Klene, J. E. Knox, J. B. Cross, V. Bakken, C. Adamo, J. Jaramillo, R. Gomperts, R. E. Stratmann, O. Yazyev, A. J. Austin, R. Cammi, C. Pomelli, J. W. Ochterski, R. L. Martin, K. Morokuma, V. G. Zakrzewski, G. A. Voth, P. Salvador, J. J. Dannenberg, S. Dapprich, A. D. Daniels, O. Farkas, J. B. Foresman, J. V. Ortiz, J. Cioslowski, D. J. Fox, Gaussian 09, Revision E.01, Gaussian, Inc., Wallingford CT, 2013.

Preface

The following chapter has been compiled for future publication.

Authors

Jens Braese, Christian Marquardt and Manfred Scheer

Author contributions

The syntheses and characterization of compounds **1-4** were performed by Dr. Christian Marquardt (Universität Regensburg). Compounds **4-13** were synthesized and characterized by Jens Braese. The manuscript (including supporting information, figures, schemes and graphical abstract) was written by Jens Braese and Dr. Christian Marquardt with equal contributions.

5 Coordination of Pnictogenylboranes Towards Monovalent Copper Compounds

Abstract: Reactions of the pnictogenylboranes $\text{H}_2\text{EBH}_2\cdot\text{NMe}_3$ (**A1**: E = P; **A2**: E = As) and $\text{Ph}_2\text{PBH}_2\cdot\text{NMe}_3$ (**A3**) with $[\text{Cu}(\text{MeCN})_4][\text{BF}_4]$ afford the homoleptic complexes $[\text{Cu}(\text{H}_2\text{EBH}_2\cdot\text{NMe}_3)_4(\text{BF}_4)]$ (**1**: E = P, **2**: E = As) and $[\text{Cu}(\text{Ph}_2\text{PBH}_2\cdot\text{NMe}_3)_3][\text{BF}_4]$ (**3**). Compound **2** represents the first structurally characterized complex of a primary arsine coordinated to a Cu center. From reactions of **A3** with CuX , a series of complexes $[\text{Cu}_n\text{X}_n(\text{Ph}_2\text{PBH}_2\cdot\text{NMe}_3)_m]$ (X = Cl, Br, I; n = 1-6, m = 2-4) (**4** – **13**) were synthesized and compared to related complexes possessing Ph_3P ligands. All complexes were characterized by single-crystal X-ray structure analysis, multinuclear NMR spectroscopy, IR spectroscopy and mass spectrometry.

5.1 Introduction

Although the coordination chemistry of phosphines towards the coinage metal Cu(I) is very well studied, complexes including primary phosphines (RPH_2) remain scarce.^[1,2] In contrast to phosphines, Cu(I) complexes of arsines^[3] are less common and for primary arsines (RAsH_2) they have only been studied by theoretical methods.^[4] Moreover, reports on complexes of primary arsines are restricted to heteroleptic complexes of the type $[\text{M}(\text{L})_n(\text{AsH}_2\text{R})]$ (M = Cr, Mo, W, Fe, Co, Ni, L = CO; M = Ti, L = Cl; M = Y, L = CH_4Me).^[5] Recently, phosphine-copper-catalysts with chiral phosphorus-ligands have been used for a variety of transformations of organic substrates, including asymmetric hydrogenation reactions.^[6] Phosphine-copper complexes also exhibit light emitting properties.^[7] Monomeric Lewis base stabilized pnictogenylboranes of the type $\text{R}_2\text{EBH}_2\cdot\text{NMe}_3$ (E = P, As; R = H, alkyl, aryl) are special phosphines and arsines: they are good σ -donors and also represent easily accessible building blocks for neutral polymeric^[8] and ionic^[9] oligomeric compounds. The backbone of these chain molecules consists of alternating group 13 and group 15 elements. The oxidation with chalcogens (O, S, Se, Te) as well as their reactivity towards main group Lewis acids has been studied thoroughly.^[10] From the reaction of $\text{H}_2\text{PBH}_2\cdot\text{NMe}_3$ (**A1**) with $[\text{Cp}_2\text{Ti}(\text{btmsa})]$ extended B-P-oligomers were obtained, which are stabilized in the coordination sphere of Cp_2Ti units.^[11] Some pnictogenylboranes and -alanes are unstable unless they are stabilized through coordination to $\text{W}(\text{CO})_5$. This can be observed in the phosphanylalane $[\text{W}(\text{CO})_5(\text{PH}_2\text{-AlH}_2\cdot\text{NMe}_3)]$ ^[12] and the mixed pnictogenylboranes $[(\text{OC})_5\text{W}(\text{PH}_2\text{BH}_2\text{EH}_2\text{BH}_2\cdot\text{NMe}_3)]$ (E = P, As; also Sb).^[13] $[\text{W}(\text{CO})_5(\text{EH}_2\text{BH}_2\cdot\text{NMe}_3)]$ (E = P, As) can be used as a starting

material for the synthesis of Lewis acid free $\text{H}_2\text{EBH}_2\cdot\text{NMe}_3$ (**A1** E = P; **A2** E = As).^[10] Furthermore, they undergo E-H activation to form complexes like $\text{cis}-(\text{Ph}_3\text{P})_2\text{Pt}(\text{H})(\mu\text{-EHBH}_2\cdot\text{NMe}_3)\text{W}(\text{CO})_5$ (E = P, As).^[14] **A1** and **A2** coordinating to Au(I) centers afford complexes with aurophilic interactions acting as blue-green light emitters.^[15] Reaction of the phosphanylborane **A1** with CuI leads to two Cu-I-P-clusters.^[16] Therefore, these distinct primary phosphine and arsine ligands (**A1**, **A2**) are of interest for a methodical study if novel Cu complexes are achievable. Additionally, the coordination behavior of $\text{Ph}_2\text{PBH}_2\cdot\text{NMe}_3$ (**A3**), which can be viewed as a special derivative of the well-known ligand Ph_3P , will be investigated. Because coordination towards transition metal centers represents the first step in the coordination chemistry of pnictogenylboranes, a comparison of the reactivity of $\text{Ph}_2\text{PBH}_2\cdot\text{NMe}_3$ (**A3**) with that of Ph_3P to investigate the influence of the boranyl group in pnictogenylboranes is desirable.

5.2 Results and Discussion

Herein we present the first systematic study of the coordination behavior of the special primary phosphines or arsines $\text{H}_2\text{EBH}_2\cdot\text{NMe}_3$ (**A1** E = P; **A2** E = As) towards Cu(I) complexes. From the reactions of **A3** with CuX in defined stoichiometries, a series of complexes of the type $[\text{Cu}_n\text{X}_n(\text{Ph}_2\text{PBH}_2\cdot\text{NMe}_3)_m]$ (X = Cl, Br, I; n = 1-6, m = 2-4) (**4** – **13**) were synthesized and characterized.

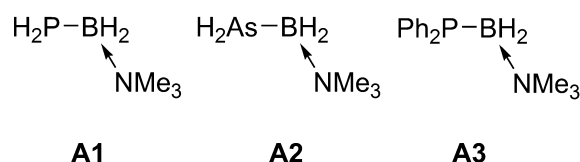
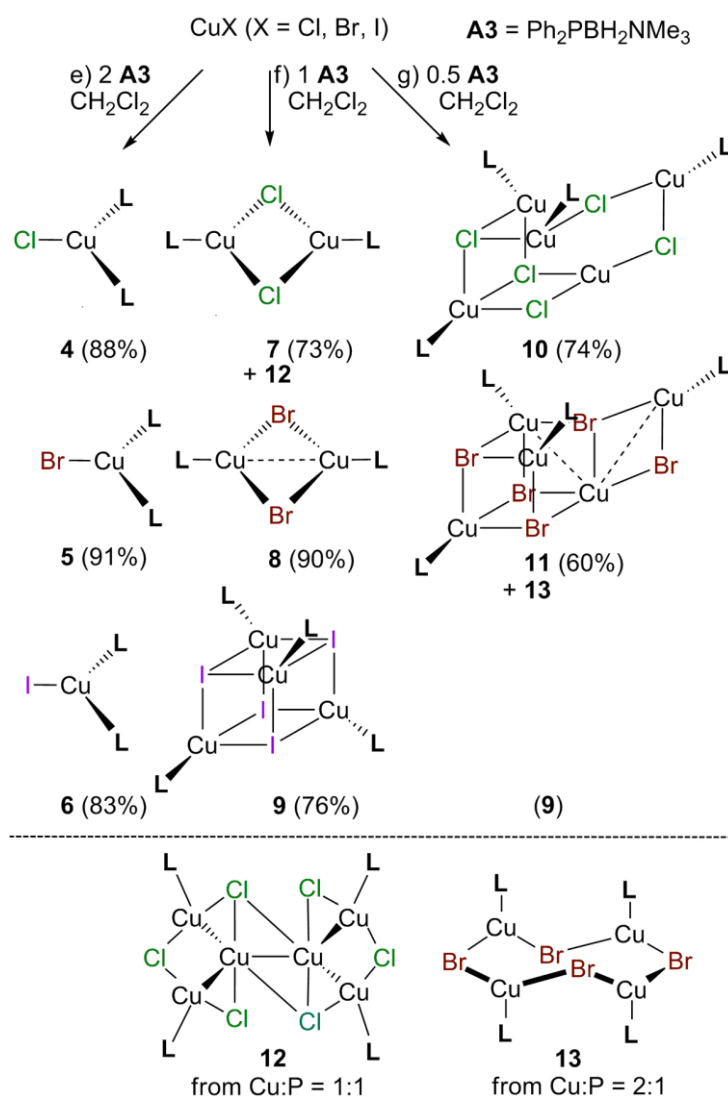


Figure 1: Pnictogenylboranes **A1**, **A2** and **A3**.

Reactions of 4 equivalents of **A1** and **A2** with $[\text{Cu}(\text{MeCN})_4][\text{BF}_4]$ in MeCN afford the homoleptic, tetracoordinated complexes $[\text{Cu}(\text{H}_2\text{PBH}_2\cdot\text{NMe}_3)_4][\text{BF}_4]$ (**1**) and $[\text{Cu}(\text{H}_2\text{AsBH}_2\cdot\text{NMe}_3)_4][\text{BF}_4]$ (**2**) in good isolated yields (68% for **1**, 65% for **2**). When the sterically demanding phosphanylborane **A3** is reacted with $[\text{Cu}(\text{MeCN})_4][\text{BF}_4]$ in MeCN, the trifold coordinated, trigonal planar complex $[\text{Cu}(\text{Ph}_2\text{PBH}_2\cdot\text{NMe}_3)_3][\text{BF}_4]$ (**3**) is obtained instead in 65% yield. Storing a CH_2Cl_2 solution of **3** for several weeks slowly leads to the formation of $[\text{CuCl}(\text{Ph}_2\text{PBH}_2\cdot\text{NMe}_3)_2]$ (**4**), showing the chlorinating ability of the solvent, which is sometimes observed.^[17] The structure of the products **1-4** could be determined by single-crystal X-ray structure analysis.

unresolved coupling of the EH_2 group in the ^1H NMR spectrum of **3** is indicative for an interaction to Cu and might also be influenced by dynamic processes in solution. ESI mass spectrometry shows peaks assignable to the fragments $[\text{Cu}(\text{L})_n]$ (**1**: $\text{L} = \text{A1}$, $n = 2,3$; **2**: $\text{L} = \text{A2}$, $n = 1,2$). Single-crystal X-ray diffraction analysis (Figure 2) reveals that **1** and **2** contain a central Cu atom with a nearly ideal tetrahedral coordination environment (E–Cu–E angle $108.81(2) - 110.79(3)^\circ$ for **1** and $108.32(2) - 111.79(3)^\circ$ for **2**). The E–Cu bond lengths of $2.2980(5) \text{ \AA}$ for **1** (E = P) and $2.3915(6) \text{ \AA}$ for **2** (E = As), which are slightly longer than the calculated sum of the covalent radii ($\sum r_{\text{cov}}(\text{Cu-P}) = 2.23 \text{ \AA}$, $\sum r_{\text{cov}}(\text{Cu-As}) = 2.33 \text{ \AA}$).^[18] The P–B bond length of $1.963(3) \text{ \AA}$ in **1** and the As–B bond length of **2** ($2.079(5) \text{ \AA}$) are similar to the corresponding bond lengths in the starting materials (**A1**: $1.976(2) \text{ \AA}$, **A2**: $2.071(4) \text{ \AA}$). Compound **2** represents the first structurally characterized Cu complex containing a primary arsine. Complex **3** exhibits a distorted trigonal planar coordination environment ($\sum(\text{P–Cu–P})$ angles = 359.84°), with P–Cu–P angles ranging from $111.45(3)$ to $124.85(3)^\circ$. The P–Cu bond lengths in **3** vary from $2.3075(7)$ to $2.3293(7)$, which corresponds to the values in **1**. The P–B bond lengths range from $1.982(3)$ to $1.990(3) \text{ \AA}$ for **3** which are slightly longer compared to the starting material (**A3**: $1.975(3) \text{ \AA}$). In the solid state each boranyl group adopts a different orientation; one lies within the P_3Cu plane while the others are above and below (Figure 2 (c)). In contrast, the Cu(I) center in complex $[\text{Cu}(\text{Ph}_3\text{P})_3][\text{BF}_4]$ is also coordinated by the BF_4^- group, resulting in a pseudotetrahedral coordination geometry.^[19]

After using the pnictogenylboranes as ligands towards $[\text{Cu}(\text{MeCN})_4][\text{BF}_4]$, also the reaction towards Cu(I) halides was investigated, especially because $[\text{CuCl}(\text{Ph}_2\text{PBH}_2\cdot\text{NMe}_3)_2]$ (**4**) was identified as a subsequent product obtained by storing a CH_2Cl_2 solution of **3** for several weeks. The targeted synthesis of **4** from the reaction of 2 equivalents of **A3** with CuCl was successful. Therefore, we synthesized further copper halide complexes from the reaction of the CuX (X = Cl, Br, I) with the ligand $\text{Ph}_2\text{PBH}_2\cdot\text{NMe}_3$ (**A3**) in different stoichiometries (scheme 2). The reaction of 2 equivalents of **A3** with CuX (X = Cl, Br, I) in CH_2Cl_2 afforded the complexes $[\text{CuX}(\text{Ph}_2\text{PBH}_2\cdot\text{NMe}_3)_2]$ (**4**: X = Cl; **5**: X = Br; **6**: X = I) (Scheme 2, Figure 3) in good crystalline yields (**4**: 88%; **5**: 91%; **6**: 83%). They crystalline compounds are isomorphous to each other and show isostructural motives, which are similar to the solid state structures of $[\text{CuX}(\text{Ph}_3\text{P})_2]$.^[20] For all three complexes **4**, **5** and **6**, the ^{31}P NMR spectra in CD_2Cl_2 reveal a broad singlet at $\delta = -42.8 \text{ ppm}$. FD mass spectrometry shows peaks assignable to the fragments $[\text{Cu}_l\text{X}_m(\text{L})_n]$ ($l = 1-3$; $m = 0-3$; $n = 1-3$), showing increasing cluster size with increasing atomic number of the halogen atom. The solid state structure show a trigonally coordinated Cu center by two ligands **A3** and one halogenide. Exemplary geometric parameters for **4** are a P–Cu–P angle of $131.49(3)^\circ$ and a P–Cu–Cl



Scheme 2: Reactions of **A3** with CuX (X = Cl, Br, I) in different stoichiometric ratios.

angle of 115.67(2). The P–Cu bond lengths in **4**, **5** and **6** are 2.2571(6) Å, 2.2485(4) Å and 2.2563(11) Å, respectively. The P–B bond lengths, 1.975(3), 1.975(2) and 1.979(5) Å for **4**, **5** and **6**, respectively are nearly identical to the starting material (**A3**: 1.975(3) Å).

The reactions of just one equivalent of **A3** with CuX (X = Cl, Br, I) in CH₂Cl₂ affords molecular complexes of the type [CuX(Ph₂PBH₂·NMe₃)_n] (**7**: X = Cl, n = 2; **8**: X = Br, n = 2; **9**: X = I, n = 4) (Figure 4) in good isolated yields (**7**: 73%; **8**: 90%; **9**: 76%) as well as the complex **12** (Scheme 2). [CuCl(Ph₂PBH₂·NMe₃)₂] (**7**) and [CuBr(Ph₂PBH₂·NMe₃)₂] (**8**) reveal similar dinuclear complexes with trigonal coordinated Cu centers bearing one phosphine ligand and two halides in bridging positions. On the other hand, [CuI(Ph₂PBH₂·NMe₃)₄] (**9**) shows a heterocubane structure with a Cu₄I₄ core and one phosphine ligand coordinating to each Cu(I) center, resulting in a coordination number of

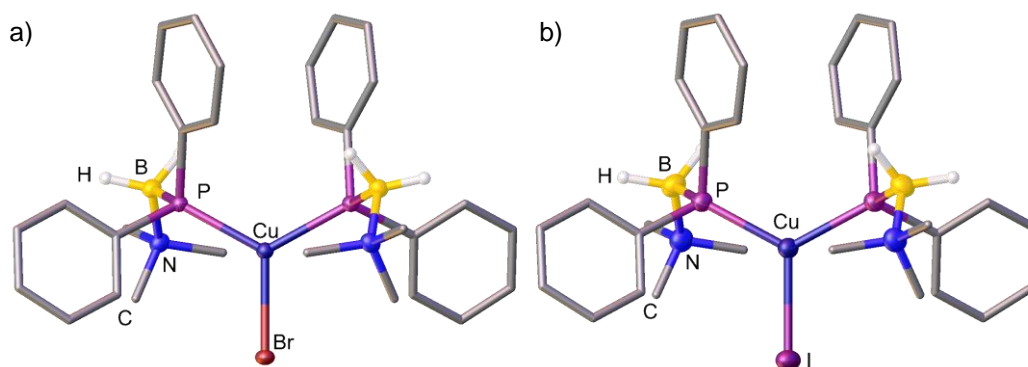


Figure 3: Molecular structures of the Cu complexes **5** (a) and **6** (b). Hydrogen atoms on carbon and counter ions are omitted for clarity. Selected bond lengths [Å] and angles [°]: **5** P–Cu 2.2485(4), Cu–Br 2.4264(3), P–B 1.975(2), B–P–Cu 119.24(6), P–Cu–P 122.95(2), P–Cu–Br 118.52(1); **6** P–Cu 2.2563(11), Cu–I 2.5682(10), P–B 1.979(5), B–P–Cu 118.86(17), P–Cu–P 123.67(7), P–Cu–I 118.17(3).

4. A comparison with Cu(I) halide complexes of Ph_3P reveals that only $[\text{CuCl}(\text{Ph}_3\text{P})_4]$ displays a heterocubane structure similar to **9**, while $[\text{CuBr}(\text{Ph}_3\text{P})_4]$ and $[\text{CuI}(\text{Ph}_3\text{P})_4]$ display a ladderlike (open-cube) structure.^[21] Comparable dimeric structures as displayed in compounds **7** and **8** are not observed in Cu(I) halide complexes of Ph_3P . Sufficiently large phosphine ligands eventually stop the oligomerization process in the coordination chemistry of copper halides. For example, $\text{CuBr}(\text{Mes}_3\text{P})$ does not form oligomers in the solid state and remains monomeric.^[22] As an additional product, $[\text{Cu}_6\text{Cl}_6(\text{Ph}_2\text{PBH}_2\cdot\text{NMe}_3)_4]$ (**12**) can be found in scarce multi-component molecular crystals alongside complex **7**, where one molecule of **7** and one molecule of **12** are present in the unit cell. **12** shows a 6:4 ratio of CuCl to **A3**, displaying an unusual structure of two connected Cu_3Cl_3 six membered rings (Figure 4 (d)). The conditions of all crystallization experiments were kept constant, repeated experiments delivered the same results. Complexes **7** and **8** reveal in the ^{31}P NMR spectra in CD_2Cl_2 broad singlets at similar values of $\delta = -34.7$ ppm and -37.2 ppm, respectively. Complex **9** shows a less downfield shifted singlet at $\delta = -42.4$ ppm. FD mass spectrometry of complexes **7-9** show peaks assignable to the fragments $[\text{CuX}_m(\text{L})_n]$ ($l = 1-5$; $m = 0 - 4$; $n = 1 - 4$), showing variable cluster compositions, some even bigger than observed in the solid state. Single-crystal X-ray diffraction analysis shows that the distance between two bridged Cu atoms is 2.993(1) Å for **7** and 2.785(1) to 2.914(1) Å for **8** and Å 3.220(1) to 3.478(1) Å for **9**. For **12**, the distance ranges from 2.865(1) to 3.029(1) Å. Regarding the big differences in the Cu...Cu distances, these values appear rather flexible. For example, there are two independent molecules present in the unit cell of **8** that show big differences in the intermetallic distances. Some are in range of the van-der-Waals

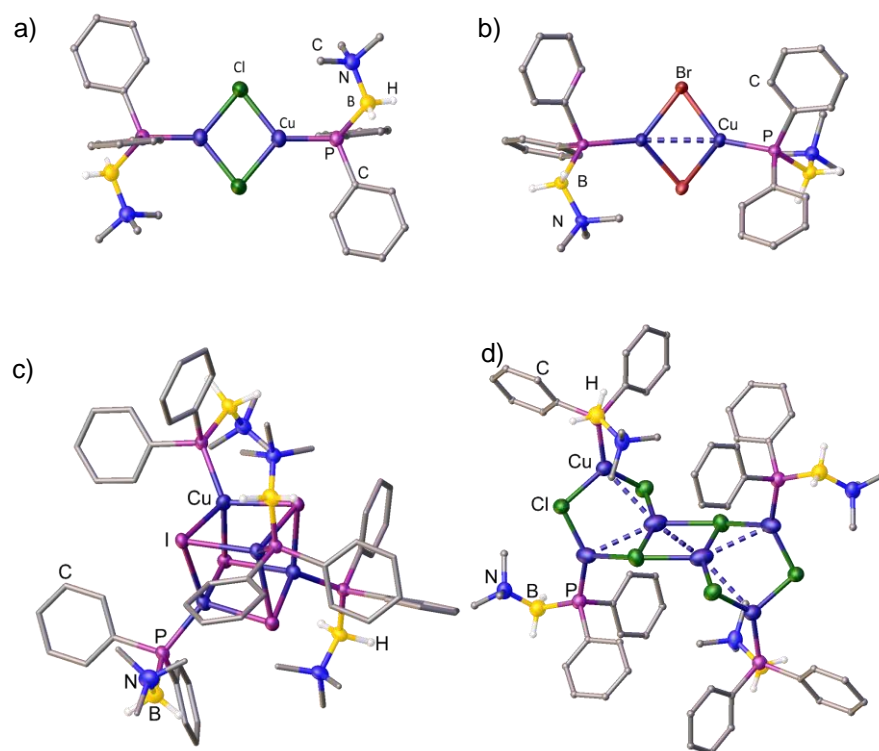


Figure 4: Molecular structures of the Cu complexes **7** (a), **8** (b), **9** (c) and **12** (d; **12** crystallizes together with **7**). Hydrogen atoms on carbon are omitted for clarity. Selected bond lengths [Å] and angles [°]: **7** P–Cu 2.1903(14), Cu··Cu 2.9931(14), Cu–Cl 2.291(1), P–B 1.9836(1), B–P–Cu 124.136(3), P–Cu–Cl 129.33(1) - 131.65(2); **8** P–Cu 2.2025(7) - 2.2140(7), Cu··Cu 2.7847(5) - 2.9139(5), Cu–Br 2.3935(5) - 2.4552(4), P–B 1.974(3) - 1.981(3), B–P–Cu 117.94(9) - 123.44(9), P–Cu–Br 123.71(2) - 129.35(2); **9** P–Cu 2.2438(16) - 2.2521(15), Cu··Cu 3.220(1) - 3.478(1), Cu–I 2.6756(9), P–B 1.981(6) - 2.001(8), B–P–Cu 121.3(2) - 121.73(18), P–Cu–I 113.88(5) - 121.71(5); **12** P–Cu 2.2042(1) - 2.2091(1), Cu··Cu 2.8653(1) - 3.02932(14), Cu–Cl 2.2157(2) - 2.6166(1), P–B 1.973(1) - 1.990(1), B–P–Cu 119.18(1) - 121.50(1), P–Cu–Cl 114.99(1) - 140.02(1).

distance between two copper atoms (2.8 Å) and some are longer.^[23] Despite the fact that weak Cu(I)··Cu(I) interactions have been studied for a long time,^[24] the existence of a bonding situation between two Cu centers is beyond the scope of this article.^[25,26] Although it should be noticed that **A1** and **A2** coordinating to Au(I) centers do show attractive aurophilic interactions which are resulting in luminescence properties.^[15]

If two equivalents of the copper salt CuX (X = Cl, Br, I) are reacted with one equivalent of **A3** in CH₂Cl₂, complexes **9**, [Cu₅Cl₅(Ph₂PBH₂·NMe₃)₄] (**10**) and [Cu₅Br₅(Ph₂PBH₂·NMe₃)₄] (**11**) (Scheme 2, Figure 5) are obtained in good crystalline yields (**10**: 74%; **11**: 60% based on **A3**). The latter two complexes do not show the initially used stoichiometry, but rather the maximum relative amount of metal halide to **A3** possible under these conditions. **9** reveals the same stable cubane structure as obtained from the 1:1 reaction, while **10** and **11** can be viewed as edge open cubanes with an additional CuX (X = Cl, Br) unit attached to the Cu₄X₄ core. From the reaction of two equivalents of CuBr with one equivalent of **A3**, additionally to compound **11** also complex [Cu₄Br₄(Ph₂PBH₂·NMe₃)₄] (**13**) is formed as a side product, which shows a Cu₄Br₄ eight

membered ring in a ladderlike structure (Figure 5 (c)). The targeted synthesis of **13** is difficult, the initial stoichiometry of the reaction is better represented in product **11**, while a direct synthesis in a 1:1 ratio of CuBr to **A3** leads to formation of complex $[\text{CuBr}(\text{Ph}_2\text{PBH}_2\cdot\text{NMe}_3)]_2$ (**8**).

For complexes **10** and **11**, the ^{31}P NMR spectra in CD_2Cl_2 reveal just one broad singlet at $\delta = -33.6$ ppm and -34.7 ppm, respectively. We were interested if structural changes can be observed upon solvation of the complexes compared to their solid state structures. Dissolving crystals of **10** and **11** in CD_2Cl_2 at -80 °C, the recorded ^{31}P NMR spectra at that temperature show only one broad signal which is slightly highfield shifted with increasing temperature up to room temperature. Therefore, we assume that the complexes either dissociate to smaller units in solution or some intramolecular dynamic processes occur, which are too fast on the NMR timescale.

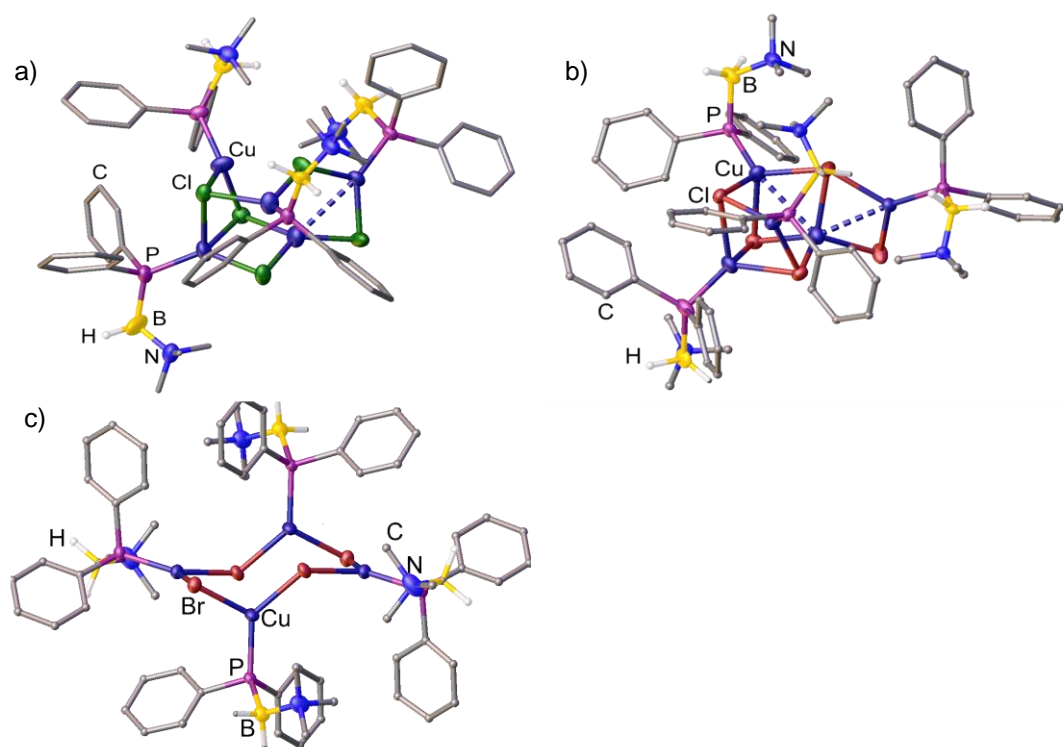


Figure 5: Molecular structure of the Cu complexes **10** (a), **11** (b) and **13** (c). Hydrogen atoms on carbon are omitted for clarity. Selected bond lengths [Å] and angles [°]: **10** P–Cu 2.2000(18) - 2.2111(2), Cu···Cu 2.9301(18), Cu–Cl 2.215(2) - 2.3564(19), P–B 1.944(11) - 1.972(14), B–P–Cu 117.6(3) - 123.8(4), P–Cu–Cl 116.73(9) - 134.98(9); **11** P–Cu 2.2009(14) - 2.2276(15), Cu···Cu 2.7219(11) & 2.9563(13), Cu–Br 2.4034(9) - 2.7288(11), P–B 1.971(6) - 1.987(7), B–P–Cu 118.91(7) - 125.2(4), P–Cu–Br 114.04(6) - 133.37(6); **13** P–Cu 2.221(2) - 2.2246(15), Cu···Cu 3.289(1) - 3.849(1), Cu–Br 2.429(3) - 2.464(1), P–B 1.973(8) - 1.994(7), B–P–Cu 122.3(2) - 125.5(2), P–Cu–Br 116.30(5) - 132.26(5).

A difference to the solid state structures can also be observed in the gas phase, as FD mass spectrometry of **10** and **11** shows fragments of $[\text{Cu}_l\text{X}_m(\text{L})_n]$ ($l = 1-5$; $m = 0 - 4$; $n = 1 - 4$), similar to fragments from complexes **7 - 9**. In the solid state, the shortest distances between two Cu atoms are 2.930(2) Å for **10** and 2.722(1) and 2.956(1) Å for **11**. For **13**

the closest distances are 3.289(1) Å and 3.849(1) Å, which are larger by 0.29 Å and 0.40 Å than in the ladderlike structure of $[\text{Cu}_4\text{Br}_4(\text{Ph}_3\text{P})_4]$.^[21] Therefore, **13** might be rather viewed as an eight membered Cu_4Br_4 ring than a ladder structure. It should be mentioned that the CuI containing complexes $[\text{Cu}(\text{Ph}_2\text{PBH}_2\cdot\text{NMe}_3)_2]$ (**6**) and $[\text{Cu}(\text{Ph}_2\text{PBH}_2\cdot\text{NMe}_3)_4]$ (**9**) show orange emission under an UV lamp in the solid state. **6** and **9** don't show any short intermetallic distances, so the emission is likely caused by some other effects, which will be investigated in the future.

5.3 Conclusion

In summary, it was shown that the pnictogenylboranes $\text{H}_2\text{EBH}_2\cdot\text{NMe}_3$ (**A1** E = P; **A2** E = As) and $\text{Ph}_2\text{PBH}_2\cdot\text{NMe}_3$ (**A3**) can be used for the generation of homoleptic complexes of Cu(I). The use of the special primary phosphine **A1** and the primary arsine **A2** lead to the tetrahedral complexes $[\text{Cu}(\text{L})_4]^+$ (L = **A1**(**1**), **A2**(**2**)), for which complex **2** represents the first Cu complex of a primary arsine. The use of the sterically demanding compound **A3** leads to a trigonal planar coordination of the Cu^+ ion. Especially the use of ligand **A3**, that mimics Ph_3P as ligand, gave rise to a series of new copper(I) halide complexes. Complexes $[\text{CuX}(\text{Ph}_2\text{PBH}_2\cdot\text{NMe}_3)_2]$ (**4**: X = Cl, **5**: X = Br, **6**: X = I) possessing a 2:1 ration of **A3** to CuX show similar trigonal structures to their Ph_3P counterparts. The same is true for the tetrameric product $[\text{Cu}_4\text{Cl}_4(\text{Ph}_2\text{PBH}_2\cdot\text{NMe}_3)_4]$ (**13**). The other complexes, possessing a ratio of CuX to **A3** that is greater or equal to 1 tend to stabilize geometries which are less favoured when Ph_3P is used. This behaviour can be observed in the dimeric species $[\text{Cu}_2\text{X}_2(\text{Ph}_2\text{PBH}_2\cdot\text{NMe}_3)_2]$ (**7**: X = Cl, **8**: X = Br), but also in $[\text{Cu}_4\text{I}_4(\text{Ph}_2\text{PBH}_2\cdot\text{NMe}_3)_4]$ (**9**), $[\text{Cu}_5\text{X}_5(\text{Ph}_2\text{PBH}_2\cdot\text{NMe}_3)_4]$ (**10**: X = Cl, **11**: X = Br) or $[\text{Cu}_6\text{Cl}_6(\text{Ph}_2\text{PBH}_2\cdot\text{NMe}_3)_4]$ **12**, and even in complexes **3** and **13**. Therefore they show the differences of the special phosphine and arsine ligands that were employed to the Ph_3P chemistry. The current study conclusively shows the versatility of the easily accessible primary phosphine **A1**, the primary arsine **A2** or the more sterical demanding phosphine **A3**, that all contain a boranyl group, as ligands in coordination chemistry. Despite the fundamental interest, these ligands may be interesting for catalytic studies and a large variety of different complexes should be accessible.

5.4 References

- [1] a) I. V. Kourkine, S. V. Maslennikov, R. Ditchfield, D. S. Glueck, G. P. A. Yap, L. M. Liable-Sands, A. L. Rheingold, *Inorg.Chem.* **1996**, 35, 6708 – 6716; b) P. G. Edwards, B. M. Kariuki, P. D. Newman, H. A. Tallis, C. Williams; *Dalton Trans.* **2014**, 43, 15532 – 15545.
- [2] P. G. Jones, H. W. Roesky, H. Gruetzmacher, G. M. Sheldrick; *Z. Naturforsch., B: Chem. Sci.* **1985**, 40, 590–593.
- [3] a) O. M. A. Salah, M. I. Bruce, P. J. Lohmeyer, C. L. Raston, B. W. Skelton, A. H. White; *J.Chem.Soc.,Dalton Trans.* **1981**, 962–967; b) G. A. Bowmaker, Effendy, R. D. Hart, J. D. Kildea, E. N. de Silva, B. W. Skelton, A. H. White; *Aust.J.Chem.* **1997**, 50, 539–552; c) M. F. Davis, M. Jura, W. Levason, G. Reid, M. Webster; *J.Organomet.Chem.* **2007**, 692, 5589–5597; d) T. Kern, G. Knor, M. Zabel, U. Monkowius; *Acta Crystallogr., Sect.E: Struct. Rep. Online* **2008**, 64, m99; e) J. R. Black, W. Levason, M. D. Spicer, M. Webster; *J. Chem. Soc., Dalton Trans.* **1993**, 3129–3136.
- [4] L. Galiano, M. Alcamí, O. Mó, M. Yáñez, *J. Phys. Chem. A* **2002**, 106, 9306–9312.
- [5] a) E. Röttinger, H. Vahrenkamp, *J. Organomet. Chem.* **1981**, 213, 1–9; b) T. Thomas, D. Pugh, I. P. Parkin, C. J. Carmalt, *Dalton Trans.* **2010**, 39, 5325–5331; c) T. Pugh, A. Kerridge, R. A. Layfield, *Angew. Chem. Int. Ed.* **2015**, 54, 4255 – 4258, *Angew. Chem.* **2015**, 127, 4329–4332.
- [6] a) S. Rendler, M. Oestreich, *Angew. Chem. Int. Ed.* **2007**, 46, 498 – 504; *Angew. Chem.* **2007**, 119, 504–510; b) D. H. Appella, Y. Moritani, R. Shintani, E. M. Ferreira, S. L. Buchwald, *J. Am. Chem. Soc.* **1999**, 121, 9473–9474; c) S. Lal, H. S. Rzepa, S. Díez-González, *ACS Catal.* **2014**, 4, 2274–2287; d) K. Ramakrishna, M. Murali, C. Sivasankar, *Org. Lett.* **2015**, 17, 3814–3817.
- [7] a) J. Min, Q. Zhang, W. Sun, Y. Cheng, L. Wang, *Dalton Trans.* **2011**, 40, 686–693; b) A. Wada, Q. Zhang, T. Yasuda, I. Takasu, S. Enomoto, C. Adachi, *Chem. Commun.* **2012**, 48, 5340–5342; c) X.-L. Chen, R. Yu, Q.-K. Zhang, L.-J. Zhou, X.-Y. Wu, Q. Zhang, C.-Z. Lu, *Chem. Mater.* **2013**, 25, 3910–3920; d) Q. Zhang, J. Chen, X.-Y. Wu, X.-L. Chen, R. Yu, C.-Z. Lu, *Dalton Trans.* **2015**, 44, 6706–6710; e) Y. Sun, V. Lemaur, J. I. Beltrán, J. Cornil, J. Huang, J. Zhu, Y. Wang, R. Fröhlich, H. Wang, L. Jiang, G. Zou, *Inorg. Chem.* **2016**, 55, 5845–5852; f) C. S. Smith, C. W. Branham, B. J. Marquardt, K. R. Mann, *J. Am. Chem. Soc.* **2010**, 132, 14079–14085; g) R. Czerwieniec, K. Kowalski, H. Yersin, *Dalton Trans.* **2013**, 42, 9826–9830; h) L. Bergmann, J. Friedrichs, M. Mydlak, T. Baumann, M. Nieger, S. Bräse, *Chem. Commun.* **2013**, 49, 6501–6503; i) C. L. Linfoot, M. J. Leidl, P. Richardson, A. F. Rausch, O. Chepelin, F. J. White, H. Yersin, N. Robertson, *Inorg. Chem.* **2014**, 53, 10854–10861; j) M. Nishikawa, S. Sawamura, A. Haraguchi, J. Morikubo, K. Takao, T. Tsubomura, *Dalton Trans.* **2015**, 44, 411–418; k) Z. Wang, C. Zheng, W. Wang, C. Xu, B. Ji, X. Zhang, *Inorg. Chem.* **2016**, 55, 2157–2164; l) J.-L. Chen, X.-H. Zeng, Y.-S. Luo, W.-M. Wang, L.-H. He, S.-J. Liu, H.-R. Wen, S. Huang, L. Liu, W.-Y. Wong, *Dalton Trans.* **2017**, 46, 13077–13087.
- [8] a) C. Marquardt, T. Jurca, K.-C. Schwan, A. Stauber, A. V. Virovets, G. R. Whittell, I. Manners, M. Scheer, *Angew. Chem.* **2015**, 127, 13315–13318; *Angew. Chem. Int. Ed.* **2015**, 54, 13122–13125; b) C. Marquardt, A. Adolf, A. Stauber, M. Bodensteiner, A. V. Virovets, A. Y. Timoshkin, M. Scheer, *Chem. Eur. J.* **2013**, 19, 11887–11891.
- [9] a) C. Marquardt, C. Thoms, A. Stauber, G. Balázs, M. Bodensteiner, M. Scheer, *Angew. Chem.* **2014**, 126, 3801–3804; *Angew. Chem. Int. Ed.* **2014**, 53, 3727–3730; b) C. Marquardt, G. Balázs, J. Baumann, A. V. Virovets, M. Scheer, *Chem. Eur. J.* **2017**, 23, 11423–11429; c) C. Marquardt, T. Kahoun, A. Stauber, G.

- Balázs, M. Bodensteiner, A. Y. Timoshkin, M. Scheer, *Angew. Chem. Int. Ed.* **2016**, *55*, 14828–14832.
- [10] a) K.-C. Schwan, A. Y. Timoshkin, M. Zabel, M. Scheer, *Chem. Eur. J.* **2006**, *12*, 4900–4908; b) C. Marquardt, O. Hegen, T. Kahoun, M. Scheer, *Chem. Eur. J.* **2017**, *23*, 4397–4404; C. Marquardt, T. Kahoun, J. Baumann, A. Y. Timoshkin, M. Scheer, *Z. Anorg. Allg. Chem.* **2017**, *643*, 1326–1330; c) O. Hegen, A. V. Virovets, A. Y. Timoshkin, M. Scheer, *Chem. Eur. J.* **2018**, *24*, 16521–16525.
- [11] C. Thoms, C. Marquardt, M. Bodensteiner, M. Scheer, *Angew. Chem.* **2013**, *125*, 5254–5259; *Angew. Chem. Int. Ed.* **2013**, *52*, 5150–5154.
- [12] U. Vogel, K.-C. Schwan, M. Scheer, *Eur. J. Inorg. Chem.* **2004**, *10*, 2062–2065.
- [13] O. Hegen, C. Marquardt, A. Y. Timoshkin, M. Scheer, *Angew. Chem. Int. Ed.* **2017**, *56*, 12783–12787.
- [14] U. Vogel, K.-C. Schwan, P. Hoemensch, M. Scheer, *Eur. J. Inorg. Chem.* **2005**, *8*, 1453–1458.
- [15] J. Braese, A. Schinabeck, M. Bodensteiner, H. Yersin, A. Y. Timoshkin, M. Scheer, *Chem. Eur. J.* **2018**, *24*, 10073–10077.
- [16] K. Schwan, A. Adolf, M. Bodensteiner, M. Zabel, M. Scheer, *Z. Anorg. Allg. Chem.* **2008**, *634*, 1383–1387.
- [17] For an example: Y. Ling, G. K. Koyanagi, D. Caraiman, V. Baranov, D. K. Bohme, *Int. J. Mass. Spectrom.* **1999**, *182/183*, 349–356; and literature therein.
- [18] P. Pyykkö, M. Atsumi, *Chem. Eur. J.* **2009**, *15*, 186–197
- [19] A. P. Gauchan, Z. Dori, J. A. Ibers, *Inorg. Chem.* **1974**, *13*, 1657–1667.
- [20] G. A. Bowmaker, J. C. Dyason, P. C. Healy, L. M. Engelhardt, C. Pakawatchai, A. H. White, *J. Chem. Soc., Dalton Trans.* **1987**, *0*, 1089–1097.
- [21] a) M. R. Churchill, K. L. Kalra, *J. Am. Chem. Soc.* **1973**, *95*, 5772–5773; b) P. Schwerdtfeger, R.P. Krawczyk, A. Hammerl, R. Brown, *Inorg. Chem.* **2004**, *43*, 6707–6716.
- [22] Alyea, E. C.; Ferguson, G.; Malito, J.; Ruhl, B. J. *Inorg. Chem.* **1985**, *24*, 3719–3720.
- [23] A. Bondi, *J. Phys. Chem.* **1964**, *68*, 441–451.
- [24] J. Beck, J. Strähle, *Angew. Chem.* **1985**, *97*, 419–420; *Angew. Chem. Int. Ed. Engl.* **1985**, *24*, 409–410.
- [25] W.-F. Fu, X. Gan, C.-M. Che, Q.-Y. Cao, Z.-Y. Zhou, N. N. Zhu, *Chem. Eur. J.* **2004**, *10*, 2228–2236.
- [26] a) For a review: P. Pyykkö, *Chem. Rev.* **1997**, *97*, 597–636; b) P. Pyykkö, F. Mendizabal, *Inorg. Chem.* **1998**, *37*, 3018–3025; c) J. M. Zuo, M. Kim, M. Oprea, J. C. H. Spence, *Nature* **1999**, *401*, 49–52; d) C. M. Che, Z. Mao, V. M. Miskowski, M. C. Tse, C. K. Chan, K. K. Cheung, D. L. Phillips, K. H. Leung, *Angew. Chem.* **2000**, *112*, 4250–4254; *Angew. Chem. Int. Ed. Engl.* **2000**, *39*, 4084–4088; e) H. L. Hermann, G. Boche, P. Schwerdtfeger, *Chem. Eur. J.* **2001**, *7*, 5333–5342; f) A. Vega, J.-Y. Saillard, *Inorg. Chem.* **2004**, *43*, 4012–4018.

5.5 Supporting Information

5.5.1 General information

All manipulations were performed under an atmosphere of dry argon using standard glove-box and Schlenk techniques. All solvents were degassed and purified by standard procedures. The compounds $\text{H}_2\text{EBH}_2\cdot\text{NMe}_3$ (E = P, As), $\text{Ph}_2\text{PBH}_2\cdot\text{NMe}_3$, were prepared according to literature procedures.^[1] Other chemicals were obtained from commercial sources ($[\text{Cu}(\text{MeCN})_4][\text{BF}_4]$, CuCl , CuBr , CuI). NMR spectra were recorded on a Bruker Avance 400 spectrometer (^1H : 400.13 MHz, ^{31}P : 161.976 MHz, ^{11}B : 128.378 MHz, $^{13}\text{C}\{^1\text{H}\}$: 100.623 MHz) with δ [ppm] referenced to external SiMe_4 (^1H , ^{13}C), H_3PO_4 (^{31}P), $\text{BF}_3\cdot\text{Et}_2\text{O}$ (^{11}B). IR spectra were recorded on a DIGILAB (FTS 800) FT-IR spectrometer and on a Thermo Scientific Nicolet iS5. Mass spectra were recorded on a ThermoQuest Finnigan TSQ 7000 (ESI-MS) and on a Finnigan MAT 95 (FDMS). The C, H, N analyses were measured on an Elementar Vario EL III apparatus.

5.5.2 Syntheses of described compounds

Synthesis of $[\text{Cu}(\text{H}_2\text{PBH}_2\cdot\text{NMe}_3)_4]^+[\text{BF}_4]^-$ (**1**): A solution of 84 mg (0.8 mmol) $\text{H}_2\text{PBH}_2\cdot\text{NMe}_3$ in 1 mL toluene is added to a solution of 63 mg (0.2 mmol) $[\text{Cu}(\text{MeCN})_4]^+[\text{BF}_4]^-$ in 10 ml MeCN. After stirring the mixture for 18 h, all volatiles are removed under reduced pressure. After dissolving the solid in CH_2Cl_2 the solution is filtrated and over layered by the 6 fold amount of *n*-hexane. **1** crystallises at r.t. as colourless needles. The crystals are separated and washed with *n*-hexane (3x5 mL).

Yield of $[\text{Cu}(\text{H}_2\text{PBH}_2\cdot\text{NMe}_3)_4]^+[\text{BF}_4]^-$: 66 mg (58%). ^1H NMR (CD_2Cl_2 , 25 °C): δ = 2.10 (q, 2H, BH_2), 2.20 (dm, $^1J_{\text{H,P}}$ = 258 Hz, 4H, PH_2), 2.69 (s, 9H, NMe_3). ^{31}P NMR (CD_2Cl_2 , 25 °C): δ = -183.8 (t, br, $^1J_{\text{H,P}}$ = 258 Hz). $^{31}\text{P}\{^1\text{H}\}$ NMR (CD_2Cl_2 , 25 °C): δ = -183.8 (s, br). ^{11}B NMR (CD_2Cl_2 , 25 °C): δ = -7.8 (m, br, BH_2), -1.4 (s, BF_4). $^{11}\text{B}\{^1\text{H}\}$ NMR (CD_2Cl_2 , 25 °C): δ = -8.7 (s, br, BH_2), -1.4 (s, BF_4). ^{19}F NMR (CD_2Cl_2 , 25 °C): δ = -152.81 (s, $^{11}\text{BF}_4$), -152.87 (s, $^{10}\text{BF}_4$). $^{13}\text{C}\{^1\text{H}\}$ NMR (CD_2Cl_2 , 25 °C): δ = 53.2 (d, $^4J_{\text{P,H}}$ = 4 Hz). IR (KBr): $\tilde{\nu}$ = 3020 (w, CH), 2948 (w, CH), 2920 (w, CH), 2890 (w, CH) 2835 (w, CH), 2386 (s, br, BH), 2323 (s, PH), 2309 (s, PH), 2250 (w), 2215 (w), 2178 (w), 2143 (w), 2011 (w), 1817 (w), 1735 (w), 1481 (s), 1470 (s), 1408 (m), 1287 (w), 1249 (m), 1151 (s), 1125 (s), 1100 (s), 1061 (vs, BF_4), 978 (m), 849 (vs), 754 (vs), 696 (w), 611 (w), 521 (w), 464 (vw), 434 (vw). ESI-MS (THF): m/z = 273 (100 %, $[\text{Cu}(\text{H}_2\text{PBH}_2\cdot\text{NMe}_3)_2]^+$), 378 (66%, $[\text{Cu}(\text{H}_2\text{PBH}_2\cdot\text{NMe}_3)_3]^+$). Elemental analysis (%) calculated for $\text{C}_{12}\text{H}_{52}\text{P}_4\text{B}_5\text{Cu}_1\text{F}_4\text{N}_4$ (**1**): C: 25.25, H: 9.19, N: 9.82; found: C: 25.72, H: 9.09, N: 9.85.

Synthesis of $[\text{Cu}(\text{H}_2\text{AsBH}_2\cdot\text{NMe}_3)_4]^+[\text{BF}_4]^-$ (2**):** A solution of 60 mg (0.4 mmol) $\text{H}_2\text{AsBH}_2\cdot\text{NMe}_3$ in 0.8 mL toluene is added to a solution of 31 mg (0.1 mmol) $[\text{Cu}(\text{MeCN})_4]^+[\text{BF}_4]^-$ in 10 ml MeCN. After stirring the mixture for 18 h, all volatiles are removed under reduced pressure. After dissolving the solid in CH_2Cl_2 the solution is filtrated and over layered by the 6 fold amount of *n*-hexane. **2** crystallises at r.t. as colourless needles. The crystals are separated and washed with *n*-hexane (3×5 mL).

Yield of $[\text{Cu}(\text{H}_2\text{AsBH}_2\cdot\text{NMe}_3)_4]^+[\text{BF}_4]^-$: 48 mg (65 %). ^1H NMR (CD_2Cl_2 , 25 °C): $\delta = 1.21$ (m, AsH_2), 2.37 (q, 2H, BH_2), 2.72 (s, 9H, NMe_3). ^{11}B NMR (CD_2Cl_2 , 25 °C): $\delta = -7.8$ (t, $^1J_{\text{B,H}} = 110$ Hz, BH_2), -1.4 (s, BF_4). $^{11}\text{B}\{^1\text{H}\}$ NMR (CD_2Cl_2 , 25 °C): $\delta = -7.8$ (s, br, BH_2), -1.4 (s, BF_4). $^{19}\text{F}\{^1\text{H}\}$ NMR (CD_2Cl_2 , 25 °C): $\delta = -152.25$ (s, $^{11}\text{BF}_4$), -152.19 (s, $^{10}\text{BF}_4$). ^{19}F NMR (CD_2Cl_2 , 25 °C): $\delta = -152.25$ (s, $^{11}\text{BF}_4$), -152.19 (s, $^{10}\text{BF}_4$). $^{13}\text{C}\{^1\text{H}\}$ NMR (CD_2Cl_2 , 25 °C): $\delta = 53.7$ (s, NMe_3). IR (KBr): $\tilde{\nu} = 3017$ (w, CH), 3000 (w, CH), 2948 (w, CH), 2920 (w, CH), 2839 (w), 2409 (m, BH), 2382 (m, BH), 2294 (w), 2121 (m, AsH), 2104 (m, AsH), 1484 (m), 1469 (m), 1409 (w), 1249 (w), 1135 (w), 1120 (m), 1099 (m), 1059 (vs, BF_4), 1009 (m), 977 (m), 959 (m), 851 (m), 711 (w), 670 (m), 552 (w), 520 (w). ESI-MS (MeCN): $m/z = 253$ (54 %, $[\text{Cu}(\text{H}_2\text{AsBH}_2\cdot\text{NMe}_3)\text{MeCN}]^+$), 361 (100 %, $[\text{Cu}(\text{H}_2\text{AsBH}_2\cdot\text{NMe}_3)_2]^+$). Elemental analysis (%) calculated for $\text{C}_{12}\text{H}_{52}\text{As}_4\text{B}_5\text{Cu}_1\text{F}_4\text{N}_4$ (**2**): C: 19.32, H: 7.03, N: 7.51; found: C: 19.52, H: 7.06, N: 7.25.

Synthesis of $[\text{Cu}(\text{Ph}_2\text{PBH}_2\cdot\text{NMe}_3)_3]^+[\text{BF}_4]^-$ (3**):** A solution of 154 mg (0.6 mmol) $\text{Ph}_2\text{PBH}_2\cdot\text{NMe}_3$ in 10 mL MeCN is added to a solution of 63 mg (0.2 mmol) $[\text{Cu}(\text{MeCN})_4]^+[\text{BF}_4]^-$ in 10 ml MeCN. After stirring the mixture for 18 h, all volatiles are removed under reduced pressure. The solid is dissolved in CH_2Cl_2 and the solution is filtrated. The solution is over layered with twice the amount of *n*-hexane. **3** crystallises at -28 °C as colourless blocks. The crystals are separated and washed with *n*-hexane (3×5 mL).

Yield of $[\text{Cu}(\text{Ph}_2\text{PBH}_2\cdot\text{NMe}_3)_3]^+[\text{BF}_4]^-$: 126 mg (65 %). ^1H NMR (CD_2Cl_2 , 25 °C): $\delta = 2.37$ (s, 9H, NMe_3), 2.49 (br, 2H, BH_2), 7.15 (m, 2H, *m*-Ph), 7.22 (m, 2H, *p*-Ph), 7.36 (m, 4H, *o*-Ph). ^{31}P NMR (CD_2Cl_2 , 25 °C): $\delta = -38.9$ (s, br). $^{31}\text{P}\{^1\text{H}\}$ NMR (CD_2Cl_2 , 25 °C): $\delta = -38.9$ (s, br). ^{11}B NMR (CD_2Cl_2 , 25 °C): $\delta = -5.9$ (s, br, BH_2), -1.4 (s, BF_4). $^{11}\text{B}\{^1\text{H}\}$ NMR (CD_2Cl_2 , 25 °C): $\delta = -5.9$ (s, br, BH_2), -1.4 (s, BF_4). ^{19}F NMR (CD_2Cl_2 , 25 °C): $\delta = -152.91$ (s, $^{11}\text{BF}_4$), -152.85 (s, $^{10}\text{BF}_4$). $^{19}\text{F}\{^1\text{H}\}$ NMR (CD_2Cl_2 , 25 °C): $\delta = -152.91$ (s, $^{11}\text{BF}_4$), -152.85 (s, $^{10}\text{BF}_4$). $^{13}\text{C}\{^1\text{H}\}$ NMR (CD_2Cl_2 , 25 °C): $\delta = 54.4$ (s, NMe_3), 128.4 (s, *p*-Ph), 128.6 (s, *m*-Ph), 134.2 (s, *o*-Ph), 136.3 (s, *i*-Ph). IR (KBr): $\tilde{\nu} = 3052$ (w, CH), 3005 (w, CH), 2949 (w, CH), 2877 (w, CH), 2842 (w, CH), 2390 (m, br, BH), 1963 (vw), 1892 (vw), 1818 (vw), 1584 (w), 1481 (s), 1463 (s), 1434 (s), 1410 (w), 1426 (w), 1158 (w), 1124 (s), 1063 (vs, BF_4), 970 (m), 856 (m), 739 (s), 698 (s), 512 (m). ESI-MS (pos.,

MeCN): $m/z = 577$ (100%, $[\text{Cu}(\text{Ph}_2\text{PBH}_2\cdot\text{NMe}_3)_2]^+$), ESI-MS (neg., MeCN): $m/z = 87$ (100%, $[\text{BF}_4]^-$). Elemental analysis (%) calculated for $\text{C}_{45}\text{H}_{63}\text{B}_4\text{Cu}_1\text{F}_4\text{N}_3\text{P}_3$ (**3**): C: 58.60, H: 6.89, N: 4.56; found: C: 58.40, H: 6.94, N: 4.14.

Transformation of $[\text{Cu}(\text{Ph}_2\text{PBH}_2\cdot\text{NMe}_3)_3]^+[\text{BF}_4]^-$ (**3**) to $[\text{CuCl}(\text{Ph}_2\text{PBH}_2\cdot\text{NMe}_3)_2]$ (**4**):

Storing a solution of **3** in CH_2Cl_2 for more than 20 days leads to traces of **4**. Some crystals were obtained by over layering a solution with *n*-hexane and storing it at r.t..

Synthesis of $[\text{CuCl}(\text{Ph}_2\text{PBH}_2\cdot\text{NMe}_3)_2]$ (**4**): A solution of 64 mg (0.25 mmol) $\text{Ph}_2\text{PBH}_2\cdot\text{NMe}_3$ in 5 mL CH_2Cl_2 is added to 12 mg (0.125 mmol) CuCl. After stirring the mixture for 18 h, the solution is filtrated. The solution is over layered with thrice the amount of *n*-hexane. **4** crystallises at room temperature as colourless blocks. The crystals are separated and washed with *n*-hexane (3×5 mL). Unit cell from targeted synthesis differs from the crystals of **4** obtained from storing **3** in CH_2Cl_2 .

Yield of $[\text{CuCl}(\text{Ph}_2\text{PBH}_2\cdot\text{NMe}_3)_2]$: 65 mg (88 %). ^1H NMR (CD_2Cl_2 , 25 °C): $\delta = 2.49$ (br, 2H, BH_2), 2.68 (s, 9H, NMe_3), 7.17 (m, 6H, *m/p*-Ph), 7.60 (m, 4H, *o*-Ph). ^{31}P NMR (CD_2Cl_2 , 25 °C): $\delta = -42.9$ (s, br). $^{31}\text{P}\{^1\text{H}\}$ NMR (CD_2Cl_2 , 25 °C): $\delta = -42.9$ (s, br). ^{11}B NMR (CD_2Cl_2 , 25 °C): $\delta = -4.3$ (s, br, BH_2). $^{11}\text{B}\{^1\text{H}\}$ NMR (CD_2Cl_2 , 25 °C): $\delta = -4.3$ (s, br, BH_2). IR (ATR): $\tilde{\nu} = 3070$ (w, CH), 3049 (m, CH), 3013 (w, CH), 2985 (w, CH), 2945 (w, CH), 2833 (w, CH), 2411 (m, br, BH), 2380 (m, br, BH), 2311 (w, BH), 1585 (m), 1480 (s), 1470 (m), 1446 (w), 1432 (s), 1402 (m), 1320 (w), 1254 (m), 1244 (m), 1187 (w), 1162 (m), 1124 (s), 1093 (w), 1072 (s), 1062 (s), 1019 (m), 1001 (w), 979 (m), 855 (s), 764 (m), 741 (m), 727 (s), 690 (vs), 639 (m), 618 (w). FD-MS (pos., CH_2Cl_2): $m/z = 257$ (100%, $(\text{Ph}_2\text{PBH}_2\cdot\text{NMe}_3)^+$), 577 (36%, $[\text{Cu}(\text{Ph}_2\text{PBH}_2\cdot\text{NMe}_3)_2]^+$). Elemental analysis (%) calculated for $\text{C}_{30}\text{H}_{42}\text{B}_2\text{ClCuN}_2\text{P}_2$ (**4**): C: 58.76, H: 6.90, N: 4.57; found: C: 58.63, H: 6.49, N: 4.29.

Synthesis of $[\text{CuBr}(\text{Ph}_2\text{PBH}_2\cdot\text{NMe}_3)_2]$ (**5**): A solution of 64 mg (0.25 mmol) $\text{Ph}_2\text{PBH}_2\cdot\text{NMe}_3$ in 5 mL CH_2Cl_2 is added to 18 mg (0.125 mmol) CuBr. After stirring the mixture for 18 h, the volume is reduced to the half and the concentrated solution is filtrated. The solution is over layered with thrice the amount of *n*-hexane. **5** crystallises at room temperature as colourless blocks. The crystals are separated and washed with *n*-hexane (3×5 mL).

Yield of $[\text{CuBr}(\text{Ph}_2\text{PBH}_2\cdot\text{NMe}_3)_2]$: 75 mg (91 %). ^1H NMR (CD_2Cl_2 , 25 °C): $\delta = 2.47$ (br, 2H, BH_2), 2.68 (s, 9H, NMe_3), 7.18 (m, 6H, *m/p*-Ph), 7.60 (m, 4H, *o*-Ph). ^{31}P NMR (CD_2Cl_2 , 25 °C): $\delta = -42.8$ (s, br). $^{31}\text{P}\{^1\text{H}\}$ NMR (CD_2Cl_2 , 25 °C): $\delta = -42.8$ (s, br). ^{11}B NMR (CD_2Cl_2 , 25 °C): $\delta = -4.5$ (s, br, BH_2). $^{11}\text{B}\{^1\text{H}\}$ NMR (CD_2Cl_2 , 25 °C): $\delta = -4.5$ (s, br,

BH₂). IR (ATR): $\tilde{\nu}$ = 3071 (w, CH), 3049 (w, CH), 3014 (w, CH), 2984 (w, CH), 2944 (w, CH), 2832 (w, CH), 2800 (w, CH), 2423 (m, BH), 2410 (m, BH), 2383 (m, br, BH), 2312 (w, BH), 1585 (m), 1570 (w), 1480 (s), 1468 (m), 1446 (w), 1433 (s), 1402 (m), 1323 (w), 1253 (m), 1243 (m), 1186 (w), 1163 (m), 1123 (s), 1093 (w), 1071 (s), 1062 (s), 1019 (m), 1001 (w), 978 (m), 914 (w), 855 (s), 764 (m), 741 (s), 727 (s), 690 (vs), 654 (w), 639 (m), 618 (w). FD-MS (pos., CH₂Cl₂): m/z = 257 (100%, (Ph₂PBH₂·NMe₃)⁺), 336 (12%, (BrPh₂PBH₂·NMe₃)⁺), 401 (12%, [CuBr(Ph₂PBH₂·NMe₃)]⁺), 577 (100%, [Cu(Ph₂PBH₂·NMe₃)₂]⁺), 721 (22%, [Cu₂Br(Ph₂PBH₂·NMe₃)₂]⁺), 802 (2%, [Cu₂Br₂(Ph₂PBH₂·NMe₃)₂]⁺), 978 (4%, [Cu₂Br(Ph₂PBH₂·NMe₃)₃]⁺), 1122 (3%, [Cu₃Br₂(Ph₂PBH₂·NMe₃)₃]⁺). Elemental analysis (%) calculated for C₃₀H₄₂B₂BrCuN₂P₂ (**5**): C: 54.79, H: 6.44, N: 4.26; found: C: 55.52, H: 6.33, N: 3.84.

Synthesis of [CuI(Ph₂PBH₂·NMe₃)₂] (**6**): A solution of 64 mg (0.25 mmol) Ph₂PBH₂·NMe₃ in 5 mL CH₂Cl₂ is added to 24 mg (0.125 mmol) CuI. After stirring the mixture for 18 h, the volume is reduced to the half and the concentrated solution is filtrated. The solution is over layered with thrice the amount of *n*-hexane. **6** crystallises at room temperature as colourless blocks. The crystals are separated and washed with *n*-hexane (3×5 mL).

Yield of [CuI(Ph₂PBH₂·NMe₃)₂]: 73 mg (83 %). ¹H NMR (CD₂Cl₂, 25 °C): δ = 2.54 (br, 2H, BH₂), 2.68 (s, 9H, NMe₃), 7.20 (m, 6H, *m/p*-Ph), 7.63 (m, 4H, *o*-Ph). ³¹P NMR (CD₂Cl₂, 25 °C): δ = -42.7 (s, br). ³¹P{¹H} NMR (CD₂Cl₂, 25 °C): δ = -42.7 (s, br). ¹¹B NMR (CD₂Cl₂, 25 °C): δ = -4.6 (s, br, BH₂). ¹¹B{¹H} NMR (CD₂Cl₂, 25 °C): δ = -4.6 (s, br, BH₂). IR (ATR): $\tilde{\nu}$ = 3069 (w, CH), 3048 (w, CH), 3016 (w, CH), 3000 (w, CH), 2984 (w, CH), 2942 (w, CH), 2875 (w, CH), 2425 (m, BH), 2405 (m, BH), 2390 (m, br, BH), 2311 (w, BH), 1583 (m), 1569 (w), 1478 (s), 1461 (s), 1432 (s), 1406 (m), 1326 (w), 1308 (w), 1266 (w), 1252 (m), 1243 (m), 1186 (w), 1160 (m), 1122 (s), 1090 (m), 1063 (s), 1026 (m), 1015 (s), 1000 (w), 977 (m), 956 (w), 930 (w), 910 (w), 855 (s), 763 (w), 749 (m), 739 (s), 692 (vs), 523 (w), 636 (m), 618 (w). FD-MS (pos., CH₂Cl₂): m/z = 257 (100%, (Ph₂PBH₂·NMe₃)⁺), 384 (48%, (IPh₂PBH₂·NMe₃)⁺), 447 (2%, [CuI(Ph₂PBH₂·NMe₃)]⁺), 577 (46%, [Cu(Ph₂PBH₂·NMe₃)₂]⁺), 767 (11%, [Cu₂I(Ph₂PBH₂·NMe₃)₂]⁺), 894 (3%, [Cu₂I₂(Ph₂PBH₂·NMe₃)₂]⁺), 1085 (<1%, [Cu₃I₃(Ph₂PBH₂·NMe₃)₂]⁺), 1216 (2%, [Cu₃I₂(Ph₂PBH₂·NMe₃)₃]⁺). Elemental analysis (%) calculated for C₃₀H₄₂B₂CuIN₂P₂ (**6**): C: 51.13, H: 6.01, N: 3.98; found: C: 50.79, H: 5.81, N: 3.52.

Synthesis of [Cu₂Cl₂(Ph₂PBH₂·NMe₃)₂] (**7**): A solution of 64 mg (0.25 mmol) Ph₂PBH₂·NMe₃ in 5 mL CH₂Cl₂ is added to 25 mg (0.25 mmol) CuCl. After stirring the mixture for 18 h, the solution is filtrated. The solution is over layered with thrice the

amount of *n*-hexane. **7** crystallises at room temperature as colourless blocks. The crystals are separated and washed with *n*-hexane (3×5 mL).

Yield of [Cu₂Cl₂(Ph₂PBH₂·NMe₃)₂]: 65 mg (73 %). ¹H NMR (CD₂Cl₂, 25 °C): δ = 2.61 (q, 2H, ¹J_{H,B} = 88 Hz, BH₂), 2.78 (s, 9H, NMe₃), 5.33 (s, CH₂Cl₂, from crystals), 7.32 (m, 6H, *m/p*-Ph), 7.72 (m, 4H, *o*-Ph). ³¹P NMR (CD₂Cl₂, 25 °C): δ = -34.7 (s, br). ³¹P{¹H} NMR (CD₂Cl₂, 25 °C): δ = -34.7 (s, br). ¹¹B NMR (CD₂Cl₂, 25 °C): δ = -4.3 (d, ¹J_{B,P} = 68 Hz, BH₂). ¹¹B{¹H} NMR (CD₂Cl₂, 25 °C): δ = -4.3 (dq, ¹J_{B,P} = 68 Hz, ¹J_{B,H} = 88 Hz, BH₂). IR (ATR): $\tilde{\nu}$ = 3049 (w, CH), 2999 (w, CH), 2942 (w, CH), 2417 (m, BH), 2383 (m, br, BH), 2307 (w, BH), 1583 (w), 1569 (w), 1478 (s), 1460 (s), 1432 (s), 1406 (m), 1387 (w), 1329 (vw), 1305 (w), 1251 (m), 1239 (m), 1183 (w), 1160 (m), 1122 (s), 1092 (m), 1074 (m), 1063 (s), 1026 (m), 1016 (m), 1007 (m), 1000 (m), 976 (m), 920 (vw), 855 (s), 807 (w), 737 (s), 692 (vs), 641 (s), 618 (w). FD-MS (pos., CH₂Cl₂): *m/z* = 257 (100%, (Ph₂PBH₂·NMe₃)⁺), 292 (36%, (ClPh₂PBH₂·NMe₃)⁺), 355 (8%, [CuCl(Ph₂PBH₂·NMe₃)]⁺), 518 (5%, [Cu₃Cl₂(Ph₂PBH₂·NMe₃)]⁺), 577 (52%, [Cu(Ph₂PBH₂·NMe₃)₂]⁺), 677 (27%, [Cu₂Cl(Ph₂PBH₂·NMe₃)₂]⁺), 712 (6%, [Cu₂Cl₂(Ph₂PBH₂·NMe₃)₂]⁺), 775 (2%, [Cu₃Cl₂(Ph₂PBH₂·NMe₃)₂]⁺), 934 (10%, [Cu₂Cl(Ph₂PBH₂·NMe₃)₃]⁺), 1032 (12%, [Cu₃Cl₂(Ph₂PBH₂·NMe₃)₃]⁺), 1389 (2%, [Cu₄Cl₃(Ph₂PBH₂·NMe₃)₄]⁺). Elemental analysis (%) calculated for C₃₀H₄₂B₂Cl₂Cu₂N₂P₂ (**7**) · (CH₂Cl₂)_{0.7}: C: 47.78, H: 5.67, N: 3.63; found: C: 47.89, H: 5.46, N: 3.57.

Synthesis of [Cu₂Br₂(Ph₂PBH₂·NMe₃)₂ (**8**): A solution of 64 mg (0.25 mmol) Ph₂PBH₂·NMe₃ in 5 mL CH₂Cl₂ is added to 25 mg (0.25 mmol) CuBr. After stirring the mixture for 18 h, the solution is filtrated. The solution is over layered with thrice the amount of *n*-hexane. **8** crystallises at room temperature as colourless blocks. The crystals are separated and washed with *n*-hexane (3×5 mL).

Yield of [Cu₂Br₂(Ph₂PBH₂·NMe₃)₂]: 90 mg (90 %). ¹H NMR (CD₂Cl₂, 25 °C): δ = 2.59 (q, 2H, ¹J_{H,B} = 101 Hz, BH₂), 2.77 (s, 9H, NMe₃), 7.30 (m, 6H, *m/p*-Ph), 7.73 (m, 4H, *o*-Ph). ³¹P NMR (CD₂Cl₂, 25 °C): δ = -37.2 (s, br). ³¹P{¹H} NMR (CD₂Cl₂, 25 °C): δ = -37.2 (s, br). ¹¹B NMR (CD₂Cl₂, 25 °C): δ = -5.0 (d, ¹J_{B,P} = 65 Hz, BH₂). ¹¹B{¹H} NMR (CD₂Cl₂, 25 °C): δ = -4.3 (dq, ¹J_{B,P} = 65 Hz, ¹J_{B,H} = 101 Hz, BH₂). IR (ATR): $\tilde{\nu}$ = 3069 (w, CH), 3049 (w, CH), 3014 (w, CH), 2999 (w, CH), 2986 (w, CH), 2942 (w, CH), 2872 (w, CH), 2384 (m, br, BH), 2397 (w, BH), 1584 (m), 1570 (w), 1479 (s), 1461 (m), 1432 (s), 1407 (s), 1333 (w), 1308 (w), 1253 (m), 1242 (m), 1184 (w), 1157 (m), 1122 (s), 1092 (m), 1063 (s), 1026 (m), 1014 (m), 1000 (m), 978 (m), 854 (s), 801 (m), 738 (s), 692 (vs), 638 (m), 618 (w). FD-MS (pos., CH₂Cl₂): *m/z* = 257 (100%, (Ph₂PBH₂·NMe₃)⁺), 336 (52%, (BrPh₂PBH₂·NMe₃)⁺), 401 (5%, [CuBr(Ph₂PBH₂·NMe₃)]⁺), 577 (86%, [Cu(Ph₂PBH₂·NMe₃)₂]⁺), 721 (29%, [Cu₂Br(Ph₂PBH₂·NMe₃)₂]⁺), 802 (4%,

$[\text{Cu}_2\text{Br}_2(\text{Ph}_2\text{PBH}_2\cdot\text{NMe}_3)_2]^+$, 978 (2%, $[\text{Cu}_2\text{Br}(\text{Ph}_2\text{PBH}_2\cdot\text{NMe}_3)_3]^+$, 1122 (7%, $[\text{Cu}_3\text{Br}_2(\text{Ph}_2\text{PBH}_2\cdot\text{NMe}_3\text{Z}_3)^+$, 1201 (2%, $[\text{Cu}_3\text{Br}_3(\text{Ph}_2\text{PBH}_2\cdot\text{NMe}_3)_3]^+$). Elemental analysis (%) calculated for $\text{C}_{30}\text{H}_{42}\text{B}_2\text{Br}_2\text{Cu}_2\text{N}_2\text{P}_2$ (**8**): C: 44.98, H: 5.28, N: 3.50; found: C: 45.18, H: 5.36, N: 3.34.

Synthesis of $[\text{Cu}_4\text{I}_4(\text{Ph}_2\text{PBH}_2\cdot\text{NMe}_3)_4]$ (**9**): A solution of 51 mg (0.2 mmol) $\text{Ph}_2\text{PBH}_2\cdot\text{NMe}_3$ in 4 mL CH_2Cl_2 is added to 51 mg (0.2 mmol) CuI . After stirring the mixture for 18 h, the solution is filtrated. The solution is over layered with thrice the amount of *n*-hexane. **9** crystallises at room temperature as colourless blocks. The crystals are separated and washed with *n*-hexane (3x5 mL).

Yield of $[\text{Cu}_4\text{I}_4(\text{Ph}_2\text{PBH}_2\cdot\text{NMe}_3)_4]$: 68 mg (76%). ^1H NMR (CD_2Cl_2 , 25 °C): δ = 2.56 (br, 2H, BH_2), 2.72 (s, 9H, NMe_3), 7.26 (m, 6H, *m/p*-Ph), 7.72 (m, 4H, *o*-Ph). ^{31}P NMR (CD_2Cl_2 , 25 °C): δ = -42.4 (s, br). $^{31}\text{P}\{^1\text{H}\}$ NMR (CD_2Cl_2 , 25 °C): δ = -42.4 (s, br). ^{11}B NMR (CD_2Cl_2 , 25 °C): δ = -4.7 (s, br, BH_2). $^{11}\text{B}\{^1\text{H}\}$ NMR (CD_2Cl_2 , 25 °C): δ = -4.7 (s, br, BH_2). IR (ATR): $\tilde{\nu}$ = 3049 (w, CH), 3014 (w, CH), 2998 (w, CH), 2940 (w, CH), 2384 (m, br, BH), 2305 (w, BH), 1583 (w), 1569 (w), 1479 (s), 1460 (m), 1432 (s), 1406 (w), 1307 (w), 1252 (m), 1242 (m), 1184 (w), 1156 (w), 1121 (s), 1092 (m), 1063 (s), 1026 (m), 1014 (m), 1000 (w), 977 (m), 854 (s), 805 (m), 738 (s), 692 (vs), 638 (m), 617 (w). FD-MS (pos., CH_2Cl_2): m/z = 257 (94%, $(\text{Ph}_2\text{PBH}_2\cdot\text{NMe}_3)^+$), 384 (65%, $(\text{IPh}_2\text{PBH}_2\cdot\text{NMe}_3)^+$), 447 (1%, $[\text{CuI}(\text{Ph}_2\text{PBH}_2\cdot\text{NMe}_3)]^+$), 577 (100%, $[\text{Cu}(\text{Ph}_2\text{PBH}_2\cdot\text{NMe}_3)_2]^+$), 767 (6%, $[\text{Cu}_2(\text{Ph}_2\text{PBH}_2\cdot\text{NMe}_3)_2]^+$), 1216 (2%, $[\text{Cu}_3\text{I}_2(\text{Ph}_2\text{PBH}_2\cdot\text{NMe}_3)_3]^+$), 1663 (<1%, $[\text{Cu}_4\text{I}_3(\text{Ph}_2\text{PBH}_2\cdot\text{NMe}_3)_4]^+$), 1853 (<1%, $[\text{Cu}_5\text{I}_4(\text{Ph}_2\text{PBH}_2\cdot\text{NMe}_3)_4]^+$). Elemental analysis (%) calculated for $\text{C}_{60}\text{H}_{84}\text{B}_4\text{Cu}_4\text{I}_4\text{N}_4\text{P}_4$ (**9**) · $(\text{CH}_2\text{Cl}_2)_{1.5}$: C: 38.79, H: 4.60, N: 2.95; found: C: 39.11, H: 4.76, N: 2.88.

Synthesis of $[\text{Cu}_5\text{Cl}_5(\text{Ph}_2\text{PBH}_2\cdot\text{NMe}_3)_4]$ (**10**): A solution of 64 mg (0.25 mmol) $\text{Ph}_2\text{PBH}_2\cdot\text{NMe}_3$ in 5 mL CH_2Cl_2 is added to 50 mg (0.50 mmol) CuCl . After stirring the mixture for 18 h, the cloudy solution is filtrated. The solution is over layered with thrice the amount of *n*-hexane. **10** crystallises at room temperature as colourless blocks. The crystals are separated and washed with *n*-hexane (3x5 mL).

Yield of $[\text{Cu}_5\text{Cl}_5(\text{Ph}_2\text{PBH}_2\cdot\text{NMe}_3)_4]$: 66 mg (74 %). ^1H NMR (CD_2Cl_2 , 25 °C): δ = 2.60 (q, 2H, $^1J_{\text{H,B}} = 87$ Hz, BH_2), 2.78 (s, 9H, NMe_3), 7.32 (m, 6H, *m/p*-Ph), 7.71 (m, 4H, *o*-Ph). ^{31}P NMR (CD_2Cl_2 , 25 °C): δ = -33.6 (s, br). $^{31}\text{P}\{^1\text{H}\}$ NMR (CD_2Cl_2 , 25 °C): δ = -33.6 (s, br). ^{11}B NMR (CD_2Cl_2 , 25 °C): δ = -4.3 (d, $^1J_{\text{B,P}} = 69$ Hz, BH_2). $^{11}\text{B}\{^1\text{H}\}$ NMR (CD_2Cl_2 , 25 °C): δ = -4.3 (dq, $^1J_{\text{B,P}} = 69$ Hz, $^1J_{\text{B,H}} = 87$ Hz, BH_2). IR (ATR): $\tilde{\nu}$ = 3065 (w, CH), 3053 (w, CH), 3048 (w, CH), 3023 (w, CH), 2998 (w, CH), 2942 (w, CH), 2913 (w, CH), 2417 (m, br, BH), 2382 (m, br, BH), 2309 (w, BH), 1583 (w), 1560 (w), 1478 (s), 1460 (s), 1432

(s), 1406 (m), 1399 (w), 1388 (vw), 1305 (w), 1250 (m), 1239 (m), 1183 (w), 1161 (m), 1122 (m), 1092 (w), 1074 (m), 1063 (s), 1026 (m), 1016 (m), 1008 (m), 1000 (m), 976 (m), 955 (w), 855 (s), 768 (w), 745 (s), 736 (s), 692 (vs), 642 (m), 618 (w). FD-MS (pos., CH₂Cl₂): m/z = 257 (100%, (Ph₂PBH₂·NMe₃)⁺), 292 (63%, (ClPh₂PBH₂·NMe₃)⁺), 355 (11%, [CuCl(Ph₂PBH₂·NMe₃)⁺]), 518 (4%, [Cu₃Cl₂(Ph₂PBH₂·NMe₃)⁺]), 577 (68%, [Cu(Ph₂PBH₂·NMe₃)₂]⁺), 677 (38%, [Cu₂Cl(Ph₂PBH₂·NMe₃)₂]⁺), 712 (8%, [Cu₂Cl₂(Ph₂PBH₂·NMe₃)₂]⁺), 775 (<2%, [Cu₃Cl₂(Ph₂PBH₂·NMe₃)₂]⁺), 934 (11%, [Cu₂Cl(Ph₂PBH₂·NMe₃)₃]⁺), 1032 (18%, [Cu₃Cl₂(Ph₂PBH₂·NMe₃)₃]⁺), 1067 (3%, [Cu₃Cl₃(Ph₂PBH₂·NMe₃)₃]⁺), 1389 (3%, [Cu₄Cl₃(Ph₂PBH₂·NMe₃)₄]⁺), 1424 (<2%, [Cu₄Cl₄(Ph₂PBH₂·NMe₃)₄]⁺). 1487 (<2%, [Cu₅Cl₄(Ph₂PBH₂·NMe₃)₄]⁺). Elemental analysis (%) calculated for C₆₀H₈₄B₄Cl₅Cu₅N₄P₄ (**10**): C: 47.30, H: 5.56, N: 3.68; found: C: 47.79, H: 5.40, N: 3.57.

Synthesis of [Cu₅Br₅(Ph₂PBH₂·NMe₃)₄] (**11**): A solution of 64 mg (0.25 mmol) Ph₂PBH₂·NMe₃ in 5 mL CH₂Cl₂ is added to 72 mg (0.50 mmol) CuBr. After stirring the mixture for 18 h, the cloudy solution is filtrated. The solution is over layered with thrice the amount of *n*-hexane. **11** crystallises at room temperature as colourless blocks. The crystals are separated and washed with *n*-hexane (3x5 mL).

Yield of [Cu₅Br₅(Ph₂PBH₂·NMe₃)₄]: 65 mg (60%). ¹H NMR (CD₂Cl₂, 25 °C): δ = 2.54 (br, 2H, BH₂), 2.78 (s, 9H, NMe₃), 7.32 (m, 6H, *m/p*-Ph), 7.71 (m, 4H, *o*-Ph). ³¹P NMR (CD₂Cl₂, 25 °C): δ = -34.7 (s, br). ³¹P{¹H} NMR (CD₂Cl₂, 25 °C): δ = -34.7 (s, br). ¹¹B NMR (CD₂Cl₂, 25 °C): δ = -5.3 (d, ¹J_{B,P} = 63 Hz, BH₂). ¹¹B{¹H} NMR (CD₂Cl₂, 25 °C): δ = -5.3 (m, br, BH₂). IR (ATR): $\tilde{\nu}$ = 3066 (w, CH), 3052 (w, CH), 2998 (w, CH), 2943 (w, CH), 2912 (w, CH), 2380 (s, br, BH), 2308 (w, BH), 1583 (w), 1569 (w), 1588 (w), 1549 (w), 1477 (s), 1459 (s), 1432 (s), 1406 (m), 1362 (w), 1333 (w), 1305 (w), 1274 (w), 1246 (m), 1182 (w), 1169 (m), 1122 (s), 1092 (w), 1063 (s), 1026 (m), 1014 (m), 1000 (m), 977 (m), 914 (w), 858 (s), 767 (w), 737 (s). FD-MS (pos., CH₂Cl₂): m/z = 257 (49%, (Ph₂PBH₂·NMe₃)⁺), 336 (21%, (BrPh₂PBH₂·NMe₃)⁺), 577 (100%, [Cu(Ph₂PBH₂·NMe₃)₂]⁺), 721 (16%, [Cu₂Br(Ph₂PBH₂·NMe₃)₂]⁺), 802 (1%, [Cu₂Br₂(Ph₂PBH₂·NMe₃)₂]⁺), 978 (4%, [Cu₂Br(Ph₂PBH₂·NMe₃)₃]⁺), 1122 (6%, [Cu₃Br₂(Ph₂PBH₂·NMe₃)₃]⁺), 1523 (1%, [Cu₄Br₃(Ph₂PBH₂·NMe₃)₄]⁺). Elemental analysis (%) calculated for [C₆₀H₈₄B₄Br₅Cu₅N₄P₄]_{0.14} (**11**) [C₆₀H₈₄B₄Br₄Cu₄N₄P₄]_{0.86} (**13**): C: 44.46, H: 5.22, N: 3.46; found: C: 44.46, H: 5.21, N: 3.34.

The X-ray diffraction experiments were performed on either an Rigaku Oxford Diffraction Gemini R Ultra diffractometer with Cu-K_α radiation (λ = 1.54178 Å) (**1-4**, **6-13**) and Mo-K_α radiation (λ = 0.71073 Å) (**5**). The measurements were performed at 123 K.

Crystallographic data together with the details of the experiments are given below. Absorption corrections were applied semi-empirically from equivalent reflections or analytically (SCALE3/ABSPACK algorithm implemented in CrysAlis PRO software by Agilent Technologies Ltd).^[2] All structures were solved using SHELXT,^[3] and OLEX 2.^[4] Refinements against F^2 in anisotropic approximation were done using SHELXL.^[3] The hydrogen positions of the methyl groups were located geometrically and refined riding on the carbon atoms. Hydrogen atoms belonging to BH₂ and PH₂ groups were located from the difference Fourier map. The figures were created with OLEX 2.^[4]

Table 1. Crystallographic data for compounds 1 - 3.

Compound	1	2	3
Formula	H ₅₂ C ₁₂ N ₄ F ₄ P ₄ CuB ₅	H ₅₂ C ₁₂ N ₄ F ₄ CuAs ₄ B ₅	C ₄₇ H ₆₇ B ₄ Cl ₄ CuF ₄ N ₃ P ₃
<i>D</i> _{calc.} / g cm ⁻³	1.197	1.511	1.350
<i>m</i> /mm ⁻¹	3.160	5.688	3.652
Formula Weight	570.04	745.85	1091.52
Colour	colourless	colourless	colourless
Shape	needle	needle	block
Size/mm ³	0.23×0.15×0.08	0.85×0.07×0.03	0.17×0.09×0.07
<i>T</i> /K	123.05(10)	122.9(4)	123.1(4)
Crystal System	tetragonal	tetragonal	monoclinic
Space Group	<i>I</i> -4	<i>I</i> -4	<i>P</i> 2 ₁ / <i>c</i>
<i>a</i> /Å	15.84420(10)	16.1323(4)	13.36102(11)
<i>b</i> /Å	15.84420(10)	16.1323(4)	15.06251(11)
<i>c</i> /Å	6.30060(10)	6.3010(4)	26.9426(2)
<i>α</i> ^o	90	90.00	90
<i>β</i> ^o	90	90.00	98.0289(7)
<i>γ</i> ^o	90	90.00	90
<i>V</i> /Å ³	1581.69(3)	1639.84(12)	5369.07(7)
<i>Z</i>	2	2	4
<i>Z'</i>	0.25	0.25	1
Wavelength/Å	1.54178	1.54178	1.54184
Radiation type	CuK _α	CuK _α	CuK _α
<i>θ</i> _{min} ^o	3.946	3.87	3.313
<i>θ</i> _{max} ^o	66.469	66.37	66.660
Measured Refl.	6298	2473	27225
Independent Refl.	1394	1172	9399
Reflections with <i>I</i> > 2(<i>I</i>)	1366	1073	8299
<i>R</i> _{int}	0.0305	0.0443	0.0342
Parameters	87	83	656
Restraints	0	4	24
Largest Peak	0.289	0.843	0.572
Deepest Hole	-0.154	-0.478	-1.236
GooF	1.058	1.019	1.050
<i>wR</i> ₂ (all data)	0.0552	0.0829	0.1468
<i>wR</i> ₂	0.0550	0.0822	0.1402
<i>R</i> ₁ (all data)	0.0225	0.0366	0.0530
<i>R</i> ₁	0.0220	0.0337	0.0473

Table 2. Crystallographic data for compounds **4** - **5**

Compound	4	4 (from CuCl)	5
Formula	C ₃₀ H ₄₂ B ₂ ClCuN ₂ P ₂	C ₃₀ H ₄₂ B ₂ N ₂ P ₂ ClCu	C ₃₀ H ₄₂ B ₂ BrCuN ₂ P ₂
<i>D</i> _{calc} / g cm ⁻³	1.291	1.282	1.358
<i>m</i> /mm ⁻¹	2.869	2.848	2.042
Formula Weight	613.20	613.20	657.66
Colour	colourless	colourless	colourless
Shape	block	block	block
Size/mm ³	0.09×0.08×0.05	0.24×0.20×0.11	0.58×0.45×0.35
<i>T</i> /K	123(1)	123.00(10)	123(1)
Crystal System	monoclinic	monoclinic	monoclinic
Space Group	<i>C2/c</i>	<i>C2/c</i>	<i>C2/c</i>
<i>a</i> /Å	35.8068(5)	12.5715(8)	12.5613(4)
<i>b</i> /Å	8.78028(10)	19.5464(8)	19.5217(4)
<i>c</i> /Å	20.8866(3)	13.9352(9)	14.1640(4)
<i>α</i> ^o	90	90	90
<i>β</i> ^o	106.1251(14)	111.879(7)	112.148(4)
<i>γ</i> ^o	90	90	90
<i>V</i> /Å ³	6308.26(14)	3177.6(3)	3216.98(17)
<i>Z</i>	8	4	4
<i>Z</i> '	1	0.5	0.5
Wavelength/Å	1.54184	1.54184	0.71073
Radiation type	CuK _α	CuK _α	MoK _α
<i>θ</i> _{min} ^o	4.407	4.414	3.587
<i>θ</i> _{max} ^o	66.619	74.388	32.263
Measured Refl.	15303	5476	9038
Independent Refl.	5504	3080	5203
Reflections with <i>I</i> > 2(<i>I</i>)	4823	2415	3655
<i>R</i> _{int}	0.0316	0.0431	0.0218
Parameters	414	182	184
Restraints	0	2	0
Largest Peak	0.583	1.288	0.567
Deepest Hole	-0.353	-0.604	-0.651
GooF	1.068	0.989	0.933
<i>wR</i> ₂ (all data)	0.0936	0.1578	0.0611
<i>wR</i> ₂	0.0894	0.1514	0.0595
<i>R</i> ₁ (all data)	0.0418	0.0687	0.0460
<i>R</i> ₁	0.0354	0.0571	0.0289

Table 3. Crystallographic data for compounds 6 - 8, 12.

Compound	6	7, 12	8
Formula	C ₃₀ H ₄₂ B ₂ CuIn ₂ P ₂	C ₉₀ H ₁₂₆ B ₆ Cl ₆ Cu ₈ N ₆ P ₆	C ₃₀ H ₄₂ B ₂ N ₂ P ₂ Cu ₂ Br ₂
<i>D</i> _{calc.} / g cm ⁻³	1.413	1.480	1.547
<i>m</i> /mm ⁻¹	9.305	4.826	5.285
Formula Weight	704.65	2334.56	801.11
Colour	colourless	colourless	colourless
Shape	block	block	block
Size/mm ³	0.06×0.04×0.02	0.17×0.07×0.03	0.31×0.15×0.12
<i>T</i> /K	123.1(3)	123.0(4)	123.0(6)
Crystal System	monoclinic	triclinic	triclinic
Space Group	<i>C</i> 2/ <i>c</i>	<i>P</i> -1	<i>P</i> -1
<i>a</i> /Å	12.6038(11)	8.3734(4)	14.1523(4)
<i>b</i> /Å	19.6086(13)	14.3042(5)	14.1578(4)
<i>c</i> /Å	14.4725(14)	22.4244(10)	18.2501(5)
<i>α</i> /°	90	98.386(3)	89.672(2)
<i>β</i> /°	112.121(11)	94.196(3)	70.189(2)
<i>γ</i> /°	90	97.934(3)	89.264(2)
<i>V</i> /Å ³	3313.5(5)	2619.75(19)	3439.98(17)
<i>Z</i>	4	1	4
<i>Z</i> '	0.5	0.5	2
Wavelength/Å	1.54184	1.54184	1.54184
Radiation type	CuK _α	CuK _α	CuK _α
<i>θ</i> _{min} /°	4.407	3.159	3.122
<i>θ</i> _{max} /°	75.012	62.380	66.591
Measured Refl.	11977	14316	27610
Independent Refl.	3314	8107	11705
Reflections with <i>I</i> > 2(<i>I</i>)	2578	5935	10640
<i>R</i> _{int}	0.0631	0.0473	0.0310
Parameters	184	591	765
Restraints	2	2	0
Largest Peak	1.261	1.288	0.567
Deepest Hole	-1.212	-0.604	-0.651
GooF	1.054	0.989	0.933
<i>wR</i> ₂ (all data)	0.1126	0.1578	0.0611
<i>wR</i> ₂	0.1068	0.1514	0.0595
<i>R</i> ₁ (all data)	0.0613	0.0687	0.0460
<i>R</i> ₁	0.0441	0.0571	0.0289

Table 4. Crystallographic data for compounds **9**, **10**.

Compound	9	10
Formula	C ₆₀ H ₈₄ B ₄ Cu ₄ I ₄ N ₄ P ₄ * CH ₂ Cl ₂	C ₆₀ H ₈₄ B ₄ Cl ₅ Cu ₅ N ₄ P ₄
<i>D</i> _{calc.} / g cm ⁻³	1.658	1.454
<i>m</i> /mm ⁻¹	15.909	4.621
Formula Weight	3806.70	1523.38
Colour	colourless	colourless
Shape	block	block
Size/mm ³	0.16×0.09×0.06	0.20×0.12×0.07
<i>T</i> /K	122.8(5)	123.01(16)
Crystal System	triclinic	monoclinic
Space Group	<i>P</i> -1	<i>P</i> ₂ / <i>c</i>
<i>a</i> /Å	13.6885(2)	29.6655(15)
<i>b</i> /Å	23.0719(3)	9.8699(7)
<i>c</i> /Å	27.3926(4)	26.3795(15)
<i>α</i> /°	113.8800(10)	90
<i>β</i> /°	95.0530(10)	115.743(7)
<i>γ</i> /°	101.2000(10)	90
<i>V</i> /Å ³	7624.7(2)	6957.2(8)
<i>Z</i>	2	4
<i>Z</i> '	1	1
Wavelength/Å	1.54178	1.54184
Radiation type	CuK _α	CuK _α
<i>θ</i> _{min} /°	3.297	3.351
<i>θ</i> _{max} /°	74.101	67.063
Measured Refl.	68934	38776
Independent Refl.	29906	12281
Reflections with <i>I</i> > 2(<i>I</i>)	20263	6687
<i>R</i> _{int}	0.0427	0.1599
Parameters	1678	755
Restraints	52	9
Largest Peak	1.606	1.430
Deepest Hole	-0.828	-0.910
GooF	0.896	0.956
<i>wR</i> ₂ (all data)	0.1032	0.2121
<i>wR</i> ₂	0.0968	0.1946
<i>R</i> ₁ (all data)	0.0595	0.1352
<i>R</i> ₁	0.0397	0.0798

Table 5. Crystallographic data for compounds **11**, **13**.

Compound	11	13
Formula	C ₆₀ H ₈₄ B ₄ Br ₅ Cu ₅ N ₄ P ₄	C ₆₀ H ₈₄ B ₄ Br ₄ Cu ₄ N ₄ P ₄
<i>D</i> _{calc.} / g cm ⁻³	1.647	1.594
<i>m</i> /mm ⁻¹	6.148	5.445
Formula Weight	1745.68	1602.23
Colour	colourless	colourless
Shape	block	block
Size/mm ³	0.08×0.03×0.03	0.07×0.04×0.04
<i>T</i> /K	122.9(2)	122.9(2)
Crystal System	monoclinic	monoclinic
Space Group	<i>P</i> 2 ₁ / <i>c</i>	<i>P</i> 2 ₁ / <i>c</i>
<i>a</i> /Å	28.9443(7)	12.5449(3)
<i>b</i> /Å	10.0574(2)	9.9152(3)
<i>c</i> /Å	26.0925(6)	26.8677(6)
<i>α</i> ^o	90	90
<i>β</i> ^o	112.082(3)	92.392(2)
<i>γ</i> ^o	90	90
<i>V</i> /Å ³	7038.5(3)	3339.03(15)
<i>Z</i>	4	2
<i>Z</i> '	1	0.5
Wavelength/Å	1.54184	1.54184
Radiation type	CuK _α	CuK _α
<i>θ</i> _{min} ^o	3.656	3.293
<i>θ</i> _{max} ^o	73.772	73.952
Measured Refl.	36416	18819
Independent Refl.	13763	6541
Reflections with <i>I</i> > 2(<i>I</i>)	10568	5439
<i>R</i> _{int}	0.0373	0.0279
Parameters	810	410
Restraints	52	82
Largest Peak	1.547	1.614
Deepest Hole	-1.519	-0.816
GooF	1.023	1.106
<i>wR</i> ₂ (all data)	0.1142	0.1312
<i>wR</i> ₂	0.1073	0.1272
<i>R</i> ₁ (all data)	0.0704	0.0656
<i>R</i> ₁	0.0505	0.0548

5.5.3 References

- [1] a) C. Marquardt, T. Jurca, K.-C. Schwan, A. Stauber, A. V. Virovets, G. R. Whittell, I. Manners, M. Scheer, *Angew. Chem. Int. Ed.* **2015**, *54*, 13122-13125; b) C. Marquardt, A. Adolf, A. Stauber, M. Bodensteiner, A. V. Virovets, A. Y. Timoshkin, M. Scheer, *Chem. Eur. J.* **2013**, *19*, 11887–11891.
- [2] Agilent Technologies **2006-2011**, CrysAlisPro Software system, different versions, Agilent Technologies UK Ltd, Oxford, UK.
- [3] G. M. Sheldrick, *Acta Cryst.* **2008**, *A64*, 112–122.
- [4] O.V. Dolomanov, L.J. Bourhis, R.J. Gildea, J.A.K. Howard, H.Puschmann, OLEX2: A complete structure solution, refinement and analysis program, **2009**. *J. Appl. Cryst.*, *42*, 339-341.

6 Thesis Treasury

The following chapter includes preliminary results. Some of the products are not fully characterized, but the results provide a basis for further research targets and might be included in future publications.

6.1 Reactivity of Phosphyboranes towards Rh(I) complexes

Transition metal complexes containing a Rh(I) center have already been discussed in chapter 1.3 for their use as precatalysts in dehydrocoupling reactions of amine- and phosphine-borane adducts.^[1] Previous research in our group started investigating the reactivity of Lewis base stabilized phosphyboranes towards $[\text{Rh}(\mu\text{-Cl})(\text{COD})]_2$.^[2] The coordination products **1** and **3** as well as the derived multinuclear complex **2** could be isolated and characterized (Figure 1). The transformation of the labile compound **1** to product **2** happens by warming up the starting material from $-80\text{ }^\circ\text{C}$ to room temperature. This reaction includes hydrogen evolution, originating from the P-H moieties, resulting in two ligands $\text{HPBH}_2\text{NMe}_3$ in a bridging position between two Rh centers. Compound **3**, containing no hydrogen atoms bonded to the phosphorus atom, shows no subsequent reaction. Based on these findings, the reaction of $t\text{BuHPBH}_2\text{NMe}_3$ towards $[\text{Rh}(\mu\text{-Cl})(\text{COD})]_2$ should be investigated, on the one hand side because of the presence of one hydrogen substituent on the phosphorus atom, which would allow for

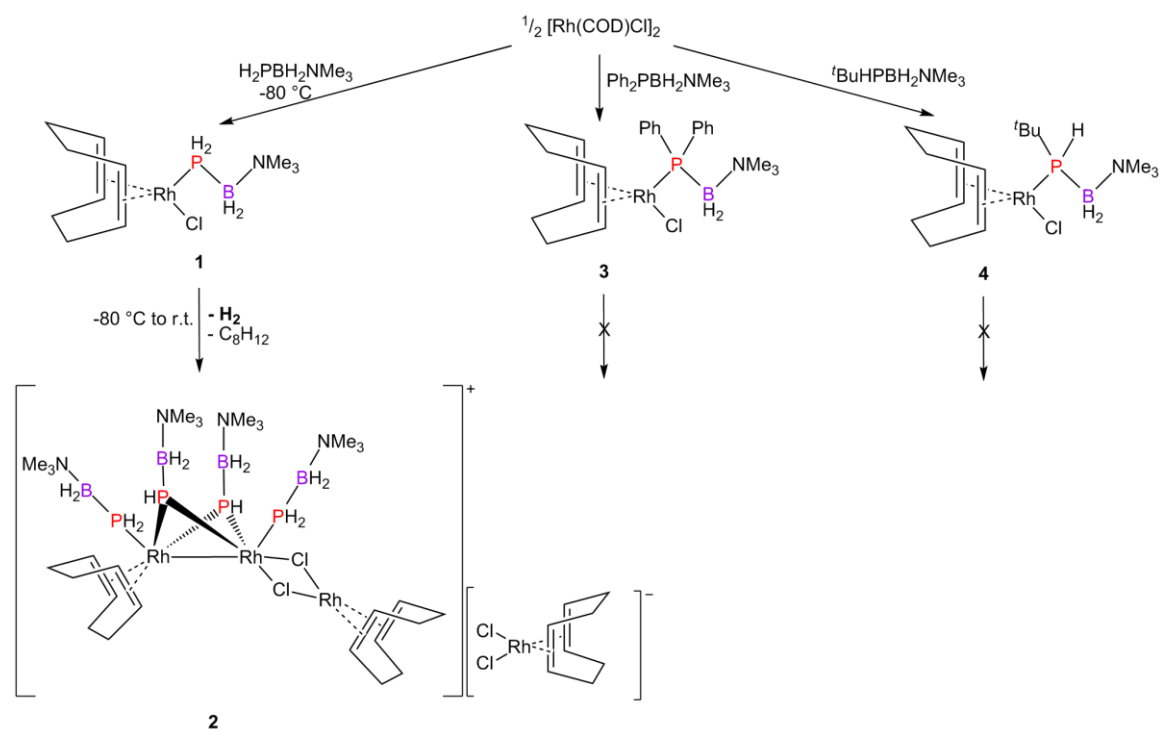


Figure 1. Reaction of $[\text{Rh}(\mu\text{-Cl})(\text{COD})]_2$ with different substituted phosphonylboranes.

indicating that subsequent reactions proceed. From this reaction, crystals of $[\text{Rh}(\text{COD})(t\text{BuHPBH}_2\text{NMe}_3)_2][\text{B}(\text{C}_6\text{H}_3\text{Cl}_2)_4]$ (**6**) could be obtained and were analyzed by single crystal X-ray diffraction (Figure 5). NMR spectroscopy of the isolated crystals of **6** was not successful due to a bad signal to noise ratio, nevertheless this coordination product is assumedly assigned to the main signal at $\delta = -18$ ppm.

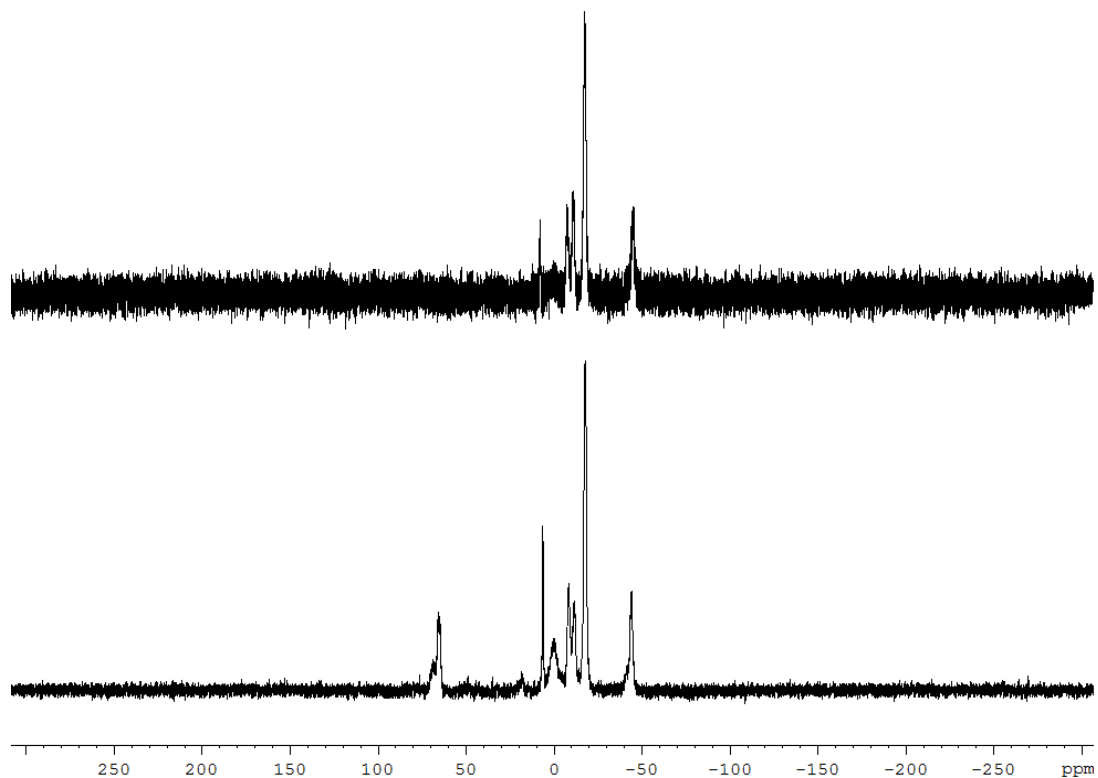


Figure 4. $^{31}\text{P}\{^1\text{H}\}$ NMR spectra of reaction of 2 equivalents of $t\text{BuHPBH}_2\cdot\text{NMe}_3$ with $[\text{Rh}(\text{COD})\{\text{B}(\text{C}_6\text{H}_3\text{Cl}_2)_4\}]$ (**5**) short after addition (top) and approximately 24h later (bottom).

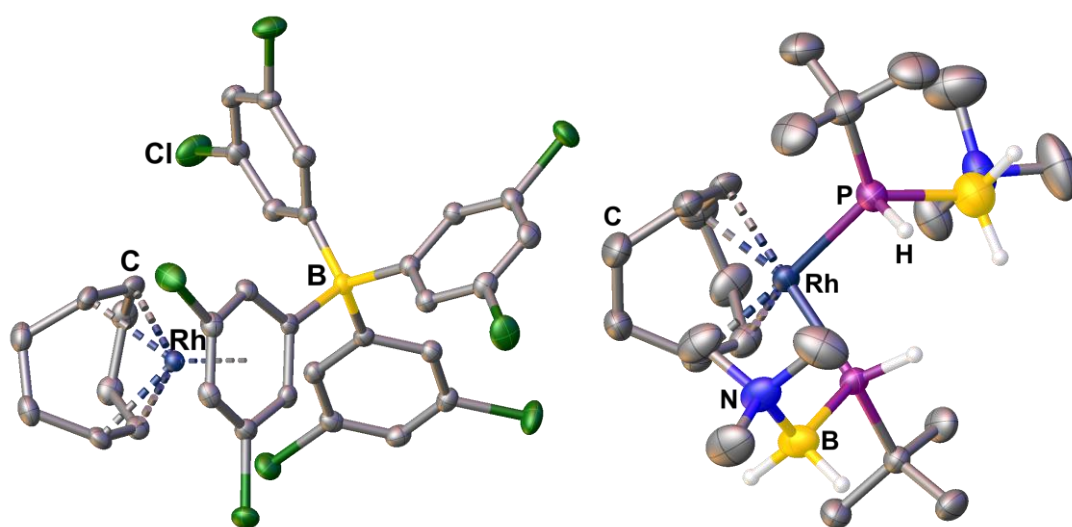


Figure 5. Molecular structure of **5** (left) and **6** (right) in the solid state. $[\text{B}(\text{C}_6\text{H}_3\text{Cl}_2)_4]$ counter ion for **6** not shown. Hydrogen atoms bonded to carbon are omitted for clarity. Thermal ellipsoids are drawn with 50% probability.

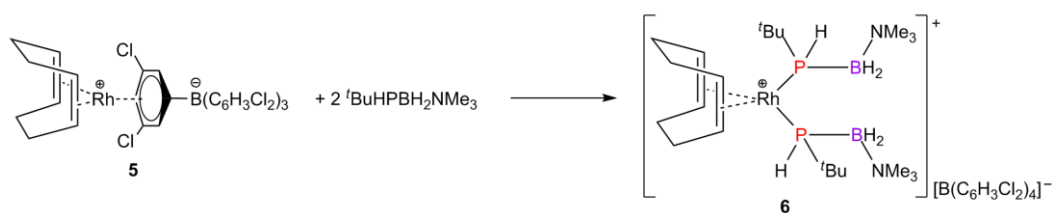


Figure 6. Formation of **6** from reaction of $[\text{Rh}(\text{COD})\{\text{B}(\text{C}_6\text{H}_3\text{Cl}_2)_4\}]$ (**5**) with $t\text{BuHPBH}_2\text{NMe}_3$.

Similar observations were made by the reaction of $[\text{Rh}(\text{COD})\{\text{B}(\text{C}_6\text{H}_3\text{Cl}_2)_4\}]$ (**5**) with two equivalents of the parent compound $\text{H}_2\text{PBH}_2\cdot\text{NMe}_3$. The initial signal at $\delta = -115$ ppm in the $^{31}\text{P}\{^1\text{H}\}$ NMR spectrum displays a broad doublet ($J = 102$ Hz), accompanied with one small side product ($\delta = -127$ ppm, d, $J = 102$ Hz). The main signal vanishes over the time, whereas an unidentified side product and various very broad signals arise (Figure 7). From the reaction of $[\text{Rh}(\text{COD})\{\text{B}(\text{C}_6\text{H}_3\text{Cl}_2)_4\}]$ (**5**) with two equivalents of $\text{Ph}_2\text{PBH}_2\cdot\text{NMe}_3$, in the $^{31}\text{P}\{^1\text{H}\}$ NMR spectrum of the reaction mixture the main signal can be found at $\delta = 23$ ppm as a broad singlet with an unidentified side product at $\delta = 4$ ppm. The main signal decreases over the time, while the signals of the side product as well as new ones are rising (Figure 8). For further insight, the initial products have to be indubitably characterized, but are assumed to be similar to complex **6**. Subsequent reactions could be observed by ^{31}P NMR spectroscopy in all of the reactions using $[\text{Rh}(\text{COD})\{\text{B}(\text{C}_6\text{H}_3\text{Cl}_2)_4\}]$ (**5**), independent from the presence of a P-H moiety, so an increased reactivity towards Lewis base stabilized pnictogenylboranes compared to $[\text{Rh}(\mu\text{-Cl})(\text{COD})]_2$ is indeed attested.

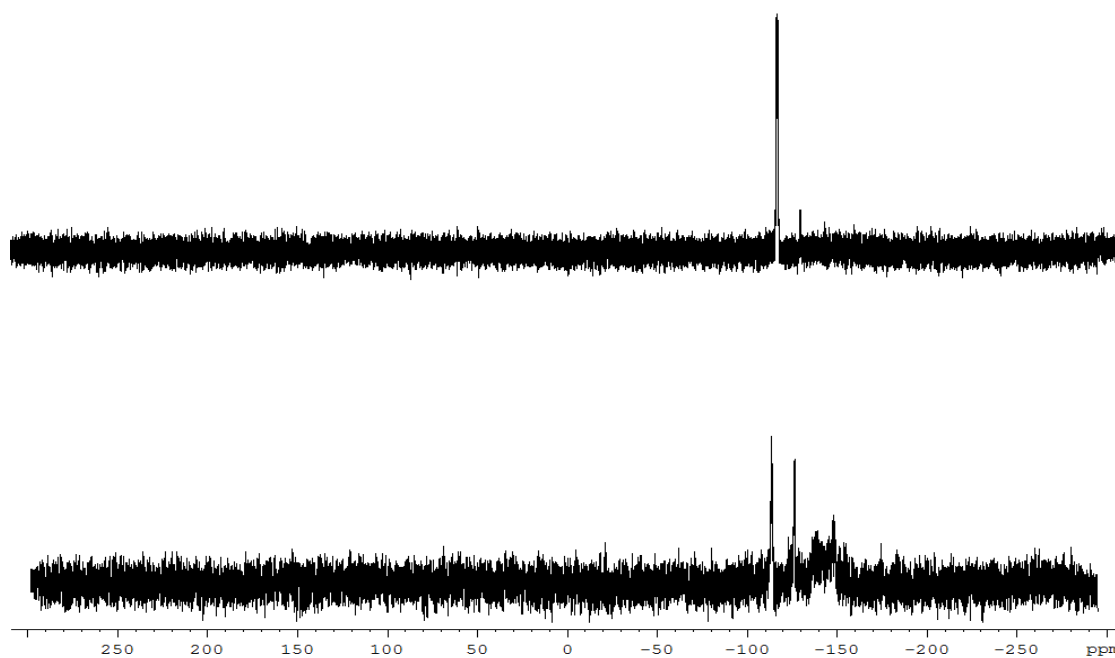


Figure 7. $^{31}\text{P}\{^1\text{H}\}$ NMR spectra of reaction of 2 equivalents of $\text{H}_2\text{PBH}_2\cdot\text{NMe}_3$ with $[\text{Rh}(\text{COD})\{\text{B}(\text{C}_6\text{H}_3\text{Cl}_2)_4\}]$ (**5**) short after addition (top) and approximately 24h later (bottom).

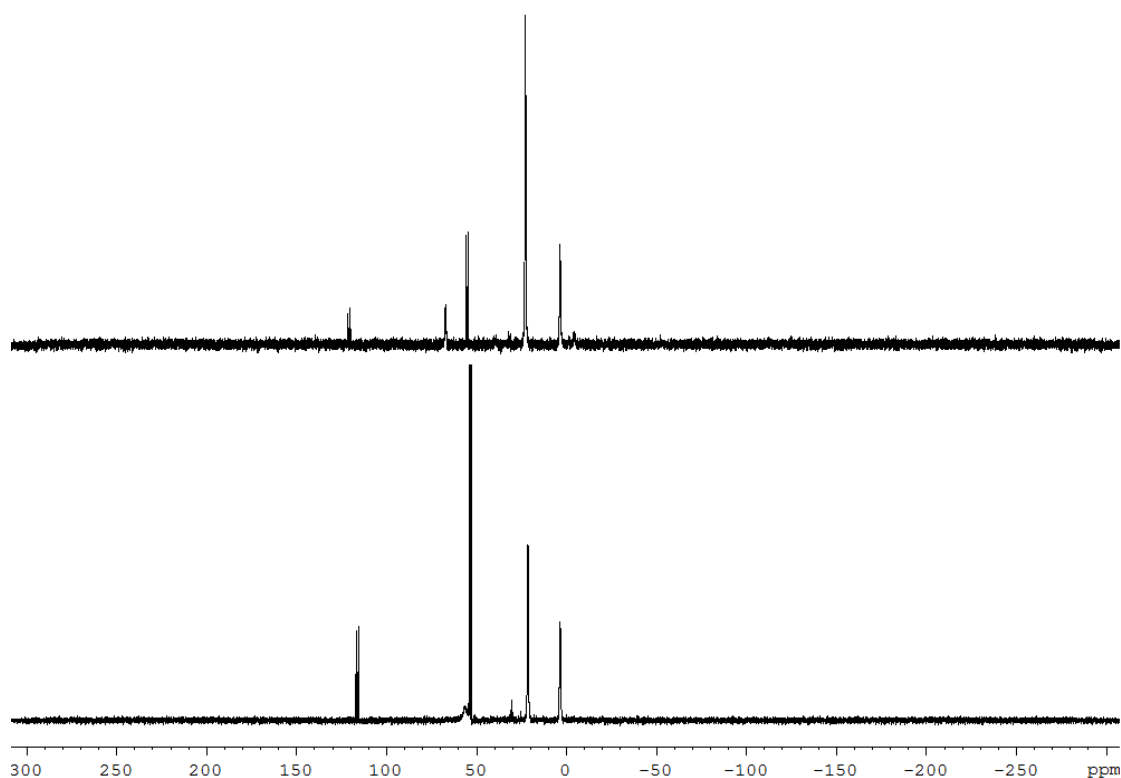


Figure 8. $^{31}\text{P}\{^1\text{H}\}$ NMR spectra of reaction of 2 equivalents of $\text{Ph}_2\text{PBH}_2\cdot\text{NMe}_3$ with $[\text{Rh}(\text{COD})\{\text{B}(\text{C}_6\text{H}_3\text{Cl}_2)_4\}]$ (**5**) short after addition (top) and approximately 24h later (bottom).

6.1.1 Syntheses of described compounds

Synthesis of $[\text{RhCl}(\text{COD})(t\text{BuHPBH}_2\text{NMe}_3)]$ (4**):** A solution of 32 mg (0.2 mmol) $t\text{BuHPBH}_2\text{NMe}_3$ in 5 mL toluene is added to a stirred solution of 49 mg (0.1 mmol) $[\text{Rh}(\mu\text{-Cl})(\text{COD})]_2$ in 5 mL toluene and stirred for 1 hour. After removing of all volatiles, the remaining solid is washed two times with small amounts of n-hexane and dried under reduced pressure. Single crystals suitable for X-ray structure analysis are obtained by storing of a concentrated toluene solution at 0 °C. **4** crystallizes as yellow blocks.

Yield of **4**: 62 mg (76%). $^1\text{H-NMR}$ (CD_2Cl_2 , 25°C): δ [ppm] = 1.95 (m, 4H, COD), 2.20 (br, 2H, BH_2), 2.25 (m, 3H, COD), 2.30 (dm, $^1J_{\text{H,P}} = 262$ Hz, 2H, PH_2), 2.44 (m, 1H, COD) 3.02 (s, 9H, $\text{N}(\text{CH}_3)_3$), 3.12 (br, 1H, COD), 3.64 (m, 1H, COD), 4.99 (m, 1H, COD), 5.14 (br, 1H, COD). $^{11}\text{B-NMR}$ (CD_2Cl_2 , 25°C): δ [ppm] = -8.22 (dt, $^1J_{\text{B,P}} = 68$ Hz, $^1J_{\text{B,H}} = 104$ Hz). $^{11}\text{B}\{^1\text{H}\}$ -NMR (CD_2Cl_2 , 25°C): δ [ppm] = -8.22 (d, $^1J_{\text{B,P}} = 68$ Hz). $^{31}\text{P-NMR}$ (CD_2Cl_2 , 25°C): δ [ppm] = 4.5 (br). $^{31}\text{P}\{^1\text{H}\}$ -NMR (CD_2Cl_2 , 25°C): δ [ppm] = 4.5 (d, br, $^1J_{\text{H,P}} = 262$ Hz). IR(KBr) : $\tilde{\nu}$ [cm^{-1}] = 2936 (s, CH), 2870 (s, CH), 2825 (m, CH), 2403 (m, BH), 2381 (m, BH), 2304 (w, PH), 2274 (m, PH), 1459 (vs), 1338 (w), 1260 (m), 1157 (m), 1129 (s), 1073 (vs), 1017 (m), 993 (m), 855 (s), 820 (m). EI-MS (70eV): $m/z = 407$ (100%,

[RhCl(COD)(*t*BuHPBH₂NMe₃)⁺]. Elemental analysis (%) calculated for C₁₅H₃₃BCINPRh (**4**): C: 44.20, H: 8.16, N: 3.44; found: C: 43.82, H: 8.12, N: 3.23.

Synthesis of [Rh(COD){B(C₆H₃Cl₂)₄}] (**5**): A solution of 325 mg (0.525 mmol) Na[B(C₆H₃Cl₂)₄] in 10 mL CH₂Cl₂ is added to a stirred solution of 123 mg (0.25 mmol) [Rh(μ-Cl)(COD)]₂ in 10 mL CH₂Cl₂ and stirred for 16 hours. The solution is filtrated, all volatiles are removed under reduced pressure. The remaining yellow solid is washed two times with small amounts of n-hexane and dried under reduced pressure. Single crystals suitable for X-ray structure analysis are obtained by overlaying of a concentrated CH₂Cl₂ solution with Et₂O and storing at -30 °C. **5** crystallizes as yellow blocks.

Yield of **5**: 323 mg (80%). ¹H-NMR (CDCl₃, 25°C): δ [ppm] = 2.15 (m, 4H, COD), 2.54 (m, 4H, COD), 3.12 (br, 1H, COD), 4.16 (br, 4H, COD), 6.30 (m, 2H, o-H Ph coord), 7.13 (m, 6H, o-H Ph), 7.16 (m, 3H, p-H Ph), 7.32 (m, 1H, p-H Ph coord). ¹¹B-NMR (CDCl₃, 25°C): δ [ppm] = -8.24 (s). ¹¹B{¹H}-NMR (CDCl₃, 25°C): δ [ppm] = -8.24 (s). IR(ATR Diamond) : $\tilde{\nu}$ [cm⁻¹] = 3077 (w, CH), 3046 (w, CH), 2960 (w, CH), 2918 (w, CH), 2879 (w, CH), 2836 (w, CH), 1562 (m), 1545 (s), 1489 (m), 1479 (m), 1451 (w), 1418 (m), 1394 (m), 1382 (m), 1369 (m), 1331 (m), 1305 (w), 1286 (w), 1261 (m), 1216 (w), 1161 (m), 1150 (m), 1136 (m), 1120 (m), 1093 (m), 1067 (m), 1015 (m) 992 (m), 960 (w), 938 (w), 912 (w), 885 (w), 874 (m), 850 (s), 784 (vs), 709 (s), 703 (s), 691 (s), 662 (m), 651 (m), 639 (m), 596 (w), 578 (w), 529 (w), 507 (m), 499 (m), 476 (m), 458 (vw), 444 (m), 435 (m), 404 (m). ESI-MS (MeCN): positive: *m/z* = 252 (67%, [Rh(COD)(MeCN)]⁺, 293 (100%, [Rh(COD)(MeCN)₂]⁺; negative: *m/z* = 595 (100%, [B(C₆H₃Cl₂)₄]⁻). Elemental analysis (%) calculated for C₃₂H₂₄BCl₈Rh (**4**): C: 47.69, H: 3.00; found: C: 47.36, H: 3.53.

Synthesis of [Rh(COD)(*t*BuHPBH₂·NMe₃)₂][B(C₆H₃Cl₂)₄] (**6**): To a stirred suspension of 45 mg (0.05 mmol) [Rh(COD){B(C₆H₃Cl₂)₄}] (**5**) in 1 mL CH₂Cl₂ 16 mg (0.1 mmol) *t*BuHPBH₂·NMe₃ is added. The suspension turns from yellow to a clear orange solution. Single crystals suitable for X-ray structure analysis are obtained by gas phase diffusion of CH₂Cl₂ into n-hexane. **6** crystallizes as orange blocks.

Table 1. Crystallographic data for compounds **4 - 6**.

Compound	4	5 (* Et ₂ O * 0.5 CH ₂ Cl ₂)	6
Formula	C ₁₅ H ₃₃ BNPCIRh	C ₁₃₇ H ₁₁₈ B ₄ Cl ₃₄ O ₂ Rh ₄	C ₄₆ H ₆₆ B ₃ Cl ₈ N ₂ P ₂ Rh
<i>D</i> _{calc.} / g cm ⁻³	1.462	1.660	1.395
<i>m</i> /mm ⁻¹	9.508	10.251	7.048
Formula Weight	407.56	3456.49	1127.88
Colour	yellow	yellow	orange
Shape	block	block	block
Size/mm ³	0.15x0.07x0.06	0.24x0.17x0.09	0.35x0.20x0.09
<i>T</i> /K	122.95(10)	122.99(11)	123(2)
Crystal System	monoclinic	triclinic	monoclinic
Space Group	<i>P</i> 2 ₁ / <i>c</i>	<i>P</i> -1	<i>I</i> 2/ <i>a</i>
<i>a</i> /Å	10.0531(2)	12.5898(4)	16.7253(2)
<i>b</i> /Å	15.9538(3)	16.3213(4)	18.1689(2)
<i>c</i> /Å	12.1507(2)	18.9439(3)	35.3442(4)
<i>α</i> /°	90	101.601(2)	90
<i>β</i> /°	108.195(2)	96.244(2)	90.0930(10)
<i>γ</i> /°	90	112.132(3)	90
<i>V</i> /Å ³	1851.35(6)	3458.35(17)	10740.4(2)
<i>Z</i>	4	1	8
<i>Z</i> '	1	0.5	1
Wavelength/Å	1.54184	1.54184	1.54184
Radiation type	CuK _α	CuK _α	CuK _α
<i>θ</i> _{min} /°	4.630	3.029	3.592
<i>θ</i> _{max} /°	66.759	74.866	66.311
Measured Refl.	8605	38247	36142
Independent Refl.	3267	13659	9379
Reflections with <i>I</i> > 2(<i>I</i>)	3036	12550	8283
<i>R</i> _{int}	0.0292	0.0329	0.0365
Parameters	199	822	591
Restraints	3	0	12
Largest Peak	0.546	1.259	1.806
Deepest Hole	-0.390	-0.758	-0.834
GooF	1.049	1.015	1.049
<i>wR</i> ₂ (all data)	0.0532	0.0777	0.1589
<i>wR</i> ₂	0.0516	0.0753	0.1533
<i>R</i> ₁ (all data)	0.0260	0.0329	0.0655
<i>R</i> ₁	0.0233	0.0298	0.0586

6.1.2 References

- [1] a) C. A. Jaska, K. Temple, A. J. Lough, I. Manners, *J. Am. Chem. Soc.* **2003**, *125*, 9424–9434; b) H. Dorn, R. A. Singh, J. A. Massey, A. J. Lough, I. Manners, *Angew. Chem. Int. Ed.* **1999**, *38*, 3321–3323, *Angew. Chem.* **1999**, *111*, 3540–3543; c) C. A. Jaska, K. Temple, A. J. Lough, I. Manners, *Chem. Commun.* **2001**, 962–963.
- [2] J. Braese, Master's Thesis, University of Regensburg, **2013**.

7 Conclusion

7.1 Polymerization of Pnictogenylboranes

For the synthesis of oligomers and polymers of group 13/15 compounds, the most in depth examined reaction pathways include a dehydrocoupling step utilizing transition metal complexes as catalysts.^[1] They represent well-established ways to produce high molecular inorganic polymers, although certain starting materials proved to be inferior for these kinds of reactions and the resulting materials might show undesirable properties like low molecular masses or high polydispersity.^[2] The reactions work best when electron withdrawing substituents are present on the pnictogen atom, resulting in a more electropositive hydrogen substituent on the same atom, allowing for a more facile elimination of dihydrogen together with the rather hydridic B-H moiety.^[3] The use of Lewis base stabilized pnictogenylboranes for the synthesis of inorganic group 13/15 polymers encounters precisely this problem, giving rise to high molecular mass polymers, especially with electron donating substituents on the pnictogen atom, which are otherwise not obtained. Thus, they represent a perfect complementary reaction to the already established synthetic routes. Additionally, organic substituents offer a better solubility of the resulting materials, preventing an early termination of the polymerization process through precipitation of the product, which would result in lower molecular masses.^[4] An increased solubility of the polymer is also facilitating the characterization. One possible pathway towards poly(alkylphosphinoborane)s that was established in our group is the mild thermolysis (I) of *t*BuHPBH₂NMe₃ (**1a**),^[5] that gives rise to a high molecular mass polymer [*t*BuPH-BH₂]_{*n*} (**2a**), which is hard to access via a dehydrocoupling reaction (Figure 1). For comparison, a dehydrocoupling reaction towards the same product using *t*BuH₂P·BH₃ and [Cp(CO)₂Fe(OSO₂CF₃)] as catalysts (II) needs higher temperatures as well as longer reaction times while offering only low molecular mass products. During this thesis, a completely new reaction pathway towards poly(alkylphosphinoborane)s could be established (III), making use of Lewis base stabilized phosphanylboranes as well as a transition metal catalysts bis(η⁵:η¹-adamantylidenepentafulvene)titanium (**3**). This new pathway significantly reduces the reaction times while offering even milder reaction conditions and comparable features of the resulting polymer (Figure 1).

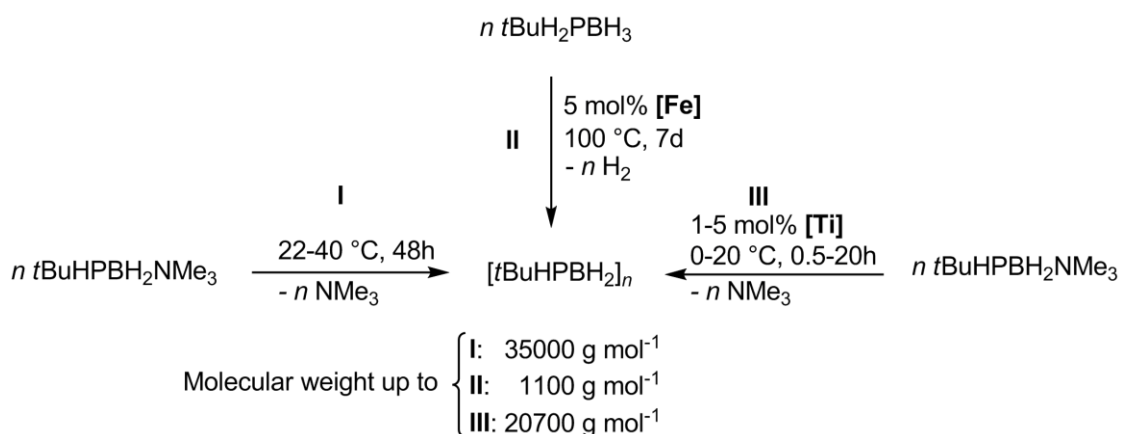


Figure 1. Comparison of different routes for the synthesis of poly[(*tert*-butylphosphino)boranes]. I: metal free thermolysis, II: dehydrocoupling using [Fe] = [Cp(CO)₂Fe(OSO₂CF₃)], III: new route using [Ti] = [(η⁵:η¹-C₅H₄C₁₀H₁₄)₂Ti].

Not only in the field of polymerization, but also the synthesis of the Lewis base stabilized monomers has steadily improved through ongoing research by our group, especially for the phosphanylborane species. Deprotonation of the corresponding phosphines and subsequent reaction with BH₂I·NMe₃ affords the desired phosphanylboranes in good yields and high purity (**IV**, Figure 2), i.e. the parent compound H₂PBH₂NMe₃ as well as its aryl- and alkyl-substituted congeners.^[5] In addition to this, a subsequent functionalization of the parent compound H₂PBH₂NMe₃ (**1b**) is also feasible by addition of iodoalkanes to generate [RPH₂–BH₂·NMe₃]I (R = *n*-alkyl) and further HI elimination by addition of a Brønsted base (**V**).^[6]

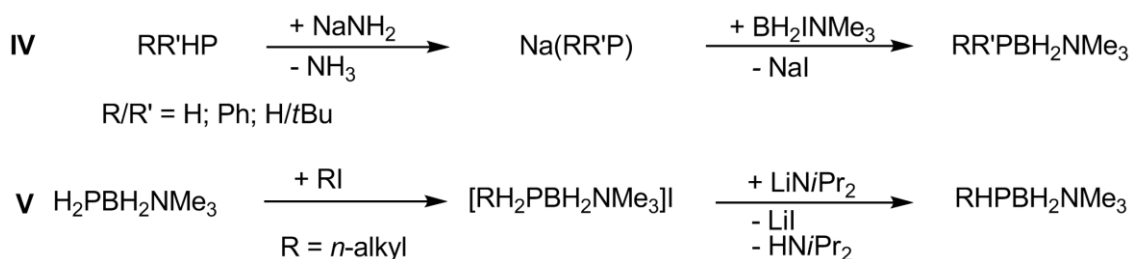


Figure 2. Synthesis of Lewis base stabilized pnictogenylboranes.

Based on these procedures, the compounds RR'EBH₂NMe₃ (**1a**: E = P, R = H, R' = *t*Bu; **1b**: E = P, R = R' = H; **1c**: E = P, R = H, R' = Me; **1d**: E = P, R = H, R' = *n*Pr; **1e**: E = P, R = H, R' = *n*Hex; **1f**: E = P, R = Me, R' = *t*Bu; **1g**: E = P, R = R' = Ph, **1h**: E = As, R = R' = H; **1i**: E = As, R = H, R' = *t*Bu) were synthesized within the course of this thesis (**1f/i** synthesized by Oliver Hegen). The monomers have been tested for oligo- or polymerization via the established thermolysis pathway (I) and also the newly discovered titanium catalyzed polymerization pathway (III). If an oligomerization or polymerization

reaction proceeded, the results from the different pathways were compared. For *n*PrHPBH₂NMe₃ (**1d**) and *n*HexHPBH₂NMe₃ (**1e**), similar oligomeric products could be obtained in either way, but the ratio is strongly influenced by the chosen reaction pathway. Best results were obtained from the polymerization reaction of *t*BuHPBH₂NMe₃ (**1a**), taking place in the presence of 1 mol% of bis(η⁵:η¹-adamantylidene)pentafulvene)titanium (**3**) at room temperature in less than an hour for a full conversion to the polymer [*t*BuPH-BH₂]_{*n*} (**2a**). The influence of temperature, catalyst loading and purification steps on the resulting polymer were investigated. A comparison to the well characterized thermal polymer^[5] shows significantly reduced reaction times and temperatures at the cost of reduced molecular weights and a higher polydispersity. The reaction was monitored by multinuclear NMR spectroscopy. The resulting polymers were investigated by mass spectrometry in order to determine the repeating units (*m/z* = 102 Da, [*t*BuHPBH₂]) and end groups. Molecular weight and size distribution was investigated via dynamic light scattering and GPC (*M_n* = 20732 g mol⁻¹, *M_w* = 44937 g mol⁻¹, PDI = 2.2).

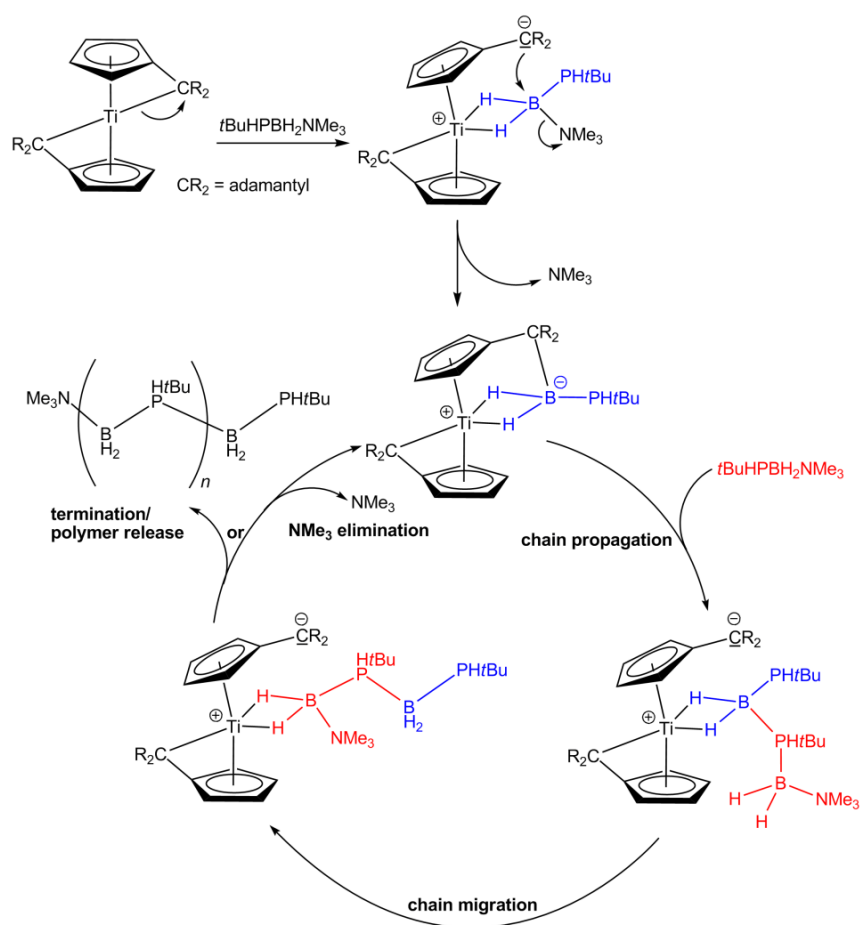


Figure 3. Proposed catalytic cycle for the chain-growth coordination polymerization of **1a** (scheme showing only one insertion event).

Derived from reports on oligomerization on titanium centers,^[7] the obtained experimental results as well as from preliminary computational studies, a first order chain growth mechanism is proposed (Figure 3). This mechanism includes the initial fixation of the first monomer on the metal center, the assisted elimination of the stabilizing Lewis base and a chain propagation step, followed up by a chain migration. From there, the polymer growth can continue via further Lewis base elimination or it can be terminated by release of the free polymer [*t*BuPH-BH₂]_{*n*} (**2a**). Further investigation should offer more insight for this new reaction pathway, that might help to facilitate polymerization reactions in future research.

[Rh(μ-Cl)(COD)]₂ represents a potent precatalyst for dehydrocoupling reactions of amine- and phosphine-borane adducts.^[8] In the reaction with Lewis base stabilized phosphanyboranes, no polymerization could be observed but rather the formation of coordination compounds. Only in the case of the parent compound H₂PBH₂NMe₃ (**1b**), a subsequent reaction including P-H activation and hydrogen evolution towards multinuclear complex $[\{(\text{COD})\text{Rh}\}(\mu\text{-Cl})_2\text{Rh}(\mu,\eta^{1:1}\text{-PHBH}_2\text{NMe}_3)_2\{\eta^1\text{-PH}_2\text{BH}_2\text{NMe}_3\}_2]^+$ [Rh(COD)Cl₂]⁻ (**4**) takes place.^[9] Further experiments produced a new Rh(I) complex [Rh(COD){B(C₆H₃Cl₂)₄}] (**5**), which shows the initial formation of coordination products like [Rh(COD)(*t*BuHPBH₂·NMe₃)₂][B(C₆H₃Cl₂)₄] (**6**). The formation of assumed complexes [Rh(COD)(R₂PBH₂·NMe₃)₂][B(C₆H₃Cl₂)₄] (**A1**: R = Ph, **A2**: R = H) is indicated by NMR spectroscopic investigations. All these complexes offer subsequent reactions, which will have to be further characterized in forthcoming experiments (Figure 4).

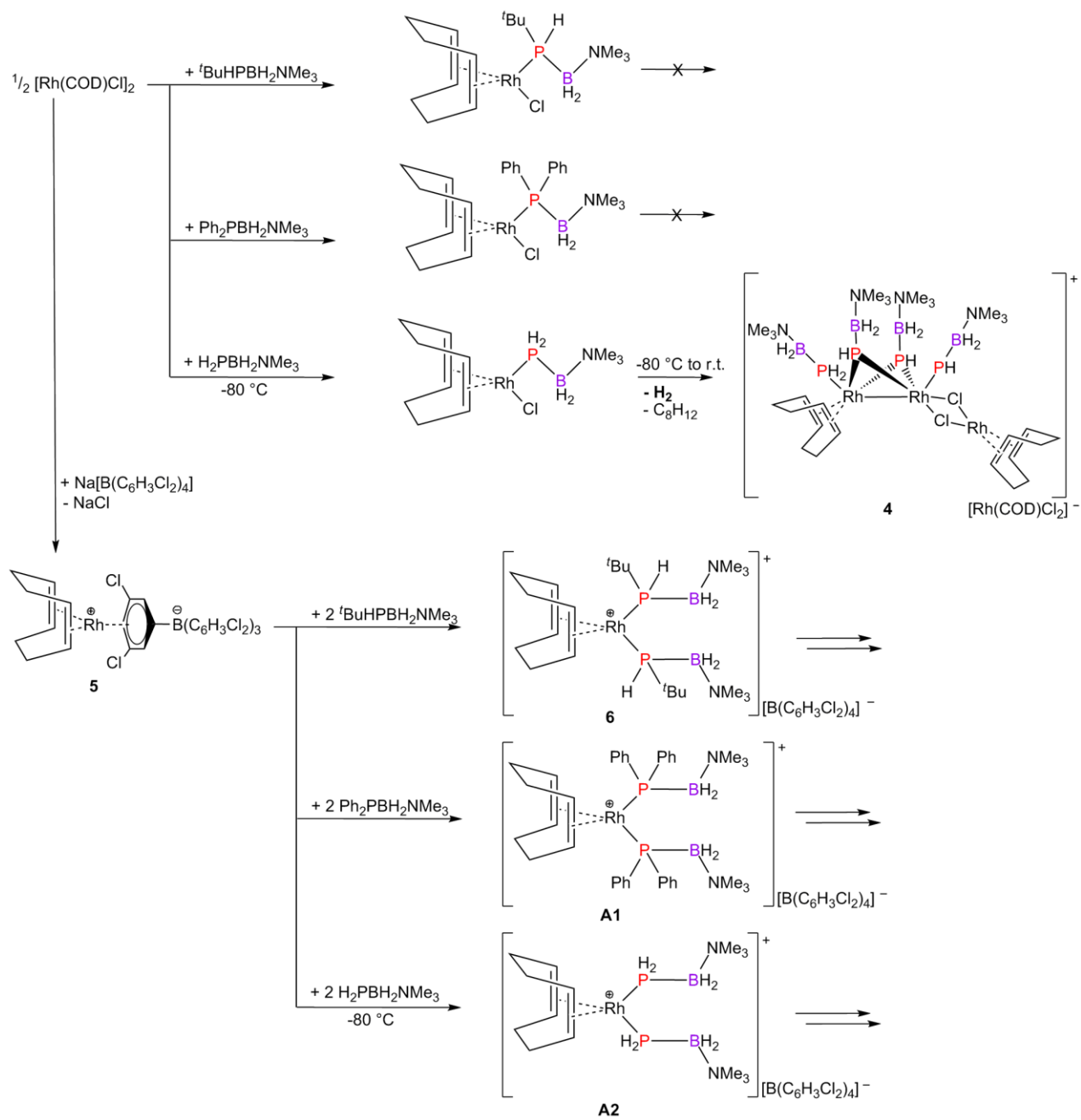


Figure 4. Reactivity of Rh(I) complexes with different substituted phosphanylboranes.

7.2 Coordination towards Au(I) and Cu(I) compounds

Reactions of Lewis base stabilized pnictogenylboranes with transition metal complexes does not necessarily leads to oligomerization/polymerization reactions but can yet produce new complexes with interesting properties. Reaction of $RR'EBH_2NMe_3$ (**1a**: E = P, R = H, R' = *t*Bu; **1b**: E = P, R = R' = H; **1g**: E = P, R = R' = Ph, **1h**: E = As, R = R' = H) with a source of AuCl affords the linear complexes $[AuCl(RR'EBH_2NMe_3)]$ (**7a-d**). Depending on the nature of the ligands, aurophilic interactions could be observed for the only hydrogen substituted ligands $H_2EBH_2NMe_3$ (E = P, As; Figure 5). This was not found for the organic substituted phosphanylboranes which reveal monomeric $[AuCl(RR'PBH_2NMe_3)]$ complexes (**7c**: R = H, R' = *t*Bu; **7d**: R = R' = Ph). $[AuCl(H_2PBH_2NMe_3)]_2$ (**7a**) dimerizes in the solid state, showing unsupported intermolecular aurophilic interactions with short Au...Au distances ($d(Au...Au) = 3.103(1)$ Å). $[AuCl(H_2AsBH_2NMe_3)]_n$ (**7b**) aggregates to form a 1D coordination polymer ($d(Au...Au) = 3.251(1)$ Å). Further reactions include the abstraction of the chloride substituent by $AlCl_3$ and addition of a second equivalent of the corresponding pnictogenylborane ligand. Cationic Au(I) complexes $[Au(RR'EBH_2NMe_3)_2][AlCl_4]$ (**8a-d**) are formed, which reveal discrete molecules in the solid state for organic substituted phosphanylboranes $[Au(RR'PBH_2NMe_3)_2][AlCl_4]$ (**8c**: R = H, R' = *t*Bu; **8d**: R = R' = Ph). In case of the parent ligands, increased aurophilicity is observed, in both cases showing 1D chain products $[Au(H_2EBH_2NMe_3)_2][AlCl_4]$ (**8a**: E = P, $d(Au...Au) = 3.208(2)$ Å; **8b**: E = As, $d(Au...Au) = 3.113(1)$ Å) in the solid state. Single crystal X-ray diffraction analysis reveals decreasing Au...Au distances with lower temperature. Additionally, the cationic chains **8a,b** reveal luminescence in the solid state (**8a**: $\lambda_{max} = 503$ nm at 300K; **8b**: $\lambda_{max} = 453$ nm at 300K). The emission shows a red shift with temperature decrease (**8a**: $\lambda_{max} = 523$ nm at 77K; **8b**: $\lambda_{max} = 497$ nm at 77K), being correlated with decreasing intermetallic distances. These findings were confirmed by DFT calculations, that also show an increase of the Au...Au bond strength by 2-4 kJ mol⁻¹ and the WBI by 7% upon cooling of **8a** from 300K to 90K. Therefore, light emitting cationic chain complexes of Au(I) featuring non-bridging phosphine and arsine ligands were obtained for the first time, resulting in remarkably short Au...Au distances. Furthermore, unprecedented primary arsine gold complexes could be synthesized (**7b**, **8b**), which show a higher tendency to form additional Au...Au bonds.

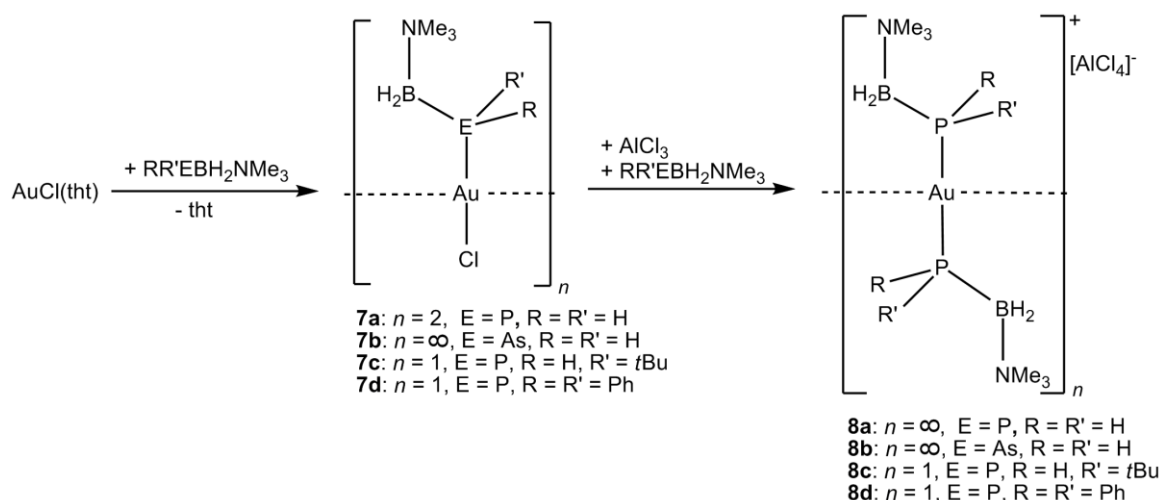


Figure 5. Reactivity of Au(I) complexes towards different substituted pnictogenylboranes.

Reactions of the pnictogenylboranes $RR'EBH_2NMe_3$ (**1b**: $E = P$, $R = R' = H$; **1g**: $E = P$, $R = R' = Ph$, **1h**: $E = As$, $R = R' = H$) with $[Cu(MeCN)_4][BF_4]$ afford the homoleptic complexes $[Cu(H_2EBH_2NMe_3)_4][BF_4]$ (**9a**: $E = P$, **9b**: $E = As$) and $[Cu(Ph_2PBH_2NMe_3)_3][BF_4]$ (**9c**). **9a,b** are tetrahedral complexes, while compound **9b** represents the first structurally characterized complex of a primary arsine coordinated to a Cu center. The use of the sterically demanding **1g** on the other hand leads to a trigonal planar coordination of the Cu^+ ion (Figure 6).

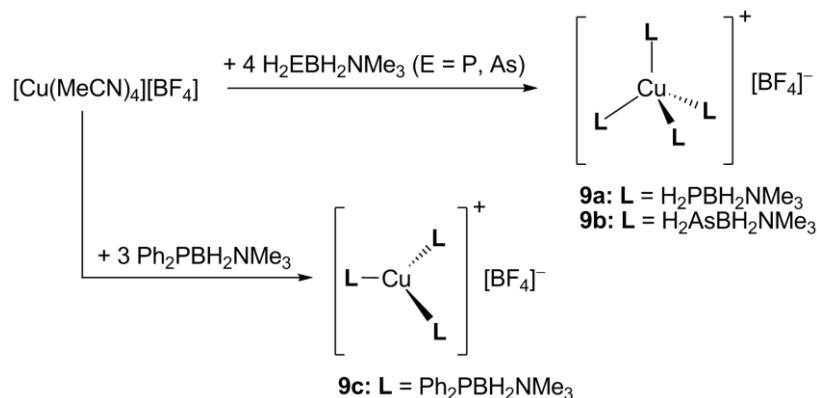


Figure 6: Coordination of different pnictogenylboranes towards Cu^+ .

Especially the use of ligand $Ph_2PBH_2NMe_3$ (**1g**), which can be described as a derivative of Ph_3P , in the reaction with copper(I) halides gave rise to a series of new complexes that were compared to related complexes featuring Ph_3P . Complexes $[CuX(Ph_2PBH_2NMe_3)_2]$ (**10**: $X = Cl$, **11**: $X = Br$, **12**: $X = I$) with a 2:1 ratio of **1g** to CuX show similar trigonal structure to their Ph_3P counterparts, the same is true for crystals of the tetrameric $[Cu_4Br_4(Ph_2PBH_2NMe_3)_4]$ (**19**), displaying an expanded ladderlike structure. The other complexes, containing a ratio of CuX to **1g** greater or equal to 1,

tend to stabilize geometries less favored when Ph_3P is used. They show structures like the dimeric, halide bridged complexes $[\text{Cu}_2\text{X}_2(\text{Ph}_2\text{PBH}_2\cdot\text{NMe}_3)_2]$ (**13**: $\text{X} = \text{Cl}$, **14**: $\text{X} = \text{Br}$) or a heterocubane $[\text{Cu}_4\text{L}_4(\text{Ph}_2\text{PBH}_2\cdot\text{NMe}_3)_2]$ (**15**) as well as $[\text{Cu}_5\text{X}_5(\text{Ph}_2\text{PBH}_2\cdot\text{NMe}_3)_4]$ (**16**: $\text{X} = \text{Cl}$, **17**: $\text{X} = \text{Br}$) and $[\text{Cu}_6\text{Cl}_6(\text{Ph}_2\text{PBH}_2\cdot\text{NMe}_3)_4]$ (**18**). Complexes **16** and **17** can be viewed as edge open cubanes with an additional CuX ($\text{X} = \text{Cl}, \text{Br}$) unit attached to the Cu_4X_4 core. (Figure 6).

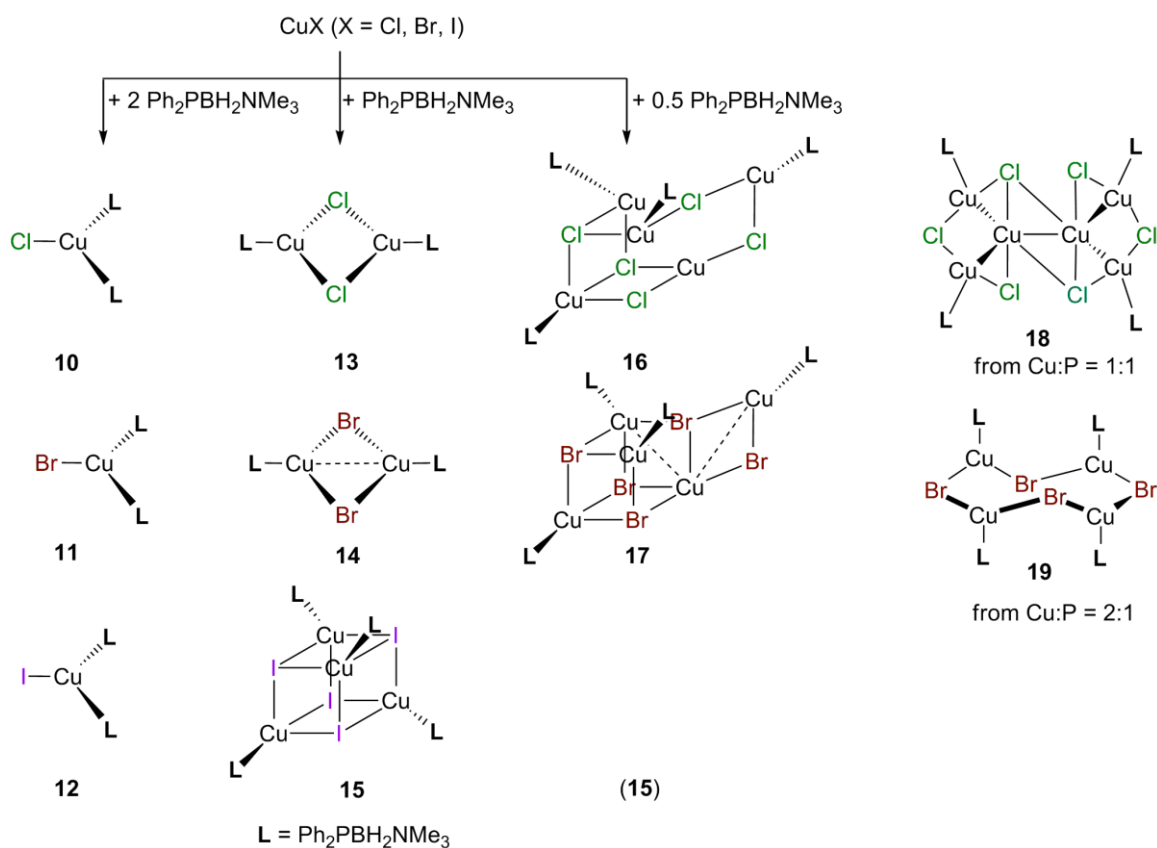


Figure 6: Reactions of $\text{Ph}_2\text{PBH}_2\text{NMe}_3$ (**1g**) with copper(I) halides in different stoichiometric ratios.

All complexes were characterized by single-crystal X-ray structure analysis, multinuclear NMR spectroscopy, IR spectroscopy and mass spectrometry. The results show that the structure present in the solid state is likely to change in solution or the gas phase. NMR spectroscopic investigations at -80°C of dissolved crystals of **16** and **17** show just one signal in the ^{31}P NMR spectra, even though the phosphorus atoms are not magnetically equivalent. The same is true for analysis by FD mass spectrometry, which reveal smaller as well as bigger aggregates than present in the solid state. Despite the academic interest, these ligands may be interesting for catalytic studies and large variety of different complexes should be accessible.

7.3 References

- [1] For a review: A. Staubitz, A. P. M. Robertson, I. Manners, *Chem. Rev.* **2010**, *110*, 4023–4078; also see chapter 1.3 and literature therein.
- [2] a) H. Dorn, J. M. Rodezno, B. Brunnhöfer, E. Rivard, J. A. Massey, I. Manners, *Macromolecules* **2003**, *36*, 291–297; b) S. Pandey, P. Lönnecke, E. Hey-Hawkins, *Eur. J. Inorg. Chem.* **2014**, 2456–2465.
- [3] a) A. Schäfer, T. Jurca, J. Turner, J. R. Vance, K. Lee, V. A. Du, M. F. Haddow, G. R. Whittell, I. Manners, *Angew. Chem. Int. Ed.* **2015**, *54*, 4836–4841; *Angew. Chem.* **2015**, *127*, 4918–4923; b) M. A. Huertos, A. S. Weller, *Chem. Commun.* **2012**, *48*, 7185–7187; c) M. A. Huertos, A. S. Weller, *Chem. Sci.* **2013**, *4*, 1881–1888; d) T. N. Hooper, M. A. Huertos, T. Jurca, S. D. Pike, A. S. Weller, I. Manners, *Inorg. Chem.* **2014**, *53*, 3716–3729; e) H. C. Johnson, T. N. Hooper, A. S. Weller, *Top. Organomet. Chem.* **2015**, *49*, 153–220.
- [4] a) X. Feng, M. M. Olmstead, P. P. Power, *Inorg. Chem.* **1986**, *25*, 4615–4616; b) J.-M. Denis, H. Forintos, H. Szelke, L. Toupet, T.-N. Pham, P.-J. Madec, A.-C. Gaumont, *Chem. Commun.* **2003**, 54–55.
- [5] C. Marquardt, T. Jurca, K.-C. Schwan, A. Stauber, A. V. Virovets, G. R. Whittell, I. Manners, M. Scheer, *Angew. Chem. Int. Ed.* **2015**, *54*, 13782–13786; *Angew. Chem.* **2015**, *127*, 13986–13991.
- [6] A. Stauber, T. Jurca, C. Marquardt, M. Fleischmann, M. Seidl, G. R. Whittell, I. Manners, M. Scheer, *Eur. J. Inorg. Chem.* **2016**, 2684–2687.
- [7] a) M. E. Sloan, A. Staubitz, T. J. Clark, C. A. Russell, G. C. Lloyd-Jones, I. Manners, *J. Am. Chem. Soc.* **2010**, *132*, 3831–3841; b) H. Helten, B. Dutta, J. R. Vance, M. E. Sloan, M. F. Haddow, S. Sproules, D. Collison, G. R. Whittell, G. C. Lloyd-Jones, I. Manners, *Angew. Chem. Int. Ed.* **2013**, *52*, 437–440; c) D. Pun, E. Lobkovsky, P. J. Chirik, *Chem. Commun.* **2007**, 3297–3299; d) T. Beweries, S. Hansen, M. Kessler, M. Klahn, U. Rosenthal, *Dalton Trans.* **2011**, *40*, 7689–7692; e) Y. Luo, K. Ohno, *Organometallics* **2007**, *26*, 3597–3600; f) M. E. Sloan, A. Staubitz, T. J. Clark, C. A. Russell, G. C. Lloyd-Jones, I. Manners, *J. Am. Chem. Soc.* **2010**, *132*, 3831–3841; g) C. Thoms, C. Marquardt, M. Bodensteiner, M. Scheer, *Angew. Chem. Int. Ed.* **2013**, *52*, 5150–5154; *Angew. Chem.* **2013**, *125*, 5254–5259.
- [8] a) C. A. Jaska, K. Temple, A. J. Lough, I. Manners, *J. Am. Chem. Soc.* **2003**, *125*, 9424–9434; b) H. Dorn, R. A. Singh, J. A. Massey, A. J. Lough, I. Manners, *Angew. Chem. Int. Ed.* **1999**, *38*, 3321–3323, *Angew. Chem.* **1999**, *111*, 3540–3543; c) C. A. Jaska, K. Temple, A. J. Lough, I. Manners, *Chem. Commun.* **2001**, 962–963.
- [9] J. Braese, Master's Thesis, University of Regensburg, **2013**.

8 Appendices

8.1 List of Abbreviations

In order of appearance:

ΔEN	electron negativity difference
e^-	electron, elemental charge
Å	Angstroem, $1 \text{ \AA} = 1 \cdot 10^{-10} \text{ m}$
wt-%	mass fraction
Ph	phenyl, C_6H_5
COD	cyclooctadiene, C_8H_{12}
Me	methyl, CH_3
Bn	benzyl, $\text{CH}_2\text{C}_6\text{H}_5$
<i>i</i> Pr	<i>iso</i> -propyl, C_3H_7
POCOP	1,3-(<i>OPtBu</i>) ₂ C_6H_3
<i>t</i> Bu	<i>tert</i> -butyl, C_4H_9
<i>n</i> Bu	<i>n</i> -butyl, C_4H_9
Cp	cyclopentadienyl, C_5H_5
Fc	ferrocenyl, $\text{C}_{10}\text{H}_9\text{Fe}$
LB	Lewis base
Mes	mesityl, C_6H_3
Cy	cyclohexyl, C_6H_{11}
DMAP	4-(Dimethylamino)pyridine, $\text{C}_7\text{H}_{10}\text{N}_2$
NHC^{Me}	N-heterocyclic carbene, 1,3,4,5-Tetramethylimidazolylidene
NHC^{Dipp}	N-heterocyclic carbene, 1,3-bis(2,6-diisopropylphenyl)imidazolin-2-ylidene
btmsa	bis(trimethylsilyl)acetylene, $\text{C}_8\text{H}_{18}\text{Si}_2$
NMR	nuclear magnetic resonance
DLS	dynamic light scattering
ESI MS	electron spray ionization mass spectrometry
GPC	Gel permeation chromatography
δ	chemical shift
ppm	parts per million
h	hour
°C	degree Celsius
M_n	number average molar mass
PDI	polydispersity index

R_h	hydrodynamic radius
k	reaction rate constant
s	second
m/z	mass to charge ratio
nPr	<i>n</i> -propyl, C_3H_7
$nHex$	<i>n</i> -hexyl, C_6H_{13}
MHz	Megahertz, 10^6 Hz
μL	microliter, 10^{-6} liter
mg	milligram, 10^{-3} gram
mL	milliliter, 10^{-3} liter
kV	kilovolt, 10^3 volt
THF	tetrahydrofurane, C_4H_8O
min	minute
μmol	micromol, 10^{-6} mol
Da	Dalton, unified mass unit
mmol	millimol, 10^{-3} mol
s(NMR)	singlet
br(NMR)	broad
d(NMR)	doublet
$J(NMR)$	coupling constant
m(NMR)	multiplet
ESR	electron spin resonance
ES^+	electron spray, positive mode
MS	mass spectrometry
M_w	weight average molecular weight
M_z	size average molecular weight
M_p	peak maximum molecular weight
DFT	density functional theory
1D	one-dimensional
r.t.	room temperature
°	degree
K	Kelvin
WBI	Wiberg bond index
Φ_{PL}	photoluminescence quantum yield
λ_{max}	Peak maximum
HOMO	highest occupied molecular orbital

LUMO	lowest unoccupied molecular orbital
sh	shoulder
τ	emission decay time
S ₀	ground state
S ₁	singlet state
T ₁	triplet state
μ s	microsecond, 10 ⁻⁶ second
FT-IR	Fourier-transform infrared spectroscopy
FD MS	field desorption ionization mass spectrometry
IR	infrared spectroscopy
w(IR)	weak
m(IR)	medium
s(IR)	strong
vs(IR)	very strong
vw(IR)	very weak

8.2 Acknowledgments

Finally, I would like to thank...

- Prof. Dr. Manfred Scheer for the opportunity to be part of his working group, providing excellent working conditions, the possibility to visit national and international workshops and conferences as well as his patience and constructive commentaries.
- Dr. Gábor Balázs for his always available, helpful advices and discussions, proof-readings and his unique enrichment to the social dynamics.
- Prof. Dr. Alexey Timoshkin for putting much effort into the DFT calculations and being an enjoyable short time office colleague.
- Prof. Dr. Hartmut Yersin for the helpful discussions and his engagement in the interpretation of the photophysical results, adding the perspective of a physicist to the work of a chemist.
- Prof. Dr. Ian Manners and Dr. Vincent Annibale for discussions and crucial measurements of the polymeric materials, improving the work with their immense theoretical and practical experience.
- Dr. Michael Bodensteiner for all of his engagement in the field of solid state structure determination, his precious help with menacing crystallographic problems as well as being an enjoyable travel companion.
- Alexander Schinabeck for his congenial efforts in the measurement and interpretation of the luminescent materials.
- All members of the Central Analytical Services of the University of Regensburg: The X-ray department, the NMR department, the mass spectrometry department and the elemental analysis department.
- My former lab colleagues (Bianca, Christian, Olli, Tobi, Matthias, Felix) for the supportive mentality in the lab and the countless hours of fun and craziness we shared.
- My training colleagues (Moritz, Eric, Valentin, Michael, Matthias), offering a precious and fun counterbalance to a researchers life.
- My former fellow students and friends (Julian, Romi, Stefan, Stefan, Steffi, Ani, Brandy and many more), battling chemistry together since the very first semester.
- All present and former members of the Scheer group, please feel personally addressed, I learned a lot from each one of you, it was a cherished time.
- My friends, my family and loved ones.